A COMPARATIVE STUDY OF THE STRUCTURAL BEHAVIOUR OF PRESTRESSED BEAMS OF BRICKWORK AND CONCRETE AND THE SHEAR STRENGTH OF BRICKWORK BEAMS

June Uduehi, B.Sc

A thesis submitted for the Degree

of Doctor of Philosophy

Department of Civil Engineering and Building Science,

The University of Edinburgh

December, 1989

To Dad and Mum, Mr. P.J Uduehi and Mrs. F.I Uduehi.

ACKNOWLEDGEMENTS

I would like to express my gratitude to Dr. B.P Sinha, my supervisor, for his advice and assistance throughout this project.

I would also like to acknowledge the financial assistance afforded by the ORS award scheme and the University of Edinburgh Bursary. Thanks are also due to the departmental technicians especially to Mr. J Hutchinson.

Finally, to my Dad and Mum, for their love, support and encouragement and for the opportunities they have given me. To Aina, Joy, Aima, Oz, Eka, Alex, Toyin and all my friends for their support, tolerance and encouragement. Most importantly, I give thanks to God who has made it all possible.

ABSTRACT

This thesis presents the results of a comparative study which has been carried out into the structural behaviour of fully and partially prestressed beams of brickwork and concrete and the shear strength of partially prestressed brickwork beams containing tensioned and non-tensioned reinforcement. Test results from twenty nine full scale brickwork and concrete beams of identical cross-sectional properties and tensile reinforcement and of similar compressive strengths are reported. The aspects of structural behaviour studied were as follows:

1. The flexural strength
2. The deformational response (load-deflection and moment-curvature)
3. Flexural cracking and
4. The shear strength

The effect of the shear span to effective depth ratio (1.5 to 6.0) on the shear strength of sixteen full scale partially prestressed brickwork beams was also investigated.

The properties of brickwork used in the theoretical analysis were obtained from small specimen tests and those for concrete were obtained from the code of practice for concrete, BS 8110, Part 2. The theoretical analysis of the flexural behaviour utilised the non-linear stress-strain relationship for brickwork and concrete at all stages of loading up to failure, accounted for the presence of the concrete cavity in the brickwork beams and also considered the tension stiffening effect in the flexurally cracked beams. A comparison was made with experimental results.

An expression for predicting the maximum crack width in fully/partially prestressed brickwork beams was developed. It was shown that the concept of the compressive force path previously developed for concrete can be used to predict the shear strength of bonded prestressed brickwork beams without shear reinforcement. Finally, the results of a non-linear finite element analysis into the shear strength of partially prestressed brickwork beams is reported.

CONTENTS

NOTATION

a, a_v	shear span
a_{ax}	location of shear failure from the support
a_i	clear shear span measured between the loading and supporting plates
a_o	sum of perimeters of reinforcement
a_{vf}	shear span marking the transition between diagonal tension failure and flexural failure
a_{vo}	shear span marking the transition between shear compression failure and diagonal tension failure
a_{vx}	ratio M_{ax}/V_{ax}
A	cross-sectional area of beam
A_p	area of tensioned reinforcement
A_{pe}	effective area of tensioned steel
A_s	area of non-tensioned reinforcement
A_{se}	effective area of tensile reinforcement
A_t	area of concrete/brickwork in tension
A_t'	cross-sectional area of transformed section
b	breadth of section
b_c	breadth of concrete cavity
b_j	distance between vertical joints at the soffit of a beam
b_v	breadth of a member, or for T-, I- and L- members the breadth of the rib
b_w	breadth of the web
b_1	effective width of the section
B	bearing area
c	cover to the tensile reinforcement
C	compressive force in section
C_o	the ratio M_o/z
C_0, C_1, C_2	tension-stiffening factors
d	effective depth of tensile reinforcement
d_e	effective depth of equivalant area of tensioned reinforcement
d_j	distance from the top fibre to the top bed joint
d_p	effective depth of tensioned reinforcement
d_r	depth to the line of action of the resultant tensile force
d_s	effective depth of non-tensioned reinforcement

D	nominal bar diameter
e	eccentricity
E	modulus of elasticity
E_c, E_o	modulus of elasticity of concrete
E'_c	initial modulus of elasticity of concrete
E_m	modulus of elasticity of brickwork
E'_m	initial modulus of elasticity of brickwork
E_p	modulus of elasticity of tensioned steel
E_s	modulus of elasticity of non-tensioned steel
f	compressive stress in brickwork/concrete
f'_c	cylinder compression strength of concrete
f_{cp}	design compressive stress at the centroidal axis due to prestress
f_{ct}	compressive stress in concrete subject to biaxial tension-compression
f_{ct}'	fictitious tensile stress
f_{cu}	characteristic compressive strength of concrete
f_f	compressive strength in the top fibre at bed joint splitting
f_k	characteristic compressive strength of masonry
f_m	average compressive strength of brickwork
f_{mt}	mean tensile stress in brickwork
f_p	stress in the tensioned reinforcement
f_{pc}	axial stress in a concrete beam
f_{pe}	design effective prestress in the tendon after all losses
f_{pu}	stress in tensioned reinforcement at ultimate
f_{py}	proof stress of tensioned reinforcement
f_r	modulus of rupture of section
f_s	tensile stress in the non-tensioned reinforcement
f_{se}	tensile stress in equivalent area of tensile reinforcement at a crack
f'_{se}	stress in equivalent area of tensioned reinforcement away from a crack
f_{secr}	stress in equivalent area of tensioned reinforcement at a crack at the cracking moment
f_{su}	stress in non-tensioned reinforcement at ultimate
f_{sy}	proof stress of non-tensioned reinforcement

f_{tc}	tensile stress in concrete subjected to biaxial tension-compression
f_y	characteristic strength of tensile steel
$F_c(\varepsilon)$	stress-strain relationship of concrete
$F_m(\varepsilon)$	stress-strain relationship of brickwork
$F_p(\varepsilon_p)$	stress-strain relationship for the tensioned reinforcement
$F_s(\varepsilon_s)$	stress-strain relationship for the non-tensioned reinforcement
F_y	yield force in the tensile reinforcement
h	overall depth of section
h_b	distances from the top of the beam to the bottom of the concrete cavity
h_{cr}	crack height
h_o	initial crack height
h_t	distance from the top of the beam to the top of the concrete cavity
H	horizontal component of the diagonal force
j_1, j_2, j_3	lever arm factors
k	tension stiffening factor
k′	constant
k_b, k_c	constant in the crack width equation for brickwork and concrete respectively
k_1,k_2	constants in the crack spacing equation for concrete
l_a	lever arm
m,m′	modular ratio
M	moment
M_{ax}	applied bending moment at a given section x
M_{cr}	cracking moment
M_{cx}	moment at a section corresponding to shear failure
M_f	flexural capacity of a beam which fails in flexure
M_{fx}	flexural moment capacity at section x
M_o	maximum flexural capacity of a beam which fails in shear compression
M_v	ultimate moment due to shear failure
M_u,M_{um},M_{ut}	ultimate moment

n	neutral axis depth
n_r	centriod of the uncracked transformed section
N_j	number of joints between cracks
P	prestressing force
P'	effective reinforcement ratio
Q	stress reduction coefficient
r_t	$\varepsilon'_1/\varepsilon'_2$
R	factor defining bond characteristics of steel
s_m	mean crack spacing
s_o	minimum crack spacing
shrr	shear retention factor
S	diagonal force
t	thickness
T	total tensile force in section
T_1, T_2	tensile forces
T_m	tensile force in brickwork
T_p	tensile force in tensioned reinforcement
T_s	tensile force in non-tensioned reinforcement
v_c	design concrete shear stress
V	shear force
V_{ax}	applied shear force at a given section x
V_c	design ultimate shear resistance of the concrete
V_{ci}	flexure-shear cracking load
V_{co}	design ultimate shear resistance of an uncracked section
V_{cr}	design ultimate shear resistance of a cracked section
V_{cw}	web-shear cracking load
V_{cx}	load corresponding to shear failure
V_p	vertical component of the prestressing force
V_u	ultimate shear force
w, w_{av}	average crack width
w_{max}	maximum crack width
x	distance along the beam
X_1, X_2, X_3	coefficients in the stress-strain relationships for brickwork and concrete
y	deflection
z	lever arm
z_f	lever arm corresponding to flexural failure

z_o	lever arm corresponding to shear compression failure
Z, Z_b, Z_t	section modulus
χ	$=e_{pa}/e_{sa}$
ε	strain in brickwork/concrete
$\varepsilon_1, \varepsilon_2$	strain in top and bottom fibre respectively
$\varepsilon_{a1}, \varepsilon_{a2}$	applied strain in top and bottom fibre respectively
ε_c	strain in concrete
$\varepsilon_{c,1}$	strain in concrete at the maximum stress
ε_{cr}	strain to cause cracking
ε_{cu}	ultimate compressive strain of concrete
ε_j	splitting strain in brickwork
ε_m	ultimate compressive strain of brickwork
ε_{max}	maximum strain
ε_{ms}	top fibre strain in brickwork at shear failure
ε_p	total strain in tensioned reinforcement
ε_{pa}	strain in tensioned reinforcement due to applied loading
ε_{pe}	strain due to precompression in brickwork at level of the tensioned steel
ε_{pp}	strain in tensioned reinforcement due to the prestressing force
ε_{py}	strain in tensioned reinforcement at the proof stress
ε_{pu}	strain in tensioned reinforcement at ultimate
ε_{p1}, ε_{p2}	prestress strains
ε_r	ultimate tensile strain of brickwork
ε_s	total strain in non-tensioned reinforcement
ε_{sa}	strain in non-tensioned reinforcement due to applied loading
ε_{se}	strain due to precompression in brickwork at level of non-tensioned reinforcement
ε_{sea}	strain in equivalent area of tensioned reinforcement due to applied loading at crack
ε_{sea}'	strain in equivalent area of tensioned steel due to applied loading away from a crack
ε_{seam}	average additional strain in equivalent area of tensioned steel
ε_{sp}	strain in non-tensioned steel due to prestressing force
ε_{su}	strain in non-tensioned steel at ultimate

ε_{sy}	strain in non-tensioned steel at proof stress
ε_t	strain in steel at cracking
ϕ	curvature of the beam
ϕ_p	curvature due to prestress
ϕ_{ave}	average curvature of the beam
ϕ_{cr}	curvature at a cracked section
Φ	reinforcement index
$\lambda_1, \lambda_2, \lambda_3$	stress block factors
ρ, ρ_s	percentage area of tensile reinforcement
ρ'	reinforcement ratio
ρ_{bal}	area of reinforcement in a balanced section
ρ_{comp}	compressive strength of concrete
$\rho_{p\ bal}$	balanced area of tensioned steel
$\rho_{s\ bal}$	balanced area of non-tensioned steel
σ_c	compressive stress in concrete
σ_{eff}	effective prestress
$\sigma_{0.2}$	0.2% stress of the prestressing reinforcement
σ_1, σ_2	stresses in top and bottom fibres due to prestressing
$\Sigma\ O$	sum of reinforcing perimeters
τ	shear stress V/b.d
τ_b	bond stress
ν_u	ultimate shear stress
κ	a/a_i
ψ	angle between the tensile steel and the principal tension direction

CHAPTER 1
INTRODUCTION

1.1 HISTORICAL DEVELOPMENT OF MODERN MASONRY

1.1.1 Unreinforced Masonry

The term masonry is defined in BS 5628[1] as an assemblage of structural units, either laid in situ or constructed in prefabricated panels, in which the structural units are bonded and solidly put together with concrete and/or mortar so as to act compositely. This definition thus covers stonework, blockwork and brickwork.

Masonry is widely acknowledged as Man's oldest building material. Its origins have been traced as far back as 20,000 years ago. Some examples of ancient masonry structures are still in evidence today. These include Stonehenge in Wiltshire, England, the Chinese Wall and many other relics of the ancient civilisations of Egypt, Greece and Rome. A majority of these ancient structures were of hewed stone and each stone unit could weigh as much as 2 tonnes. The manufacture of the first readily handled sunbaked clay bricks have been attributed to the Summerians some 5500 years ago[2].

Masonry is very strong in compression but relatively weak in tension. As a consequence, it is most commonly used in compressively loaded members, such as walls, columns and arches. However, these members can also be subjected to lateral loads due to wind and retained materials such as water, earth and crops. Traditionally, the provision of lateral stability in unreinforced masonry structures was achieved by increasing the self weight of the structure so that the resultant force due to the dead weight and lateral loading remained within the 'kern limit'. Thus no reliance was placed on the tensile strength. This culminated in the 1.6 m thick external base wall in the 16 storey Monadonack building in Chicago in 1893[2]. The rising cost of natural resources and the advent of steel and reinforced concrete priced unreinforced masonry out of the market.

In the early part of this century, the use of unreinforced masonry was

confined to low-rise buildings and as an in-fill material in framed construction. The post-war era saw a renewed interest in masonry as a structural material. This was encouraged by the departure from the traditional form of 'gravity' construction developed by Swiss engineers; rather than the provision of lateral stability through self weight, the brickwork panels were re-oriented to form shear walls. Thus an 18 storey building was built using 150 mm thick load bearing brickwork walls. Since then several alternatives to the 'gravity' form of construction have been developed. These include off-set and Pilaster walls.

The renewed interest in masonry as a structural material has been sustained through a more scientific approach to the testing and design of masonry using structural engineering principles. Masonry is now generally assumed to be comparable to concrete.

The unique advantages of masonry over concrete and steel, which include a superior durability and an ability to perform several functions such as subdivision of space, thermal and acoustic insulation as well as fire and weather protection, and its similarity to concrete led to research into the possibilities of reinforced and prestressed masonry.

1.1.2 Reinforced Brickwork

Reinforced brickwork refers to brickwork in which steel reinforcement is incorporated to enhance the resistance to tensile, compressive or shear forces[1]. The first documented use of reinforced brickwork was by Marc Isambard Brunel as part of the Thames Tunnel project in 1825[3]. Sir Marc's plan for tunnelling under the River Thames was based on the sinking of caissons on either side of the river and tunnelling between the shafts. The caissons consisted of two vertical brick tubes 15.24 m in diameter and 21.34 m high. The 762 mm thick walls were vertically reinforced with 25.4 mm diameter wrought iron bolts built into the brickwork and fastened to wooden curbs at the top and bottom with nuts at the threaded ends of the bolts. The horizontal reinforcement consisted of 228.6 mm wide and 12.7 mm thick iron hoops. The shafts were sunk by removing the earth within it so that it sunk under its own self weight. Even after severe differential settlement, 178 mm on one side and 76 mm on the other, no cracks developed in the brickwork.

Brunel's work stimulated interest in reinforced brickwork. Pasley[4] in 1837 tested beams with and without reinforcement and concluded that the presence

of reinforcement significantly increased the flexural strength of brickwork. Although work on reinforced brickwork continued after Pasley's work, the begining of modern reinforced brickwork is associated with Brebner[5] who in 1923 reported work on a large number of beams, columns and slabs. Brebner's report also included a rational theory for the design of such elements. Thereafter the use of reinforced brickwork in countries like India, New Zealand, U.S.A. and Japan became widespread. These countries are situated in earthquake zones where the requirement for buildings with a high resistence to lateral load is paramount. Reinforced brickwork still remains popular in India.

In the U.K., interest in reinforced brickwork did not begin until about 1938 when some work was carried out at the Building Research Station. The outbreak of the Second World War halted interest in reinforced brickwork and it was not until 1963 that interest was again rejuvenated. Since then a great deal of research has been carried out which has resulted in the code of practice based on limit state design philosophy. As a consequence, reinforced brickwork may become a major competitor with reinforced concrete in some sectors of the construction industry.

The advantages of reinforced brickwork over reinforced concrete are well documented. Firstly, brickwork is a low energy input material when compared to concrete. The construction process for reinforced brickwork does not in general require the erection of form work which constitutes a saving in labour and resources. By far the greatest proportion of a reinforced brickwork member is the brick unit. The quantity of cement required is thus greatly reduced. Brickwork has more aesthetic appeal than concrete and the variety of finishes which can be achieved by using different colours and textures of brick surpasses that which can be achieved in concrete. Brickwork weathers better with age and unlike concrete does not stain. Comparisons which have been made of cost between reinforced concrete and reinforced brickwork retaining walls have shown that reinforced brickwork may prove to be considerably cheaper[6,27].

Reinforced brickwork however has some disadvantages. Because of the low tensile strength of brickwork, cracking usually occurs under working loads. To limit the width of cracks, the steel stresses have to be kept low. The high tensile steel is thus been inefficiently used. Also, a number of investigations[8,9,10] have shown that reinforced brickwork beams usually fail in

shear. Thus neither the brickwork nor the steel is being fully utilized. Further, as brickwork is weak in tension, its tensile strength is not relied upon in design.

These disadvantages of reinforced brickwork can be eliminated or minimised by prestressing.

1.1.3 Prestressed Brickwork

Prestressed concrete is a well established material in the construction industry and has been used in varying degrees for over six decades. It is only recently, however, that the technique of prestressing has been applied to brickwork and attempts have been made to study the behaviour of such members. Prestressed brickwork has advantages over reinforced brickwork. The application of prestress to a member can eliminate tensile cracking under working load. Prestressing has also been shown[11,12,13,14] to enhance the shear strength. Further, in a prestressed section, all the brickwork is in compression so that the compressive strength is fully exploited. Thus the disadvantages encountered with reinforced brickwork can be eliminated or minimised by prestressing. Also there is an increase in ductility associated with a prestressed beam when compared to an ordinary reinforced beam. This results from the reduced steel area in the former arising from the fact that the yield strength of prestressing steel is between 2 and 3 times that of ordinary reinforcement.

Some notable structures[15,16,17] were constructed utilising the advantages of prestressing before the issue of the current code of practice for the design of reinforced and prestressed masonry, BS 5628: Part I: 1985[1]. This code does not consider cracked prestressed brickwork members. Thus it is assumed that sufficient prestress is applied to prevent cracking under working loads. As a result large amounts of prestress may be required in a member. This introduces problems with excessive camber. Further, experimental works[3,11] which have so far been carried out have shown that high prestressing forces can lead to cracking in the anchorage zone. In some sections, this can be counteracted by anchorage reinforcement. A logical progression will be the development of partial prestressing of masonry members which can avoid some of the problems with fully prestressed sections mentioned above.

1.1.4 Partial Prestressing

A partially prestressed section is defined as one in which the applied prestressing force is limited to counteract only a part of the tensile stresses which develop under service loads. This can be achieved in two ways. Firstly, by reducing the level of the initial prestress applied to all the tensile reinforcement. This can lead to an inefficient use of the expensive high tensile steel. Alternatively, a portion of the tensile reinforcement can consist of prestressing reinforcement stressed to the maximum allowable stress and the remaining tensile reinforcement made up of conventional reinforcement. Hereafter, partially prestressing refers to the latter method. By adopting a partially prestressed section, the camber will be reduced and excessive tensile stresses in the anchorage zone avoided.

In a prestressed beam containing tensioned reinforcement only, the location of the tensioned steel is restricted by the need to prevent tensile stresses due to the prestressing force. The prestressing reinforcement thus has to be placed within the 'kern' limit. In a partially prestressed beam, the non-tensioned steel can be placed as close to the soffit as possible thereby improving crack control. Although partial prestressing offers some advantages as mentioned, the current code BS 5628: Part I: 1985[1] does not give any guidance for the design of such members because of lack of data.

To further the development of fully and partially prestressed masonry, the present study was undertaken in this field. The principal aim of this investigation is to compare the behaviour of bonded prestressed beams of brickwork and concrete, identical in section and of similar compressive strength, under the ultimate limit states of shear and flexure and the deflection and cracking. The lower shear strength of brickwork compared to concrete imposes a limitation on the structural performance of fully and partially prestressed brickwork beams. As no work has been carried out on the shear strength of partially prestressed brickwork beams, an experimental and theoretical investigation was also undertaken in this area.

CHAPTER 2
LITERATURE REVIEW

2.1 INTRODUCTION

In this Chapter, a general review of the research work which has been carried out in the field of prestressed masonry is presented. Although this thesis also contains work on prestressed concrete beams, it was felt unnecessary for a general review to be carried out on concrete. This is because prestressed concrete is a well established form of construction in the civil/structural engineering industry, made possible by a huge amount of research work which is summarised in a large number of readily available publications[18,19]. However, a more specific and relevant review of literature for prestressed concrete was done, which can be found in the relevant chapter.

A number of prestressed masonry structures have been constructed. Some of these projects are described in Section 2.3.

2.2 RESEARCH WORK

In 1963, Thomas[3] tested two post-tensioned beams as part of an investigation into the possibility of resting suspended floors on beams constructed in this way. Both beams were constructed from three hole perforated wire-cut rustic bricks with an average compressive strength of not less than 28 N/mm^2. The cross-sections of these beams are shown in Fig. 2.2.1. In the first of these beams, the bricks were layed as soldiers. The tensioned reinforcement consisted of six 7 mm high tensile steel wires which were threaded through the lowest perforation. The perforation containing the reinforcement was left ungrouted. An initial prestressing force of 67 kN was applied to the beam which induced a maximum compressive stress of 7.2 N/mm^2. The beam was tested under a central point load over a span of 2.515 m. It was loaded up to 18 kN and then unloaded. The prestressing force was then increased to 107 kN causing a maximum compressive stress of 11.6 N/mm^2 at the soffit of the beam and was again loaded in the same way. At a somewhat lower applied load of 17 kN, the beam failed. Failure was attributed

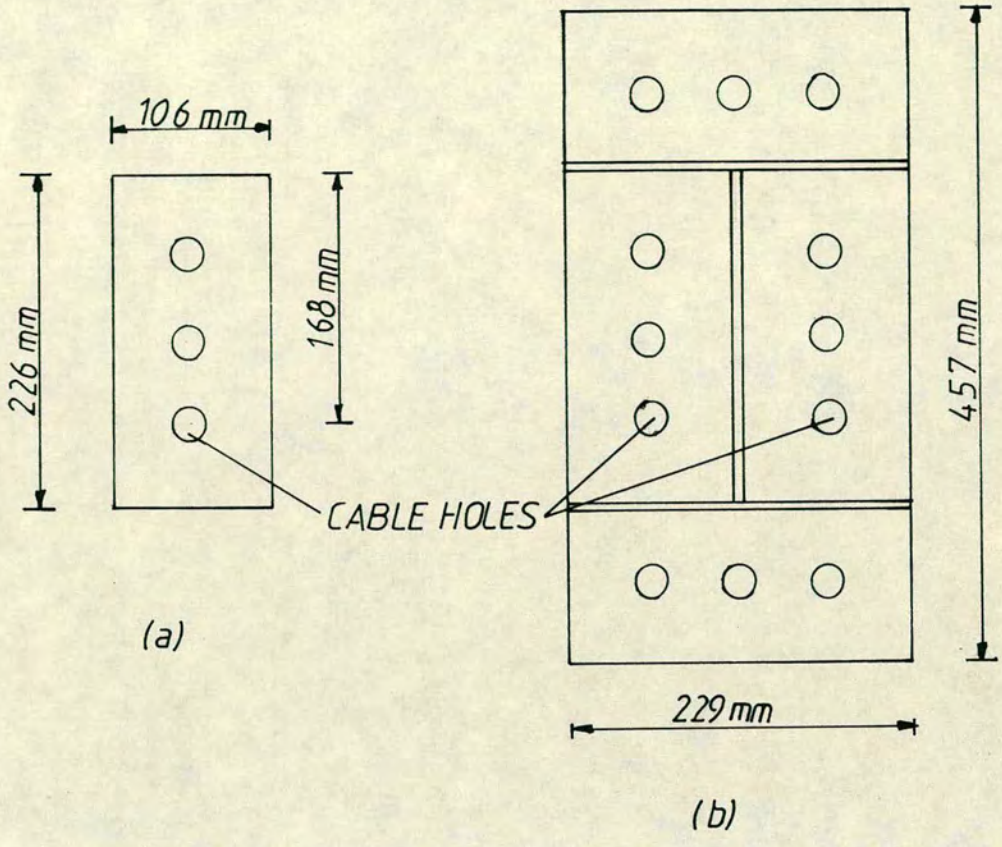

Fig. 2.2.1 Beam Section of K. THOMAS[3]

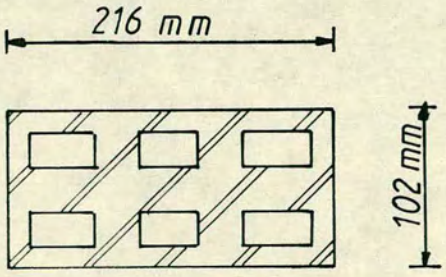

Fig. 2.2.2 Beam Section of L.S NG[3]

by Thomas to be due to the principal tensile stresses close to the support, estimated at 0.83 N/mm^2, being greater than that of the brick. This view has been upheld by other researchers[11,12]. The second beam tested by Thomas had the cross-section shown in Fig. 2.2.1b. The post-tensioned cables were also passed through the perforations and left ungrouted. This beam failed during prestressing from a crack which began immediately behind the anchorage. This was also attributed to excessive principal tensile stress adjacent to the support and the estimated value at failure was 0.62 N/mm^2. The lower principal tensile stress in this second beam resulted from the presence of brick/mortar interfaces in the cross-section which have a lower tensile strength than the brick unit in the first beam.

The tests carried out by Thomas highlighted several difficulties with prestressing masonry:

- Placing the tensioned reinforcement in perforations within the brick restricted the amount and location of the steel. In the above cases, the steel was located outside the 'middle third' thereby introducing tensile stresses due to prestressing. Further, there was no possibility of introducing non-tensioned reinforcement into the section. As it was impossible to grout the perforations containing the stressed steel, problems with corrosion may have resulted. Considerable difficulties were also encountered by the bricklayer in aligning the bricks and keeping the perforations clear of mortar.

- In both beams failure occured in the anchorage zones. To achieve smaller stresses adjacent to these regions Thomas suggested the following: larger-cross sectional areas, units of higher tensile strength and reinforcement in the bed joints to reduce lateral strain in the mortar. The second option might reduce anchorage problems in the first type of beam but will be ineffective in the second beam as it is the brick/mortar interface which controls the principal tensile strength. Alternatively, the use of self-supporting slabs in post-tensioned ceramics to disperse the force over a larger area and the development of new units were advocated.

Another alternative to reducing the anchorage zone stresses is the introduction of vertical reinforcement to the anchorage zone. In the sections considered by Thomas this would have been impractical as these would have

had to be drilled.

In 1965, Plowman[3] also undertook preliminary investigations to ascertain whether ceramics were suitable for post-tensioning and to assess their suitability for floors. In order to exclude tensile stresses due to prestressing, specially manufactured brick units with holes at the middle third position were made. Similar to the first beam tested by Thomas (see Fig. 2.2.1a), these beams were layed as soldiers. The tensile reinforcement consisted of 10 mm diameter mild steel bars threaded through the holes at the third points and left ungrouted. These were tested under a central point load over a span of 3.048 m. The effect of varying the brick strength from 27-55 N/mm^2 and amount of prestress at the soffit from 1.48 N/mm^2-7.72 N/mm^2 were studied. In all 13 beams were tested. Most of the beams failed in flexure by crushing of the compression zone. Plowman however, made no comparisons between the flexural and the compressive strengths. As the tendons were ungrouted, they were free to move. Using the limits of eccentricity, the loads at which normal prestressing theory predicts zero tension at the soffit were determined. Using this load as the design load, a factor of safety of not less than 2.0 was obtained in each case. Two of the beams tested by Plowman did not fail in compression. One of these failed by fracture of the stressing wire close to an anchor grip. The maximum deflection at failure was 108 mm. The other beam also failed in tension and at failure there was a little crushing of the brickwork. The maximum deflection at failure in this case was 152 mm. Thomas's commentary on Plowman's results[3] concluded that failure by fracture of the steel was sudden and complete. However, the load-deflection relationship for the former beam showed large deflections which could only have been caused by yielding of the steel and the authors comments were probably based on the results of the latter beam.

The constructional difficulties encountered here were similar to those described above for Thomas' sections. Also, most of the limitations imposed by placing the tensioned steel in the ungrouted perforations were also present here. In addition, the use of specially manufactured units to accomodate the reinforcement can be an expensive solution. Among the comments made were that: ceramics could be prestressed satisfactorily, post-tensioned ceramics behave in a manner similar to concrete beams and that shear failure was not a major concern. However, the last comment was probably made from comparisons with reinforced brickwork. Another important comment made was

the possibility of introducing shear reinforcement adjacent to the anchorages to solve the problem of anchorage zone failure.

In 1965/66, Ng[3] also carried out preliminary tests on three post-tensioned hollow clay block beams. The blocks used in this investigation were cheap and light-weight when compared with other building materials and the possibility existed of a new ceramic flooring system resulting from this investigation. As difficulties had been experienced by Thomas and Plowman in their investigations using traditional mortars, Ng decided to bond the ceramic units with thin joints using epoxy resin as the bonding agent in the hope that this material would exhibit a smaller lateral strain and hence delay tensile splitting of the ceramic, thus permitting much larger forces to be applied along the beam axis. The cross-section of the blocks used are shown in Fig. 2.2.2. Each beam was prestressed with 5 mm plain wires. The prestressing force was either 36 kN or 45 kN and the section was grouted after stressing with a sand/cement mix. The beams were tested under four point loading over a span of 3.048 m with the point loads at third points. All three beams failed by yielding of the steel which was followed by crushing of the compression zone. Based on the load at decompression, an average load factor of 3.5 was obtained. As a direct result of this investigation, a British patent was taken out on a pre-stressed ceramic flooring system.

In 1970, Mehta and Fincher[20] carried out tests on five prestressed grouted masonry beams. As well as exploring the feasibility of fabricating prestressed grouted cavity brickwork beams, the aim was also to study their structural behaviour under load. The variables considered were the coursing pattern and the magnitude of the prestressing force. The beams were fabricated by laying a brickwork shell in a 'U' configuration (See Fig. 2.2.3), stressing the strands in the cavity and grouting the cavity. The cross-section of these beams overcame most of the constructional difficulties encountered in the sections described above.There was much more flexibility in the position and amount of tensioned reinforcement, and the grouting of the cavity was facilitated. However the grout constituted at least 25% of the cross-sectional area of the beam and because of its location (see Fig. 2.2.3) contributed significantly to the behaviour of the beam at all stages of loading. Only tensioned steel was provided which consisted of three 10 mm diameter seven-wire stress-relieved strands in each beam. The prestressing force was either 187 kN or 94 kN. The beams were tested under concentrated loading over a span of 1.83 m. These

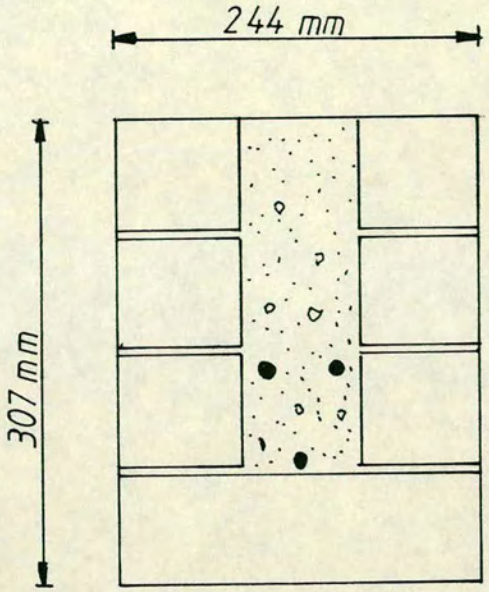

Fig. 2.2.3 Typical Section of MEHTA and FINCHER[20]

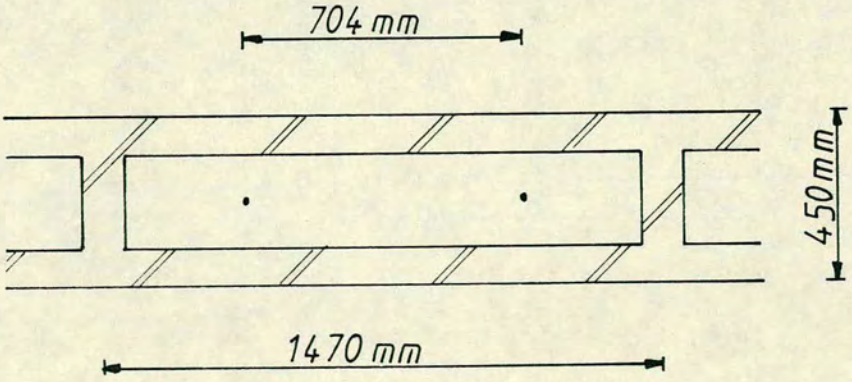

Fig. 2.2.4 Plan of Diaphragm Wall Tested by Curtin and Phipps[21]

beams showed remarkable recovery on the removal of load. The percentage recovery on the second loading cycle was generally above 95% except in one case when 78% recovery was obtained. This was considered by Mehta and Fincher[20] to be indicative of the excellent bond between the grout and the brickwork shell so that the grout and brickwork could be considered to act as a unit.

The work of Mehta and Fincher[20] showed a large discrepancy between the measured deflections when compared to those calculated using the strength of materials approach. The ratio between the measured and calculated values were between 1.46 and 2.36 for the uncracked beam. No explanation was given for this discrepancy. In the opinion of the author, this discrepancy was probably due to two reasons; firstly, the modulus of elasticity was that derived from stack-bonded brickwork prisms which were not representative of the cross-section of the beams under test. The brickwork beams in these tests were not stressed normal to the bed joint and as brickwork in an anisotropic material, the properties of a prism stressed normal to the bed joint will not adequately reflect the properties of the beam. Secondly, the properties of the brickwork shell and concrete grout were assumed to be the same while these may have been quite different. The coursing pattern was found to have no effect on the deflection of the beams.

All the beams tested in this work failed in shear and diagonal tension. The picture of a typical crack at failure showed a stepped crack in the shear span travelling towards the support. There was also a horizontal propagation of this crack towards the loading point once it reached the top bed joint. The ultimate shear capacity was calculated using modified equations for prestressed concrete given by the ACI code. Inspite of the simplifying assumptions made in applying this formula to prestressed masonry namely; ignoring the self weight, assuming that the masonry and the grout had the same modulus of elasticity and neglecting losses in the prestressing force, the ratio of the measured shear strength to that calculated was between 0.78 and 1.21. The coursing pattern of the bricks was found to have no effect on the shear strength. However, there was no significant variation in the coursing pattern of the beams tested as the orientation of the bricks in all beams were such that there was at least one bed joint parallel to the horizontal axis of the beam. The ultimate flexural strength of the prestressed masonry beams were also calculated using the ACI Building code. Although none of the beams failed

in flexure, in three cases, the actual ultimate moments were higher than the calculated flexural moments.

In 1982, Curtin and Phipps[21] reported the results of experimental work carried out on two full sized prestressed brickwork diaphragm walls each 7.62 m high x 7.62 m long x 0.45 m overall width (see Fig. 2.2.4). Each wall was prestressed with ten 40 mm diameter Macalloy bars. The walls were built side by side on a common reinforced concrete foundation and an air bag was placed between them to apply lateral load. The walls were pinned together at the top and were therefore assumed act like propped cantilevers. There was however, no experimental verification of this assumption. In the testing of one wall, the other was heavily post-tensioned to act as a reaction frame. The variable considered was the level of axial prestress which was increased from 0-1.38 N/mm^2 and each wall was tested to the serviceability limit which was considered to be reached at the plastic critical load (when an increase in the volume of air in the air bag produced no increase in side pressure) or when in the interest of safety, a predetermined or calculated side load was reached (elastic critical load). The walls were not tested to ultimate as this was considered to be dangerous because of falling masonry.

As expected, the results of the test showed that the load at which cracks developed was increased by the amount of prestress. A simple theory based on the elastic theory was proposed which predicted the cracking or serviceability loads accurately at all levels of prestress. The results also showed that even after cracking, prestressed diaphragm walls have a considerable in-built fail-safe capacity.

Other works which have been carried out to establish the behaviour of prestressed diaphragm walls have been carried out on beams. This is because, although full sized walls can be easily tested under side loads up to the first tensile cracking, testing to collapse, because of falling masonry, can be dangerous especially if the wall is large. It is however simple and safe to test horizontally spanning beams on the laboratory floor. By considering a diaphragm wall as a series of box or I sections (see Fig. 2.2.5) it is possible to test just a single section as a horizontal I or box beam. Several researchers[22,23,24] have adopted this method. A majority of these beams were prestressed with unbonded tendons. This was probably due to practical difficulties in grouting the tendon. Most of the unbonded beams were also

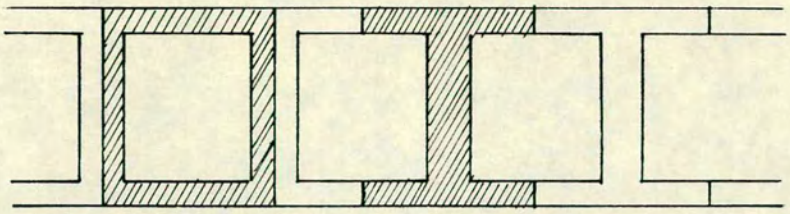

Fig. 2.2.5 Plan of Diaphragm Wall as a Series of Box and I Sections

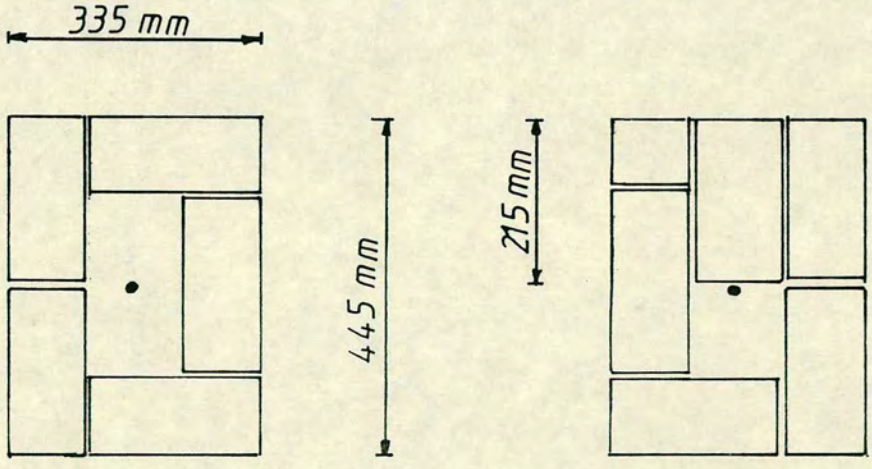

(a) Without Cross-ribs (b) With Cross-ribs

Fig. 2.2.6 Beam Sections of WILLIAMS and PHIPPS[22]

prestressed along the centroid. Although this is necessary in cases in which the lateral loads are subject to reversal, for example wind loading, the same prestressing force applied eccentrically can produce twice the amount of prestress when compared to an axially applied prestressing force.

Tests on six full-sized post-tensioned prestressed masonry box beams were reported by Williams and Phipps[22] in 1982. The main purpose of the test was to formulate design rules for the ultimate flexural limit state of prestressed diaphragm walls. As mentioned above a diaphragm wall can be considered to be a series of vertically spanning box beams and its collapse load can therefore be estimated from tests to failure of individual horizontally spanning masonry box beams. A secondary consideration was to establish whether the addition of cross-ribs to maintain the position of the tendon could be advantageously used in such walls. For this purpose 4.8 m long masonry box beams with cross-sections shown in Fig. 2.2.6 were tested under four point loading. The tensioned reinforcement consisted of a 40 mm diameter Macalloy high tensile steel bar. At three levels of prestress, between 1.1 N/mm^2 and 2.79 N/mm^2, two beams were tested, one with and the other without cross-ribs. In order to obtain a preliminary idea of the strength of the compression zone, as well as testing 215 mm x 215 mm x 4 course high standard prisms, five hollow box section prisms identical in section to those of the beams and of various heights 290 mm (h/t = 0.87) to 1500 mm (h/t = 4.48) were tested under axial compression. The results of these tests showed that there was a general increase in the load carrying capacity of a prism with decreasing height. The minimum compressive strength, obtained from the tallest specimen, was 7.2 N/mm^2, which was in good agreement with that obtained from the code (B5 5628[1])of 8.5 N/mm^2. Five of the six beams tested failed in compression by crushing of the masonry in the compression zone. The sixth beam, which contained the highest prestressing force, failed as a slender column - by buckling. The presence of the cross-ribs was found to increase the ratio of the ultimate moment to that at first cracking. Also the ultimate moment capacity was found to be increased by between 1.5 and 3.0 times by the presence of cross-ribs.

In the formulation of the theory it was assumed that the strain distribution in the tensioned reinforcement was of the same shape as the bending moment diagram although no experimental evidence was given to support this assumption. Similarly without experimental verification it was

assumed that the movement of the tendon in beams without cross-ribs was equal to the deflection. An empirical relationship between the steel stress and the neutral axis depth was derived from the experimental results. Of a total of six results, two showed considerable variation from this relationship. By consideration of the equilibrium of the tensile and compression forces, the neutral axis depth at failure was derived from the empirical relationship from which the ultimate moment could then be calculated. Although the proposed method appeared to be in good agreement with the experimental results within the range of beams tested, a more representative relationship between the steel stress and the neutral axis depth is required and also, conditions which result in buckling failure need to be identified.

In 1983, Roumani and Phipps[23] presented the results of tests carried out on 15 prestressed I and T shaped sections (See Fig. 2.2.7). The main aim of this work was to formulate design proposals for the shear strength of brickwork sections at cracking and collapse. The experimental work studied the influence of the shear span to effective depth ratio (a/d) (0.8 to 4.5), the depth (665 and 440 mm) and shape of the section (I or T), the amount of prestress (0.5 to 3.0 N/mm^2) and concentric and eccentric prestress on the behaviour of this type of beam. The prestress was applied through 40 mm unbonded Macalloy bars placed at the sides of the webs and anchored to the ends of the beam (see Fig. 2.2.7). All the beams tested failed in shear and four types of shear failure, dependent on the a/d ratio, were identified. These types of shear failure were different from those reported in the bonded beams tested by Mehta and Fincher[20].

A lower bound equation for the principal tensile stress at failure was obtained from the experimental results with the effect of low a/d ratios on enhancing the principal tensile stress being taken into account. An expression for the diagonal cracking load of beams based on the principal tension theory was developed. An empirical formula was also presented for the ultimate shear strength. This was dependent on a relationship between the average stress in brickwork due to prestress and the notional stress in the brickwork at failure due to the ultimate force in the tensioned steel. A comparison between the theoretical results and those obtained from the theory showed a great deal of overconservatism in some cases.

On the basis of the test results obtained in reference 23 Roumani and

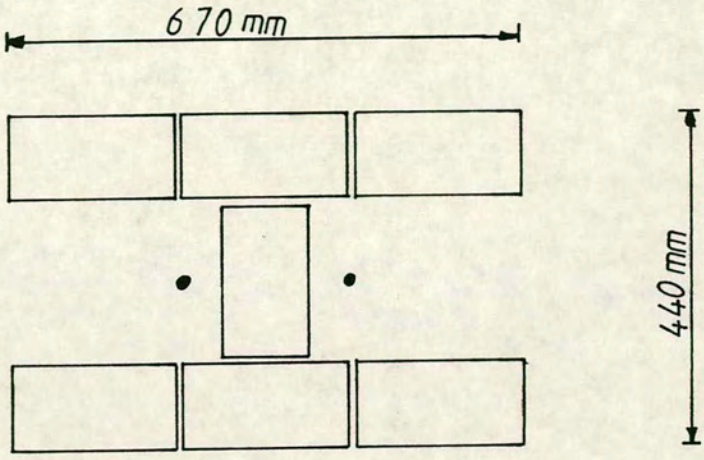

Fig. 2.2.7 Typical Section of ROUMANI and PHIPPS[23]

Phipps[24] in 1986 proposed a method for determining the ultimate shear strength of prestressed brickwork I and T section simply supported beams. The shear capacity at ultimate was assessed on the assumption that the ultimate limit state in shear was reached when diagonal cracking occurred. For a beam which was uncracked in flexure before diagonal cracking, the ultimate shear strength, as in reference 23, was obtained from the principal tension theory assuming linear elastic behaviour. The principal tensile strength was also obtained from a lower bound equation to experimental results but in this case, the influence the overall depth of the section has on reducing the principal tensile strength as well as the effect of the M/VD (a/d) ratio were taken into account. For a beam which was already cracked in flexure before the formation of a diagonal crack, it was assumed that after flexural cracking, the beam is effectively transformed into a tied arch so that the increase in the tendon force is the same at all sections along the beam. Further, it was assumed that the tied arch behaviour of the beam was still linearly elastic so that the magnitude and distribution of the stress in the critical positions in the beam where diagonal cracks will begin to form can be predicted by elastic beam theory. The inclined cracking load of a beam already cracked in flexure was therefore obtained by modifying the expression for the beam uncracked in flexure before diagonal cracking to account for the increase in the stress in the tendon. The relationship between the applied load after flexural cracking and the tendon force was obtained from the assumption that the post-flexural cracking behaviour was essentially that of a three pinned arch. The resulting relationship between the shear force and the tendon force appeared to be in agreement with experimental results. This relationship however ignored the depth of the compression zone by assuming that the lever arm was equal to the depth of the section as the compression zone in prestressed members is quite small. A major shortcoming of the above theory, however, is the assumption of linear elastic behaviour after flexural cracking which is in contradiction with observed experimental observations (see the work of Montague and Phipps[25] below).

Montague and Phipps[25] carried out tests on twelve post-tensioned blockwork box sections in order to study the behaviour of post-tensioned blockwork diaphragm walls under bending moments and shear forces. The effect of different bonding patterns and different levels of prestress were considered. The beams were tested to failure in flexure under four point

loading. After failure, the undamaged ends were tested over short shear spans to observe their behaviour under high shear force. Each beam was prestressed with a 20 mm Macalloy bar. Each bar was placed along the centroidal axis of the beam and the bars were unbonded. In some beams however, the tendons were restrained with cross-ribs. Reinforced concrete blocks were used to transfer the prestressing force from the bar into the beam. In the twelve beams tested, the prestressing force varied from 48-186 kN. The compresssive strength of the beams were obtained from box prism tests.

The load-deflection curves for all beams were initially linear until cracking. Thereafter, the behaviour of the beams were non-linear. Under four point loading, all beams failed in bending by crushing of the blockwork. Among the factors which were found to affect the ultimate moment were the form of construction (bonding pattern) and restraining the tendons. In the latter case the flexural strength increased by up to 39% in keeping with the results of Williams and Phipps[22]. In order to compute the ultimate moment, the bond factor was obtained from the strain profile at a critical section. It was taken as the ratio of the block and steel strain at mid depth. The relative tendon movement was assumed to be equal to the maximum beam deflection, although this was not checked experimentally. Further, the compressive stress at failure was assumed to be 1.2 f_k where f_k is the compressive strength of box prisms identical in cross-section and size to that of the beam. The average value for the ratio of the experimental to theoretical moment was 1.22. When tested under a point load over short shear spans, the mode of shear failure was found to be dependent on the bond pattern and the level of prestress.

A major difference exists between the work of Curtin and Phipps[21], Williams and Phipps[22], Roumani and Phipps[23,24] and Montague and Phipps[25] described above and of those carried out by Robson[26], Pedreschi[11,27] Walker[12,28] and Garwood[13,14,29] which are described below. In the first cases, the function of the prestress is to neutralise the tensile stresses induced in walls due to lateral loading from wind or retained loads. The wall still carries load primarily in compression. In the latter cases the prestress assists in a member in which the load is carried primarily in bending. Also apart from the beams tested by Pedreschi[11,27] and Walker[12,28], the end anchorages or end blocks covered most or all of the beam cross-section. Therefore as the beam deflects, the upper portions were subjected to compression along the beam axis as a result of deflection from the end anchorages.

Between 1980 and 1983, an extensive study was carried out by Pedreschi[11,27] into the behaviour of bonded post-tensioned brickwork beams. In all 51 beams were tested containing tensioned reinforcement only. The span varied from 1.75 m to 6.2 m and the beams were tested under four point loading. The aim of this work was to study the effect of the brick strength, mortar grade, steel area and prestressing force and the shear span/effective depth ratio on the deflection, cracking and ultimate load. The cross-sections of the beams tested are shown in Fig. 2.2.8. Unlike the sections tested by Mehta and Fincher[20], the grout occupied only 10% of the total cross-sectional area and did not contribute to the ultimate load of the beam. Also, unlike the sections used by Thomas[3], and Plowman[3], fabrication was relatively easy and there was relative flexibility in the location and amount of tensioned steel. The tendons were grouted into the beam section and thus adequate protection of the reinforcement against corrosion was achieved.

The compressive stresses in the beams tested by Pedreschi develop parallel to the bed joint. In the most common brickwork member, walls and piers, the compressive stresses develop normal to the bed joint. The properties of brickwork are thus given in respect of the latter direction of loading. As brickwork is an anisotropic material, as part of this study Pedreschi[11,30], carried out a comprehensive series of tests on prisms in order to obtain the properties of brickwork when stressed parallel to the bed joint. These results led to an expression for the stress-strain relationship for brickwork parallel to the bed joint[30]. Using the non-linear stress-strain relationship, obtained for brickwork parallel to the bed joint, the ultimate flexural moment was predicted from the flexural theory. The deflection and crack widths were also predicted using the actual stress-strain relationship of the brickwork and tensile reinforcement.

In order to study the effect of the shear span to effective depth ratio (a/d) on the behaviour of prestressed brickwork beams 15 beams were tested with a/d ratios between 2.0 and 11.21. Two types of shear failures were observed and these were dependent on the a/d ratio. For beams with low a/d ratios, failure occurred by crushing of the brickwork along a line joining the support and load point. In the beams with the higher a/d ratios, there was a step-wise propagation of cracks towards the support. In the direction of the load point, on reaching the top bed joint, the diagonal crack travelled along the bed joint towards the load point. The latter type of shear failure was akin to those

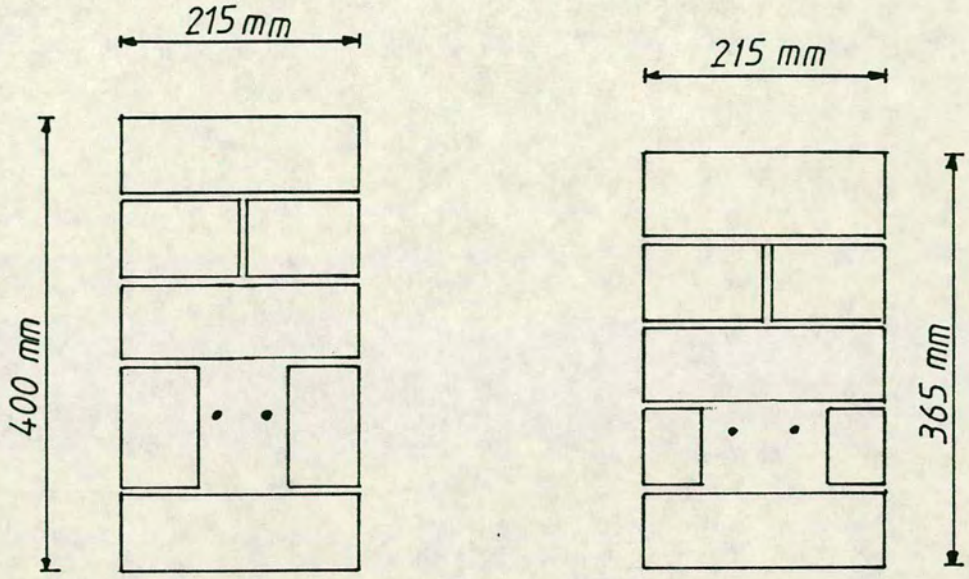

Fig. 2.28 Beam Sections of PEDRESCHI[11]

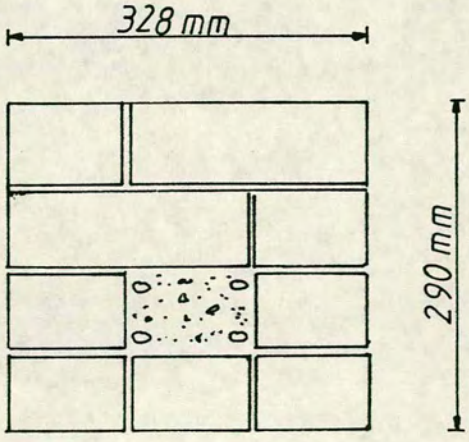

Fig. 2.2.9 Beam Section of ROBSON et al[26]

observed by Mehta and Fincher[20]. The shear strength was predicted using the plastic theory in conjunction with experimental results. The properties of the single course prisms were used in the determination of the shear strength even though the neutral axis depth at failure in the beams failing in shear was greater than the thickness of the single course prism. In the determination of the shear strength, no distinction was made between the beams with the high and low a/d ratios inspite of the observed different modes of failure. This is the only attempt which has been made to study the shear strength of bonded prestressed brickwork beams.

Some of the beams tested by Pedreschi[11] contained shear reinforcement. These consisted of single rods which were grouted into holes drilled in the brickwork. This construction procedure highlighted the difficulties involved in introducing shear reinforcement to brickwork members. All the beams tested by Pedreschi[11] contained tensioned steel only and the benefits of supplementing the tensioned steel with non-tensioned steel especially with regards to reducing anchorage zone stresses were not considered. Also, in the cross-section of these beams, it would have been difficult to accomodate non-tensioned steel.

Robson et al[26] in 1983, reported the results of tests carried out to study the behaviour of eighteen post-tensioned brickwork beams. The cross-section of the beams is shown in Fig. 2.2.9. As the section was post-tensioned after grouting, the tendons remained unbonded. The construction procedure was very complicated and involved three separate building operations. The variables considered were the percentage area of steel, the prestressing force and the a/d ratio, the last variable being between 2.74 and 5.48. Five of the six beams with the highest percentage area of steel failed in compression by crushing of the brickwork. The sixth beam failed in shear. All the other beams failed in tension. The compressive strength and elastic properties of the brickwork were obtained from prism tests. The ultimate moments obtained experimentally were compared with those obtained using the values for the compressive strength of brickwork and the stress block recommended by the code[1]. The experimental values for the compressive strength of brickwork were also used in the analysis. The best correlation with experimental results were obtained using the experimentally obtained compressive strength of brickwork. The ultimate moments in these cases was under-estimated by as much as 25% for the beams which failed in tension. A better comparison was

obtained for the beams which failed in compression. This was because the prisms tested represented the entire cross-section of the beam. In the beams which failed in tension the depth of the neutral axis was very small and could not be represented by the prisms. In the beams which failed in compression however, the depth of the neutral axis was larger and the compression zone was better represented by the prisms.

Using the experimental values for the elastic modulus gave a good agreement with experimental results. However, using the code value gave large overestimates. This was because the code value for the modulus of elasticity was obtained from stack bonded prisms loaded normal to the bed joint. In these beams however, the compressive stresses developed parallel to the bed joint.

In 1983, Garwood[13] carried out tests on bonded prestressed brickwork beams. Four post-tensioned beams were tested with different bonding arrangements and amounts of tensile reinforcement. Some of the beams also contained non-tensioned steel. Some of the beams tested by Garwood had the same cross-section as those tested by Robson et al[26] and the associated complicated construction procedure (see Fig. 2.2.9). The cross-section of the other beams tested by Garwood are shown in Fig. 2.2.10. These were constructed from a series of short 'pre-built piers'. One of these beams also contained stirrups. In each beam, the prestressing force was provided by a Macalloy bar which was grouted in after post-tensioning to form a bonded beam. The maximum compressive stress induced by the prestressing force as 5.48 N/mm^2. The tests were carried out under two point loading at third points over a span of 3.546 m. The compressive strength of the beams was obtained from prisms loaded so that the direction of stress, relative to the bricks, was the same as that at the top of the beams under test. Although all the beams failed in flexure by crushing of the brickwork in the compression zone, the increase in shear strength which can be obtained by prestressing was demonstrated by comparison with similar reinforced brickwork beams. The stresses in the tensile reinforcement were obtained indirectly from moment compatibility and could therefore only be approximate. Also, a parabolic stress-strain curve was assumed for brickwork in which the strain at the peak stress was taken as 0.0022. There was however no experimental verification of this assumption.

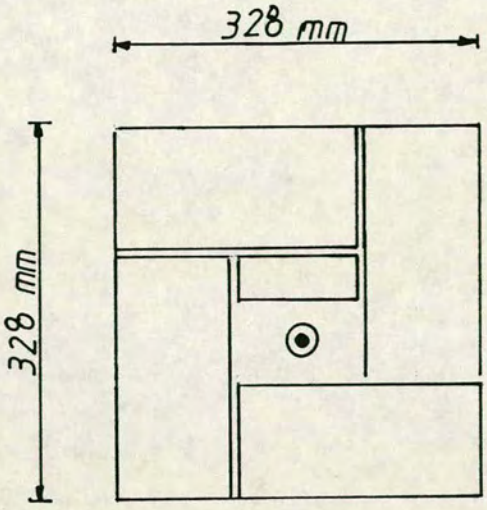

Fig. 2.2.10 Beam Section of GARWOOD[13,29]

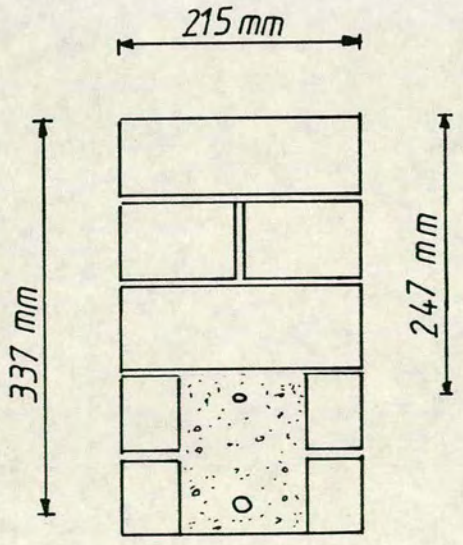

Fig. 2.2.11 Beam Section of WALKER[12]

Between 1983 and 1987, Walker[12,28] carried out a study into the behaviour of partially prestressed brickwork beams containing tensioned and non-tensioned reinforcement. The effect of the percentage area of steel, the prestressing force, the partial prestressing ratio, the cover to the non-tensioned steel, the brick strength and the strength of the mortar on the ultimate moment, deflection and cracking were studied. The cross-section of the beams is shown in Fig. 2.2.11. This was similar to the section adopted by Pedreschi[11,27] but was modified to accomodate the non-tensioned steel close to the soffit where its presence is most beneficial; increasing the lever arm of the resultant tensile force and thus the ultimate moment, and better crack control. The grout in this case occupied 18% of the cross-sectional area and did not contribute to the ultimate moment. The construction and grouting processes were much more simplified when compared to the sections tested by Garwood[13], Robson et al[26] and Pedreschi[11,27]. A total of 41 beams were tested by Walker. This was accompanied by a large number of prism tests conducted under axial and eccentric loading to obtain the compressive properties of brickwork in which the compressive stresses develop parallel to the bed joint. An interactive computer program was developed based on the direct method, which used the experimentally obtained material properties to predict flexural behaviour i.e ultimate flexural moment, deflection and cracking. The computations allowed for the presence of the grouted cavity and the stiffening effect of the brickwork and concrete between cracks after cracking. This program was however incapable of predicting a shear failure or the ultimate moment in shear.

Of the 41 beams tested by Walker, 37 failed in flexural tension of which 12 subsequently exhibited secondary shear failure. Four of the beams failed primarily in shear. In all the beams which failed in primary or secondary shear, there was a horizontal propagation of the diagonal crack which developed in the shear span towards the loading point. Inspite of the fact that 39% of the beams tested by Walker exhibited some kind of shear failure, no attempt was made to study the shear strength of partially prestressed brickwork beams either experimentally or theoretically or to identify the conditions which lead to shear failures in partially prestressed brickwork beams.

Following the work of Walker[12,28], Garwood[14] in 1984 also carried out tests to compare the flexural behaviour of three fully prestressed and partially prestressed 'pier-bond' brickwork beams. The beams and test conditions were

similar to those described above in a previous work by the author[13]. The prestressing steel was supplemented where necessary by non-tensioned steel in the tensile zone so that the flexural strength of the beams were practically the same. The depth of the cavity in each case was such that the tensioned and non-tensioned steel were placed at the same level. The advantages to be gained in placing the non-tensioned steel close to the soffit with regards to increasing the ultimate moment and a better control over cracking were thus not exploited. The prestressing force was applied through 20 or 25 mm Macalloy bars. The loss of prestress before testing was not measured but estimated using an empirical method. As in the previous work carried out by Garwood[13] (described above), the stresses in the tensile reinforcement at failure were obtained by moment compatibility. All the beams failed in flexure by crushing of the brickwork in the constant moment zone. However, comparing the behaviour of all three beams highlighted the increased shear strength which can be obtained by prestressing - the beam with the least amount of prestress was close to shear failure.

As an extension to the work carried out in reference 14, Garwood[29] also reported tests on 11 reinforced, partially and fully prestressed beams. Two series of beams each consisting of at least four beams with varying degrees of prestress and at least one conventionally reinforced beam were tested. The beams in each series had practically the same flexural capacity. A different bonding arrangement was used for each series - stretcher-quetta bond (see Fig. 2.2.9) and pier bond (See Fig. 2.2.10). As in the previous tests carried out by Garwood[13,14], the test performance of the beams were assessed with regard to serviceability and ultimate capacity but in this case, the shear strength was also of particular interest. The amount of prestress and the bonding pattern was found to influence the shear strength. Increasing the amount of prestress increased the shear strength. Comparing the two types of bonding arrangements, the test results showed that those built in pier bond had the superior shear strength; this was attributed to the presence of continuous bed joints which act as planes of weakness causing splitting failures in the stretcher-quetta bonded beams. In these beams, the diagonal crack which preceeded shear failure had a shape similar to those observed in Mehta and Fincher's[20], Pedreschi's[11] and Walker's[12] beams which failed in shear i.e. a step-wise propagation towards the support and a horizontal propagation along the bed joints towards the loading point. Garwood[29] obtained the principal

tensile stresses for the beams tested from the Mohr's circle calculation for a mid-depth element of uncracked beam close to the support at failure. Based on the test results, it was proposed that the shear design for the uncracked length of a beam should be based on limiting principal tensile stresses.

Flexural failure occurred in the beams with higher prestress by crushing of the brickwork in the compression zone. As with the previous works carried out by Garwood[13,14], the tensile stresses were not measured but obtained from moment compatibility. Again, a parabolic stress-strain relationship for brickwork was assumed. The ultimate flexural moment was calculated by using the strain compatibility method. Although the actual stress-strain curve for the steel was used, the average brickwork stress was assumed to be 0.6 times the prism strength with the centroid of compression being located at 0.4 times the neutral axis depth from the top of the beam. The ultimate brickwork strain was taken as 0.0035.

In order for prestressed masonry to continue to function efficiently over a long period of time, there should be no significant prestress losses and those that do occur should be accounted for at the design stage. Work on prestress losses in prestressed brickwork reported in the literature was carried out by Lenczner and Davies[31,34] and Lenczner[33]. Lenczner and Davies[31] carried out tests to measure the loss of prestress in post-tensioned brickwork walls and columns and the factors which influence this loss. The effects of different brick strengths, amounts of initial prestress and geometry of the specimens (walls and columns) were studied. Higher percentage losses were observed in the lower strength bricks. Also, columns were found to suffer less loss when compared with walls, but in the former, losses ocurred over a longer period of time. Theoretical estimates of the prestress losses were obtained from a guide for predicting creep in unreinforced brickwork walls and columns which was proposed earlier by Lenczner[32]. This method is however based on a constant applied stress which is not the case in post-tensioned members as the stress drops off due to creep, shrinkage and relaxation of the steel. Reasonably accurate results can however be obtained if the loss of prestress is not great. In the results reported in this reference, the maximum difference between experimental and theoretical results was 6%, with the theory underestimating the losses.

Among the results reported by Lenczner[33] in 1985 were the results of

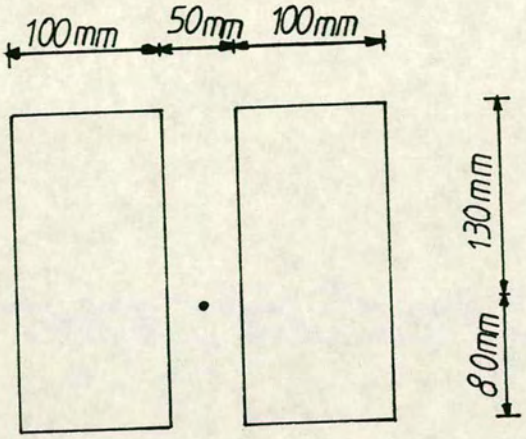

Fig. 2.2.12 Beam Section of LENCNER [33]

tests carried out on the loss of prestress and creep deflection in a post-tensioned brickwork beam (see Fig. 2.2.12). The beam was post-tensioned with a 25 mm Macalloy bar at an eccentricity of 25 mm. The beam was unbonded and monitored over a period of 1 year. The results showed that the loss of prestress was quite rapid during the first 50 days and was down to just over 90% of the initial value. Thereafter, the rate of loss of prestress decreased quite suddenly and continued at a fairly steady rate so that after 1 year, the retained prestress was about 88%. The loss in prestress was of the same order as had been obtained in walls and columns[31]. The ratio of the creep deflection to the initial deflection was 0.35. The absence of a relationship for the creep ratio in beams prevented a comparison with theoretical results as was carried out for walls and columns.

More recently, Lenczner and Davies[34] have carried out tests on two post-tensioned brickwork walls in order to investigate the creep and loss of prestress in members which have been previously prestressed for some length of time and have subsequently been post-tensioned to a higher stress level. This information can be of importance when an existing structure requires alterations e.g. to take advantage of the higher allowable stress levels in the current code of practice. It was concluded that there was a change in the behaviour of prestressed brickwork walls post-tensioned for the first time and those with a previous stress history. Creep and loss in prestress were substantially less in walls with a previous stress history. For example, in the tests described, creep after the second prestress had virtually ceased after 100 days compared with approximately 1 year after the first prestress. Walls with a previous stress history showed a loss of prestress of about 1/8 of those which have been post-tensioned for the first time even when the second prestress level exceeded the first.

2.3 PRACTICAL APPLICATIONS OF PRESTRESSED MASONRY

As a result of the high compressive and low tensile strength of masonry, its most common application has been in structures loaded mainly in compression such as walls. It is not surprising therefore that the most common practical application of post-tensioned masonry to date has been in

the vertical stabilization of laterally loaded walls and similar structures. In these type of structures, the precompression replaces the load that would normally be applied by the self weight of the structure above. Most of the following are examples of this application.

In 1966, Neil[16] reported the construction of the external walls of a factory in Darlington using post-tensioned brickwork as a means of providing lateral stability. The walls were 7.3 m high. The building frame work was generally of high tensile steel and as part of the steelwork contract, high tensile steel rods were provided to hang from the high level fascia beams. These were built into the foundations and lightly tensioned after threading on to them the special steel spacer plates which were later built into the brickwork skins. The steel rods were post-tensioned concentrically through the flange of the beam and a maximum prestress of 0.7 N/mm^2 was applied. After prestressing, the steel facia beams were welded to steel columns designed to carry vertical loads. Post-tensioning enabled a 280 mm cavity brickwork solution which would otherwise have had to be of the order of 460 mm solid brickwork construction. Also the need for intermediate framing or buttressing was eliminated. According to Neil, the cost of the wall including tensioning was comparable to an additional 115 mm of brickwork.

In 1971, Foster[15] reported the design and construction of a prestressed water tank. This application of post-tensioned brickwork is a departure from the above and all other applications, but one, which will be described in this section. A brick factory using butane gas for firing its products required a 120,000 gal. capacity water tank. Foster's solution was a vertically and circumferentially prestressed brickwork tank, 12.2 m in diameter and 4.9 m deep. The actual bonded thickness of the tank was 229 mm. The solid bricks were layed in flemish bond. This provided vertical spaces at intervals of 172 mm for the vertical reinforcement. Due to the high hydraulic head at the base of the tank, a water proof render was applied to the internal surface of the tank. An external decorative skin of 114 mm thick brickwork provided external shuttering for a grouted cavity which contained the circumferantial tensioned reinforcement, providing an overall wall thickness of 394 mm. The vertical and circumferential tensioned reinforcement were provided by 7 mm dia wires. The vertical precompression was 0.85 N/mm^2 and the circumferential prestress was 2 N/mm^2.

In 1982, Curtin et al[17] reported on the construction of a hall for religious services. The dimensions of the main hall was to be 25 m long x 15 m wide x 8.5 m high. Though these dimensions were by no means exceptional, the top of the wall could not be propped because the client and architect wanted a clerestory window running round the top of the wall. Additionally, the plane of the roof was not constant. Although an ordinary brickwork diaphragm wall was known by the authors to be capable of catering for such a structure as a propped caintilever, the four fold increase in moment as a free cantilever was beyond its capabilities. The economic solution but for the ongoing research on post-tensioned diaphragm walls was the incorporation of a steel frame with cladding. Nevertheless, the satisfactory results which had so far been obtained at the time of the preliminary design stage encouraged the adoption of a 665 mm thick post-tensioned diaphragm wall solution. The diaphragm wall was post-tensioned with two 32 mm diameter concentrically located Macalloy bars per section introducing a compressive stress of 0.5 N/mm^2 at transfer. These were anchored to the raft foundations. The tensioning force was applied through a torque wrench. At the top of the wall the anchorage was embeded into a precast concrete capping beam. Adequate protection to the Macalloy bars were provided with denso paste and tape.

In 1982, Bradshaw et al[35] described the conception and construction of a post-tensioned diaphragm wall in a multi-purpose farm building. This example of the application of prestressed masonry highlighted other desirable aspects of brickwork as a construction material. The overall size of the building was 30 m square on plan and was required to retain crops such as carrots, potatoes and grain and to provide various workshop facilities. Traditionally these buildings are constructed as steel portal frames with asbestos cladding above traditional galvanised steel grain walling. This form of construction was known to have several drawbacks. These included problems with the long term maintenance of steel galvanised grain walling due to acid attack from stored materials (carrots and other high sugar content crops), the difficulties in using acid solutions to sterilize the surfaces and the cleaning out of such buildings between crops, particularly around the stanchions which can lead to hygiene and infestation problems. Also, in these forms of construction, the stored crops are susceptible to frost attack through the thin steel walling. Such buildings also have an unattractive appearance and can be draughty between crops when used for other purposes. The post-tensioned diaphragm wall

proved to be a solution to the above problems and also gave advantages of its own. Construction in a dense, high strength acid resistant brick removed problems of acid attack from stored crops and cleaning solutions and also provided a design life far in excess of steel grain walling with less maintainance inspite of its higher initial cost. Brickwork also offered a greater resistance to frost penetration, easy cleaning of the smooth interior faces and an aesthetically pleasing appearance. The solution adopted was a steel portal frame supporting the roof and partial side cladding and post-tensioned brickwork vertical free cantilever walls to retain the stored crops acting independently of the steel portal frame.

The tensioned reinforcement was a high strength precision tie 18 mm in diameter loaded with a torque wrench. The total height of the wall was 2.4 m with an overall thickness of 777 mm. Cross-ribs were provided at 1.3 m intervals. Because the lateral loading was due to retained crops which is not subject to reversal, the tendons were placed as close to the retaining face as was allowed by the section properties without inducing tension under the prestresing loading alone. The maximum tendon force was 45 kN and the maximum compressive stress in the brickwork was 0.3 N/mm^2.

Also in 1982, the George Armitage Head Office in Wakefield was awarded The Structural Brickwork Award[36]. This was a two storey building and incorporated a storey height post-tensioned brickwork wall and post-tensioned twin fin piers. The post-tensioned storey height wall contained Macalloy bars located at intervals within a grouted cavity. The bars were sheathed in plastic ducts to permit free movement during post-tensioning and were therefore not bonded to the brickwork section. The bars projected through the roof slabs into the parapet, which was also of brickwork, where they were tensioned by tightening anchor nuts with a calibrated torque spanner. A prestressing force of 100 kN was applied which induced a maximum compressive stress in the brickwork of 1.7 N/mm^2 based on the net area of brickwork only. The piers were also post-tensioned with a Macalloy bar sheathed in a plastic tube in a grouted cavity. The bars were anchored in the foundation ring beams and terminated at the parapet level above a reinforced concrete pad which distributed the compressive stress over the total brickwork area. The bars were tensioned by tightening anchor nuts to 90 kN, giving a precompression in the brickwork of 1 N/mm^2, ignoring the grout in the core.

The Oak Tree Lane Community Centre in Mansfield, Nottinghamshire[37] was awarded a certificate of merit in 1982 by the Brick Development Association. The adoption of post-tensioned brickwork diaphragm walls provided a solution to the problems created by mining subsidence. Post-tensioning rods were introduced into the walls and anchored into the raft foundation. These were tightened down over steel spreader plates bearing on in situ concrete ring beam at the tops of the walls, to a calculated torque. The effect of the torqued rods was to cause the raft foundation and the diaphram walls to act compositely, thus providing greater stiffness and much increased resistance to the induced tensile stresses. The structure has successfully sustained the driving of a series of mine shafts, with the accompaning wave of settlement totalling over 1 m and differential settlements of over 125 mm.

In the design of the Rushden Fire Station[38], lateral stability was required for the upper portion of a wall 4.5 m high (total height of the wall was 9.5 m) exposed to wind loading. The required stability was provided by totally anchoring the unsupported portion of the tall wall and the roof load on the shorter adjacent external wall. The taller wall was designed as an unreinforced wall spanning between the upper and lower chord members of the roof structure. The roof was then designed not only for the normal loads but also for the compression force required to prop the wall. The smaller wall was designed to resist not only the wind force, but also a point load at roof level (i.e at capping beam level) equal to the propping force transferred to it from the taller wall through the roof structure. A 440 mm unreinforced brick diaphragm wall was adopted for the tall wall and a 440 mm thick post-tensioned free-cantilever for the short wall (height 5.0 mm). A prestress of 1 N/mm^2 was provided by Macalloy bars.

A very recent application of post-tensioned brickwork in lateral stabilisation was by Cambridgeshire County Council[39] in which the abutments of two bridges were constructed in post-tensioned brickwork. This work was hailed as the 'first commercial use of post-tensioned brickwork in civil engineering'.

Prestressed masonry has also been used in flooring systems an example of which is the Stahlton flooring system developed in Switzerland[40]. In this case, the tensioned wires were embeded in mortar packed grooves within the burnt clay units. These formed the lower flange of the floor beam and

provided tensile resistance. These acted in structural cooperation with the cast-in-situ concrete web and compression flange.

As outlined above, with two exceptions, all the applications, to date, of prestressed brickwork has been limited to the introduction of vertical precompression as a means of providing lateral stability to laterally loaded walls/columns. In this form of construction, the effect of the prestress is effectively one of increasing the dead weight of the structure and therefore provides no major alternative to the more conventional forms of construction in which brickwork is used solely as a compression element.

To the author's knowledge, prestressed brickwork has not been used in practice as a structural member in which the load is primarily carried in bending. This is inspite of the encouraging results which have so far been obtained through research work[11,12]. This in the author's opinion can be attributed to three main reasons; the absence of data comparing the improved structural behaviour which can be achieved by prestressing brickwork to a well established construction material of similar nature such as prestressed concrete, the absence of complete information concerning the shear strength of prestressed brickwork in general (and partially prestressed brickwork in particular) and finally, the absence of adequate design guidance especially in the areas of cracking and on the shear strength. To ameliorate the situation, this study was undertaken.

2.4 SCOPE OF PRESENT INVESTIGATION

Although the advantages of prestressing brickwork are well documented, no information exists on how its improved structural behaviour compares with other well established building materials such as prestressed concrete. In order for prestressed brickwork beams to compete with prestressed concrete in buildings, it has to satisfy two main criteria from a structural engineering point of view (as opposed to an aesthetic or architectural point of view); it has to be structurally comparable to prestressed concrete and secondly it has to be an economically comparable or cheaper solution.

The scope of this thesis has been confined to the first criterium. In order to compare the structural behaviour of prestressed beams of brickwork and

concrete, an experimental and theoretical investigation was undertaken. Twenty nine full-scale prestressed brickwork and concrete beams of identical cross-sectional properties, similar compressive strengths and containing the same area of tensile reinforcement were compared under the following:

1. The ultimate flexural strength

2. Deflection

3. Cracking

4. The ultimate shear strength

Although prestressed brickwork and concrete beams may fail primarily in shear, the shear strength of a concrete beam can be readily increased by the provision of shear reinforcement. The introduction of shear reinforcement into a brickwork beam is not always straightforward and may lead to impracticable design details. This imposes a limitation on brickwork which is absent in concrete. In view of the undesirable nature of most shear failures; sudden and brittle, and the complete absence of experimental and theoretical information on the shear strength of partially prestressed brickwork, sixteen partially prestressed brickwork beams with shear span to effective depth ratios between 1.5 and 6.0 were tested.

Also, in view of the consequent importance of rational methods of predicting the shear strength of prestressed brickwork beams, the plastic theory was applied to predict the shear strength of partially prestressed brickwork beams. However, this method is dependent on an effectiveness factor which was introduced to compensate for the fact that brickwork does not behave in a perfectly plastic manner as assumed in the theory. This factor is obtained from experimental results of the ultimate shear stress and it is therefore not unexpected that a good correlation with experimental results can be obtained. Because of this dependency on experimental results of beams tested up to failure, an alternative approach of determining the shear strength of prestressed brickwork beams based on the concept of the 'compressive force path' has been suggested.

CHAPTER 3
MATERIALS PROPERTIES, CONSTRUCTIONAL DETAILS AND TEST METHODS

3.1 INTRODUCTION

This Chapter contains the results of tests which have been carried out to determine the properties of the materials used in this investigation. The cross-section and constructional details of the beams, and the test methods are also described.

The brick unit used throughout this investigation was anisotropic with its strength in the three orthogonal directions varying considerably. The strength of a brick unit is usually specified with respect to the direction of the bed joint i.e when tested flat. This arose because in the most common form of brickwork construction (walls and piers) the compressive stresses develop normal to the bed joint. However, in brickwork members which are subject to flexural stresses such as beams, the compressive stresses may develop parallel to the bed joint. Therefore a comprehensive description of the strength of an anisotropic brick unit requires specification in all three orthogonal directions.

Two types of prisms have been used to represent the compression zone of the prestressed brickwork beams tested in this work, in order to obtain the compressive strength, the ultimate strain and the stress/strain relationship. The merits of each of these prism types will be discussed. Also, the compression zone of a flexural member is subject to a linear variation in strain with depth i.e a strain gradient. This has lead to eccentrically loaded prism tests to investigate the effect of the strain gradient on the compressive strength. Some experimental work[41] has been carried out on eccentrically loaded single course prisms tested parallel to the bed joint. The results are also summarised.

In a prestressed beam, the amount of load that can be sustained after the neutralisation of the prestress is dependent on the flexural tensile strength of brickwork i.e the modulus of rupture. This can be obtained from three or four point loading tests on suitable unreinforced specimens which adequately

represent conditions at the soffit of the beam. For the two types of sections reported here, values have been obtained[11,12] for the combination of brick unit and mortar grade reported in this study. These results will be presented.

The compressive strength of concrete was obtained from tests on cubes and cylinders. The stress-strain relationship given in BS 8110:Part 2:1985[42] Section 2 was adopted. The modulus of elasticity on which the stress-strain relationship is dependent on was obtained from the tests on cylinders. The modulus of rupture of concrete was also obtained experimentally from unreinforced beams.

The mechanical properties of the tensioned and non-tensioned reinforcement were obtained from uniaxial tests on appropriate samples.

The stress-strain relationship for brickwork and the tensile reinforcement obtained experimentally were idealised. For brickwork, a third degree polynomial was obtained. Tri-linear relationships were adopted for the tensile reinforcement. Although the stress-strain relationship for concrete was obtained from BS 8110: Part 2: 1985[42], the theoretical analysis required this relationship to be expressed in non-dimensional form. This curve was idealised by a three degree polynomial using the method of least squares.

Finally, the beam section, constructional details and the prestressing procedure are described. This is preceded by the instrumentation and test method employed for the beams.

3.2 PROPERTIES OF THE BRICK UNIT

Extruded class A engineering clay bricks with three holes were used throughout this investigation (see Fig. 3.2.1). The average area of perforations was 14.9%. Compressive strength tests were carried out in three orthogonal directions (see Fig. 3.2.1) in accordance with BS 3291[43]. The test results are presented in Table 3.2.1. Compressive strengths have been based on both the gross and net cross-sectional areas.

Based on the gross cross-sectional area, the highest compressive strength is obtained when the brick unit is tested normal to the bed joint i.e

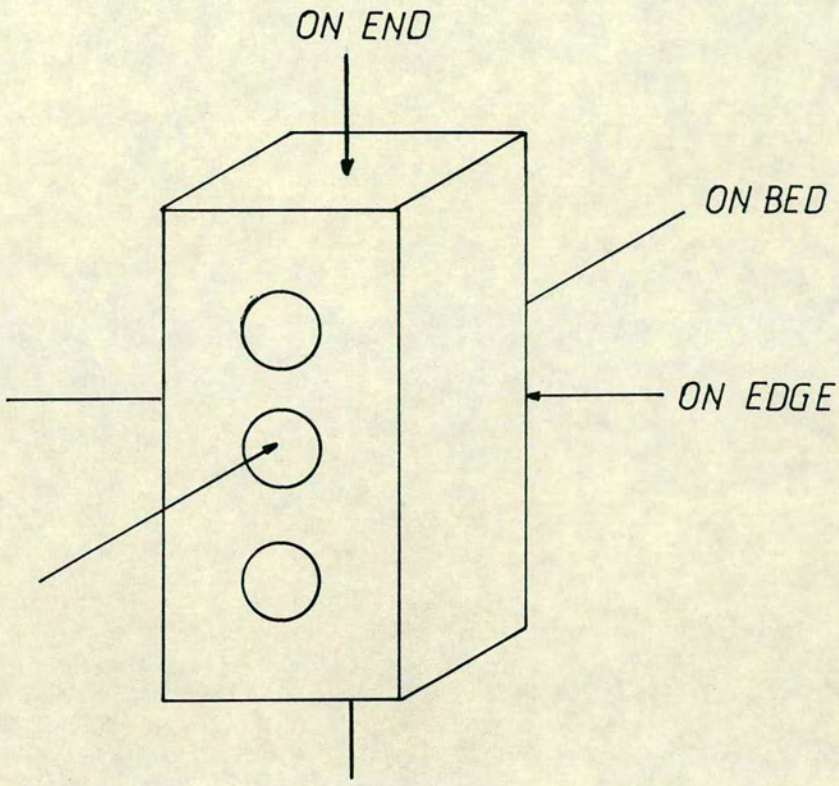

Fig. 3.2.1 Brick Type and Compressive Test Directions

Table 3.2.1 The Compressive Strength of the Brick Units and the Water Absorption Test Results

	Compressive Strength (N/mm^2)						water absorption % by weight 5 hr
	'on bed'		'on edge'		'on end'		
area	gross	net	gross	net	gross	net	
average	113.16	132.86	50.06	104.67	32.60	52.30	4.89
range	108.2–115.1	127.1–135.4	35.8–61.1	74.0–128.1	25.5–43.2	40.9–69.3	4.6–6.1
standard deviation	2.75	3.31	7.56	16.19	5.86	9.67	0.145
coeff. of var. (%)	2.43	2.49	15.1	15.47	17.98	18.49	2.96

Table 3.2.2 Comparison of brick strength in three directions

Area	Ratio of the bed joint Strength		
	'On Bed'	'On Edge'	'On End'
Gross	1.0	0.44	0.29
Net	1.0	0.79	0.39

'on bed' and is a minimum when bricks are tested 'on end'. A similar trend is also obtained when the compressive strength is based on the net cross-sectional area. In Table 3.2.2, the compressive strength of the brick unit when tested 'on edge' and 'on bed' are given as a ratio of the bed joint strength. Based on the gross cross-sectional area, the strength 'on edge' is only 44% of the strength 'on bed' while that 'on end' is 29% of that 'on bed'. However, when the compressive strength is based on the net cross-sectional area, the strength on edge increases to 79% of that on bed and that 'on end' is also increased to 39% of the bed joint strength. The variations in compressive strength in the three orthogonal directions can be attributed to platen restraint and the aspect ratio, and also to the orientation of the perforations with respect to the direction of loading. When the bricks are tested 'on bed', the effect of platen friction is more significant than in the other two directions and results in an enhancement of the compressive strength. As the aspect ratio of the specimen increases, the effect of platen restraint reduces and a corresponding reduction in the compressive strength is obtained. However, there is a minimum aspect ratio above which the effect of platen restraint does not affect the compressive strength. Previous experimental work[44] carried out on solid and perforated bricks with aspect ratios between 0.36 and 3.03 under confined and unconfined compression, showed that at low values of the aspect ratio, the confined strength was as much as twice that of the unconfined test. At an aspect ratio of 3.03 however, there was no difference in the compressive strength under similar test conditions.

Test results show that the mode of failure of the bricks depended on the orientation of the perforations. When tested 'on edge' or 'on bed' failure occurred by spalling of the brick which eventually led to crushing. When tested 'on edge', spalling occurred around the perforations. However, when tested 'on end' failure occurred by tensile splitting along the centre line of the brick. Stress concentrations which occur in the vicinity of the perforations have the effect of reducing the compressive strength. This effect was more significant when the bricks were tested 'on end'. In these bricks, spalling occurred around the perforations.

Similar variations in compressive strength in the three orthogonal directions have been observed by previous researchers[11,12,30,45]. Ratios of the 'on edge' to 'on bed' strengths of 0.554 based on the gross area and 0.879 based on the net area have been obtained[12]. The corresponding ratio of 'on

end' to 'on bed' strengths were 0.339 and 0.448 respectively[12].

To determine the water absorption, the 5h boiling test was carried out in accordance with BS 3291[43]. The results are also presented in Table 3.2.1.

3.3 MORTAR

Grade I mortar consisting of cement, lime and sand in a ratio of 1:0.25:3 by volume respectively was used throughout. The sand was oven dried prior to mixing. The water content was adjusted by the bricklayer to give a workable mix. Three 102 mm cubes were cast from each mix and tested at 28 days. The average compressive strength of the mortar was 23.13 N/mm^2.

3.3.1 Cement and Lime

Ordinary portland cement and lime conforming to BS 12[46] and BS 890[47] respectively were used in the mortar mix throughout this investigation.

3.3.2 Building Sand

Building sand was obtained from Edzell in Fife. The sieve analysis is presented in Table 3.3.1 and falls within the limits specified in BS 1200[48] which is also given in the table.

3.4 GROUT

Different grout mixes were used for the brickwork and concrete beams. For the brickwork beams, the grout consisted of ordinary portland cement as described above, concrete sand and coarse aggregate (described below) in the mix proportion 1:2.5:2 by volume respectively. A plasticiser known as conbex was also used and was always in the same proportion to the cement content. Its function was to shorten the setting time and reduce shrinkage. The above grout mix was also used in a few of the concrete beams tested.

In the grout mix for the concrete beams, the same materials were used

Table 3.3.1 Sieve analysis for building sand

BS sieve	% by weight passing through sieve size	
	Test Result	BS 1200 limit (Table 2)
5.00 mm	100	100
2.36 mm	100	90 - 100
1.18 mm	98	70 - 100
600 µm	71	40 - 80
300 µm	40	5 - 40
150 µm	10	0 - 10

Table 3.4.1 Sieve analysis for concrete sand

BS sieve	% by weight passing through sieve size	
	Test Result	BS 1200 limit (Table 5)
5.00 mm	99	89 - 100
2.36 mm	91	60 - 100
1.18 mm	84	30 - 100
600 µm	77	15 - 100
300 µm	51	5 - 70
150 µm	7	0 - 15

except the cement which was rapid hardening and conformed to BS 12[46]. The mix was proportioned by volume in the ratio 1:1.333:2 cement: concrete sand: coarse aggregate.

In each mix, the water content was adjusted to give a slump of between 200–250 mm. Three 102 mm cubes were cast from each mix, cured in water and tested at 7 days. The average compressive strength of the brickwork grout and concrete grout were 24.46 N/mm^2 and 42.20 N/mm^2 respectively.

3.4.1 Concrete Sand

The sieve analysis for the concrete sand is presented in Table 3.4.1. It complies with the overall limits given in BS 882: 1983[49] for fine aggregate (also presented in Table 3.4.1)

3.4.2 Coarse Aggregate

The coarse aggregate conformed to the BS 882: 1983[49] limit for 10 mm aggregate. The results of the sieve analysis and the limits for 10 mm aggregate[49] are presented in Table 3.4.2.

3.5 PROPERTIES OF BRICKWORK

3.5.1 Prism Types

Two types of prisms have been used to simulate conditions in the compression zone of the prestressed brickwork beam tested herein, in order to obtain representative estimates of the compressive strength, ultimate strain and stress–strain relationship. These prisms, shown in Fig. 3.5.1a and 3.5.1b, represent the top course and the three top courses of the beam and are designated as single and three course prism respectively.

The three course prism is a representation of the upper three courses of a brickwork beam and is one of the prism types recommended in BS 5628: Part 2[1] for use in the determination of the characteristic compressive strength of

Table 3.4.2 Sieve analysis for coarse aggregate

BS sieve	% by weight passing through sieve size	
	Test Result	BS 1200 limit (Table 4)
14.00 mm	100	100
10.00 mm	96	85 - 100
5.00 mm	6	0 - 25
2.36 mm	1.5	0 - 5

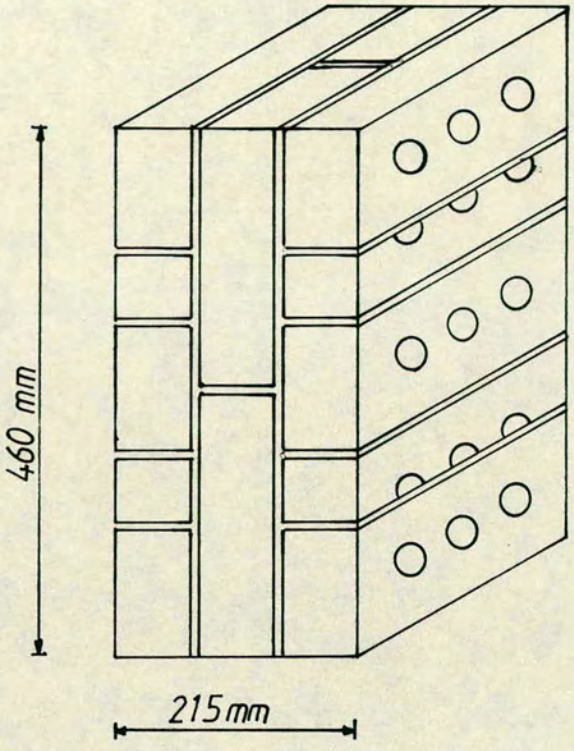

(a) Three Course Prism

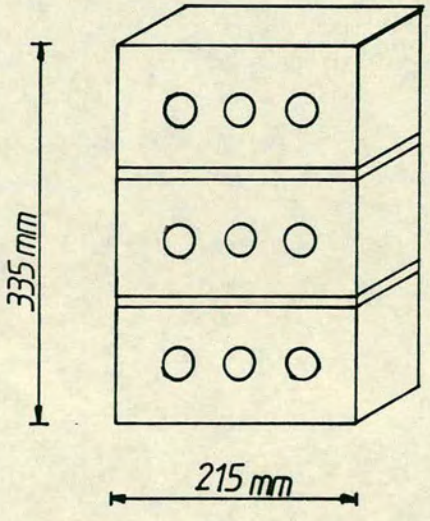

(b) Single Course Prism

Fig. 3.5.1 Brickwork Prisms

masonry. However, experimental observations on prestressed beams which fail in flexure have shown that just before failure splitting occurred in the top bed joint. Also, flexural cracking usually extends to the top bed joint when failure is in flexure. Thus, only the top course at this stage resists the compressive force hence the single course prism (also among those recommended in BS 5628[1]), was thought to be more representative of the conditions at flexural failure.

This assumption was also borne out in the modes of failure of each of these prisms types. In the three course prisms, at loads as low as 53%[12] of the failure load, horizontal splitting occurred along the bed joints seperating the prism into three individual courses each acting independently. The compressive load was thus redistributed between them. This was confirmed from strain readings taken from each course up to failure. Prior to bed joint splitting, the strains in all courses were uniform. However, marked variations in strain were observed between bed joint splitting and failure. Failure of the three course prism occurred when one or two of the brickwork courses collapsed. Simultaneous collapse of all three courses was not observed in the large number of prisms made from various brick strengths and mortar grades which have been tested[11,12]. In the single course prisms, the strain distribution remained uniform up to failure even after cracking of the prism which usually occurred at about 76%[12] of the ultimate load. Failure has been attributed to vertical tensile cracks which develop parallel to the axis of loading. Collapse was caused by explosive spalling of the brickwork.

To establish which prism type is the better representation of the compressive zone of a prestressed beam of the type tested here, the behaviour of each prism, has to be considered in relation to that of a beam. In a beam section under flexure, the strain distribution is well defined up until failure with the maximum strain occurring in the extreme compressive fibres. Splitting of the bed joints will increase the strain in the outer fibres and not result in a redistribution of load away from this region, so that flexural failure occurs when the outer fibre has attained the ultimate compressive strain. Therefore the average strain of the three course prism at failure will be less than that of a beam and also, as simultaneous crushing of the three courses does not occur the average compressive strength of the prisms will be less than that in a beam. A single course prism is therefore a better representation of conditions at flexural failure than is the three course prism. Theoretical results

using the properties of brickwork obtained from single course prisms have shown better agreement with experimental results than obtained from the three course prism. Thus in this work the properties of the brickwork have been obtained from single course prisms.

3.5.2 Test Type

Prism tests are usually conducted under uniaxial compression. Therefore, there is no variation in strain across the specimen i.e there is no strain gradient. In a flexural situation, a strain gradient is present. Eccentrically loaded prism tests simulate the conditions in the compressive zone more accurately. Tests on eccentrically loaded prisms normal to the bed joint[50,51] have shown an increase in the compressive strength over that obtained from axially loaded prisms. This increase has been attributed to the presence of a strain gradient[12]. To investigate this issue for prisms loaded parallel to the bed joint, Walker et al[41] carried out a number of tests on axially and eccentrically loaded single course prisms. The test set-up for the eccentrically loaded prisms is shown in Fig. 3.5.2. The variables included the strength of the brick unit and grade of the mortar.

Walker[12] concluded that the maximum stress developed at the time of failure of eccentrically loaded brickwork prisms built with different grades of mortar and brick strengths and stressed parallel to the bed joint appeared to be the same as obtained under axial compression.

3.5.3 The Compressive Strength of Brickwork

The compressive strength of brickwork parallel to the bed joint was obtained from tests on axially loaded single course prisms as shown in Fig. 3.5.1(a). The prisms were cured under polythene sheets and tested at 28 days. Prior to testing they were capped with a mortar mix or dental plaster. The load was applied via 3 mm thick plywood sheets which were used only once. Initially, to ensure axial loading, equal increments of strain measured with a 200 mm demec gauge were required on both faces of the prism for each load increment. Cracking generally occurred at about 70% of the ultimate load. After cracking, the increase in load per increment was reduced. In general, there were 12-15 load increments and strain readings were taken up to about

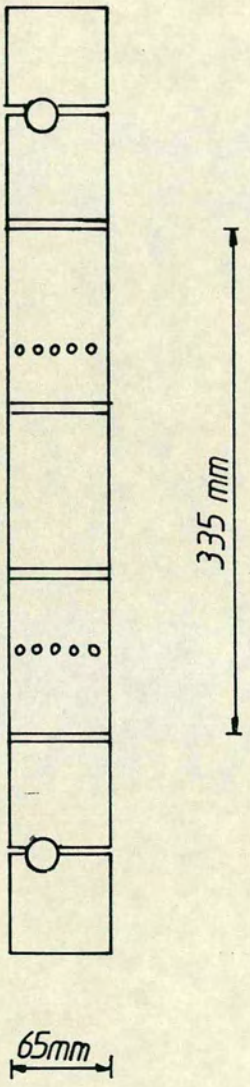

Fig. 3.5.2 Eccentrically Loaded Single Course Prism

92% of the ultimate load. Plate 3.1 shows a single course prism at failure.

The compressive strengths of the prisms tested in this work are given in Table 3.5.1. The average value of 32.69 N/mm^2 is in good agreement with those obtained for similar prisms tested by other researchers[11,12,30,41,45]. The corresponding characteristic strength[1] was 20.17 N/mm^2.

3.5.4 The Ultimate Strain in Brickwork

In the prism test, it was not possible to measure the ultimate strain. However, by mathematical extrapolation of the experimental stress-strain relationship, the ultimate strain was obtained. The ultimate strain for each of the prisms tested is presented in Table 3.5.1. The average value of 0.00327 is in good agreement with that recommended in the code of practice for reinforced and prestressed masonry[1] (0.0035) and also those obtained in references 11 (0.00326) and 12 (0.00353) for high strength bricks in grade I mortar.

3.5.5 The Stress-Strain Relationship for Brickwork

The stress-strain relationship for each prism was obtained from the average stress and strain readings at each load increment. Typical relationships are plotted in Fig. 3.5.3. Initially there is a linear relationship between the stress and strain. Thereafter, there is a more rapid increase in strain up until failure. In each case, the maximum stress occurred at the maximum strain i.e there was no falling branch. It was not possible to obtain a falling branch from the test method employed. However, unlike prisms tested normal to the bed joint, researchers[52] did not detect a falling branch in prisms tested parallel to the bed joint.

3.5.5.1 The Idealised Stress-Relationship For Brickwork

The stress-strain relationship for the prisms tested (see Fig. 3.5.3) showed considerable variations even though the brick strength and mortar grade were unchanged. These variations can be minimised by plotting the stress-strain relationship in a non-dimensional form. This is achieved by normalising the

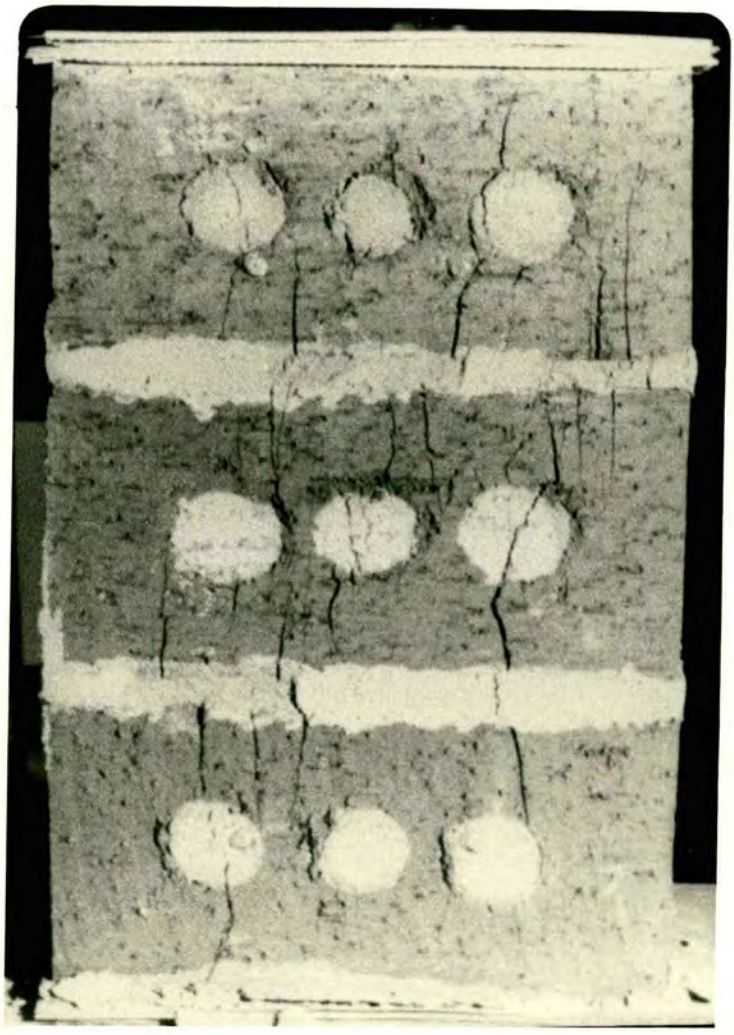

Table 3.5.1 Properties of the single course prisms

Prism	Compressive strength N/mm^2	Ultimate strain	Young's Modulus kN/mm^2
1	27.38	0.00280	18.8
2	27.78	0.00330	16.7
3	30.20	0.00360	17.5
4	32.92	0.00345	19.4
5	35.64	0.00285	19.0
6	32.80	0.00310	18.1
7	38.60	0.00365	17.7
8	36.20	0.00340	20.9
Average	32.69	0.00327	18.5

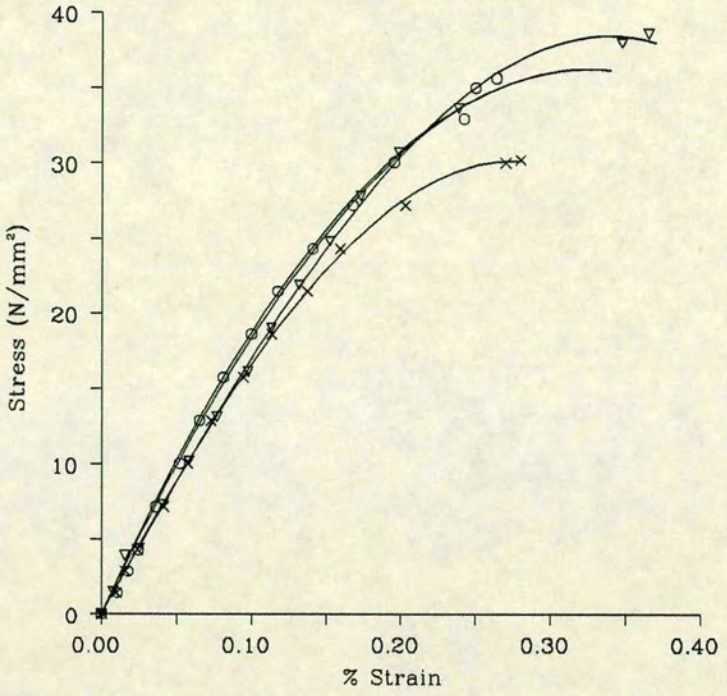

Fig. 3.5.3 Experimental Stress–Strain Relationship for Brickwork

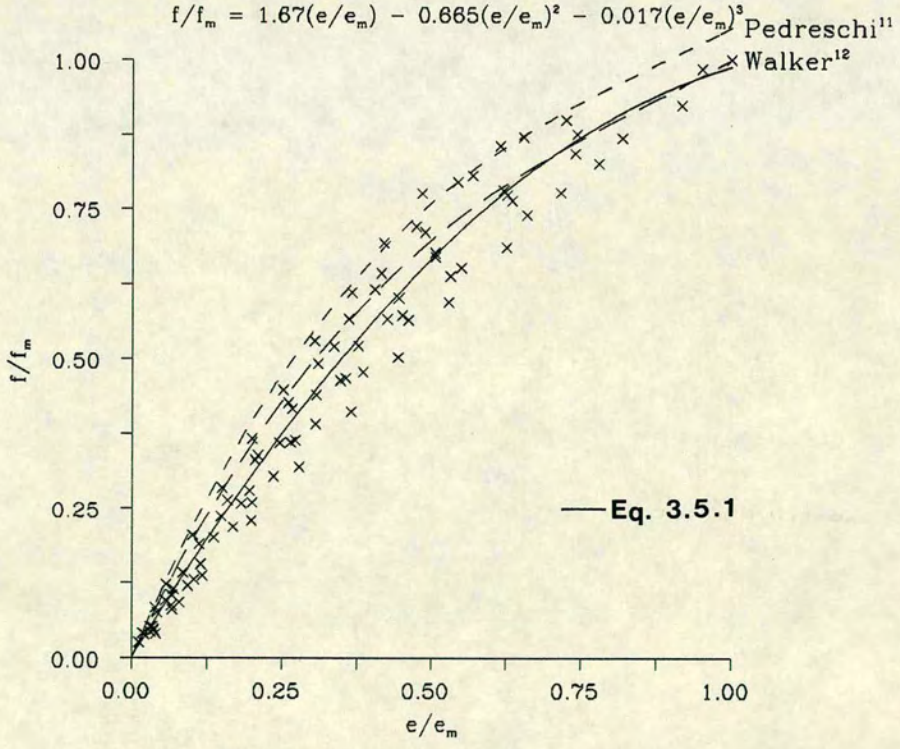

Fig. 3.5.4 Non–Dimensional Stress–Strain Relationship for Brickwork

stress and strains by their maximum values f_m and ε_m respectively. This idealised relationship, for all the prisms tested, is shown in Fig. 3.5.4.

As well as minimising experimental variations, idealisation enables all the various test results to be combined and represented by a single mathematical expression. A regression analysis was carried out on all the non-dimensional data points. The best fit equation was found to be a third degree polynomial as follows:

$$f/f_m = X_1(\varepsilon/\varepsilon_m) + X_2(\varepsilon/\varepsilon_m)^2 + X_3(\varepsilon/\varepsilon_m)^3$$

where
$X_1 = 1.67$
$X_2 = -0.665$
$X_3 = -0.017$

... 3.5.1

This relationship is in keeping with other experimental works which have found that the stress-strain relationship for brickwork parallel to the bed joint is best represented by a third degree polynomial[11,12,30]. Some of the brickwork beams reported in this study were obtained from reference 11. The idealised stress-strain relationship obtained for these beams (of high strength bricks in grade I mortar) had the coefficients 2.373, -2.095 and 0.776 for X_1, X_2 and X_3 in equation 3.5.1 respectively. The constants in equation 3.5.1 obtained by Walker[12] from a large number of tests on single and three course prisms of high and medium strength bricks in grade I and grade II mortar was as follows: $X_1 = 2.12$, $X_2 = -1.78$, $X_3 = 0.66$. In Fig. 3.5.4, the relationships obtained by Walker[12] and Pedreschi[11] are also plotted.

3.5.5.2 The Stress Block Factors

The stress block factors λ_1 and λ_2 are properties of the non-dimensional stress-strain curve which together completely describe the distribution of compressive stresses in the compression zone and are necessary for the prediction of the ultimate flexural strength.

λ_1 is a measure of the average compressive stress in the compression zone in relation to the compressive strength of brickwork. It is equivalent to the area under the non-dimensional stress-strain curve and is given by:

$$\lambda_1 = \int_0^{1.0} [X_1(\varepsilon/\varepsilon_m) + X_2(\varepsilon/\varepsilon_m)^2 + X_3(\varepsilon/\varepsilon_m)^3] d\ \varepsilon/\varepsilon_m$$

λ_2 is the distance of the centroid of the area under the non-dimensional stress-strain curve measured from $\varepsilon/\varepsilon_m$=1.0, and represents the line of action of the resultant compressive force in the compression zone. It is given by:

$$\lambda_2 = 1 - \int_0^{1.0} \varepsilon/\varepsilon_m [X_1(\varepsilon/\varepsilon_m) + X_2(\varepsilon/\varepsilon_m)^2 + X_3(\varepsilon/\varepsilon_m)^3] d\ \varepsilon/\varepsilon_m / [\lambda_1]$$

... 3.5.3

There is a third stress block factor λ_3 which relates the failure stress to the average compressive strength obtained from the brickwork prism tests. Its value in brickwork is equal to 1.0[53] i.e the failure stress in a brickwork beam is equal to the average compressive strength of the brickwork prisms.

The stress blocks factors λ_1 and λ_2 obtained from the non-dimensional stress-strain curve in Fig. 3.5.4 are as follows:

λ_1 = 0.61

λ_2 = 0.387

The values of λ_1 and λ_2 obtained for high strength bricks in grade I mortar in reference 11 were 0.652 and 0.372 respectively.

Several values have been proposed for λ_1 and λ_2 . A summary of the types of stress blocks and the corresponding values for λ_1 and λ_2 which have been proposed for brickwork is given in reference 11. Here, it shall only be mentioned that these factors are essentially independent of the type of test: axial or eccentric[12], the type of prism[11]; single or three course, and the strength of the brick or grade of mortar[11]. The values obtained here are in agreement with those of other authors[11,12,30,53].

3.5.6 Modulus of Elasticity

The modulus of elasticity for brickwork was obtained by linear regression of the stress-strain relationship (described in Section 3.5.5) up to about a third of the ultimate prism strength. The results are given in Table 3.5.1. The average modulus of elasticity obtained was 18.5 kN/mm^2 which compares

favourably with the results obtained from Walker's equation[12] given as:

$$E_m = 1308\ f_m^{0.74} \qquad \ldots 3.5.4$$

This relationship was obtained for various strengths of brickwork prisms loaded in a similar direction as those in this work and gave a value of 17.27 kN/mm^2. Earlier, Pedreschi[11] proposed an expression for the modulus of elasticity for brickwork based on a large number of tests on prisms loaded normal and parallel to the bed joint:

$$E_m = 1180\ f_m^{0.83} \qquad \ldots 3.5.5$$

If one ignores the significance of the direction of loading such as normal or parallel to the bed joint, the modulus of elasticity for this work using equation 3.5.5 will be 21.27 kN/mm^2 which overestimates the experimental value by 15%. Equations 3.5.4 and 3.5.5 reflect the increase in the modulus of elasticity of brickwork with increasing compressive strength. The modulus of elasticity obtained from both these equations could have been used to obtain the deflection in the linear range for this work but would have underestimated or slightly overestimated the deflection. Hence the value obtained in this work was used.

3.5.7 The Modulus of Rupture

As mentioned in the introduction (Section 3.1), the amount of load which can be sustained by a prestressed beam between the neutralisation of the prestress and cracking is dependent on the flexural tensile strength, otherwise known as the modulus of rupture. In order to obtain realistic estimates of the effects of load such as deflections and curvatures, it is important to know its value.

In brickwork, cracking is initiated at the brick–mortar interface as the brick and mortar have higher tensile strengths. In this work, two types of brickwork sections are reported (see Section 3.8) and in previous works[11,12] suitable specimens have been tested to estimate the modulus of rupture for these sections. These specimens are unreinforced beams and represent the conditions at the soffit of the beam under test (see Fig. 3.5.5 a and b). Tests

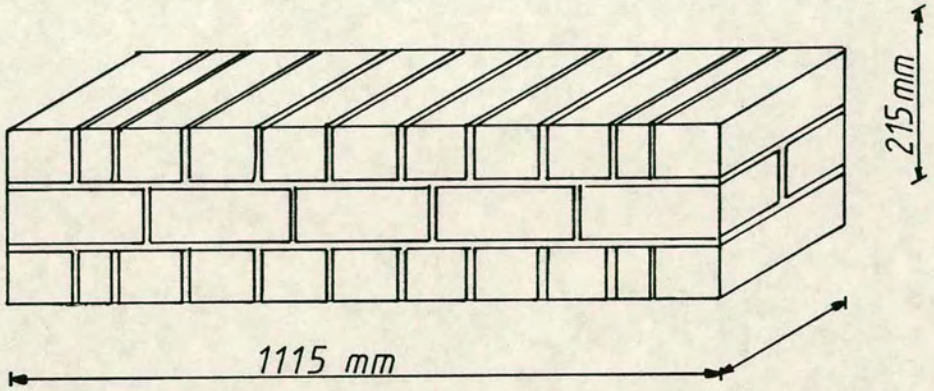

(a) Specimen for Fully Prestressed Beams[11]

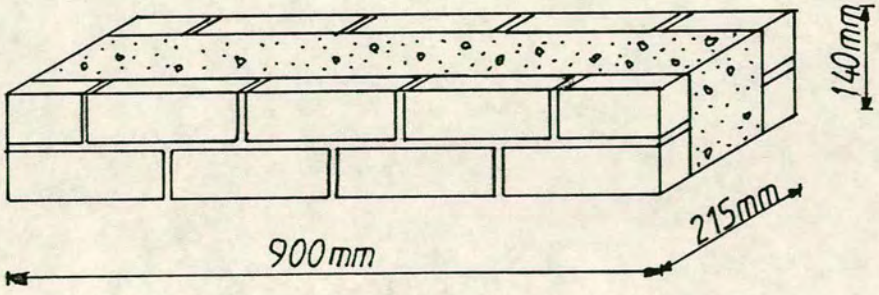

(b) Specimen for Partially Prestressed Beams[12]

Fig. 3.5.5 Modulus of Rupture Test Specimens in Brickwork

were carried out under four point loading. Once cracking began the section became incapable of sustaining any more load and collapsed. The modulus of rupture was obtained from the failure moment and was based on the gross cross-section.

The modulus of rupture has been found to be independent of the brick type[11] and grade of mortar[12]. It is however, dependent on the type of specimen. The average modulus of rupture for specimen type (a) (see Fig. 3.5.5a) was found to be 1.49 N/mm^2. The presence of the concrete grout in specimen type (b) increased the modulus of rupture by 23% to 1.83 N/mm^2. The modulus of rupture of the composite section was 19% less than that for an equivalent concrete section, at 2.26 N/mm^2.

3.6 PROPERTIES OF THE CONCRETE BEAMS

The main purpose of the tests carried out on the concrete beams was to enable a comparison with brickwork beams, identical in section and of similar flexural strength. Above, it was seen that the best method for determining the flexural strength of the type of brickwork beam tested in this work is from tests on single course prisms. Also, the failure stress is equivalent to the average compressive strength of the prism. On the other hand, the compressive strength of a concrete member may be obtained either from uniaxial tests on cylinders or cubes but currently the latter specimen is usually specified. Unlike in brickwork, the failure stress in a concrete beam is not equal to the compressive strength of the cube or cylinder but is a fraction of these strengths. Because the crushing strength of the cylinder was previously specified, several ratios of the failure stress to the compressive strength of the cylinder have been proposed[54,55,56,57] which have ranged from 0.85 to 1.0. In BS 8110: Part 2: 1985[42], it is implied that the failure stress is 0.8 times the cube crushing strength. It was therefore necessary to account for the different relationships between the failure stress and the compressive strength of the test specimen in selecting a strength of concrete comparable to that of brickwork.

For comparison with high strength brickwork (average compressive strength = 33 N/mm^2), the following concrete strength was selected in

accordance to recommendations given in references 59, 60 and 61:

Average cube crushing strength = 42 N/mm^2

Corresponding failure stress = 42 N/mm^2 x 0.8 = 34 N/mm^2

Characteristic strength = 35 N/mm^2

3.6.1 Mix Proportion

The mix was designed according to reference 59 and was in the proportion 1: 2: 2.5 cement: concrete sand: coarse aggregate by volume. The water cement ratio was 0.6. This gave a slump of about 50mm.

3.6.2 The Stress-Strain Relationship For Concrete

The stress-strain relationship adopted for concrete in this work was that proposed in BS 8110: Part 2: 1985[42] and is given as follows:

$$f = 0.8\, f_{cu}\, [(\kappa\nu - \nu^2)/(1 + (\kappa - 2)\nu] \qquad \ldots 3.6.1$$

$$\nu = \varepsilon/\varepsilon_{c,1} = \varepsilon/0.0022 \qquad \ldots 3.6.2$$

$$\kappa = 1.4\, \varepsilon_{c,1}\, E_o/f_{cu} = 3\, E_o/f_{cu} \qquad \ldots 3.6.3$$

where
f = stress in concrete

E_o = modulus of elasticity of concrete in kN/mm^2

ε = strain in concrete

$\varepsilon_{c,1}$ = strain in concrete at the maximum stress

Equation 3.6.1 requires the modulus of elasticity of concrete. In BS 8110: Part 2: 1985[42], the typical range of values for the static modulus of elasticity at 28 days for normal weight concrete with a characteristic strength of 35 N/mm^2 is between 21 kN/mm^2 and 33 kN/mm^2 with a mean value of 27 kN/mm^2 (by extrapolation). As the load-deflection response is dependent on the static modulus of elasticity, it was felt necessary to determine its value

experimentally.

The static modulus of elasticity was determined from tests on 150 mm x 300 mm cylinders in accordance with BS 1881: Part 121: 1983[62]. The results are shown in Table 3.6.1. The resulting stress-strain relationship for concrete is shown in Fig. 3.6.1.

In the partially prestressed brickwork beams tested in this work, the grouted cavity made up 18% of the total cross-sectional area. The stress-strain relationship for concrete given by equations 3.6.1 to 3.6.3 was also used.

3.6.3 The Non-Dimensional Stress-Strain Relationship for Concrete

In order to express the stress-strain relationship for concrete in a similar manner as previously done for brickwork (Section 3.5.5.1), the relationship given by the code (see Fig. 3.6.1) was expressed in non-dimensional form by normalising the stress and strain with respect to the maximum values, $0.8f_{cu}$ and ε_u respectively (see Fig. 3.6.2). The best-fit equation in this case was also found to be a third degree polynomial given as:

$$f/0.8\ f_{cu} = 3.347(\varepsilon/\varepsilon_u) - 3.049(\varepsilon/\varepsilon_u)^2 + 0.406(\varepsilon/\varepsilon_u)^3 \quad \text{... 3.6.4}$$

From this relationship, the stress block factors λ_1 and λ_2 defined above in Section 3.5.5.2 are as follows:

$\lambda_1 = 0.759$

$\lambda_2 = 0.427$

As mentioned above, the stress block factor $\lambda_3 = 0.8$.

For design purposes, the stress block factors λ_1 and λ_2 are given in BS 8110: Part 1: 1985[58] as 0.90 and 0.45 respectively - slightly different from those obtained from the curve.

Table 3.6.1 Static modulus of elasticity for concrete

Sample	Static modulus of elasticity	Average cylinder crushing strength
	kN/mm^2	N/mm^2
1	23.6	32.6
2	21.3	35.7
3	25.8	34.5
Average	23.6	34.3

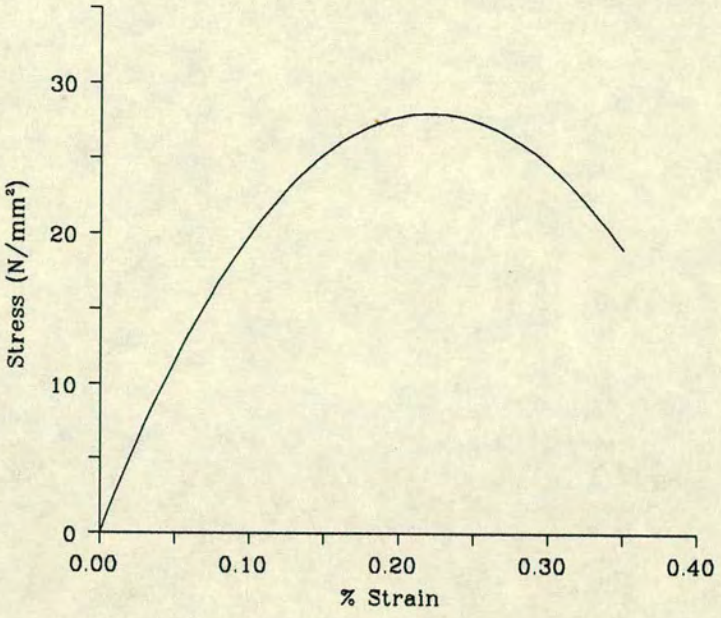

Fig. 3.6.1 Stress–Strain Relationship for Concrete[43]

$$f/(0.8\ fcu) = 3.347(e/eu) - 3.049(e/eu)^2 + 0.406(e/eu)^3$$

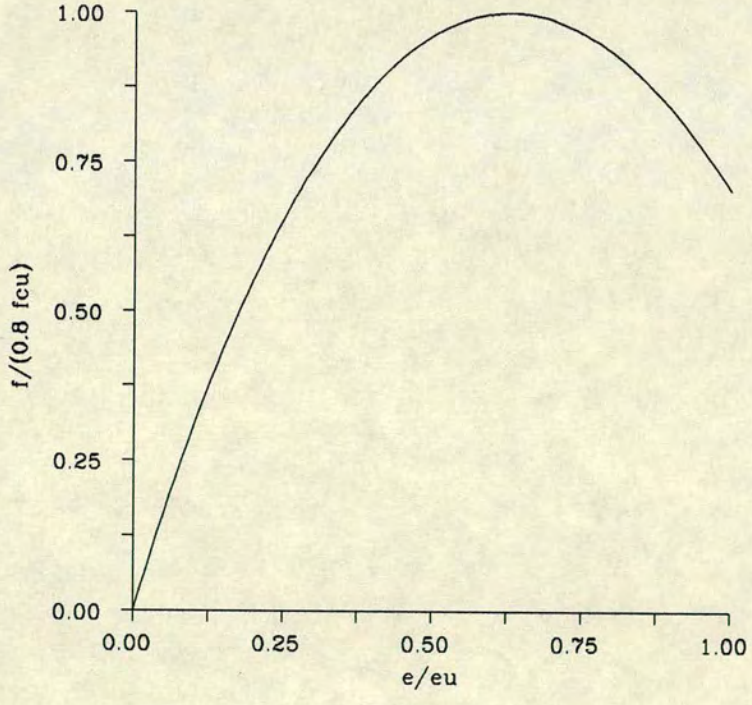

Fig. 3.6.2 Non–Dimensional Stress–Strain Relationship for Concrete

3.6.4 The Flexural Tensile Strength of Concrete

The flexural tensile strength for the concrete beams were obtained from four point loading tests on unreinforced concrete beams with cross-sectional dimensions of 102 mm x 102 mm and 500 mm long in accordance with BS 1881: Part 109: 1983[62]. The average value obtained was 3.37 N/mm^2.

3.7 PROPERTIES OF THE TENSILE REINFORCEMENT

Two types of tensile reinforcement were used in the beams tested: tensioned and non-tensioned reinforcement.

3.7.1 Properties of the Tensioned Reinforcement

Seven wire stabilised steel strands were used as the tensioned reinforcement. The strand consisted of a straight core wire around which was wound six helical wires in one layer. The diameter of the strand was 10.9 mm with a cross-sectional area of 72 mm^2 and conformed to BS 5896: 1980[63]. To obtain the mechanical properties of the prestressing strand, three specimens were tested in uniaxial tension. The experimental results are presented in Fig. 3.7.1 and Table 3.7.1. The experimental stress-strain relationship was idealised into a tri-linear form, shown in Fig. 3.7.1, for use in theoretical and computer based calculations. The properties of the tensioned reinforcement used in reference 11 from which the fully prestressed brickwork beams reported here were obtained was very similar to that shown in Fig. 3.7.1.

3.7.2 Properties of the Non-Tensioned Reinforcement

A 25 mm diameter high yield deformed bar with a cross-sectional area of 491 mm^2 and conforming to BS 4449[64] was used throughout this investigation. The stress-strain relationship was obtained as above. The results are also summarised in Table 3.7.1 and Fig. 3.7.2. The idealised stress-strain relationship also took a tri-linear form as shown in Fig. 3.7.2.

The following sections contain a description of the beam section, the

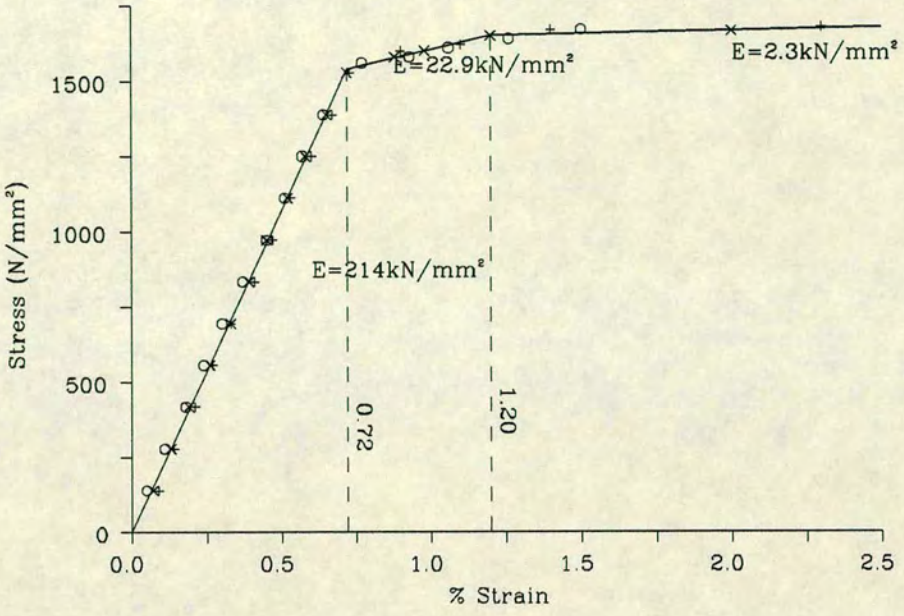

Fig. 3.7.1 Idealised Stress-Strain Relationship
for the Tensioned Steel

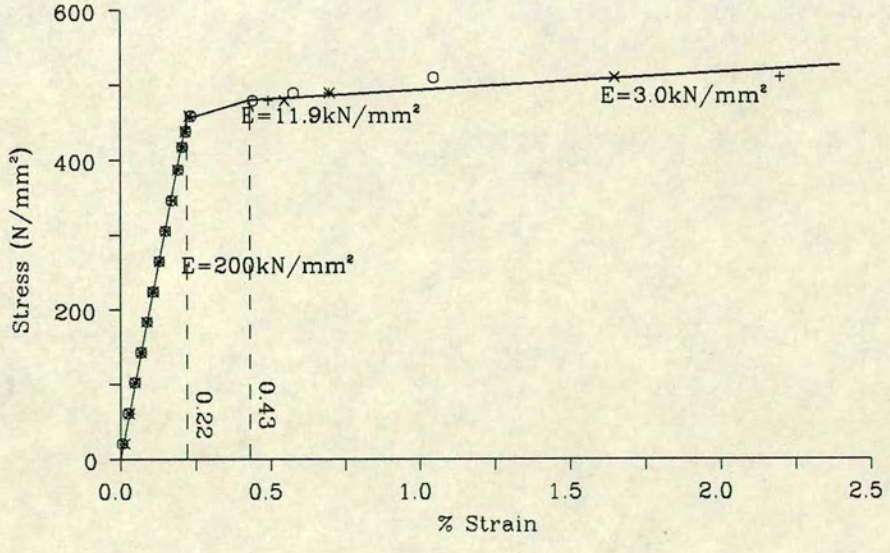

Fig. 3.7.2 Idealised Stress-Strain Relationship
for the Non-Tensioned Reinforcement

Table 3.7.1 Mechanical properties of the tensioned non-tensioned reinforcement

Type	Nominal diameter mm	Ultimate tensile strength N/mm^2	0.2% proof stress N/mm^2	Young's modulus kN/mm^2
seven wire stablised steel strand	10.9	1727	1590	214
Hot rolled deformed high yield tensile bars	25	642	480	200

construction details and the prestressing procedure. The instrumentation and test method are also described.

3.8 THE BEAM SECTION

The section chosen for the partially prestressed beams tested in this study is shown in Fig. 3.8.1a. By restricting the depth of the cavity to accommodate the required depth of the prestressing strand and the non-tensioned steel, an optimum use of brickwork was achieved. The cavity occupied 18% of the total cross-sectional area. Although the presence of the grout at the beam soffit increased the modulus of rupture of the beam section as seen in Section 3.5.7, it did not contribute to the ultimate flexural moment as the neutral axis in all the beams tested was always above the grout at failure.

The most common bonding pattern used for the construction of walls is the English bond. Hence this was used for the beams, which meant no special skill requirement from the bricklayer. The first three courses consisted of the normal English bond. The fourth and fifth courses were built from half bricks obtained by splitting a brick lengthwise. These were placed flush with the beam faces thereby forming the cavity. The side elevation of a typical beam is shown in Fig. 3.8.2.

The fully prestressed brickwork beams discussed in the later Chapters were obtained from the work of Pedreschi[11] and have cross-sections as shown in Fig. 3.8.1b. The concrete sections were identical to the brickwork sections.

3.9 ANCHORAGE REINFORCEMENT

These were provided in the "lead lengths" of each beam to resist the transverse tensile forces which develop as a result of post-tensioning. In brickwork this may cause horizontal splitting along the bed joint. The anchorage reinforcement consisted of four pairs of 6mm mild steel rods at a pitch of 100 mm. These were provided over the full depth of the beam and

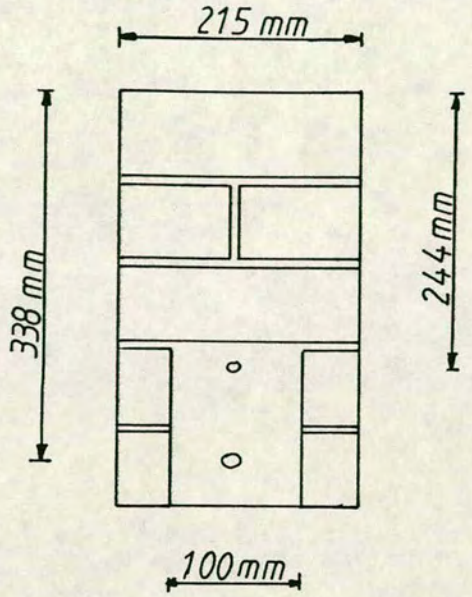

(a) Partially Prestressed Beams

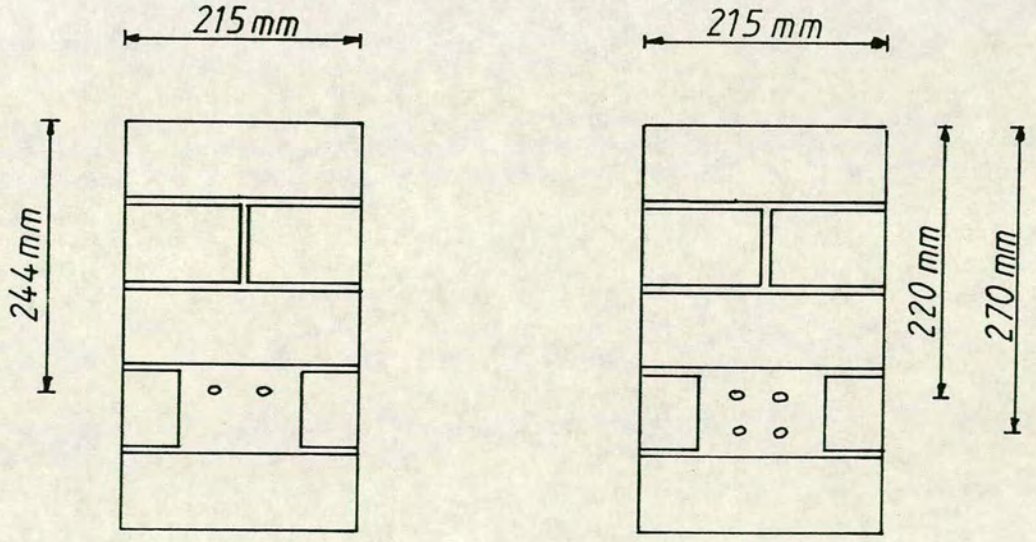

(b) Fully Prestressed Beams (11)

Fig. 3.8.1 Beam Sections

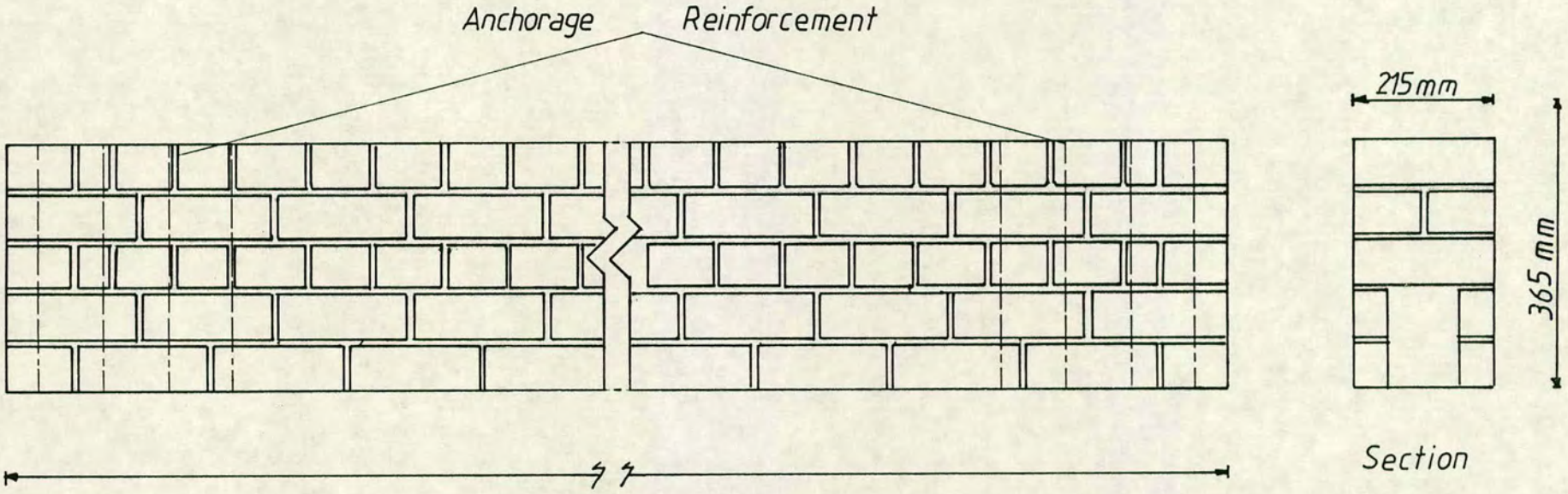

Fig. 3.8.2 Beam Section and Elevation showing the Coursing Pattern and Anchorage Reinforcement

were placed at each side of the cavity in the outer brick perforations which were then mortared against the sides of the cavity. This is illustrated in Fig. 3.8.2 and Plate 3.2.

In concrete, anchorage reinforcement was provided according to BS 8110: Part 1: 1985[58] section 4.11.2. These consisted of 4 No. 6 mm closed links at a pitch of 100 mm.

3.10 CONSTRUCTION DETAILS

3.10.1 Brickwork

The beams were built on the floor of the laboratory by an experienced bricklayer with average skills. An even surface was provided by laying wooden planks on sawdust. The planks were lined with building paper to prevent adhesion to the beams. The beams were built upside down. This simplified the building process, made prestressing easier to monitor and facilated grouting of the beams.

In the first three courses, the perforations in each brick were filled with compacted mortar. The anchorage reinforcement was then introduced at each end. Between the next two courses of 1/2 bricks, galvanised steel vertical-twist wall ties were layed at a spacing of 500mm and at both ends of the beam. These prevented separation of the leaves of the cavity during prestressing.

When all five courses had been laid the anchorage reinforcement was then mortared against the leaves of the cavity. The beams were cured under polythene sheets until testing.

3.10.2 Concrete Beams

As previously mentioned the main purpose of the concrete beams tested in this study was to enable a direct comparison to be made with an identical beam section in brickwork of similar strength. The concrete beams were also required to satisfy the requirements of BS 8110[58].

Plate 3.2 Construction of Brickwork Beams showing Anchorage Reinforcement

The concrete beams were cast in a rectangular steel mould of the same cross-sectional dimensions as the brickwork beams. Compaction was carried out with an electrical vibrator. The exposed surface was covered with polythene sheets. After seven days the beams were demoulded and cured under polythene sheets until prestressing.

3.10.3 Prestressing

In order to transfer the prestressing force from the tendons to the beam, the tendons were anchored to 200 mm x 200 mm x 25 mm thick mild steel plates mortared to each end of the beam. These plates were placed so that the resultant force on it was acting at the 'lower kern' limit of the beam. Thus, maximum use was made of the prestressing force without introducing tensile stresses.

In the partially prestressed beams, the ordinary reinforcing bars were suspended from a frame placed over the beam. In this way the required cover could be achieved. The ordinary reinforcement was thus independent of the beam until it was grouted.

The tendons were secured by using CCL XL barrel and wedge type open grips. Stressing was carried out using a CCL stress-o-matic pump with a type 300 manual control stressing head. It was capable of delivering a maximum prestressing force of 300 kN.

The load on the tendon was measured in two ways. Firstly, by the load cell fitted to the stressing head and connected to a battery operated meter. The meter could measure the force applied to the tendon but not the losses. However, the effective prestressing forces after losses were obtained from the electrical strain gauges attached to the tendon.

In general the tendons were stressed to 70% of their ultimate load. In the case of concrete beams which were to be compared with existing brickwork beams, the amount of prestress was modified so that the effective prestress after losses were about the same. In beams containing four tendons, those nearest the centroid were stressed first. This prevented tensile stresses which would otherwise have arisen from the tendons further away from the centroid.

The lock-off losses varied with the length of the beam from about 35% in the shortest beams to 12% in the longest. The variation in lock-off losses with length arises from the more or less constant amount of slip at the wedges for a given type of anchorage. The greatest loss thus occurs in the shortest beams.

After prestressing, the beam was grouted manually. Prior to grouting, a cement slurry was splashed on the surfaces of the cavity to ensure a good bond between the grout and the brickwork shell. The grout was compacted with a tamping rod. The beams were cured under polythene sheets for a further seven days until testing.

3.11 INSTRUMENTATION

3.11.1 Strain Measurement

Strain measurements were taken on the surface of the brickwork/concrete, in the grout at the level of the steel and on the surface of the steel.

3.11.1.1 Strain Measurements on the Surface of the Brickwork/Concrete

These were measured using demountable demec gauges over a gauge length of 200 mm capable of measuring strains to 8 με. Brickwork and concrete strains were measured within the region of constant bending moment. Fig. 3.11.1 shows the arrangement of demec points in the constant moment region. The depths at which strains were measured varied slightly depending on the types and number of reinforcement present. Apart from the demecs which were placed at the depths of the various reinforcements, the soffit, the extreme compression fibre and at the effective depth of the section, the positions were arbitrary. However, more points were located in the compression zone.

The demec points were mounted prior to prestressing. The sequence of operations leading up to testing of the beam (see Section 3.12.2), enabled the strain distribution due to prestressing and that due to prestressing and self weight of the beam to be determined.

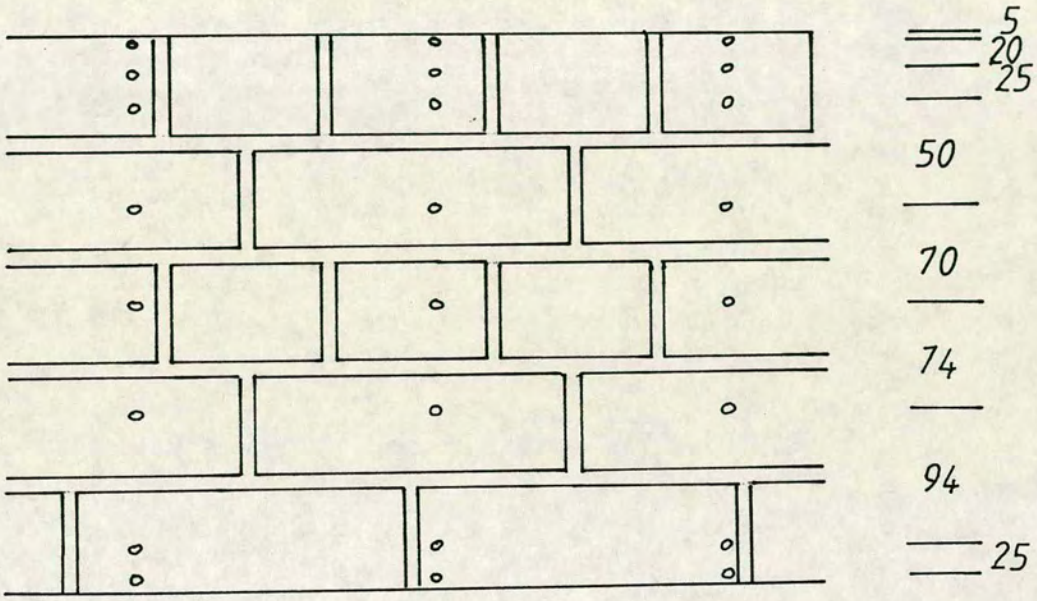

Fig. 3.11.1 Arrangment of 'Demec' Points in the Constant Moment Region

3.11.1.2 Strain Measurements in the Grout at the Level of the Steel

These strains were measured using electrical resistance embedment gauges with a gauge length of 60 mm. The purpose of this strain measurement was to compare the strain in the steel with that in the adjacent grout. The strain readings were obtained in a similar manner to that described in 3.11.1.3 below. There was virtually no difference between the strain measured in the grout and that on the steel at that level which implied that the reinforcement was fully bonded to the beam section.

3.11.1.3 Strain Measurement on the Surface of the Steel

The strain on the surface of the steel was measured in the constant moment region with electrical resistance strain gauges. The gauges were of foil and were capable of measuring strain beyond the yielding of the reinforcement. The gauge lengths selected depended on the type of reinforcement. For the 10.9 mm diameter seven wire strand, the gauge length of 2 mm was imposed by the size of each wire. A gauge length of 5 mm was used for the 25 mm deformed bar.

The 'Orion' data logger was used to monitor the output from the strain gauges. The strain readings were given directly (to an accuracy of 0.1 $\mu\varepsilon$).

3.11.2 Deflection

The deflection at various points along the span of the beam was measured using mechanical dial gauges. These gauges were supported on magnetic bases attached to a rig independent of the test rig. Deflection readings were taken at midspan and at the middle of each shear span using gauges reading down to 0.01 mm. The settlement at the supports were measured using 0.002 mm dial gauges. Towards failure when the midspan deflections became excessive or when there were signs of iminent failure, the dial gauges were removed in order to avoid damage. The midspan deflection was then measured with a ruler reading to the nearest millimeter.

3.11.3 Measurement of Crack Widths

In a brickwork beam, the bonding pattern enables the probable locations of cracks at the soffit to be predicted - at the brick/mortar interface. This enables the crack widths to be measured using a vernier calliper between two demec points mounted across these positions prior to testing. The vernier calliper reads down to 0.02 mm. In concrete, it is not possible to predict the exact position of a crack. Thus the ultra-lomora moving microscope was used to measure crack widths. This instrument was such that crack widths could only be measured from 10mm above the soffit. The smallest measurement was 0.02 mm. By placing pairs of demec points at random at the soffit within the constant moment region, some crack widths were also measured using the vernier callipers. Crack widths were measured on both faces of the beam within the constant moment region.

3.11.4 Load Application and Measurement

The load was applied through two hydraulic jacks connected to a single feed hydraulic pump. The applied load was measured at the jacking points using 100 kN or 200 kN capacity load cells depending on the expected ultimate load. The load cells were calibrated before testing using a voltmeter.

The applied load was recorded with a voltmeter connected to a power supply. The load cells were also connected to a penchart recorder which automatically traced the loading history up to failure.

The test set-up is shown in Plate 3.3.

3.12 TESTING OF BEAMS

All beams were tested at a minimum age of 28 days, that is at least 7 days after prestressing.

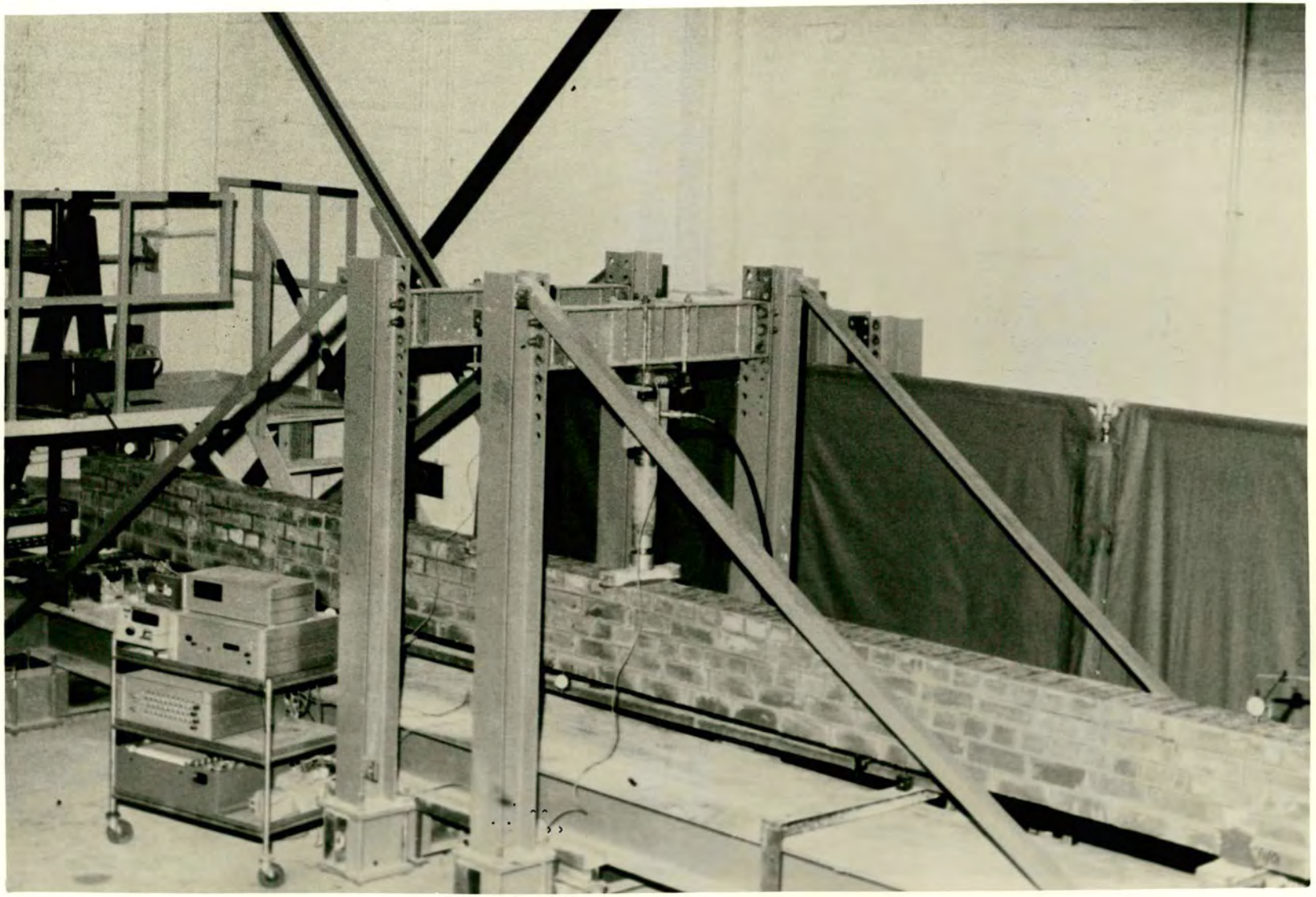

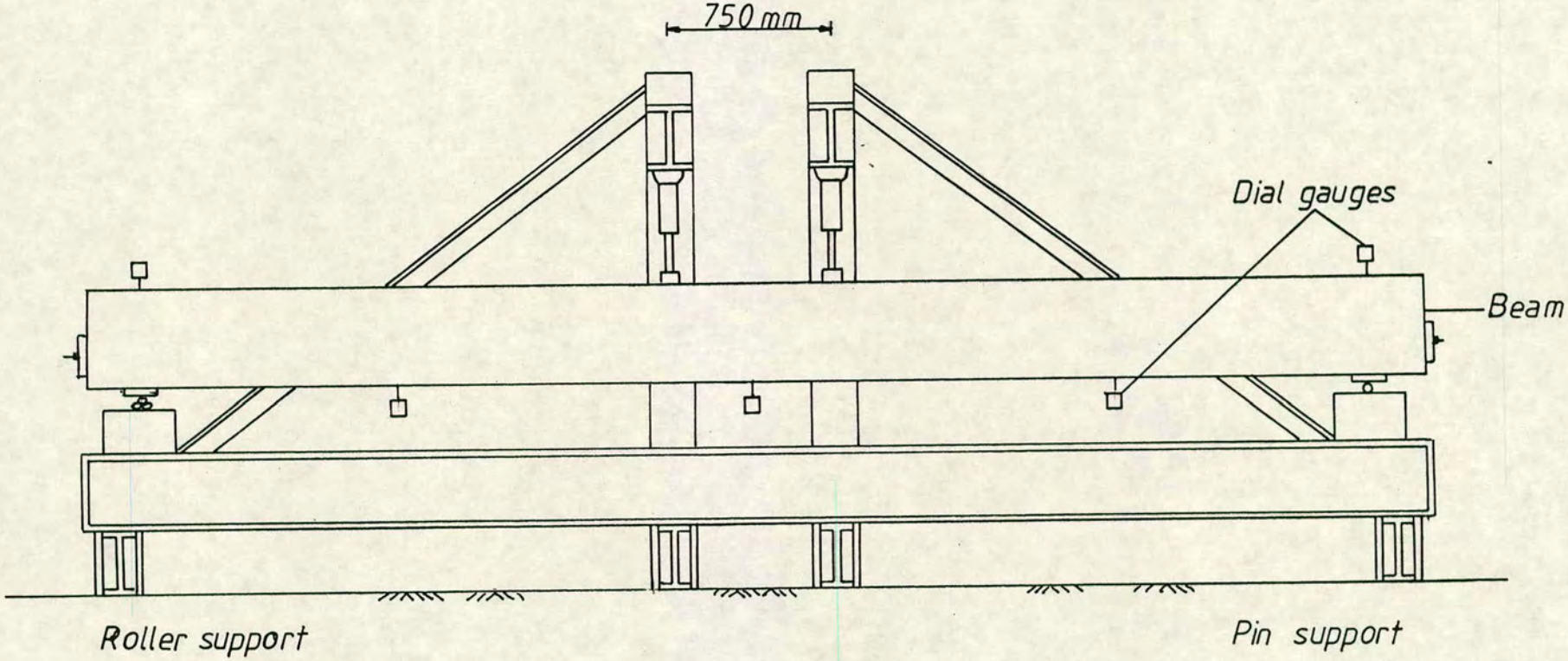

Fig. 3.12.1 Test Set-Up

3.12.1 The Test Rig

The beams were tested in the test rig as shown in Fig. 3.12.1 which is capable of testing beams up to a total length of 6.8 m. The beams were simply supported and tested under four point loading, the loading points being at a fixed distance apart. The simple supports were provided by a pin and a roller whose positions could be adjusted to give any span up to 6.2 m. At each support the beam rested on a bed of mortar carried by 25 mm thick mild steel bearing plates. The loading jacks were supported by 40 mm x 40 mm x 500 mm long mild steel plates placed on a bed of mortar. The test rig was self restraining.

3.12.2 The Test Procedure

All beams were prestressed and grouted upside down. Just before testing, they were turned the right way up using an overhead crane and slings. Each beam was then weighed using a load cell attached to the crane and transferred into the test rig. The average self weight for the fully prestressed brickwork beams, the partially prestressed brickwork beams and the concrete beams were 1.5 kN/m, 1.8 kN/m and 1.85 kN/m respectively.

Before any load was applied, all the initial readings were taken and the load cells connected to the pen chart recorder. The load increments were arranged so that a minimum of four sets of readings were taken before cracking, one at the first sight of a crack and about eight more before failure. At each load increment before cracking, the following data were recorded: the deflection readings on each of the five dial gauges, the brickwork/concrete strain in the constant moment zone, the strain readings on the tendons and where applicable on the reinforcing bar. After cracking, in addition to the above data , the crack widths within the constant moment zone were measured and the progress of these cracks marked on the beam. The ultimate load was reached when the beam became incapable of taking any further load.

In beams which failed in tension, because there was ample warning of impending failure, it was possible to take strain readings in the region of maximum compression very close to failure. In beams which failed in shear, for reasons of safety, this was not always possible.

CHAPTER 4
THE ULTIMATE MOMENT OF PRESTRESSED BEAMS

4.1 INTRODUCTION

The current British codes of practice for the structural use of concrete[58] and of reinforced and prestressed masonry[1] are based on the limit state method of design. The limit state method of design and the ultimate load or load factor method which it replaced are a better representation of flexural behaviour than the elastic method of design which they superseded. In the ultimate load method, the aim was to ensure that the design strength of the structure calculated using the actual material strength expected was sufficient to support the ultimate load obtained by increasing the service load by an overall safety factor. This overall safety factor was introduced to compensate for uncertainties in the loading, workmanship, strengths of materials, the construction process and in the current state of knowledge of structural behaviour. In the limit state method, the overall safety factor has been replaced by partial safety factors, one for each material and type of loading. The relative values of each partial safety factor reflects the relative uncertainty associated with the various loads and material strengths.

The use of partial safety factors overcomes an inherent weakness encountered with the overall safety factor approach when a structure is subjected to different types of loading simultaneously, where a more critical condition is achieved when one loading is at its maximum and the other at its minimum. An example of this is found with wind and vertical loading in a shear wall. The critical case is obtained with the maximum wind load and the minimum vertical load. The global safety factor approach automatically increases both the wind and the vertical load giving rise to a less critical condition than if only the wind load was increased.

The limit state method of design aims to ensure that the probabilty of a structure reaching a particular limit state is acceptable. The limit states are the ultimate limit state which covers collapse, buckling and overturning and the serviceability limit states of deflection, cracking and vibration. The scope of

this project has been confined to the ultimate limit state of collapse induced by the flexural and shear capacities being exceeded and the serviceability limit states of deflection and cracking. The general approach in both brickwork and concrete is to design for the most critical limit state and then check that the remaining limit states will not be reached. The failure of a structure to satisfy any limit state is tantamount to failure.

In reinforced brickwork and concrete, the ultimate limit state is assumed to be the critical limit state. The serviceability limit states of deflection and cracking will not normally be reached if the recommendations given for the span/effective depth ratios and reinforcement spacings are followed. However, in prestressed brickwork and concrete, the section has to be designed to suit the actual service load in order to determine the magnitude and position of the prestressing forces. Therefore, it is not possible to assume that a particular limit state will always be a critical one. As a result, the comparative study on the structural behaviour of prestressed beams of brickwork and concrete involved a detailed investigation under the ultimate limit states of flexure and shear and the serviceability limit states of deflection and cracking.

In this chapter, the ultimate moment and flexural strength of prestressed beams of brickwork and concrete with identical sectional properties and of similar compressive strength are compared (the shear strength of prestressed beams is examined in Chapter 7). Comparisons are also made with theoretical predictions including those obtained from the appropriate code of practice[1,58].

4.2 THEORY

The ultimate strength in flexure is reached when the brickwork (or concrete) or the tensile reinforcement or both, become incapable of resisting the internal forces necessary to provide flexural capacity. This is distinct from a shear failure which may occur at a lower moment than the ultimate flexural moment of resistance. When flexural failure is caused by the yielding of the tensile reinforcement, the section is under-reinforced. If on the other hand, flexural failure is precipitated by the crushing of the brickwork/concrete in the compression zone, the section is referred to as an over-reinforced section. When the yielding of the tensile reinforcement and the crushing of the

brickwork/concrete occur simultaneously, the section is known as a balanced section. The behaviour of a section at ultimate is dependent on whether the section is under-reinforced or over-reinforced.

In this section, the flexural theory for a rectangular fully bonded prestressed brickwork/concrete beam containing tensioned and non-tensioned tensile reinforcement at different levels is presented. The conditions necessary for a balanced failure in this type of section is also presented.

4.2.1 The Flexural Theory

The following assumptions are made in the development of the flexural theory for brickwork and concrete beams containing fully bonded tensioned and non-tensioned tensile reinforcement:

1. The strain distribution in brickwork/concrete in compression and of the tensile reinforcement in tension is derived from the assumption that plane sections remain plane. As will be seen in Section 4.3.1.1, this is a valid assumption.

2. The stress distribution in brickwork/concrete in the compression zone may be determined from the stress-strain relationship obtained from uniaxial tests on representative specimens (see Chapter 3).

3. The maximum strain in the outermost compression fibre at failure is known. As crushing of the compression zone will occur irrespective of whether the section is under- or over-reinforced, it can be assumed that the compression zone is fully developed.

4. The tensile strength of brickwork/concrete is ignored. This is because its value in brickwork and concrete is very low when compared to their compressive strengths. Therefore, the tensile stress distribution below the neutral axis depth will be very small. The combination of a small tensile strength and a small lever arm results in a very small contribution to the flexural strength.

5. The stresses in the tensioned and non-tensioned reinforcement are derived from the appropriate stress-strain relationship.

6. The magnitude of any initial strain in the tensioned reinforcement is known. This is necessary to obtain the total strain and hence the total tensile force in the tensioned reinforcement.

Consider the case of a prestressed brickwork beam containing tensioned and non-tensioned tensile reinforcement at different levels as shown in Fig. 4.2.1:

The stress-strain relationship for brickwork in compression is given as:

$$f_m = F_m(\varepsilon)$$

... 4.2.1

where
f_m = the stress in brickwork
$F_m(\varepsilon)$ = the stress-strain relationship for brickwork

The stress-strain relationship for the non-tensioned reinforcement is given as:

$$f_s = F_s(\varepsilon_s)$$

... 4.2.2

where
f_s = stress in the non-tensioned steel
$F_s(\varepsilon_s)$ = stress-strain relationship for the non-tensioned steel

$$\varepsilon_s = \varepsilon_{sp} + \varepsilon_{sa} + \varepsilon_{se}$$

... 4.2.3

where
ε_s = total strain in the non-tensioned reinforcement
ε_{sp} = strain in the non-tensioned steel due to prestress (assumed to be equal to zero)
ε_{sa} = strain in the non-tensioned reinforcement due to applied loads
ε_{se} = strain in the brickwork at the level of the steel due to the prestressing force and dead load

The stress-strain relationship for the tensioned reinforcement is:

$$f_p = F_p(\varepsilon_p)$$

... 4.2.4

where
f_p = stress in the tensioned steel
$F_p(\varepsilon_p)$ = stress-strain relationship for the tensioned steel

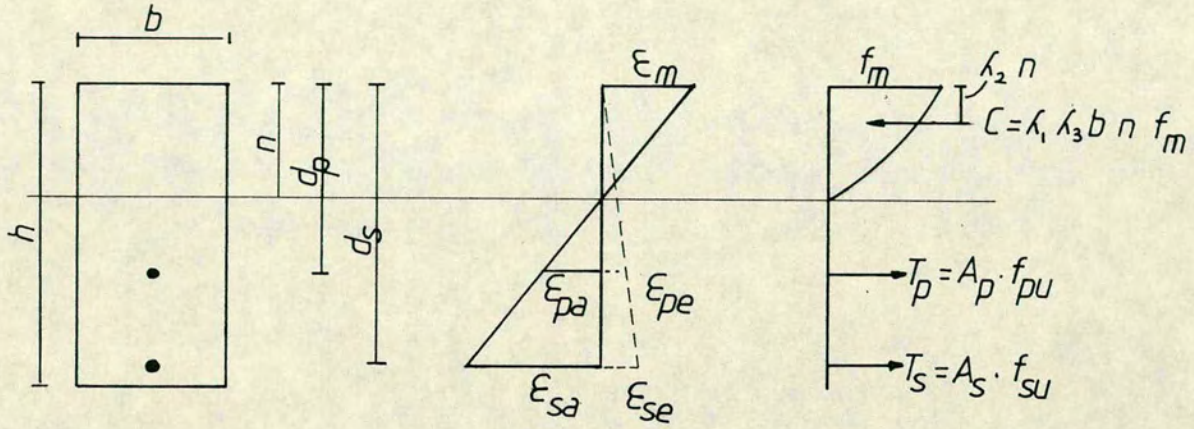

Fig. 4.2.1 Conditions in a Partially Prestressed Brickwork Beam at Failure

$$\varepsilon_p = \varepsilon_{pp} + \varepsilon_{pa} + \varepsilon_{pe}$$

... 4.2.5

where
ε_p = total strain in the tensioned reinforcement
ε_{pp} = strain in the tensioned steel due to effective prestress
ε_{pa} = strain in the tensioned steel due to applied loads
ε_{pe} = strain in the brickwork at the level of the tensioned steel due to the effects of the prestress and dead load.

Assuming that the maximum strain in the brickwork at failure is ε_m, the strain in the non-tensioned reinforcement due to applied load is:

$$\varepsilon_{sa} = \varepsilon_m . (d_s - n)/n$$

... 4.2.6

where d_s is the depth to the non-tensioned steel and n is the depth of the neutral axis.

The strain in the tensioned steel due to applied load is given by:

$$\varepsilon_{pa} = \varepsilon_m . (d_p - n)/n$$

... 4.2.7

where d_p is the depth to the tensioned steel.

The total compressive force in the section is given by:

$$C = b \int_0^n F_m(\varepsilon)\ \delta x$$

... 4.2.8

where $\varepsilon = \varepsilon_m(1 - x/n)$

The total tensile force T is given by:

$$T = T_s + T_p$$

... 4.2.9

Where T_s and T_p are the total tensile forces in the non-tensioned and tensioned steel respectively given by:

$$T_s = F_s(\varepsilon_s)\ A_s$$

... 4.2.10

$$T_p = F_p(\varepsilon_p)\ A_p$$

... 4.2.11

A_s and A_p are the areas of non-tensioned and tensioned steel respectively.

For equilibrium,

$$C = T$$

$$b \int_0^n F_m(\varepsilon)\, dx = F_s(\varepsilon_s)A_s + F_p(\varepsilon_p)A_p$$

... 4.2.12

The neutral axis depth n, is obtained by solving equation 4.2.12. The ultimate flexural moment of resistance is then obtained by taking moments of the forces about the neutral axis depth i.e.

$$M_u = b\int_0^n F_m(\varepsilon)x\delta x + F_s(\varepsilon_s)A_s(d_s - n) + F_p(\varepsilon_p)A_p(d_p - n)$$

... 4.2.13

A more convenient way of describing the compressive stress distribution in the compressive zone is in terms of the stress block factors λ_1, λ_2 and λ_3 discussed in Chapter 3. Using these factors, the compressive force C in equation 4.2.12 can be written as:

$$C = \lambda_1 . \lambda_3 . f_m . b . n$$

... 4.2.14

From equations 4.2.9-4.2.11, the tensile force at failure, T may also be expressed as:

$$T = f_{su} . A_s + f_{pu} . A_{pu}$$

... 4.2.15

where f_{su} and f_{pu} are the stresses in the non-tensioned and tensioned steel at ultimate respectively.

From equations 4.2.14 and 4.2.15, the equilibrium equation can be written as:

$$\lambda_1.\lambda_3.f_m.b.n = f_{su}.A_s + f_{pu}.A_p$$

... 4.2.16

The neutral axis depth can again be obtained from equation 4.2.16.

Once the neutral axis depth n, has been obtained, since the maximum strain in the brickwork ε_m is known (see assumption 3) and the prestrain in the tensioned steel is also known (see assumption 6), the total strain in the tensioned and non-tensioned reinforcement can be calculated from equations 4.2.6, 4.2.7, 4.2.3 and 4.2.5. The corresponding stresses are obtained from the appropriate stress-strain relationships, equations 4.2.2 and 4.2.4 and the tensile forces, T_s and T_p can then be calculated from equations 4.2.10 and 4.2.11.

Taking moments about the line of action of the compressive force, the ultimate flexural moment of resistance is given by:

$$M_{um} = f_{su}.A_s(d_s - \lambda_2.n) + f_{pu}.A_p(d_p - \lambda_2.n) \quad \text{... 4.2.17}$$

Alternatively, the ultimate flexural moment of resistance can be obtained by taking moments of the resultant compressive force about the line of action of the resultant tensile force:

$$M_{ut} = \lambda_1.\lambda_3.f_m.b.n(d_r - \lambda_2.n) \quad \text{... 4.2.18}$$

where

$$d_r = [T_s.d_s + T_p.d_p]/[T_s + T_p] \quad \text{... 4.2.19}$$

The ultimate flexural moment for a fully or partially prestressed concrete beam can also be obtained in the same way by substituting the properties of the concrete where appropriate.

4.2.2 The Balanced Section

It was mentioned above that the behaviour of a section which fails in flexure depends on whether the section is under- or over-reinforced. An under-reinforced section fails in tension by yielding of the tensile reinforcement. Therefore, large deflections and considerable widening of cracks are evident before failure. In a flexural compression failure which is associated with over-reinforced sections, crushing of the brickwork/concrete

occurs before the tensile reinforcement yields. Consequently, this type of flexural failure generally occurs with very little warning. It also leads to an inefficient use of the materials. In practice it is therefore important to know whether a design solution is over- or under-reinforced. An under-reinforced section is favoured in design as this gives adequate warning of impending collapse and results in an efficient use of the tensile reinforcement which is expensive.

Whether or not a section is over- or under-reinforced can be ascertained from the area of steel required for a balanced section i.e one in which the yielding of the steel occurs simultaneously with the crushing of the brickwork/concrete in the compression zone.

In a beam containing non-tensioned steel only, the determination of a balanced section is a simple procedure. The steel area corresponding to a balanced reinforced section (in this case, brickwork) is given as follows:

$$\rho_{bal} = \lambda_1.\lambda_3.\ f_m/f_{sy}.\ \varepsilon_m/(\varepsilon_m + \varepsilon_{sy})$$

... 4.2.20

where
ε_{sy} = yield strain of the non-tensioned reinforcement

A balanced prestressed section containing tensioned steel only is rather more complex as the steel stress at failure and hence the balanced steel area is dependent on the prestrain in the tensioned steel. The steel area for a balanced fully prestressed beam is given as:

$$\rho_{bal} = \lambda_1.\lambda_3.f_m/f_{py}.\varepsilon_m/[\varepsilon_m + \varepsilon_{py} - (\varepsilon_{pe} + \varepsilon_{pp})]$$

... 4.2.21

In the general case of a section containing tensioned and non-tensioned steel at different levels, the determination of the balanced section is even more complicated. This will be examined in the following section.

4.2.2.1 A Balanced Partially Prestressed Section

For a partially prestressed section containing tensioned and non-tensioned tensile reinforcement with different yield strengths placed at different levels, the conventional definition of a balanced section is inappropriate for most practical applications. This is because the condition necessary for simultaneous yielding of both types of tensile reinforcements are unacceptable in practice. Thurlimann[65] has shown that when both types of tensile reinforcement are present at the same level, for both to yield simultaneously, the tensioned reinforcement must be stressed to the difference between its proof stress and the yield strength of the non-tensioned reinforcement. From the figures quoted in BS 5896: 1980[63] for high tensile steel strand and in BS 4449[64] for hot rolled steel, the tendons need to retain 70% of the breaking load after all losses have taken place. This figure of 70% is coincident with the maximum jacking force recommended by BS 5628: Part 2: 1985[1] and is sligthly lower than the normal recommended by BS 8110: Part 1: 1985[58] of 75%. When lock-off losses and losses due to creep and shrinkage etc are taken into account such amounts of effective prestress can not be obtained without violating these design recommendations.

With both types of tensile reinforcement at different levels, Walker[12] has shown that for the condition of balanced failure where the tensioned and non-tensioned steel yield simultaneously, as the depth of the non-tensioned steel increases, so also does the amount of prestress necessary to achieve balanced behaviour i.e effective prestressing forces in excess of 70% of the breaking load is necessary to achieve balanced behaviour when the non-tensioned steel is placed nearer the soffit.

Therefore it is extremely unlikely that both types of tensile reinforcement will yield simultaneously. Another approach to the problem of a balanced partially prestressed section is to consider one type of reinforcement yielding first followed by the simultaneous yielding of the other tensile reinforcement and crushing of the brickwork/concrete. Firstly, it is necessary to establish which of the tensile reinforcement will yield first - the tensioned reinforcement with its prestrain or the non-tensioned reinforcement with is comparatively low yield strain.

Consider the case where it is the non-tensioned reinforcement which

yields first in a brickwork section (see Fig. 4.2.1) with f_{pu} and f_{su} replacing f_p and f_s, respectively. The relationship between the additional strain due to applied loads in both the tensioned reinforcement (ε_{pa}) and the non-tensioned reinforcement (ε_{sa}) is given by:

$$\varepsilon_{pa}/\varepsilon_{sa} = [d_p - n]/[d_s - n] = \chi$$

... 4.2.22

As the non-tensioned steel yields before the tensioned steel, then:

$$\varepsilon_{sa} = \varepsilon_{sy} - \varepsilon_{se}$$

... 4.2.23

and

$$\varepsilon_{pe} + \varepsilon_{pp} + \varepsilon_{pa} < \varepsilon_{py}$$

... 4.2.24

From 4.2.22-4.2.24,

$$\varepsilon_{pe} + \varepsilon_{pp} + (\varepsilon_{sy} - \varepsilon_{se}).\chi < \varepsilon_{py}$$
or
$$(\varepsilon_{pe}/\varepsilon_{py}) + (\varepsilon_{pp}/\varepsilon_{py}) + (\varepsilon_{sy}/\varepsilon_{py}).\chi - (\varepsilon_{se}/\varepsilon_{py}).\chi < 1$$

... 4.2.25

The maximum value of the left hand side of equation 4.2.25 is obtained when χ=1.0 i.e when the tensioned and non-tensioned steel are at the same level. Then $\varepsilon_{pe}/\varepsilon_{py} = \varepsilon_{se}/\varepsilon_{py}$ and equation 4.2.25 becomes:

$$[\varepsilon_{pp}/\varepsilon_{py}] + [\varepsilon_{sy}/\varepsilon_{py}] < 1$$

... 4.2.26

From references 11, 12, 63, and 64, typical values of $\varepsilon_{pp}/\varepsilon_{py}$ and $\varepsilon_{sy}/\varepsilon_{py}$ are around 0.44 and 0.45 respectively. Therefore equation 4.2.26 will always hold implying that the non-tensioned reinforcement will always yield before the tensioned steel.

Conversely, let us assume that it is the tensioned reinforcement which yields before the non-tensioned reinforcement. For this to occur;

$$\varepsilon_{py} = \varepsilon_{pp} + \varepsilon_{pa} + \varepsilon_{pe}$$

... 4.2.27

From equation 4.2.22,

$$\varepsilon_{sa} = \varepsilon_{pa}/\chi$$

... 4.2.28

Also,

$$\varepsilon_{se} + \varepsilon_{sa} < \varepsilon_{sy}$$

... 4.2.29

Equations 4.2.27–4.2.29 give:

$$\varepsilon_{se} + [\varepsilon_{py} - \varepsilon_{pp} - \varepsilon_{pe}]/\chi < \varepsilon_{sy}$$

... 4.2.30

or

$$[(\varepsilon_{se}/\varepsilon_{sy})\chi + \varepsilon_{py}/\varepsilon_{sy} - \varepsilon_{pp}/\varepsilon_{sy} - \varepsilon_{pe}/\varepsilon_{sy}]\ 1/\chi < 1$$

As before, the maximum value of the l.h.s is obtained when χ=1.0. Then

$$[\varepsilon_{py}/\varepsilon_{sy} - \varepsilon_{pp}/\varepsilon_{sy}] < 1$$

... 4.2.31

With typical values of $\varepsilon_{py}/\varepsilon_{sy}$ of 2.22 and $\varepsilon_{pp}/\varepsilon_{sy}$ of 1.13 equation 4.2.31 is always false.

There is experimental evidence to support the theory that the non-tensioned reinforcement will yield before the tensioned reinforcement. In the partially prestressed brickwork beams tested by Walker[12], of the 41 beams tested, 37 failed in flexure with the non-tensioned steel always yielding before the tensioned steel. In the partially prestressed concrete beams tested in reference 66, even though the non-tensioned and tensioned steel were placed at the same level, the non-tensioned steel also yielded before the tensioned steel.

4.2.2.2 The Condition for a Balanced Partially Prestressed Section

It was established above that in a partially prestressed section containing tensioned and non-tensioned tensile steel with different yield strengths at different levels, the non-tensioned steel will always yield before the tensioned reinforcement. Thus for such a section to be balanced, it has to be under-reinforced with respect to the non-tensioned reinforcement in order for it to be balanced with respect to the total tensile reinforcement.

The relation for a balanced partially prestressed section will consist of

two parts. Firstly, crushing of the brickwork/concrete and yielding of the non-tensioned steel will be assumed to occur simultaneously with the contribution of the tensioned steel taken into account. Then, the yielding of the tensioned steel and crushing of the brickwork/concrete will be assumed to occur simultaneously with the contribution of the non-tensioned steel taken into account.

From Fig. 4.2.1, for a brickwork section,

$$C = T_s + T_p \qquad \text{...4.2.32}$$

$$C = \lambda_1.\lambda_3.b.n.f_m \qquad \text{... 4.2.33}$$

$$T_s = A_s.\ f_{sy} \qquad \text{... 4.2.34}$$

$$T_p = A_p.\ f_p \qquad \text{... 4.2.35}$$

When the non-tensioned steel has yielded, the additional strain in the tensioned steel due to applied load is given by:

$$\varepsilon_{pa}/(\varepsilon_{sy} - \varepsilon_{se}) = (d_p - n)/(d_s - n)$$

i.e

$$\varepsilon_{pa} = [(d_p - n)/(d_s - n)](\varepsilon_{sy} - \varepsilon_{se}) \qquad \text{... 4.2.36}$$

From equation 4.2.32

$$\lambda_1.\lambda_3.b.n.f_m = A_s.f_{sy} + A_p.f_p$$

Dividing by d_s

$$n/d_s = [A_s/b.d_s.f_{sy}/f_m + A_p/b.d_s.f_p/f_m]/[\lambda_1.\lambda_3] \qquad \text{... 4.2.37}$$

Considering the strain distribution:

$$\varepsilon_m/n = [\varepsilon_{sy} - \varepsilon_{se}]/[d_s - n] \qquad \text{... 4.2.38}$$

$$\varepsilon_m(d_s - n) = n(\varepsilon_{sy} - \varepsilon_{se})$$

$$n(\varepsilon_{sy} - \varepsilon_{se} + \varepsilon_m) = \varepsilon_m . d_s$$

$$n/d_s = \varepsilon_m/[\varepsilon_{sy} - \varepsilon_{se} + \varepsilon_m]$$

... 4.2.39

From equations 4.2.37 and 4.2.39

$$\varepsilon_m/[\varepsilon_{sy}-\varepsilon_{se}+\varepsilon_m]=[1/\lambda_1.\lambda_3].[A_s/b.d_s\ f_{sy}/f_m + A_p/b.d_s\ f_p/f_m]$$

$$[\lambda_1.\lambda_3.\varepsilon_m]/[\varepsilon_{sy}-\varepsilon_{se}+\varepsilon_m]=[A_s/b.d_s\ f_{sy}/f_m]+[A_p/b.d_s\ f_p/f_m]$$

... 4.2.40

let $\rho_{s(bal)} = A_s/b.d_s$, then

$$\rho_{s(bal)} = f_m/f_{sy}[\lambda_1.\lambda_3.\varepsilon_m/(\varepsilon_{sy}-\varepsilon_{se}+\varepsilon_m) - A_p/b.d_s.\ f_p/f_m]$$

... 4.2.41

For a conventionally reinforced beam section, ε_{se} is zero and equation 4.2.41 becomes:

$$\rho_{s(bal)} = \lambda_1.\lambda_3\ f_m/f_{sy}.\ \varepsilon_m/(\varepsilon_{sy}+\varepsilon_m)$$

which is identical to equation 4.2.20.

For the second part of the relation for a balanced partially prestressed section, the non-tensioned reinforcement has yielded and the yielding of the tensioned reinforcement and the crushing of the brickwork/concrete are assumed to occur simultaneously.

Also, from Fig. 4.2.1:

$$\varepsilon_{py} = \varepsilon_{pa} + \varepsilon_{pp} + \varepsilon_{pe}$$

...4.2.43

The strain distribution at the yielding of the tendon is given by:

$$\varepsilon_m/n = \varepsilon_{pa}/(d_p - n)$$

... 4.2.44

Equations 4.2.43 and 4.2.44 give:

$$\varepsilon_m/n = [\varepsilon_{py}-\varepsilon_{pp}-\varepsilon_{pe}]/[d_p - n]$$

$$n[\varepsilon_{py} - \varepsilon_{pp} - \varepsilon_{pe} + \varepsilon_m] = \varepsilon_m.d_p$$

$$n/d_p = \varepsilon_m/[\varepsilon_{py}-\varepsilon_{pp}-\varepsilon_{pe}+\varepsilon_m]$$

... 4.2.45

From equation 4.2.32

$$\lambda_1.\lambda_3.b.n.f_m = A_s.f_{sy} + A_p.f_{py}$$

$$n/d_p = [(A_s/b.d_p\ f_{sy}/f_m) + (A_p/b.d_p\ f_{py}/f_m)]/[\lambda_1.\lambda_3]$$

... 4.2.46

Equating 4.2.45 and 4.2.46

$$\varepsilon_m/[\varepsilon_{py}-\varepsilon_{pp}-\varepsilon_{pe}+\varepsilon_m]=[(A_s/b.d_p f_{sy}/f_m) + (A_p/b.d_p f_{py}/f_m)]/[\lambda_1.\lambda_3]$$

... 4.2.47

let $\rho_{p(bal)} = A_p/b.d_p$

... 4.2.48

Then

$$\rho_{p(bal)}=[(\lambda_1.\lambda_3.\varepsilon_m)/(\varepsilon_{py}-\varepsilon_{pp}-\varepsilon_{pe}+\varepsilon_m)-A_s/b.d_p f_{sy}/f_m]f_m/f_{py}$$

... 4.2.49

For a prestressed section containing no non-tensioned reinforcement:

$$\rho_{p(bal)} =\lambda_1.\lambda_3\ f_m/f_{py}[\varepsilon_m/(\varepsilon_m+\varepsilon_{py}-(\varepsilon_{pe}+\varepsilon_{pp})]$$

which is identical to equation 4.2.21 derived for a fully prestressed section.

The above derivations are also applicable to a concrete section as long as the properties of concrete are substituted where appropriate.

4.3 EXPERIMENTAL RESULTS, DISCUSSION AND COMPARISON WITH THEORY

In this section, the experimental results for the ultimate moment obtained for all the brickwork and concrete beams reported in this study are presented. A summary of these results and some properties of the beams are presented in Table 4.3.1. The failure mode of each beam was identified from strain readings in the tensile reinforcement and the extreme compression fibre at failure. The shear stresses in Table 4.3.1 were obtained from the ultimate load at failure irrespective of whether failure was in flexure or shear.

Table 4.3.1 Summary of Experimental Results

Beam	% area of steel	Effective prestress	Compressive* strength	Ultimate moment	Failure mode	Span	a/d ratio	Shear stress
		kN	N/mm^2	kNm		m		N/mm^2
Brickwork beams[11]								
FB1	0.274	133	32.6	56.9	Tension	6.2	11.2	0.440
FB2	"	115	"	56.4	"	"	"	0.428
FB3	"	133	"	61.5	"	"	"	0.476
FB4	"	144	"	58.4	"	"	"	0.448
FB5	"	133	"	59.2	"	"	"	0.454
FB6	"	152	"	58.8	"	"	"	0.451
Concrete beams								
CB1	0.274	137	42.8	58.8	Tension	6.2	11.2	0.458
CB2	"	132	45.0	58.1	"	"	"	0.453
CB3	"	115	38.7	59.1	"	"	"	0.461
CB5	"	136	39.9	57.6	"	"	"	0.450
Brickwork beams[11]								
BB1	0.548	275	32.6	87.2	Shear	6.2	11.2	0.657
BB2	"	213	"	72.5	"	"	"	0.547
BB3	"	212	"	71.5	"	"	"	0.549
BB4	"	199	"	75.2	"	"	"	0.572
Concrete beams								
CB4	0.548	283	41.6	103.0	Tension	6.2	11.2	0.765
CB7	"	219	43.3	103.4	"	"	"	0.775
CB8	"	183	44.1	100.1	"	"	"	0.744
Partially Prestressed Beams								
Brickwork beams								
B1	0.341+	56	32.7	66.4	Shear	1.65	1.5	2.246
B2	"	56	"	86.1	Tension[2]	"	"	2.909
B12	"	57	"	67.2	Shear	"	"	2.357
B16	"	51	"	47.8	"	"	"	1.616
Concrete beams								
CB11	0.341+	54	42.0	115.1	Tension[2]	1.65	1.5	3.922
CB12	"	57	45.0	97.1	"	"	"	3.309
Brickwork beams								
B3	0.341+	64	32.7	84.9	Tension[2]	2.55	3.0	1.444
B7	"	57	"	73.6	Shear	"	"	1.251
B11	"	61	"	59.6	"	"	"	1.037
B15	"	64	"	66.7	"	"	"	1.159
Concrete beams								
CB9	0.341+	61	42.1	87.5	Shear	2.55	3.0	1.502
CB10	"	62	43.2	94.9	Tension[2]	"	"	1.628

Table 4.3.1 contd. Summary of Experimental Results

Beam	% area of steel	Effective prestress kN	Compressive* strength N/mm^2	Ultimate moment kNm	Failure mode	Span m	a/d ratio	Shear stress N/mm^2
Brickwork beams								
B4	0.341+	69	32.7	76.0	Shear	3.3	4.3	0.912
B5	"	65	"	68.0	"	3.5	4.5	0.784
B6	"	59	"	93.8	Tension[2]	"	"	1.073
B13	"	70	"	69.6	Shear	"	"	0.801
Brickwork beams								
B8	0.341+	65	32.7	70.1	Shear	4.35	6.0	0.615
B9	"	63	"	88.8	"	"	"	0.749
B10	"	62	"	93.8	Tension[2]	"	"	0.784
B14	"	69	"	69.0	Shear	"	"	0.597

Notes
[2] = secondary shear failure
* = prism strength for brickwork or cube crushing strength for concrete
+ = effective area of tensioned steel
Shear stress=V/b.d at failure irrespective of the failure mode

The ultimate moment of prestressed beams of brickwork and concrete of identical cross-sectional properties and of similar compressive strengths are compared. A comparison is also made with theoretical results.

4.3.1 General Experimental Observations

The initial behaviour of all beams under the application of load were similar irrespective of the mode of failure. In the following sections, the strain distribution and the relationship between the moment and the tensile strain, the top fibre strain and the neutral axis depth are discussed.

4.3.1.1 The Strain Distribution

The strain distribution was obtained from strain readings taken at various depths on the surface of the brickwork/concrete (see Chapter 3). Typical strain profiles are shown in Figs. 4.3.1–4.3.3. These figures show that the strain distribution is sensibly linear throughout the loading history, thereby confirming one of the assumptions made in the development of the flexural theory in Section 4.2.

Initially, the eccentric prestressing force induces a triangular distribution of compressive strain with the maximum strain occurring at the soffit. The application of load introduces compressive strains to the upper sections of the beam and reduces those at the lower sections until the prestrain at the soffit is completely neutralised. Between prestressing and decompression at the soffit, the neutral axis lies outside the section. Further increases in load produce tensile strains at the soffit so that the curvature (the slope of the strain profile) is reversed. The neutral axis then rises into the beam section.

The neutral axis depth at failure was dependent on the area of steel and the mode of failure. In the brickwork beams which failed in flexural tension, the neutral axis depth at failure was less than 65 mm validating the adoption of the single course prisms as representative of these beams at ultimate in flexure.

The theory presented in Section 4.2 was based on the assumption that full bond exists between the tensile reinforcement and the concrete and in the

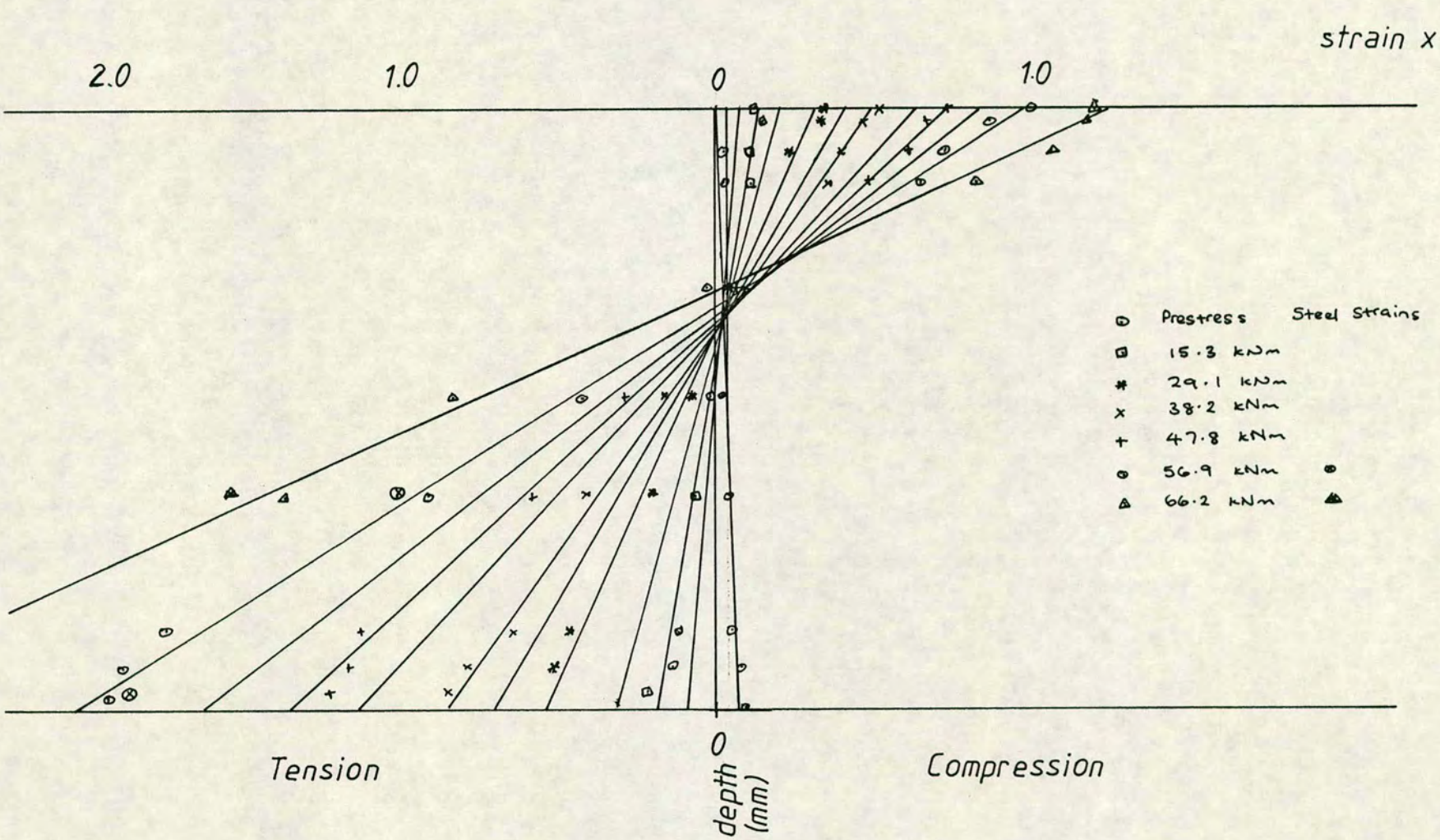

Fig. 4.3.1 Typical Strain Distribution for Partially Prestressed Brickwork

a/d = 3.0

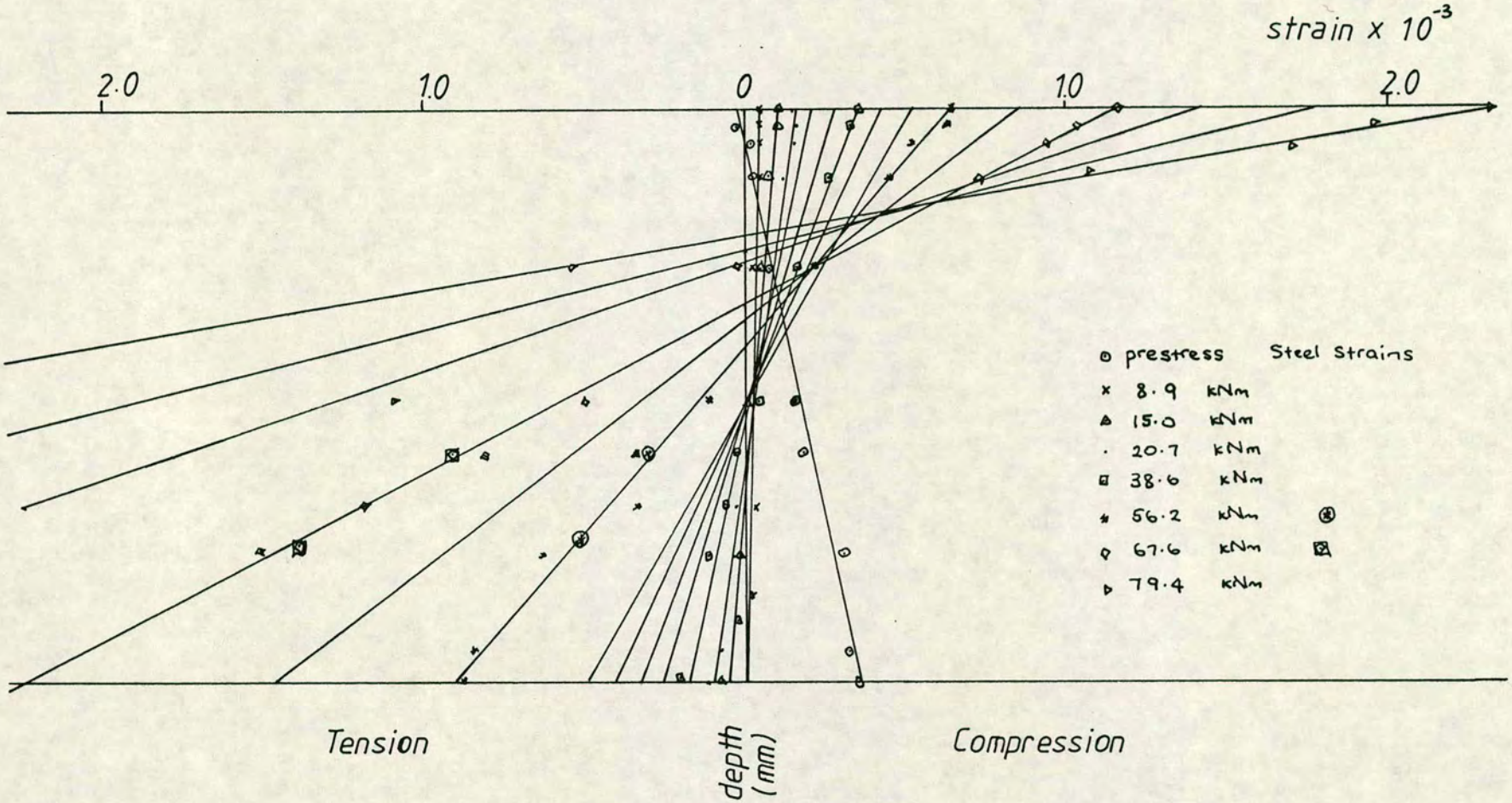

Fig. 4.3.2 Typical Strain Distribution in the Concrete Beams

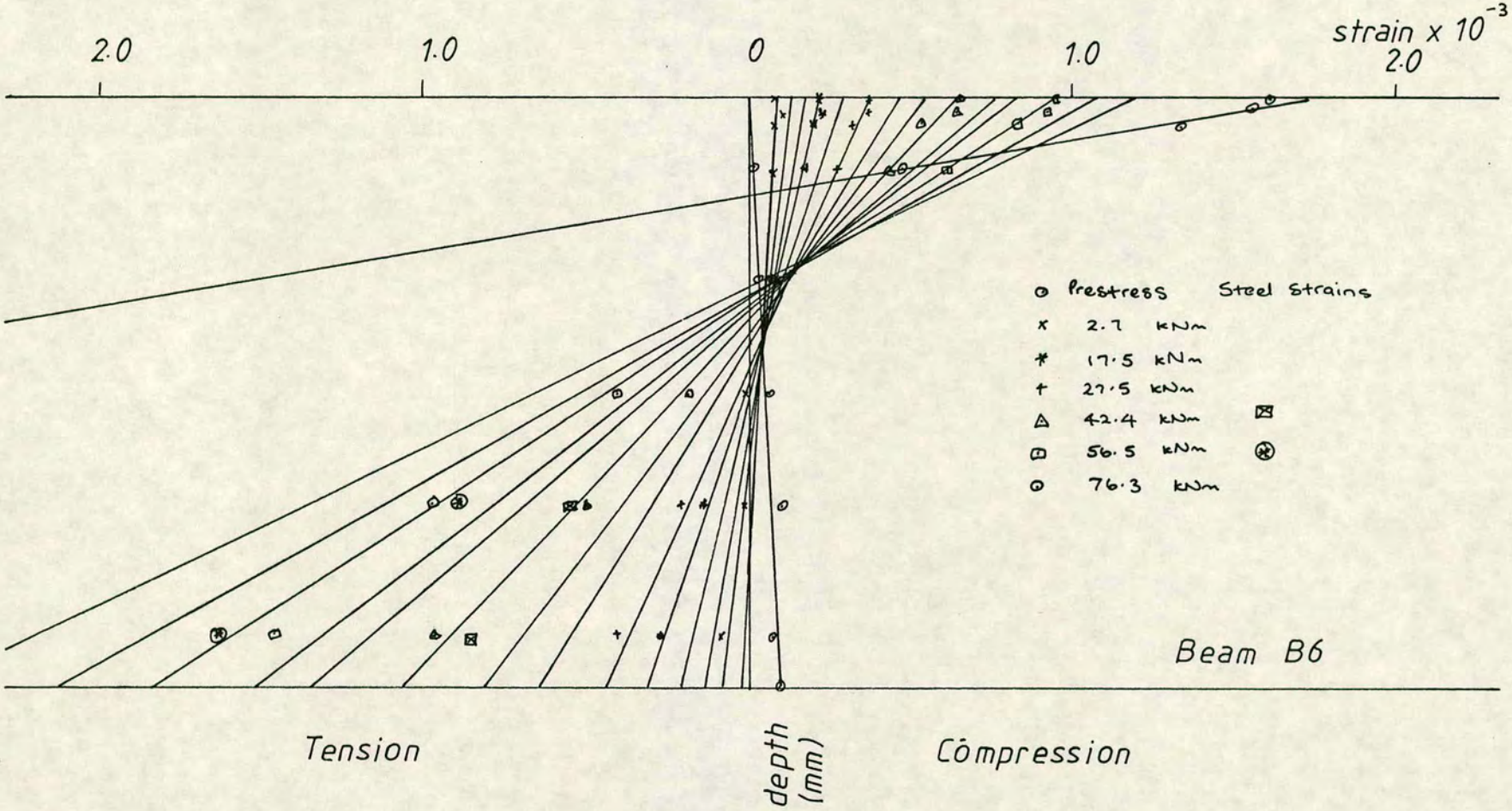

Fig. 4.3.3 Typical Strain Distribution in a Partially Prestressed Beam Exhibiting Secondary Shear Failure

brickwork beams, also between the brickwork shell and the concrete cavity. This was confirmed by strain readings taken on the surface of the tensile reinforcement with electrical resistance strain gauges which were in good agreement with those obtained from the surface of the brickwork/concrete using demec gauges (see Fig. 4.3.1–4.3.3).

4.3.1.2 The Relationship Between the Moment and the Strain in the Tensile Reinforcement

In Figs. 4.3.4–4.3.12, the relationship between the moment and the strain in the tensile reinforcement for all the beams reported in this study are presented. The relationships for the fully prestressed brickwork beams have been reproduced from reference 11. The strain in the tensile reinforcements were obtained from strain readings taken on the surface of the brickwork/concrete across a crack in the region of constant and maximum moment and so represents the maximum strains. The strain so measured in the tensioned reinforcement was therefore the additional strain due to the applied load i.e excluding that induced by the effective prestressing force.

In the partially prestressed beams, compressive strains were recorded in the non-tensioned steel after the grout had attained some strength. These were caused by the compressive stresses in the brickwork/concrete at the level of the non-tensioned steel due to the prestress, and by shrinkage and creep in the concrete surrounding the non-tensioned steel. However, the magnitude of these compressive strains were insignificant (maximum measured was 1×10^{-5}) compared to subsequent levels of strain due to the applied moment. The relationship between the moment and the tensile strain in the non-tensioned steel therefore began at the origin.

In general, the relationship between the moment and the additional strain in the tensioned reinforcement and that between the moment and the total strain in the non-tensioned reinforcement were very similar. Initially, there was a linear variation in strain with applied moment. After cracking however, there was a rapid increase in strain with applied moment until failure. Also shown on each of these figures are the average failure moment and the strain necessary for yielding of the tensile reinforcement. Close to failure, excessive deflections and widening cracks made it unsafe to take strain readings with the demec gauge. However, the maximum strains at failure were obtained by

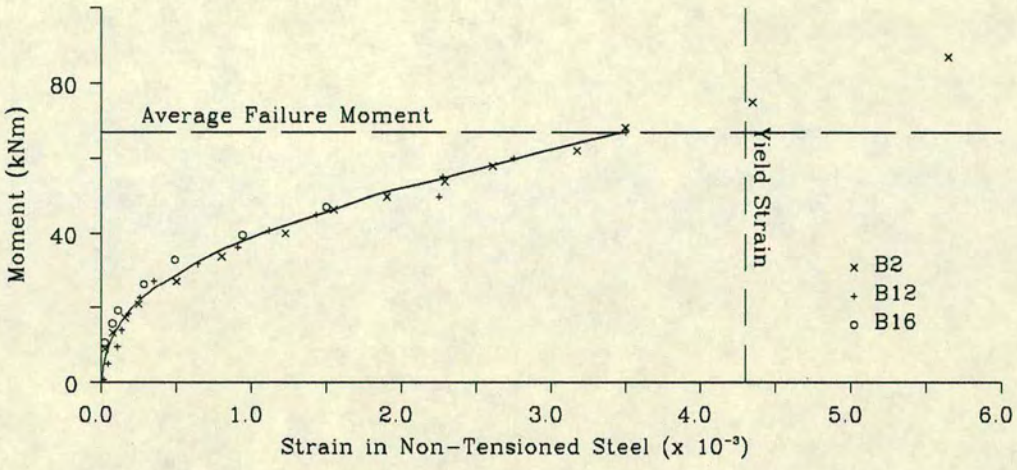

Fig. 4.3.4a Strain in the Non-Tensioned Steel
Partially Prestressed Brickwork Beams, A_{ps}=0.341%, a/d=1.5

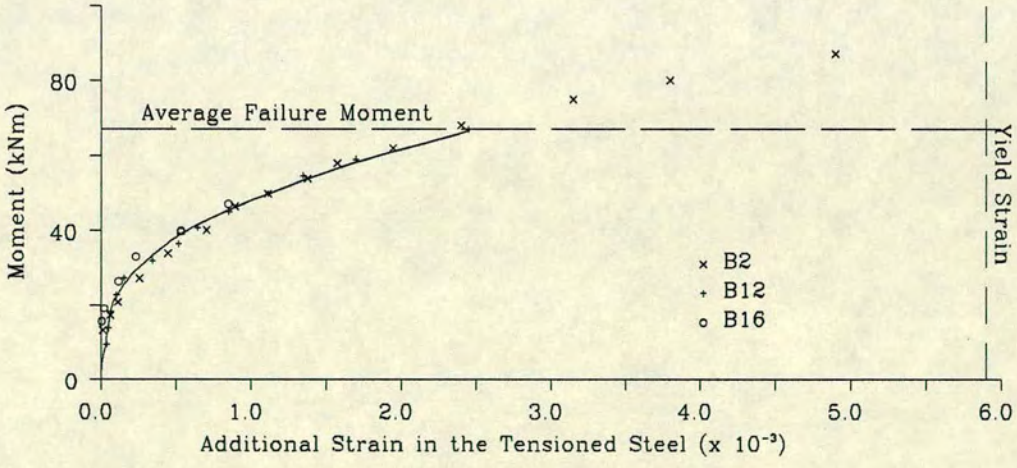

Fig. 4.3.4b Additional Strain in the Tensioned Steel
Partially Prestressed Brickwork Beams, A_p=0.341% , a/d=1.5

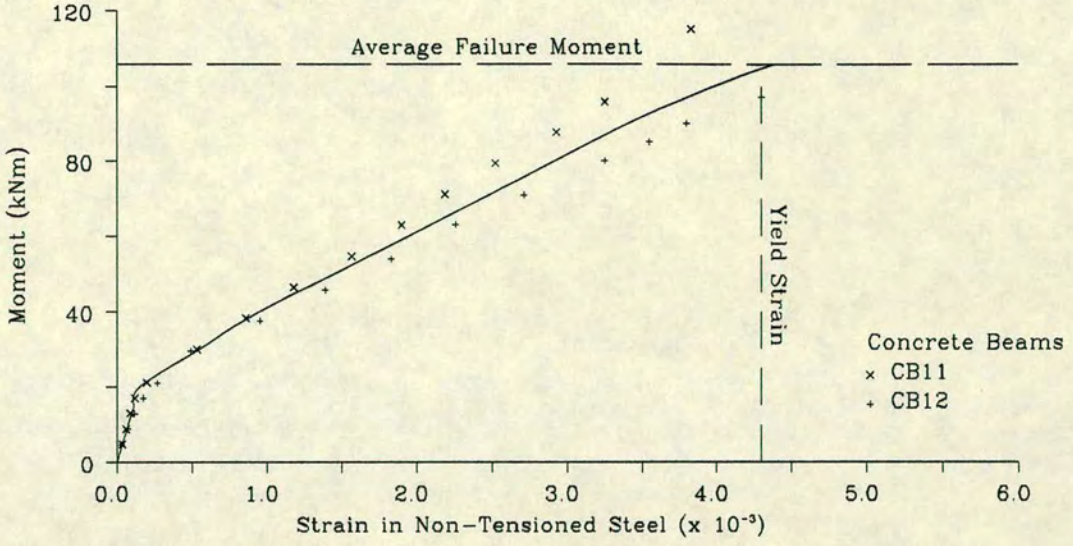

Fig. 4.3.5a Strain in the Non-Tensioned Steel
Partially Prestressed Concrete Beams, a/d=1.5

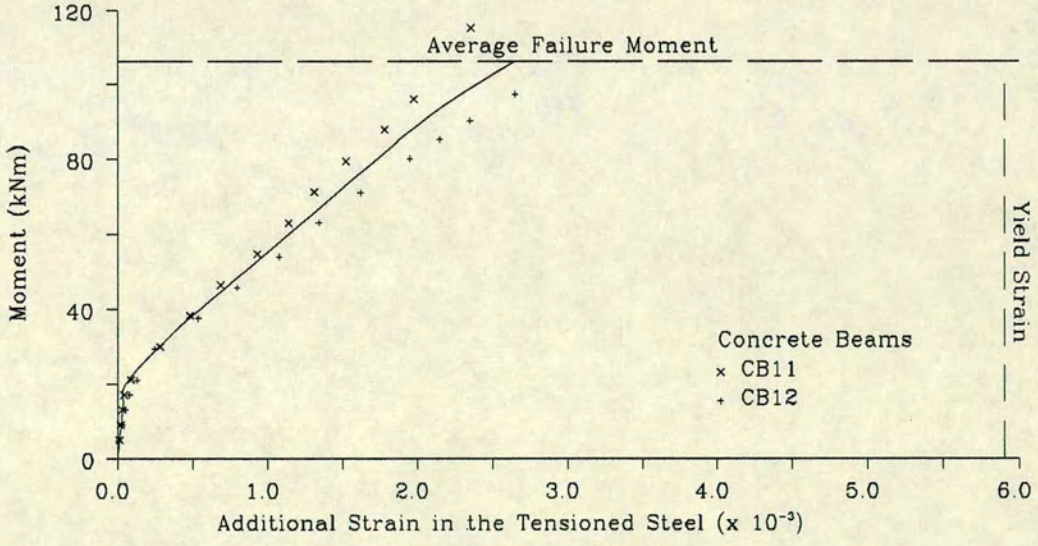

Fig. 4.3.5b Additional Strain in the Tensioned Steel
Partially Prestressed Concrete Beams, a/d=1.5

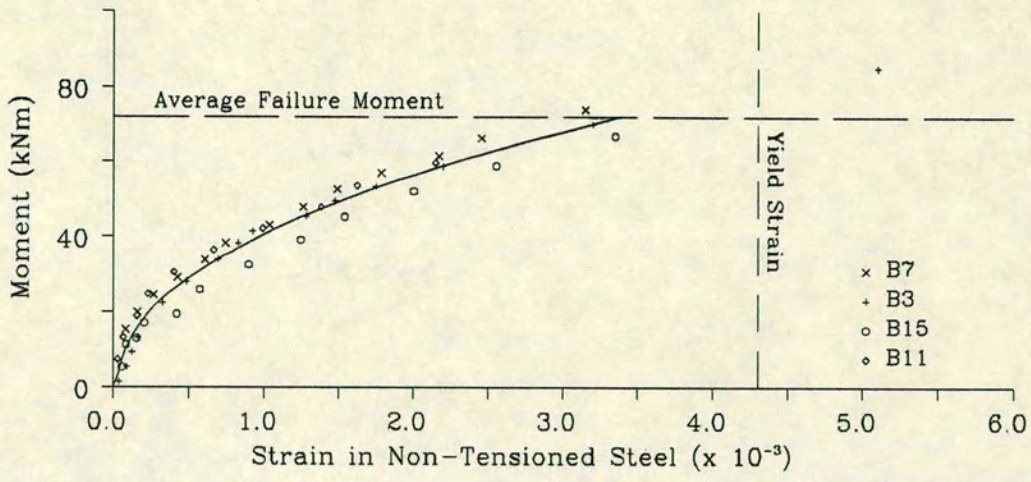

Fig. 4.3.6a Strain in the Non-Tensioned Steel
Partially Prestressed Brickwork Beams, A_p=0.341%, a/d=3.0

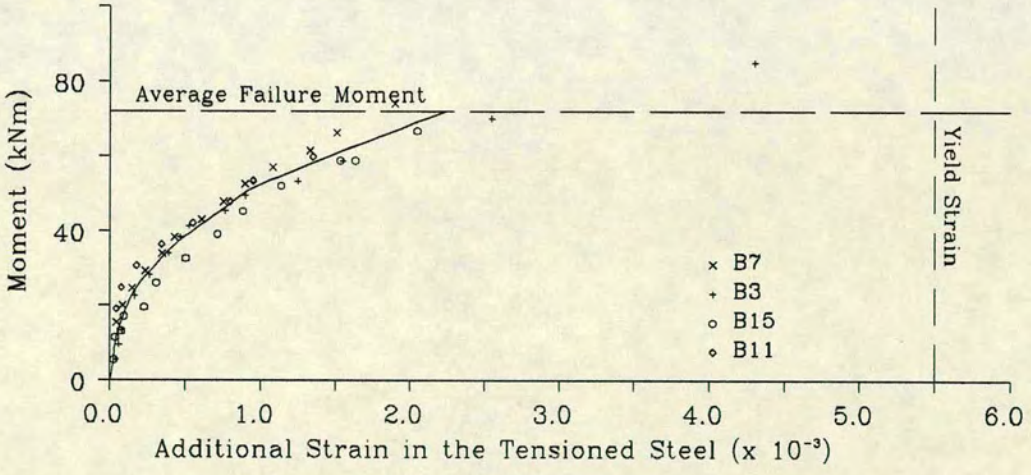

Fig. 4.3.6b Additional Strain in the Tensioned Steel
Partially Prestressed Brickwork Beams, A_p=0.341%, a/d=3.0

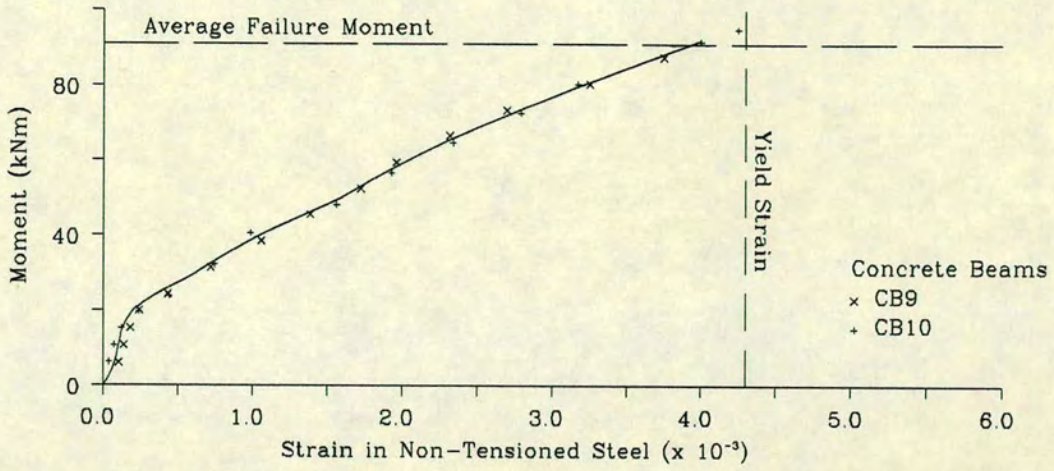

Fig. 4.3.7a Strain in the Non-Tensioned Steel
Partially Prestressed Concrete Beams, a/d=3.0

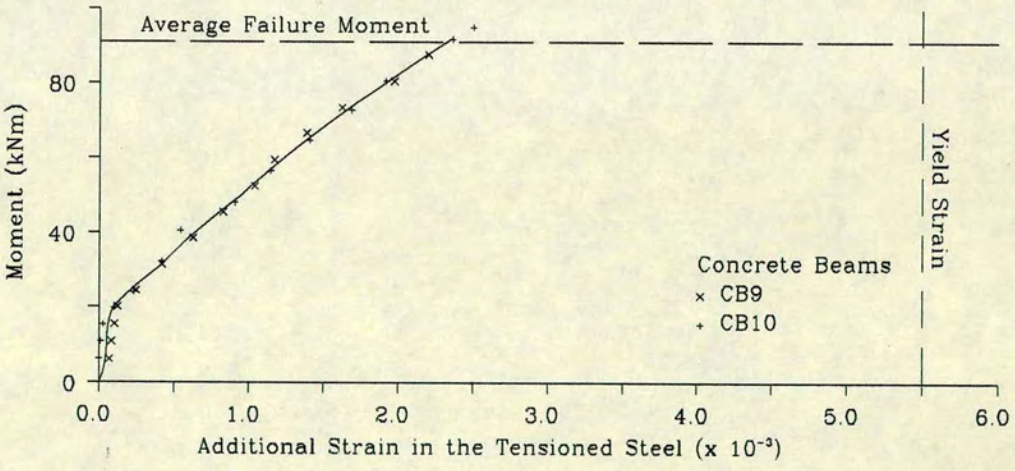

Fig. 4.3.7b Additional Strain in the Tensioned Steel
Partially Prestressed Concrete Beams, a/d=3.0

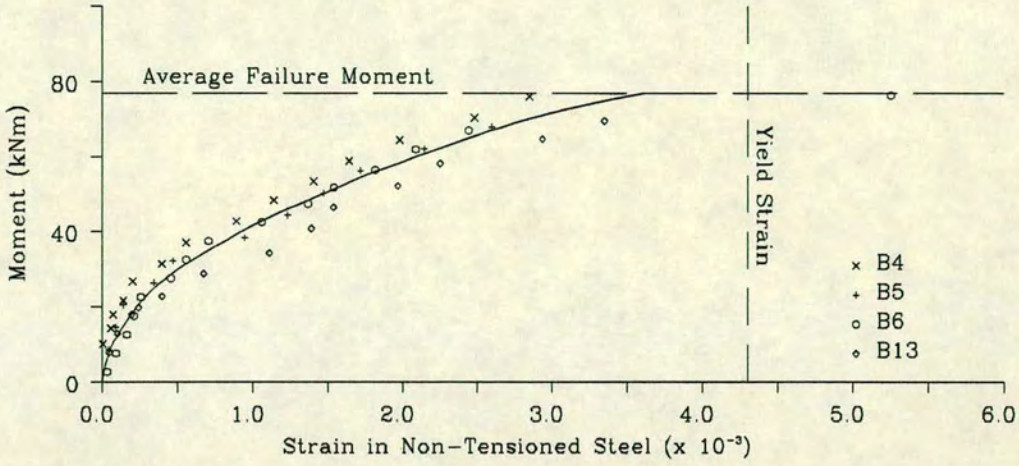

Fig. 4.3.8a Strain in the Non-Tensioned Steel
Partially Prestressed Brickwork Beams (a/d=4.5)

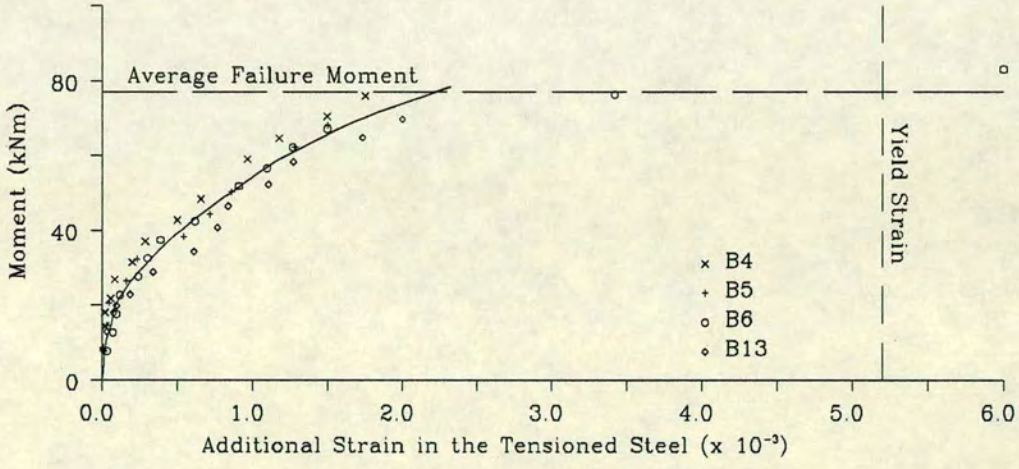

Fig. 4.3.8b Additional Strain in the Tensioned Steel
Partially Prestressed Brickwork Beams (a/d=4.5)

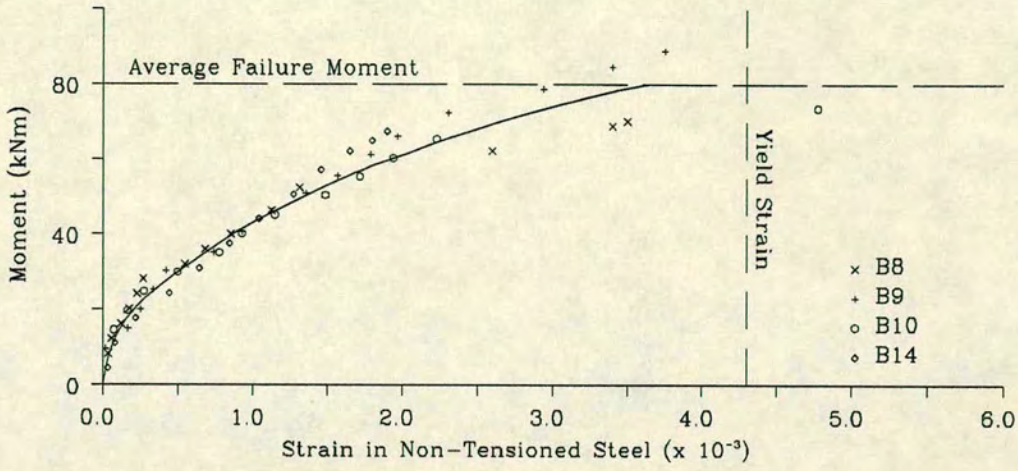

Fig. 4.3.9a Strain in the Non-Tensioned Steel
Partially Prestressed Brickwork Beams, a/d=6.0

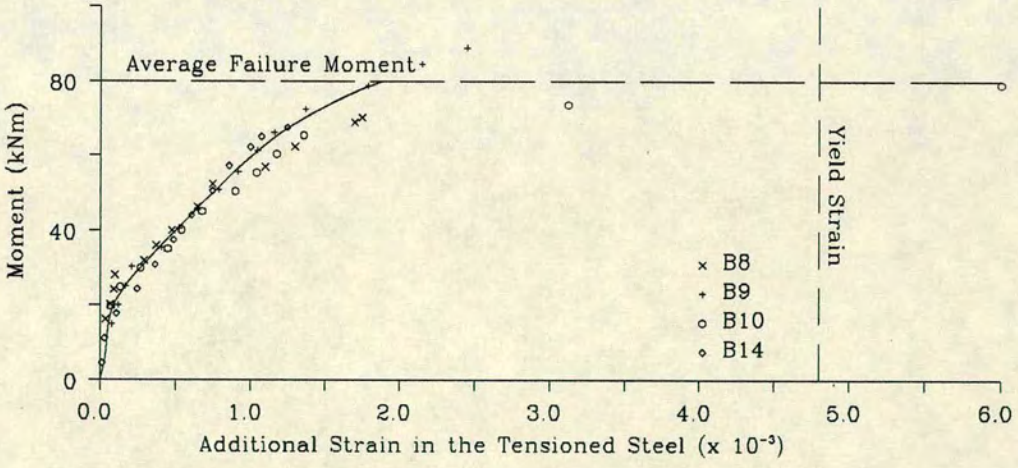

Fig. 4.3.9b Additional Strain in the Tensioned Steel
Partially Prestressed Brickwork Beams, a/d=6.0

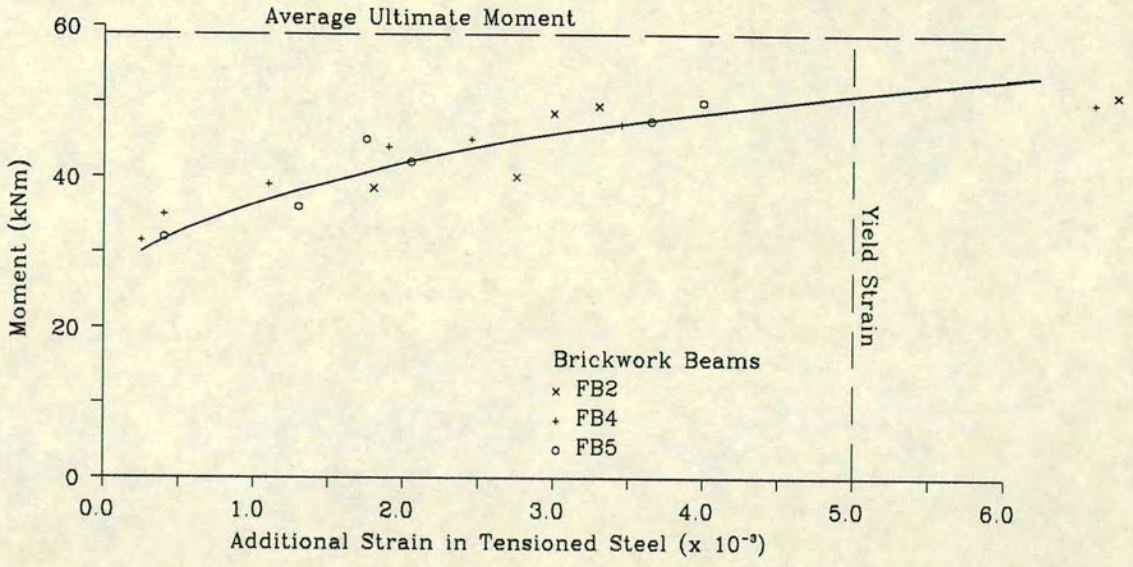

Fig. 4.3.10a Additional Strain in the Tensioned Steel
Fully Prestressed Brickwork Beams, A_p=0.274%

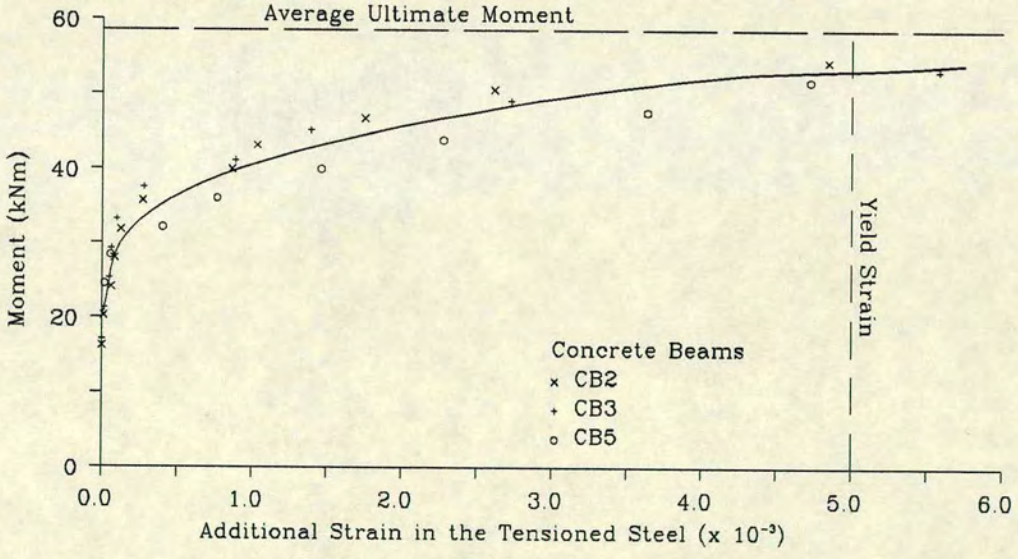

Fig. 4.3.10b Additional Strain in the Tensioned Steel
Fully Prestressed Concrete Beams, A_p=0.274%

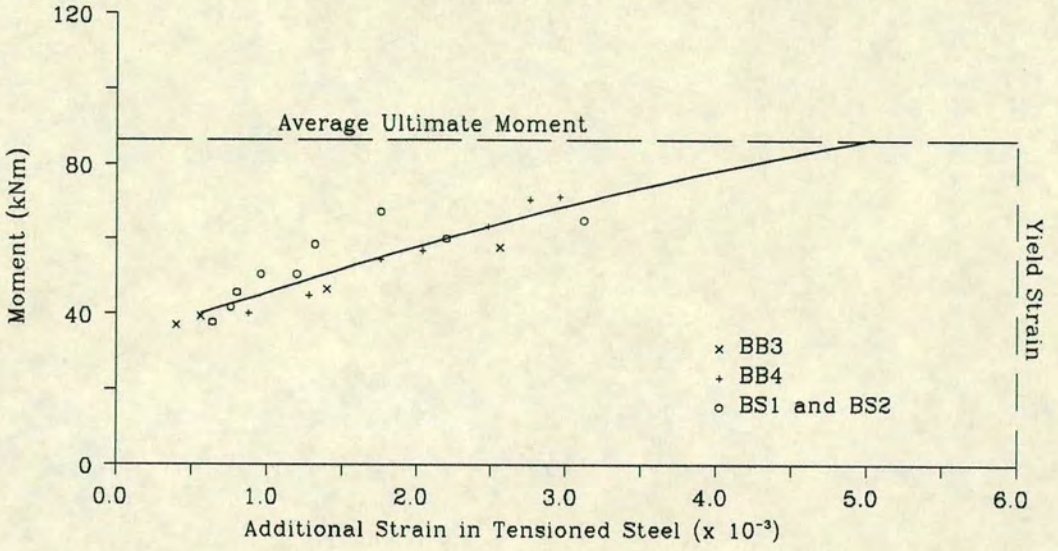

Fig. 4.3.11a Additional Strain in the Tensioned Steel
Brickwork Beams (A_p=0.548%, P_e=208 kN)

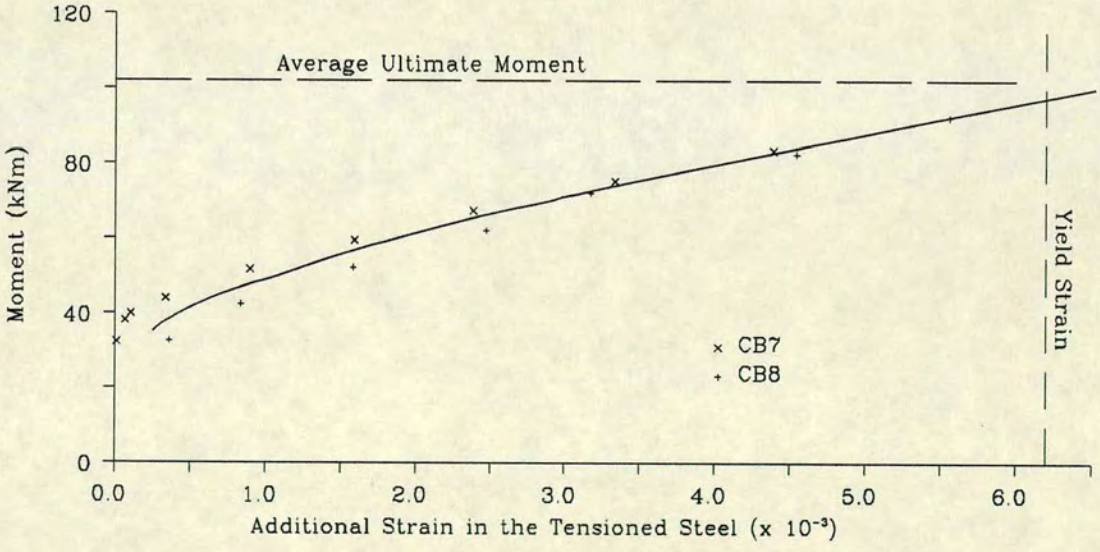

Fig. 4.3.11b Additional Strain in the Tensioned Steel
Concrete Beams (A_p=0.548%, P_e=201 kN)

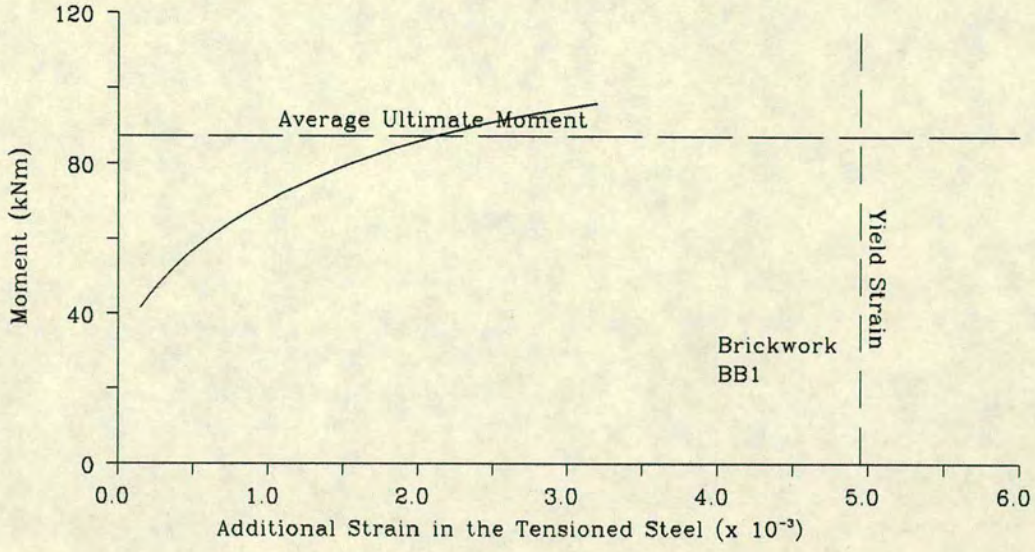

Fig. 4.3.12a Additional Strain in the Tensioned Steel
Fully Prestressed Brickwork Beam, A_p=0.548%, P_e=275 kN

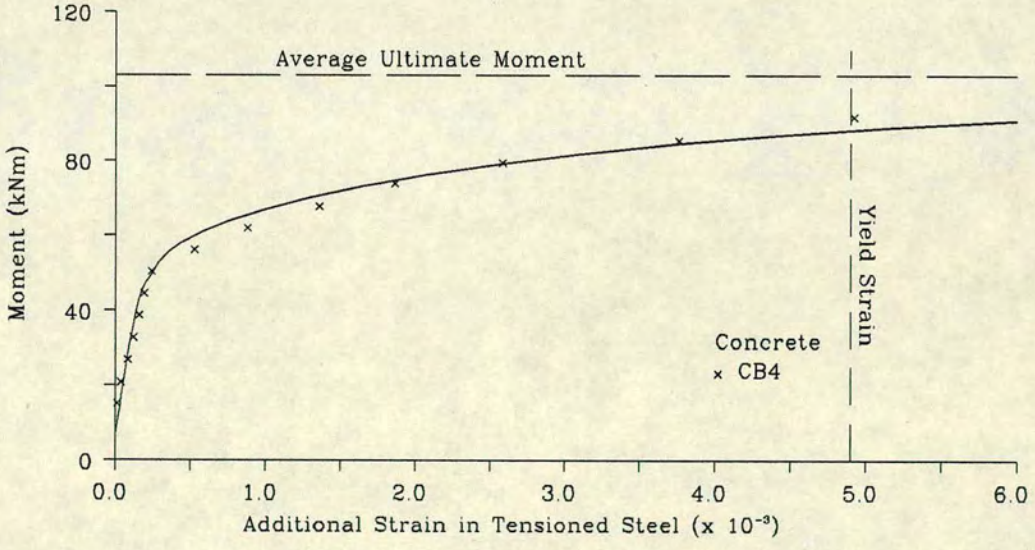

Fig. 4.3.12b Additional Strain in the Tensioned Steel
Fully Prestressed Concrete Beam, A_p=0.548%, P_e=283 kN

extrapolation and are also shown as data points in each of these figures.

In the beams containing tensioned and non-tensioned steel, as expected from Section 4.2, the strains in the latter due to applied load moment were always larger by virtue of its further distance from the neutral axis.

4.3.1.3 The Relationship between the Moment and the Top Fibre Strain

The relationship between the moment and the maximum top fibre strains for all the brickwork and concrete beams reported in this study are presented in Figs. 4.3.13 to 4.3.19. Also shown on these figures, are the average failure moment and the ultimate compressive strains obtained from the single course prism tests in the case of the brickwork beams and from the code[58] for the concrete beams (see Chapter 3). As in section 4.3.1.2, the ultimate strain at failure for each beam was obtained by extrapolation.

Before cracking in all beams, there was a linear increase in the top fibre strain with applied moment. Thereafter, rapid increases in the top fibre strain were obtained until failure. In the brickwork and concrete beams containing 0.274% area of tensioned steel only, Fig. 4.3.17 a and b respectively, the moment-top fibre strain relationship 'flattened out' so that it became parallel to the x-axis before failure. The average top fibre strain in these beams at failure were 0.0031 in brickwork and 0.0035 in concrete. The value in the brickwork beams at failure was in good agreement with that obtained from the single course prisms in Chapter 3 of 0.00327. In concrete, this value was the same as that recommended by the code of practice[58].

For the concrete beams containing 0.548% area of steel (see Fig. 4.3.18b and 4.3.19b), the average top fibre strain at failure was 0.0039. In the corresponding brickwork beams, top fibre strains at failure of up to and over 0.0031 were obtained[11]. This indicated that although failure was in shear, the constant moment region was at the point of crushing.

In the partially prestressed brickwork beams, within each group with the same shear span to effective depth ratio, there was an appreciable amount of variation in the ultimate moment. This was also reflected in the top fibre strains at failure. The maximum top fibre strains were obtained in the beams which were close to flexural failure namely, B2 (0.00315), B6 (0.0034) and B10

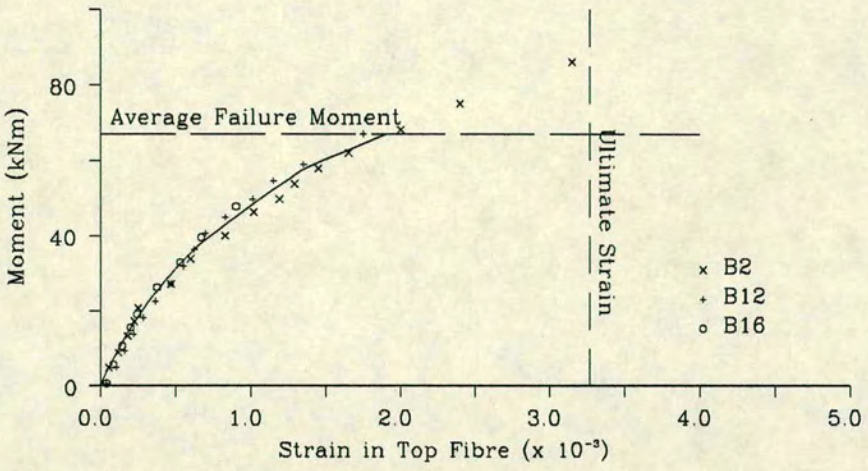

(a) Brickwork Beams

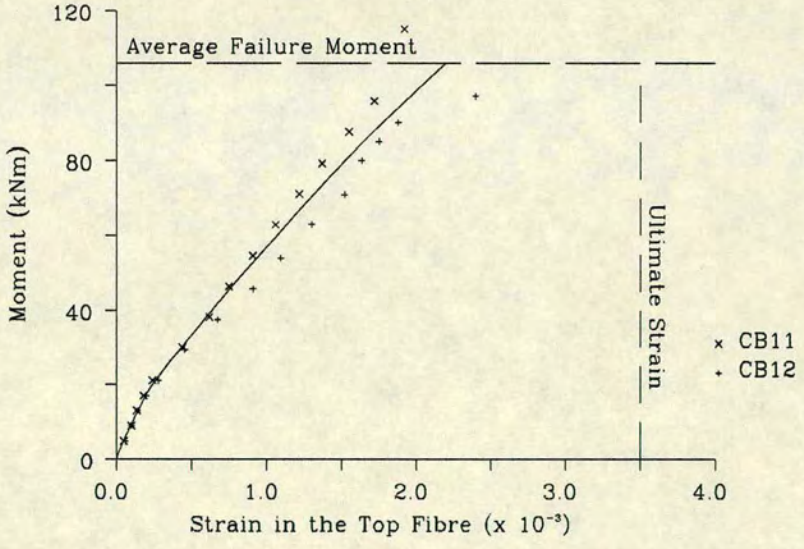

(b) Concrete Beams

Fig. 4.3.13 Strain in Top Fibre
Partially Prestressed Beams, a/d=1.5

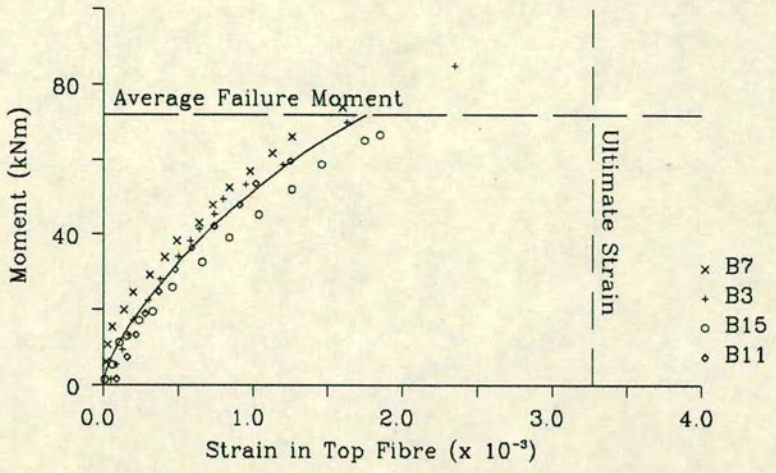

(a) Brickwork Beams

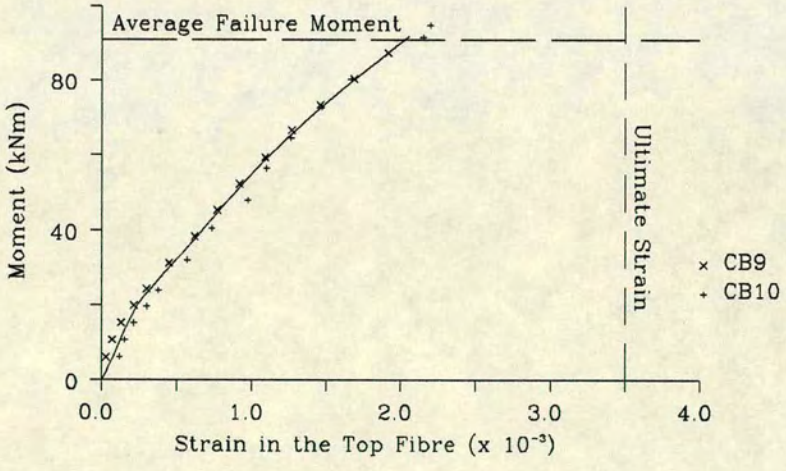

(b) Concrete Beams

Fig. 4.3.14 Strain in Top Fibre
Partially Prestressed Beams, a/d=3.0

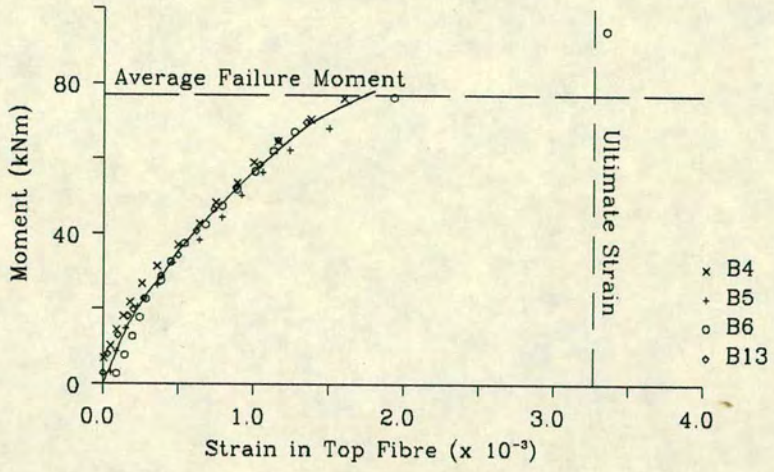

Fig. 4.3.15 Strain in the Top Fibre
Partially Prestressed Brickwork Beams, a/d=4.5

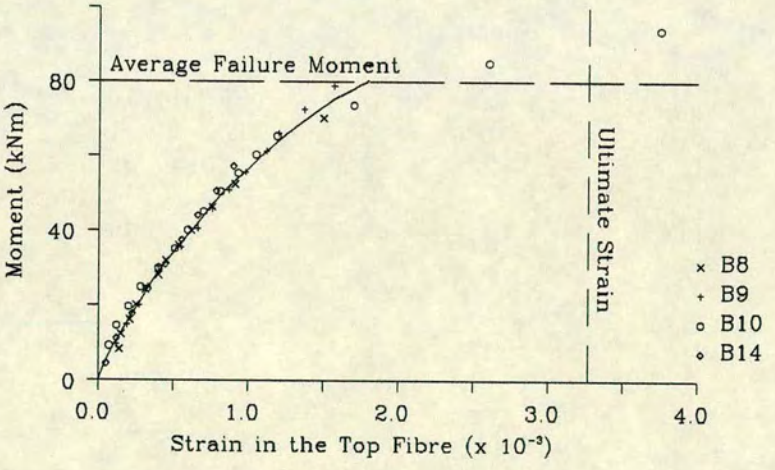

Fig. 4.3.16 Strain in the Top Fibre
Partially Prestressed Brickwork Beams, a/d=6.0

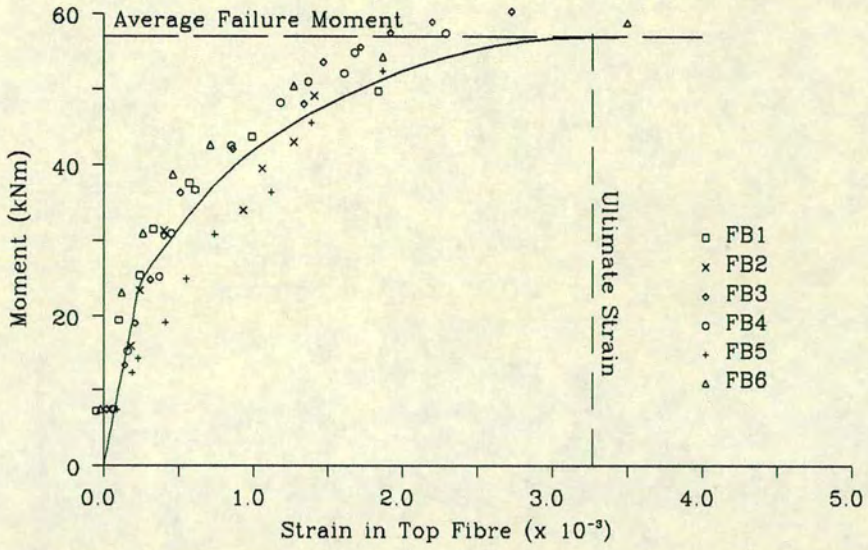

(a) Brickwork Beams

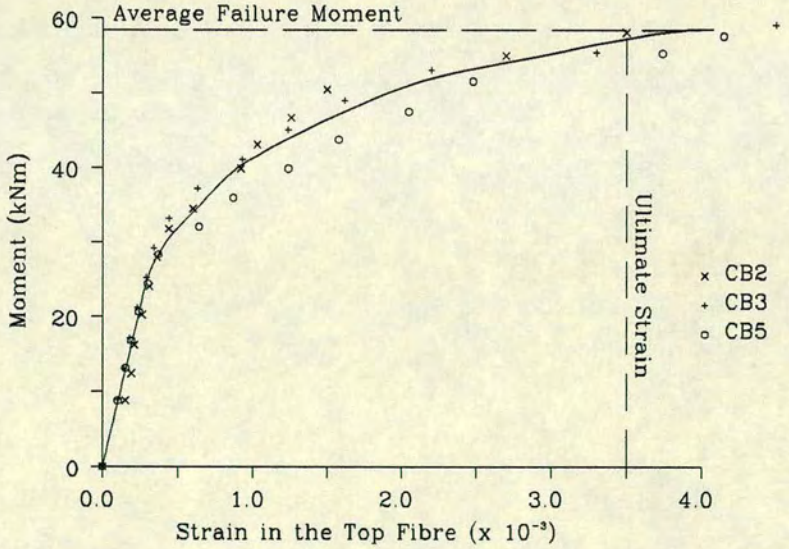

(b) Concrete Beams

Fig. 4.3.17 Strain in Top Fibre
Fully Prestressed Beams, A_p=0.274%

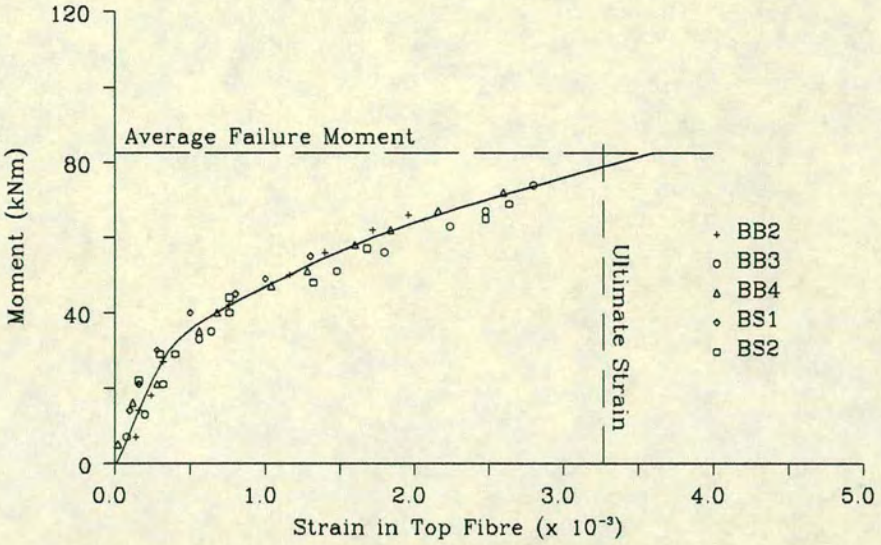

(a) Brickwork Beams

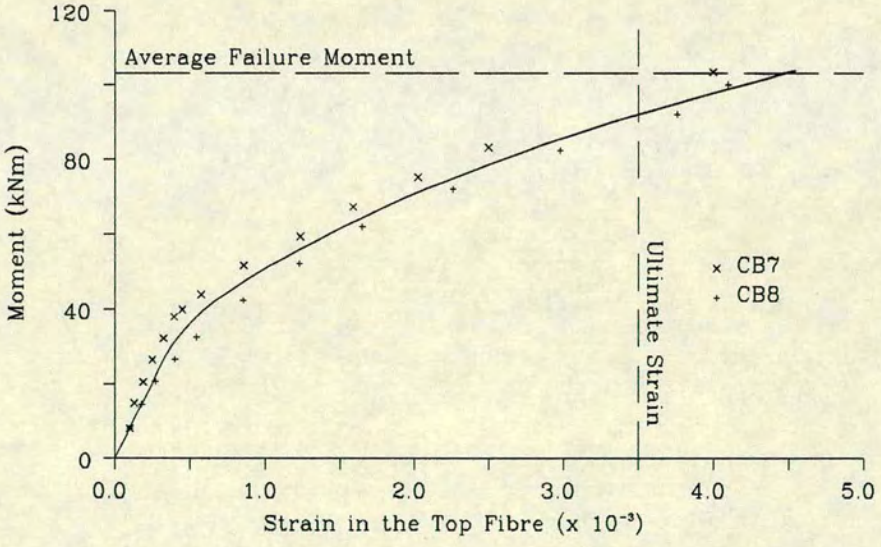

(b) Concrete Beams

Fig. 4.3.18 Strain in Top Fibre, Fully Prestressed Beams
A_p = 0.548%, P_e=200 kN

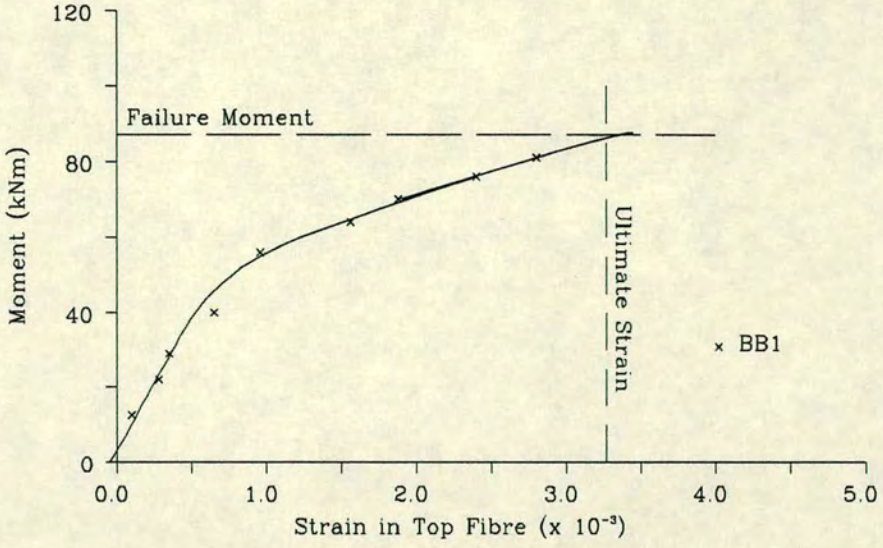

(a) Brickwork Beam

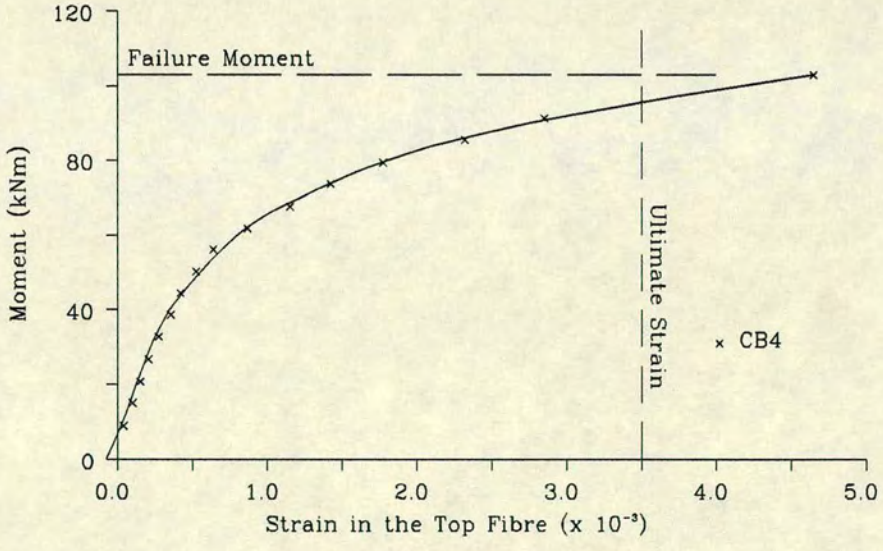

(b) Concrete Beams

Fig. 4.3.19 Strain in Top Fibre, Fully Prestressed Beams
A_p=0.548%, P_e=280 kN

(0.00375). The lowest values were obtained for B16 (0.0009), B11 (0.00125) and B5 (0.00135) which had the lowest ultimate moments in their groups. The maximum value of the top fibre strain in the partially prestressed concrete beams was obtained for CB12 (0.0024).

4.3.1.4 The Relationship Between the Neutral Axis Depth and the Moment

Typical relationships between the neutral axis depth and moment are shown in Figs. 4.3.20–4.3.22. The depth of the neutral axis from the top fibre was obtained from strain distribution diagrams (see Fig. 4.3.1–4.3.3). After decompression at the soffit of the beam, the neutral axis moved into the beam section, its depth from the top fibre reducing with increasing moment. After cracking, there is a marked drop in the neutral axis depth and thereafter it levels off with applied moment. In beams which fail in flexural tension (see Fig. 4.3.21 (CB5), after the yielding of the tensile reinforcement, the curves level off until a minimum value is reached at the ultimate moment after which the brickwork/concrete crushes.

The depth of the neutral axis at failure was dependent on the area of steel and the mode of failure. The larger the steel area, the larger will be the neutral axis depth necessary to equate the compression force to the tensile force. When failure was in primary shear as opposed to flexure, the minimum neutral axis depth was not attained (see Fig. 4.3.22).

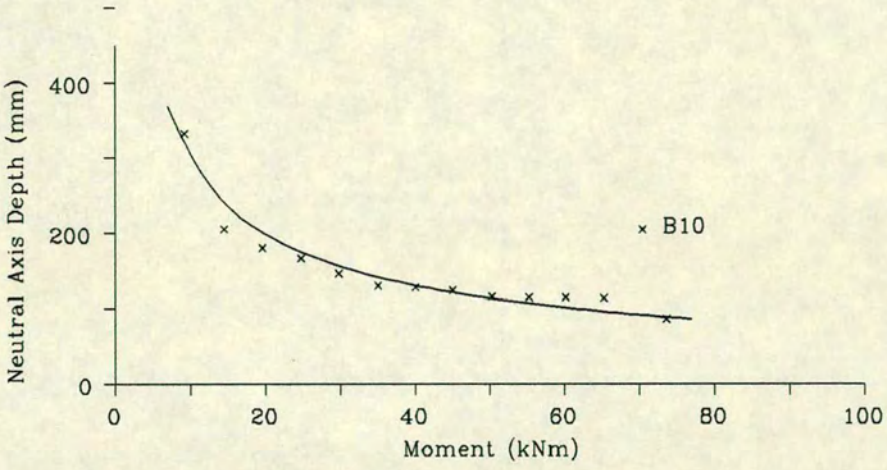

Fig. 4.3.20 Neutral Axis Depth vs Moment
Partially Prestressed Brickwork, a/d = 6.0

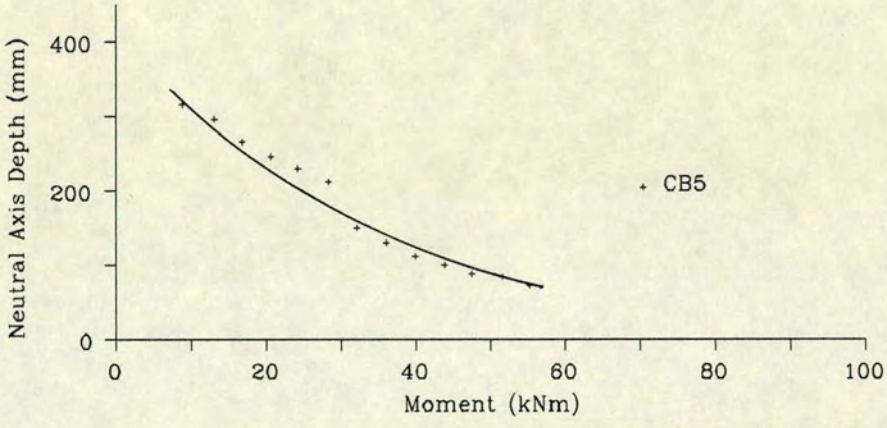

Fig. 4.3.21 Neutral Axis Depth vs Moment
Fully Prestressed Concrete, A_p=0.274%

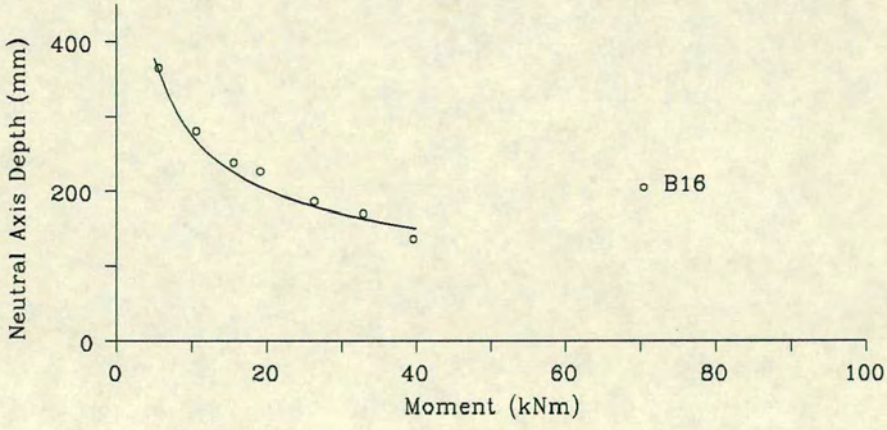

Fig. 4.3.22 Neutral Axis Depth vs Moment
Partially Prestressed Brickwork, a/d = 1.5

4.3.2 The Failure Mode

4.3.2.1 General

There were three possible modes of failure for the beams reported in this work:

1. Failure in Flexural Tension - by yielding of the tensile reinforcement in the under-reinforced beams. This results in large increases in strains for small increases in load causing the neutral axis depth to rise resulting in crushing of the compression zone. A flexural tension failure is associated with excessive deflections and cracking thus giving ample warning of impending collapse.

2. Failure in Flexural Compression - when the strain in the brickwork or concrete reaches its ultimate before the tensile reinforcement yields. Flexural compression failures are brittle.

3. Shear Failure - Shear failure can occur before the brickwork/concrete and/or the tensile reinforcement reach their ultimate strengths - a primary shear failure. This type of failure can be sudden and brittle. In some cases, a secondary shear failure can occur after some or all of the tensile reinforcement has yielded. - a secondary shear failure.

In the beams tested in this work, two modes of failure were observed, 1 and 3.

As each of the above modes of failure have distinct characteristics at ultimate, they may be determined from experimental observations. However, there may be overlap between the various modes of failure. For example, a beam can fail in shear after the tensile reinforcement has yielded or similtaneous yielding of the tensile reinforcement and crushing of the brickwork/concrete in the compression zone may occur (a balanced section). The failure mode can be more accurately determined from the tensile strains in the reinforcement and the maximum compressive strains in the brickwork/concrete at ultimate. The relationships between the moment and the maximum steel/brickwork/concrete strain for each beam were presented in

Figs. 4.3.4-4.3.19. For each beam the appropriate experimental point at ultimate, obtained by extrapolation was given. The average failure moment for each group of beams was plotted on each figure. Also, where appropriate, the ultimate strain in the brickwork/concrete obtained from Chapter 3 and the additional/total strain necessary for the tensioned and non-tensioned steel to yield respectively, were given.

4.3.2.2 Failure in Flexural Tension

The behaviour of all the brickwork and concrete beams which failed in flexural tension were similar up to failure. Typical flexural tension failures of brickwork and concrete beams are shown in Plates 4.1 a and b respectively. Cracking in the region of constant and maximum moment had penetrated deep into the compression zone so that the depth of the compression zone was quite small. This type of failure was characterised by gross deflections and excessive cracking towards failure, indicating that the tensile reinforcement had yielded. This led to crushing of the brickwork/concrete in the top fibre. There was appreciable recovery in deflection (about 40%) and reduction in the crack widths when the load was removed.

4.3.2.3 Shear Failure

Some of the fully and partially prestressed brickwork and concrete beams failed primarily in shear before the brickwork/concrete in the maximum moment region had reached its crushing strength and before the non-tensioned and tensioned reinforcement had reached their yield strengths. This type of failure was characterised by an inclined crack in the shear span. In the partially prestressed beams with a shear span to effective depth ratio (a/d) of 1.5, the inclined crack ran from the loading point to the support and in the case of brickwork, in a step-wise fashion (see Plates 4.2a and 4.2.b for brickwork and concrete respectively). In these beams, failure occurred along the inclined crack. In the fully prestressed beams and the partially prestressed beams with the higher a/d ratios, the inclined crack was initiated by a flexural crack located at about half way into the shear span. This travelled towards the loading point. In the brickwork beams, these cracks progressed in the usual step-wise manner. On reaching the top bed joint, there was a horizontal propagation of

Plate 4.1

(a) Typical Flexural Failure in a Brickwork Beam

(b) Typical Flexural Failure in a Concrete Beam

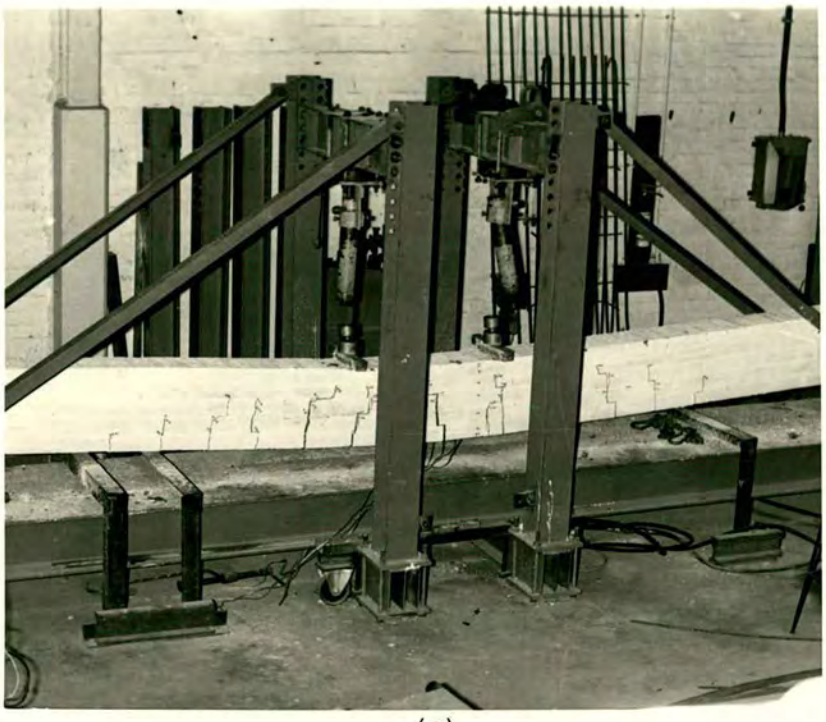

(a)

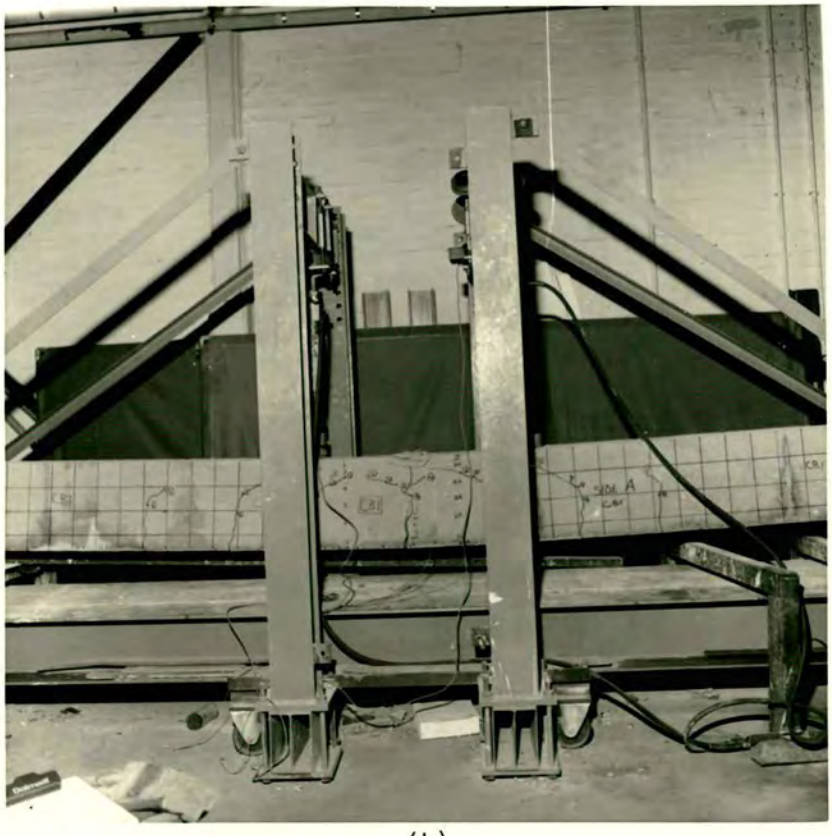

(b)

Plates 4.2

(a) Typical Shear Failure in Brickwork Beams (a/d = 1.5)

(b) Typical Shear failure in Concrete Beams (a/d = 1.5)

(a)

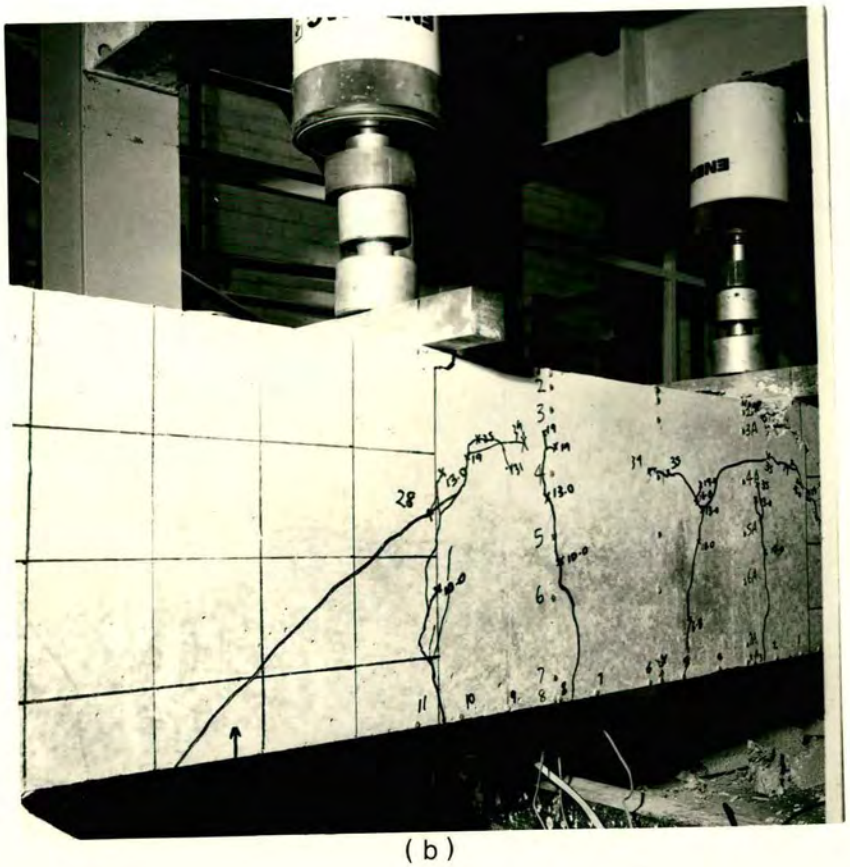

(b)

Plate 4.3

(a) Typical Shear Failure in Brickwork Beams ($a/d > 1.5$)

(b) Typical Shear Failure in Concrete Beams ($a/d = 3.0$)

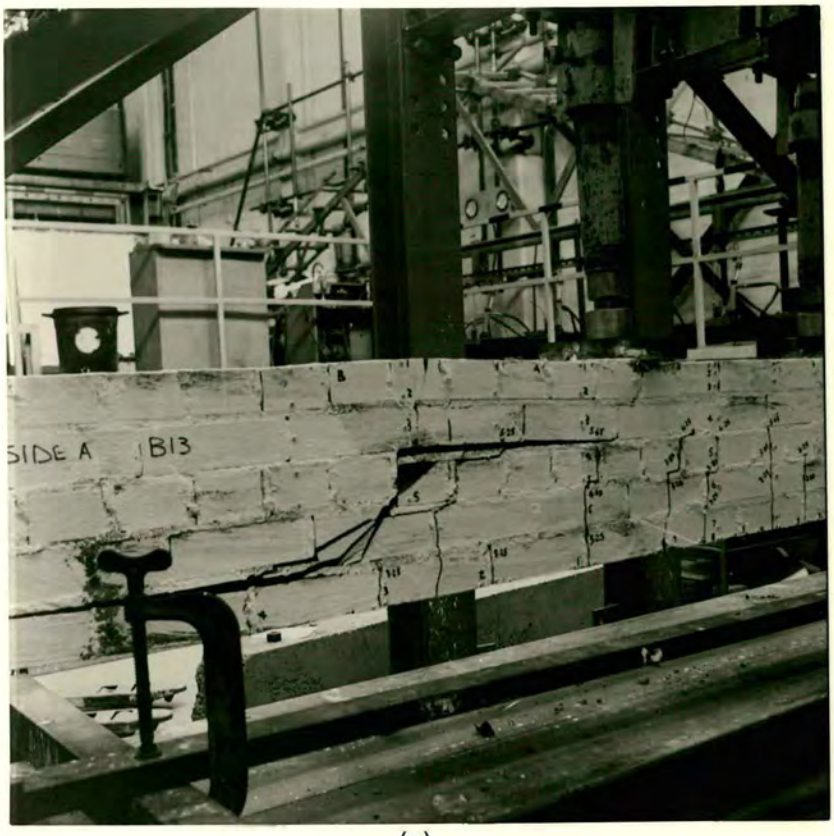

(a)

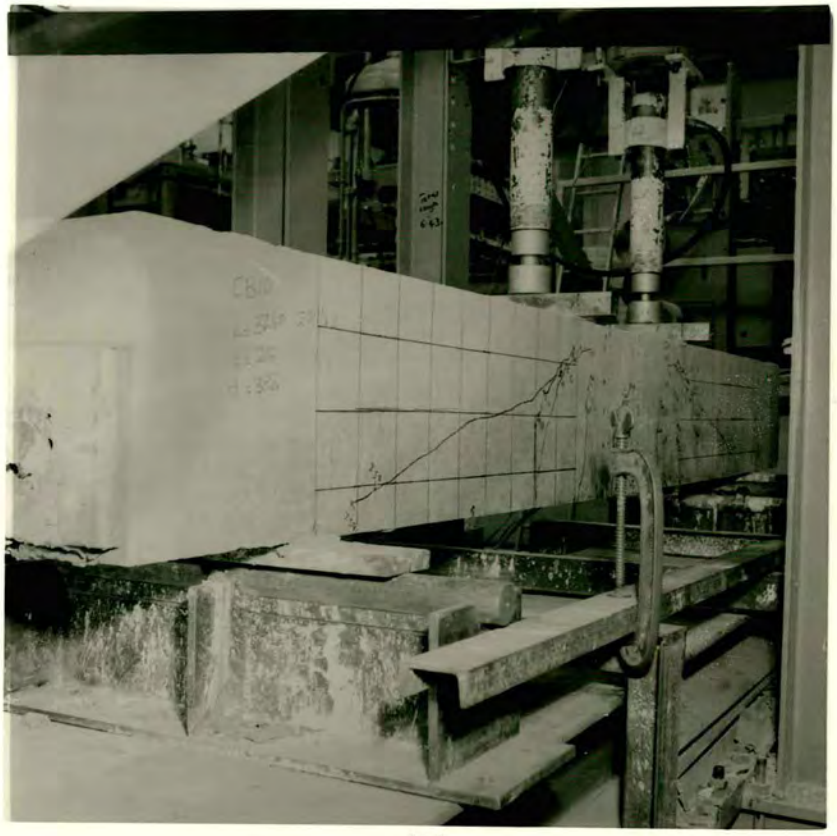

(b)

Plate 4.4 Secondary Shear Failure in a Brickwork Beam

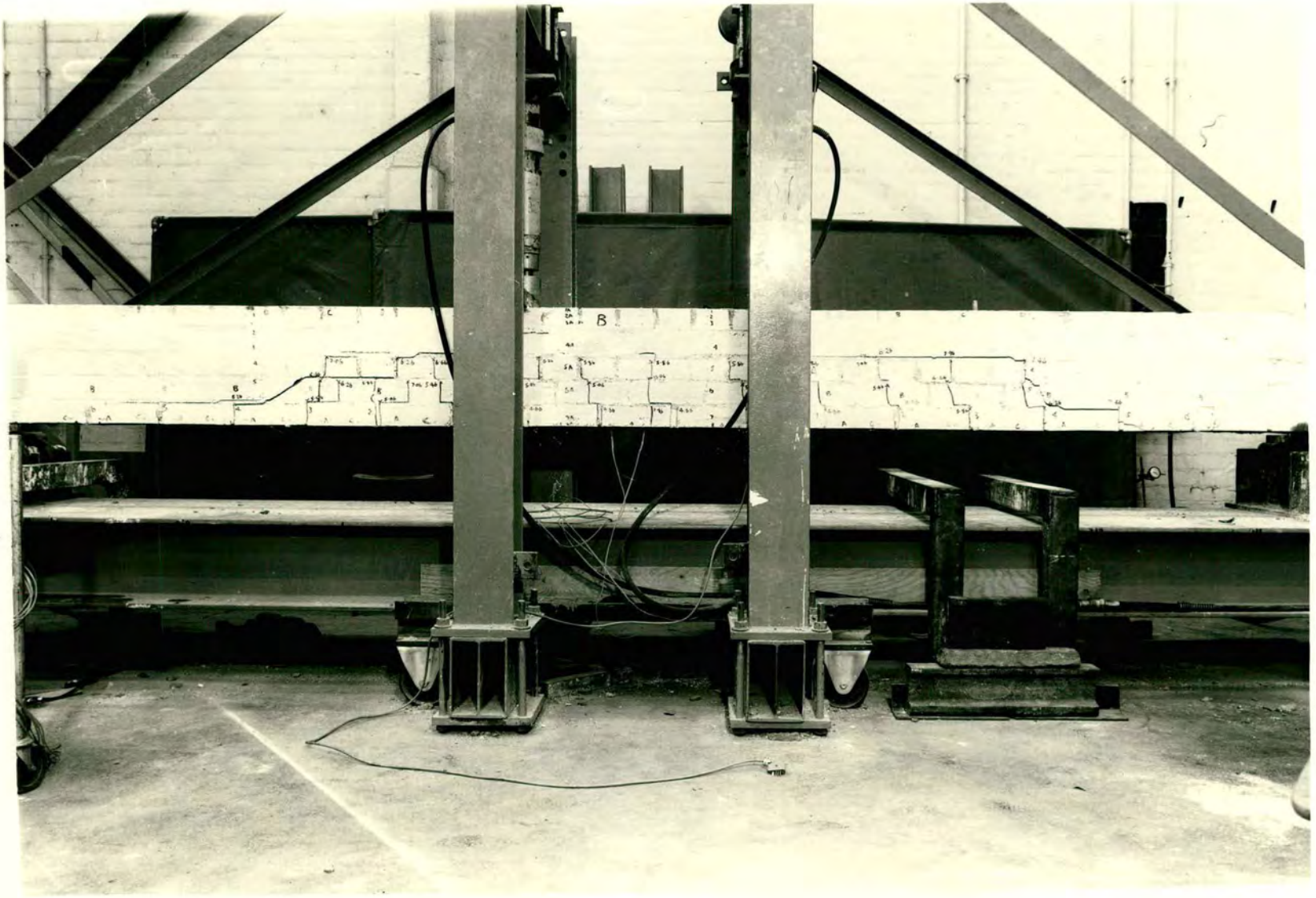

this crack along the bed joint into the constant moment region (see Plate 4.3a). The inclined crack in the concrete beams also travelled into the constant moment region terminating just beyond the load point (see Plate 4.3b). In both the brickwork and concrete beams, there was a horizontal propagation of the inclined crack towards the support. In the brickwork beams, this travelled along the bottom bed joint. In these beams, failure occurred when the inclined crack had penetrated into the constant moment region.

In the fully prestressed beams and some of the partially prestressed beams, considerable deformations were observed before the formation of the inclined crack in the shear span. Thus some or all of the tensile reinforcement had yielded and before crushing of the brickwork/concrete took place, a secondary shear failure occurred. Plate 4.4 shows a secondary shear failure in brickwork. The characteristics of the secondary shear failure is similar to that of a primary shear failure except that since some or all of the tensile reinforcement has yielded, appreciable evidence of impending collapse is given.

4.3.2.4 Failure Modes of the Partially Prestressed Beams

Shear Span/Effective Depth = 1.5

The relationship between the moment and the tensile strain for the partially prestressed brickwork and concrete beams with shear span to effective depth ratio (a/d) of 1.5 were shown in Figs. 4.3.4 and 4.3.5. In the brickwork beams, there was a considerable variation in the ultimate moment (see Table 4.3.1). However, the relationship between the moment and the strain in the non-tensioned steel shows that only the non-tensioned steel in B2 had yielded prior to failure. The additional strain in the tensioned steel in all cases was below that required for it to yield. The relationship between the moment and the top fibre strain for these beams are presented in Fig. 4.3.13a. With the exception of B2, the top fibre strain in all the beams were well below the ultimate values. The top fibre strain in B2 at ultimate was however only just below that required for crushing. Therefore B1, B12 and B16 failed primarily in shear while in B2 a secondary shear failure occurred. The moment vs tensile strain relationships for the corresponding concrete beams, CB11 and CB12 are shown in Fig. 4.3.5 and the relationships between the moment and the top fibre strain are given in Fig. 4.3.13b. In these beams a secondary shear failure

occurred just after the yielding of the non-tensioned reinforcement. The additional strains in the tensioned steel were well below that necessary for yielding.

Shear Span/Effective Depth = 3.0

The relationships between the moment and the tensile strain for the partially prestressed brickwork and concrete beams with an a/d of 3.0 are shown in Figs. 4.3.6 and 4.3.7 respectively. The relationship between the moment and the top fibre strain for the brickwork beams are shown in Fig. 4.3.14a and Fig. 4.3.14b shows this relationship for the concrete beams. With the exception of B3, all the brickwork beams in this group failed primarily in shear. A secondary shear failure occurred in B3 in which the non-tensioned steel yielded before failure. In the similar concrete beams, CB9 and CB10, the former failed primarily in shear and in the latter, the yielding of the non-tensioned steel coincided with shear failure, the additional strain in the tensioned steel and the top fibre strain being well below their ultimate values.

Shear Span/Effective Depth = 4.5

Fig. 4.3.8a and b show the relationship between the moment and the strain in the tensile reinforcement for the partially prestressed brickwork beams with an a/d ratio of 4.5. The relationships between the moment and the top fibre strain are shown in Fig. 4.3.15. These figures show that B4, B5 and B13 failed primarily in shear before the yielding of the non-tensioned and tensioned steel and prior to the ultimate strain in brickwork being attained. On the other hand, in B6, the tensioned and non-tensioned steel had yielded prior to failure and the top fibre strain at failure was higher than the average ultimate value in brickwork but crushing in the compression zone of the maximum moment region was not evident. The inclined crack in the shear span had however penetrated into the constant moment region. B6 therefore failed in tension and a secondary shear failure occurred before crushing of the brickwork. As shown in the strain distribution diagram for B6 (Fig. 4.3.3), towards failure there was a sharp rise in the position of the neutral axis which corresponded to the yielding of the tensile steel.

Shear Span/Effective Depth = 6.0

As in the previous groups of partially prestressed beams, two modes of

failure were identified in this group of beams; primary and secondary shear failures (see Figs. 4.3.9 and 4.3.16). The secondary shear failure which occur occurred in B10 was similar to that described in the previous section for B6. Both the tensioned and non-tensioned steel had yielded prior to shear failure. Also, the strain in the top fibre was higher than the average ultimate strain but crushing of the top fibre did not occur at ultimate. In some of the beams which failed in primary shear namely B8 and B9, the non-tensioned steel was very close to yielding.

4.3.2.5 Failure Modes of Fully Prestressed Beams

Beams Containing 0.274% Area of Tensioned Steel

The relationships between the moment and the additional strain in the tensioned steel and between the moment and the top fibre strain for the brickwork and concrete beams containing 0.274% area of tensioned steel were presented in Fig. 4.3.10 and 4.3.17. Clearly, at ultimate in both brickwork and concrete, the additional strain required for the tensioned steel to yield and the ultimate strain in the brickwork/concrete had been exceeded. Failure was initiated by yielding of the tensile reinforcement which gave rise to large strains in the brickwork/concrete which eventually crushed at the ultimate strain.

Beams Containing 0.548% Area of Tensioned Steel

The brickwork beams containing 0.548% area of tensioned steel with the lower prestressing force i.e BB2, BB3 and BB4 failed in primary shear with the strain in the tensioned steel being below the yield strain (see Fig. 4.3.11a). The relationship between the moment and the top fibre strain in Fig. 4.3.18a however show that the top fibre strains were very close to crushing. The relationships for the corresponding concrete beams are shown in Figs. 4.3.11b and 4.3.18b. The concrete beams failed in tension by yielding of the tensioned steel. The relationship for BB1, the brickwork beam with the higher prestressing force, and the corresponding concrete beam, CB4 were presented in Figs. 4.3.12 and 4.3.19. BB1 failed in shear with the top fibre strain being very close to the crushing value. The concrete beam failed in tension.

4.3.3 The Ultimate Moment

In this section, the ultmiate moment obtained for all the brickwork and concrete beams reported in this study are presented and discussed. The ultimate flexural moment of resistance of prestressed beams of brickwork and concrete with identical cross-sectional properties and of similar compressive strengths are compared. A comparison is also made with theoretical results obtained from the theory described in Section 4.2 using the stress block factors, compressive strengths and idealised stress-strain relationships for the tensile reinforcement given in Chapter 3. The effective prestressing forces after all losses given in Table 4.3.1 were used. The experimental ultimate flexural moments are also compared with those given by the direct method presented in Chapter 5. In addition, a comparison is made with those predicted by the appropriate codes of practice[1,58].

4.3.3.1 The Effect of the shear span/effective depth Ratio on the Ultimate Moment of Partially Prestressed Beams

In this study sixteen partially prestressed brickwork beams and four partially prestressed concrete beams with a/d ratios varying between 1.5 and 6.0 were tested. All these beams failed in shear before or after some or all of the tensile reinforcement had yielded. The shear strength of these beams will be examined in detail in Chapter 7. In this section, only the effect of the a/d ratio on the ultimate moment will be considered.

The ultimate moment at failure was dependent on the a/d ratio. This was because the shear strength was such that the beams failed in shear before a flexural failure could occur. The maximum moment was therefore dependent on the shear strength which varied with the a/d ratio (see Table 4.3.1). Although there were considerable variations in the ultimate moment within a group of beams with the same a/d ratio, there was an underlying trend of increasing ultimate moment with increasing a/d ratio. This was borne out by the modes of failure discussed in Section 4.3.2.2. In the beams with the lower a/d ratios, 1.5 and 3.0, the beams with the highest ultimate moments in each group failed in secondary shear after the non-tensioned steel only had yielded. In the beams with the highest ultimate moments within the groups with a/d ratios of 4.5 and 6.0 also failed in secondary shear but after both the tensioned

and non-tensioned steel had yielded. Conversely, there was an increase in the ultimate moment of the partially prestressed concrete beams with decreasing a/d ratio from 3.0 to 1.5. As will be discussed in Chapter 7, this results from the enhanced shear strength in beams with a/d ratios less than 2.5 due to 'tied arch' action which is less significant in brickwork beams.

4.3.3.2 A Comparison between the Ultimate Moments of Similar Prestressed Beams of Brickwork and Concrete

The ultimate moments, failure modes and some other properties of the beams studied in this work are shown in Table 4.3.1. This table shows that when prestressed brickwork and concrete beams fail in flexure, the ultimate moments are very similar. However, when a brickwork beam fails in shear, the ultimate moment can be less than in a corresponding concrete beam whether the latter also failed in shear or in flexure. In the beams containing 0.548% area of tensioned steel, the average ultimate moment of the brickwork beams at failure for the beams with the lower prestressing force was 28% less than the value in concrete. Increasing the prestressing force increases the ultimate moment of beams which fail in shear so that in the beam with the higher prestressing force the average ultimate moment in brickwork was 15% less than the value in the corresponding concrete beam.

The partially prestressed brickwork and concrete beams with a/d ratios of 1.5 and 3.0 failed in shear. In the latter case, the average ultimate moment of the brickwork beams was 18% less than the value in the concrete beams. However, the average ultimate moment of the concrete beams with an a/d ratio of 1.5 was 59% higher than the value in the corresponding brickwork beams. As discussed in Section 4.3.3.1, the increased value in the concrete beams at this a/d ratio resulted from the enhancement in the shear strength due to 'tied arch' action.

4.3.3.3 A Comparison Between the Flexural Strengths of Prestressed Brickwork and Concrete Beams

From Table 4.3.1, it can be seen that when prestressed brickwork and concrete beams fail in flexure as opposed to shear, similar ultimate moments were obtained. In this section, this issue is examined further.

The only beams which failed in flexure in both brickwork and concrete were those containing 0.274% area of tensioned steel. The average flexural moments of resistance of the brickwork beams was 58.5 kNm, practically identical to the average ultimate moment of the concrete beams of 58.4 kNm. In Table 4.3.2, experimental and theoretical ultimate moments for all the beams which failed in flexure are presented. The theoretical ultimate moments were obtained from the flexural theory presented in Section 4.2 and from the direct method which is presented in Chapter 5. In the theoretical analyses, the idealised stress-strain relationships for all the materials given in Chapter 3 and the effective prestressing forces after all losses presented in Table 4.3.1, were used.

In both brickwork and concrete, both methods give a good estimate of the ultimate flexural moment of resistance. Using the flexural theory, the ratios of experimental to theoretical ultimate moments were the same for brickwork and concrete. The direct method gave similar ratios to those obtained from the flexural theory. The similarity in the ultimate moments obtained experimentally for the brickwork and concrete beams containing 0.274% area of steel was not unexpected as these beams, as determined from section 4.2.2, were under-reinforced. Failure was therefore initiated by the yielding of the tensile reinforcement which was then followed by crushing of the brickwork/concrete in the compression zone, the latter being a secondary action. From Section 4.2, the ultimate flexural moment of beams which fail in tension is given by equation 4.2.17 i.e.

$$M_{um} = f_{py}.A_p(d_p-\lambda_2.n) + f_{sy}.A_s(d_s-\lambda_2.n)$$

The above equation shows that when a beam fails in flexural tension, the properties of the brickwork/concrete only affect the lever arm i.e. the term $\lambda_2.n$. In Chapter 3, the values of λ_2 obtained for brickwork and concrete from the idealised stress-strain relationships were 0.372 and 0.427 respectively. The neutral axis depth, n, is determined by the magnitude of the compressive force at failure which is controlled by $\lambda_1.\lambda_3.f_m$ (or f_{cu}). In this study, the compressive strengths of brickwork and concrete were such that $\lambda_3.f_{cu}$ and $\lambda_3.f_m$ were similar. The value of λ_1 in concrete is higher than that in brickwork, 0.759 and 0.652 respectively. The relative values indicate that the neutral axis depth in concrete at failure will be less than in brickwork as in the former, a smaller neutral axis depth will be required to balance the same tensile force. This was confirmed from experimental results where the neutral axis depth at failure for

Table 4.3.2 Predicted Ultimate Flexural Moments

Beam	% area of steel	Exp	Flexural Theory	Exp/Theo	Direct Method	Exp/Theo
		kNm	kNm		kNm	
Brickwork beams[11]						
FB1	0.274	56.9	54.3	1.05	53.8	1.06
FB2	"	56.4	54.3	1.04	53.8	1.05
FB3	"	61.5	54.3	1.13	53.8	1.14
FB4	"	58.4	54.4	1.07	53.8	1.09
FB5	"	59.2	54.4	1.09	53.8	1.10
FB6	"	58.8	54.4	1.08	53.8	1.09
Concrete beams						
CB1	0.274	58.8	54.3	1.08	54.1	1.09
CB2	"	58.1	54.5	1.07	54.1	1.07
CB3	"	59.1	53.8	1.10	54.1	1.09
CB5	"	57.6	53.8	1.07	54.1	1.06
Concrete beams						
CB4	0.548	103.0	97.8	1.05	97.9	1.05
CB7	"	103.4	97.6	1.06	96.6	1.07
CB8	"	100.1	97.5	1.03	96.6	1.04

the beams containing 0.274% area of steel was 53 mm in brickwork and 42 mm in concrete. The corresponding values of $\lambda_2.n$ were 20 mm and 18 mm respectively. The differences between $\lambda_2.n$ in brickwork and concrete is thus very small. Further, because the values of d_p and d_s in equation 4.2.17 are much larger than $\lambda_2.n$, any differences will not be significantly reflected in the ultimate flexural moments. Therefore, as long as failure is in flexural tension, the ultimate moment of a prestressed brickwork beam will always be very similar to that of a corresponding concrete beam irrespective of the strength of the brickwork/concrete. Higher brickwork/concrete strengths only result in a reduced neutral axis depth which will have little effect on the ultimate moment.

According to the theory in Section 4.2.2, the concrete beams containing 0.548% area of tensioned steel were under-reinforced. The similar brickwork beam with the higher prestressing force, BB1 was balanced and those with the lower prestressing forces BB2, BB3 and BB4 were over-reinforced. These differences between the brickwork and concrete beams result from the higher λ_1 value in concrete (see equation 4.2.21). Increasing the prestressing force increases the balanced steel area (see Equation 4.2.21) so that the brickwork beam with the higher prestressing force (BB1) was balanced. The concrete beams failed in tension but the brickwork beams failed in shear.

The ultimate flexural moment of over-reinforced beams which will fail in compression before the tensile steel yields is given by equation 4.2.18 i.e.

$$M_{ut} = \lambda_1.\lambda_3.f_{m\ (or\ cu)}.b.n.(d - \lambda_2.n)$$

The brickwork/concrete in the compression zone crushes before the tensile reinforcement yields so that the ultimate moment is governed by the properties of the brickwork/concrete i.e the product of $\lambda_1.n(d - \lambda_2.n)$ since λ_3 is accounted for in the compressive strength. Above, it was seen that the term in parenthesis was not very different for brickwork and concrete beams which fail in tension. Consequently, the ultimate flexural moment is governed by $\lambda_1.n$. Although λ_1 is higher in concrete (0.759) when compared to brickwork (0.652), the effect on the ultimate moment is compensated for by the lower neutral axis depth in concrete. Therefore, when identical sections of brickwork and concrete are over-reinforced and subsequently fail in compression, their ultimate flexural moments will also be similar. In this case however, the differences will be more significant than in the under-reinforced beams because of the more prominent role of λ_1.

According to the theory presented in Section 4.2.2, the partially prestressed brickwork and concrete beams were under-reinforced with respect to both the tensioned and non-tensioned steel so that in the absence of shear failure, the yielding of the non-tensioned steel will be followed by that of the tensioned steel after which crushing of the brickwork/concrete will occur. In some of the brickwork beams namely, B6 and B10 with a/d ratios of 4.5 and 6.0 repectively, both the tensioned and non-tensioned steel had yielded before shear failure occurred. Consequently, the beams were very close to tension failure. Based on the theoretical calculations (Section 4.2) using the single course prism test results, secondary shear failure in these beams occurred at 96% of the flexural moment of resistance. Therefore, the degradation in the ultimate moment due to shear failure was very small. The concrete beams with a/d ratio of 3.0 which had the highest ultimate moment in this group, CB10, had attained 95% of the theoretical flexural moment. In this case however, only the non-tensioned steel had yielded prior to failure. Although the concrete beams with a/d ratio of 1.5 failed at 97% and 116% of the computed ultimate flexural moment of resistance, only the non-tensioned steel had yielded prior to failure. This has been attributed to 'tied arch action' (see Chapter 7).

4.4 A COMPARISON BETWEEN THE ULTIMATE MOMENTS OBTAINED EXPERIMENTALLY AND THE CODE RECOMMENDATIONS

In this section the ultimate flexural moments obtained experimentally are compared with those obtained from the appropriate code of practice[1,58]. A partial safety factor of 1.0 is used for all materials.

The code of practice for structural brickwork[1] allows two methods for the determination of the characteristic compressive strength of masonry f_k. This may be obtained directly from test results on prisms as described in Appendix D of the code[1]. In the absence of direct test results, f_k may be determined from Table 3A or Fig. 1 (a) of the code[1] which give f_k values for various combinations of brick and mortar tested perpendicular to the bed face. The corresponding value for specimens tested parallel to the bed face is taken as a third this value. Both methods have been used and the results from each will be compared.

In Table 4.4.1, a comparison is given between the average compressive strength for brickwork obtained experimentally f_m, the characteristic strength obtained from prism test results as suggested by the code[1], f_{k1}, and that obtained from Table 3A of the code[1], f_{k2}. The value of f_{k2} is almost a third of the value of f_{k1}. The average stress in the compression zone at failure is given by the product $\lambda_1.f_m$ or $\lambda_1.f_k$ in a brickwork beam (see Chapter 3 and Section 4.2). These are also presented in Table 4.4.1 along with the ratios $\lambda_1.f_{k1}/\lambda_1.f_m$ and $\lambda_1.f_{k2}/\lambda_1.f_m$, which give 0.95 and 0.33 respectively. The effect of these values on the ultimate moment are discussed below.

The ultimate strain in brickwork/concrete adopted in both codes of practice[1,58] is 0.0035. These values in both cases are in good agreement with the strains measured in the beams which failed in flexural tension (see Section 4.3.1). The stress-strain relationships adopted for the tensioned reinforcement are identical. This is presented in Fig. 4.4.1 with the idealised relationship obtained in Chapter 3.

The ultimate moments obtained from the codes of practice for brickwork and concrete are compared with those obtained experimentally in Table 4.4.2. In both brickwork and concrete, as expected, the codes gave very good predictions of the experimental ultimate flexural moment. In concrete, The ultimate moment was underestimated by an average of 8%. In brickwork, the ratio of the experimental ultimate moment to the code value was dependent on the method used to determine the characteristic compressive strength f_k.

When the characteristic compressive strength is calculated from prism test results, (Appendix D of the code i.e. f_{k1}), the experimental value was underestimated by about 11%. This method also gave an accurate assessment of the behaviour of the beam; the compressive strength was sufficient to enable the tensioned reinforcement to yield and hence the beam failed in tension. With the characteristic strength obtained from Table 3A and Fig. 1 (a) of the code (a third the characteristic strength normal to the bed joint, i.e f_{k2}), the experimental ultimate flexural moment was underestimated by an average of 64%. In this case, the average compressive stress in the compression zone $\lambda_1.f_{k2}$ gave a very conservative value of the average compressive strength which was too low to enable the tensioned reinforcement to yield and hence the beam failed in compression - an inaccurate reflection of the behaviour of the beam.

Table 4.4.1 Compressive Strength of Brickwork Based on the Code of Practice[1]

Exp			BS 5628[1] Values				
f_m N/mm^2	from prism tests f_{k1} N/mm^2	1/3 bed joint strength f_{k2} N/mm^2	$\lambda_1 f_m$ N/mm^2	$\lambda_1 f_{k1}$ N/mm^2	$\lambda_1 f_{k2}$ N/mm^2	$\frac{\lambda_1 f_{k1}}{\lambda_1 f_m}$	$\frac{\lambda_1 f_{k2}}{\lambda_1 f_m}$
32.56	20.17	7.04	21.23	20.17	7.04	0.95	0.33

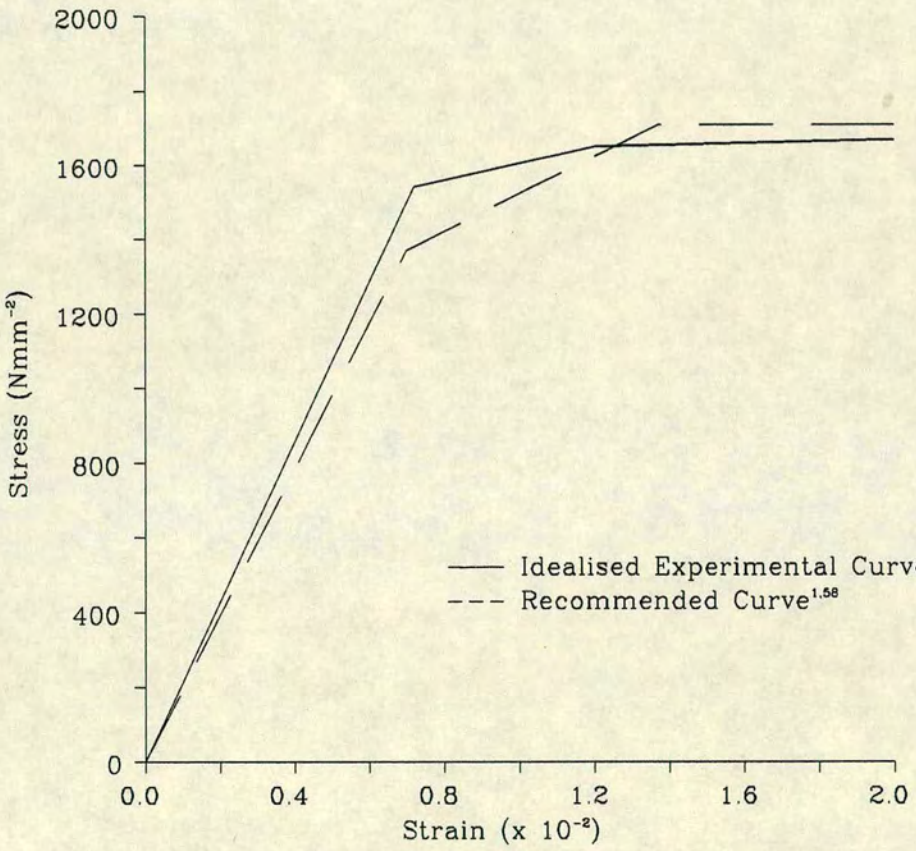

Fig. 4.4.1 Comparison Between the Idealised Experimental Curve for the Tensioned Steel and the Code[1.58] Recommendations

Table 4.4.2 Experimental and Code[1,58] Values for the Ultimate Moment

Beam	% area of steel	Exp	BS 5628[1]			
			f_{k1}		f_{k2}	
		kNm	M_{fk1} kNm	Exp/Theo	M_{fk2} kNm	Exp/Theo
Brickwork beams[11]						
FB1	0.274	56.9	53.1	1.07	35.8	1.59
FB2	"	56.4	53.1	1.06	35.8	1.57
FB3	"	61.5	53.1	1.16	35.8	1.72
FB4	"	58.4	53.1	1.10	35.8	1.63
FB5	"	59.2	53.1	1.12	35.8	1.65
FB6	"	58.8	53.1	1.11	36.2	1.62

Concrete beams			BS 8110[58]	
				Exp/Theo
CB1	0.274	58.8	54.0	1.09
CB2	"	58.1	54.0	1.08
CB3	"	59.1	54.0	1.09
CB5	"	57.6	54.0	1.07
CB4	0.548	103.0	92.8	1.11
CB7	"	103.4	90.8	1.14
CB8	"	100.1	89.7	1.12

Comparing the ultimate moment of the concrete beams predicted using the stress-strain relationship for concrete given in Chapter 3 and that for the tensioned steel obtained experimentally (see Chapter 3), with that predicted by using the code[58], the code predicts higher ultimate moments. Since the steel had yielded at failure, this difference can be attributed to the slight difference in the post-yield behaviour of the idealised stress-strain relationship obtained in Chapter 3 and that adopted by the code (see Fig. 4.4.1). On the other hand, when the ultimate moment for the brickwork beams is obtained using the characteristic compressive strength obtained from prism test results (Appendix D of the code[1]) is compared with that using the stress-strain relationship obtained experimentally (see Chapter 3), the latter gives higher results. Here, the differences in the post-yield behaviour of the tensile reinforcement is negated by the much larger increase in λ_2 (experimental value of 0.372, code value 0.5). The magnitude of the compressive force at failure is controlled by the product $\lambda_1.f_m$ or $\lambda_1.f_k$ which are similar in both methods inspite of the significant differences in λ_1 (code value for λ_1=1.0) (see Table 4.4.1).

4.5 CONCLUSIONS

In this chapter, the ultimate moment of fully and partially prestressed beams of brickwork and concrete with identical cross-sectional properties and similar compressive strengths have been compared. The following conclusions can be drawn:

1. The ultimate moment of resistance of prestressed beams of brickwork and concrete having the same cross-sectional properties and of similar compressive strengths are very similar when failure is in flexural tension.

2. The ultimate flexural moment of prestressed brickwork and concrete beams can be accurately predicted by the flexural theory and the direct method using the stress-strain relationship for brickwork and concrete respectively.

3. When a prestressed brickwork beams fails primarily in shear, the ultimate moment is lower than in a corresponding concrete beam.

4. The ultimate flexural moment of resistance of prestressed brickwork beams obtained from the code using the characteristic strength of brickwork obtained from uniaxial tests on representative prism formats are in very good agreement with experimental results. The mode of flexural failure predicted by this method is also in agreement with observed behaviour.

5. The ultimate flexural moment of resistance of prestressed brickwork beams in which the compressive stresses develop parallel to the bed joint is grossly underestimated by the code when the characteristic compressive strength is taken as a third the value normal to the bed joint. This method also gives an inaccurate reflection of the behaviour of the beam at failure.

6. The balanced steel area for a partially prestressed brickwork/concrete section containing tensioned and non-tensioned tensile reinforcement at different levels can be estimated from the method presented in this work.

CHAPTER 5
THE LOAD-DEFLECTION RESPONSE

5.1 INTRODUCTION

In the design of brickwork and concrete flexural members the effect of load is as important as the ultimate load carrying capacity. The effect of load causes deflection, cracking and vibration and are catered for in design under the serviceability requirements. In normal design, only the first two requirements are considered. This chapter is concerned with deflection. Cracking is examined in Chapter 6. The serviceability limit state of deflection aims to ensure that the deflection of a structure or any part of it does not adversely affect its appearance or efficiency. Excessive deflection can cause damage to finishings and cladding, and in extreme cases may lead to a distribution of load not considered in the design. For example, excessive sagging of a beam can cause the transfer of load to a partition wall.

Several theoretical methods are available for estimating the deflection of a member. The choice of method depends on the degree of accuracy required and the complexity of the problem. A brief summary of the existing methods is given and the most suitable for this study is described in detail. An important step in the theoretical calculation of the deflection is the determination of the moment-curvature ($M-\phi$) relationship. This relationship also provides valuable information on the ductility of a member. In this chapter, the $M-\phi$ relationship has been obtained from considerations at a cracked section. However, the load-deflection response is required to reflect average behaviour. The relationship between the deflection and curvature has been improved by accounting for the tension stiffening effect of the uncracked portions of the beam between cracks.

The experimentally obtained $M-\phi$ and load-deflection relationships for similar fully and partially prestressed beams of brickwork and concrete are compared. A comparison is also made with theory. The design of brickwork for deflection is also examined.

5.2 THEORY

5.2.1 General

In the case of beam bending the following relationship exists between the moment M and the curvature ϕ:

$$\phi = M/E.I \qquad \text{... 5.2.1}$$

where
E = Young's Modulus of Elasticity
I = Second moment of area

If the bending moment distribution along a member is known, the curvature at any section can be determined. The deflection y, is then obtained from the differential equation:

$$\phi = \delta^2 y/\delta x^2 \qquad \text{... 5.2.2}$$

where
x = distance along the beam

Concrete and brickwork are brittle materials. The tensile strength of both materials is low, hence flexural cracking occurs so that the second moment of area, I, changes. The Young's modulus of elasticity also varies with stress level. This has lead to three basic methods for calculating the curvature in bending and hence deflection of their members which take into account the varying nature of the flexural rigidity, E.I. These are as follows:

1. The moment of inertia method;

2. The direct method;

3. The finite element method.

The application of the finite element method of analysis to reinforced and prestressed concrete is well established. Recent developments in structural masonry have enabled more realistic models to be used in finite element

analysis. However such a powerful method is usually applied to complex problems/structures. In this simple beam problem such a sophisticated method of analysis for deflection is quite unnecessary. However, as will be seen in Chapter 7, a finite element analysis was carried out to investigate the shear strength of partially prestressed brickwork beams. The results produced included deflection which were used in the verification of the finite element analysis (see Chapter 7).

5.2.2 The Moment of Inertia Method

In this method, the behaviour of the section is assumed to be elastic. A bi-linear or tri-linear relationship is then obtained between the moment and curvature. Up to cracking, the moment of inertia is based on the uncracked section. It is calculated either by using the gross or transformed section. The latter accounts for the presence of the reinforcement. After cracking the moment of inertia is obtained from the area of concrete (or brickwork) in compression and the transformed area of steel. In an under-reinforced section, the moment of inertia is also calculated at a third stage[68], the yielding of the tensile reinforcement. At each stage a value of the elastic modulus is chosen to reflect the level of stress in the beam.

The curvature at a crack is always greater than the average value within any particular region. This is due to the stiffening effect of the concrete/brickwork in the tension zone between cracks. The lightly loaded parts of a beam which may remain uncracked in flexure also contribute to tension stiffening. Several formulae have been proposed for the tension stiffening effect in concrete. Among these are the proposals made by Yu and Winter[69], Branson[70], Beeby[69] and Rao et al[68]. The last method will be examined in Section 5.2.4.

The limitations of this method are as follows:

- The non-linear behaviour of brickwork and concrete is not taken into account

- In a prestressed member, after cracking, the depth of the neutral axis gradually reduces with applied load. The compression zone on which the moment of inertia of a cracked section is based is continually changing

- The elastic modulus varies continually with stress level

The moment of inertia method can not therefore be expected to accurately reflect beam behaviour. However, its relative simplicity makes it a useful design tool.

5.2.3 The Direct Method

The direct method[11,12,71,72] uses the actual stress-strain relationship of the brickwork or concrete as well as that of the tensile reinforcement. This immediately eliminates some of the limitations associated with the moment of inertia method (see Section 5.2.2). Up to cracking however, the beams are considered to be elastic and the curvature is obtained from equation 5.2.1. The cracking moment M_{cr} is obtained from the following:

$$M_{cr} = [P_e(1/A + e/Z) + f_r] Z \qquad \ldots 5.2.3$$

where
P_e = effective prestressing force
A = gross cross-sectional area
e = eccentricity of the prestressing force
Z = modulus of the section
f_r = modulus of rupture

After cracking, the curvature is obtained by applying increments of compressive strain to the extreme compression fibre. Assuming a cracked section, the tensile strain required for the equilibrium of the internal forces is obtained. The curvature is obtained from the strain profile. For a particular loading, the distribution of curvature along the beam is obtained from the computed moment-curvature relationship. The average curvature is then obtained by accounting for tension stiffening. The deflection is obtained from double integration along the span.

The direct method has been applied to prestressed brickwork by Pedreschi[11] who incorporated the stress-strain relationship for brickwork from prestressing to failure. This was further improved by Walker[12] who accounted for the properties of the composite section (see Chapter 3). Using the idealised stress-strain relationship for brickwork obtained from the single course prisms and allowing for tension stiffening, very good agreements were

obtained with experimental results. This method was also assumed to be applicable to reinforced and prestressed concrete. This method will be used to obtain the M–ϕ relationship for the brickwork and concrete beams tested in this study.

The assumptions made here are the same as those made in the flexural theory (see Chapter 4) with the exception that in this method, the tensile strength of brickwork and concrete is taken into account before cracking. The M–ϕ relationship is obtained in three stages:

1. At prestressing;

2. From prestressing to cracking; and

3. From cracking up to the ultimate flexural moment.

The following derivations have been carried out for the most complex case i.e. a brickwork section with an enclosed cavity containing tensioned and non-tensioned reinforcement at different levels. They simplify for the less complex sections and are equally applicable to concrete.

5.2.3.1 M–ϕ at Prestressing

Initially, the section is assumed to be elastic. The extreme fibre stresses are obtained from the properties of the transformed section.

$$\sigma_1 = P_e/A_t - P_e.\ e/Z_t$$

or

$$\sigma_2 = P_e/A_t + P_e.\ e/Z_t \qquad \text{... 5.2.4}$$

where
σ_1, σ_2 = stress in top and bottom fibres due to prestressing respectively
P_e = effective prestressing force
A_t = cross-sectional area of the transformed section
e = eccentricity of prestressing force
Z_t = section modulus

The corresponding extreme fibre strains ε_{p1} and ε_{p2} are then obtained by assuming a value for the initial tangent modulus of brickwork, E'_m:

$$\varepsilon_{p1(2)} = \sigma_{p1(2)}/E'_m$$

... 5.2.5

The variation in the initial tangent modulus up to the maximum compressive stress which is allowed due to pretressing, 0.4 f_k^1 (0.4 f_{cu}^{58} in concrete) is negligible. The ratio of the top and bottom fibre strains r_t, is assumed to be constant:

$$r_t = \varepsilon_{p1}/\varepsilon_{p2}$$

... 5.2.6

In the composite brickwork section, the modular ratio m' is also assumed to be constant where:

$$m' = E'_c/E'_m$$

... 5.2.7

where E'_c is the initial tangent modulus of concrete This assumption is also valid up to the maximum allowable compressive stress due to prestress.

Fig. 5.2.1 shows the conditions in a composite brickwork section, (containing an enclosed cavity) due to the prestressing force. The resultant compressive force C, due to prestress is given by:

$$C = b \int_n^{ht} F_m(\varepsilon)\ \delta x + b_c \int_{ht}^{hb} F_c(\varepsilon)\ \delta x + (b - b_c) \int_{ht}^{hb} F_c(\varepsilon)\ \delta x + b \int_{hb}^{h} F_m(\varepsilon)\ \delta x$$

... 5.2.8

where
b = breadth of section
b_c = width of the concrete cavity
n = neutral axis depth
h_t = depth to the top of the cavity
h_b = depth to the bottom of the cavity
h = overall depth of the section
$F_m(\varepsilon)$ = stress-strain relationship for brickwork
$F_c(\varepsilon)$ = stress-strain relationship for concrete

The strain ε is given by:

$$\varepsilon = \varepsilon_{p1} + (\varepsilon_{p2} - \varepsilon_{p1})\ x/h$$

... 5.2.9

For equilibrium,

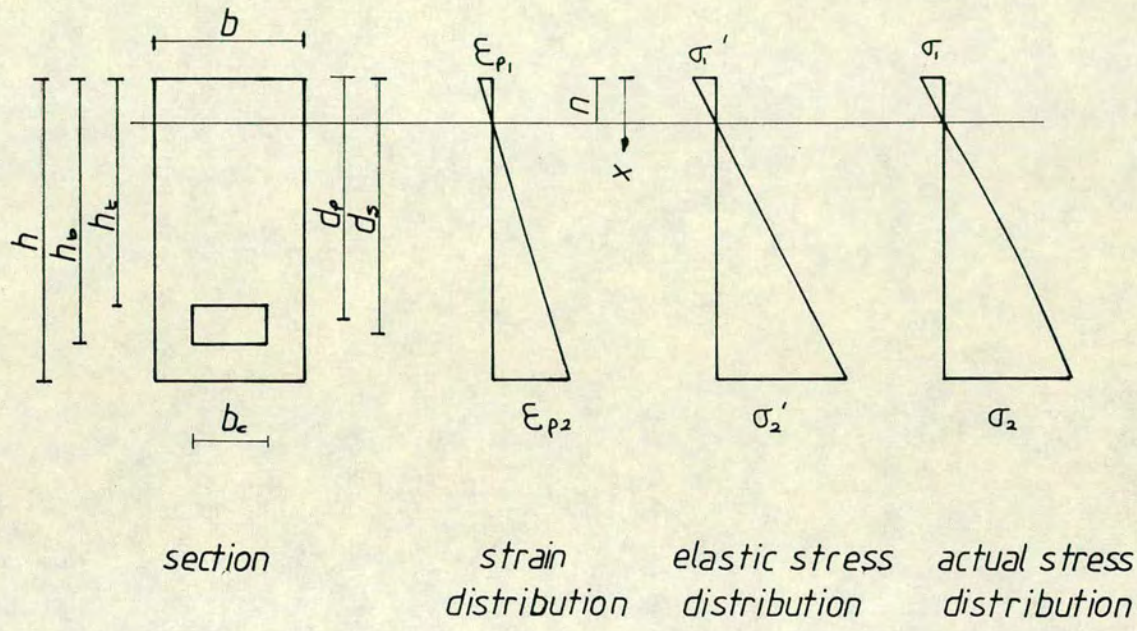

Fig. 5.2.1 Conditions in a Composite Brickwork Section due to the Effects of Prestressing

$$C = P_e$$

... 5.2.10

If equation 5.2.10 is not satisfied, the initial tangent modulus E'_m is modified to E_m such that:

$$E_m = E'_m \, (C/P_e)$$

... 5.2.11

Equations 5.2.5 and 5.2.8 are reapplied until 5.2.10 is satisfied. This is assumed to occur when C/Pe is between 0.98 and 1.02.

The curvature due to prestress is given by

$$\phi_p = [\varepsilon_{p1} - \varepsilon_{p2}]/h$$

... 5.2.12

5.2.3.2 M–ϕ From Prestressing to Cracking:

Cracking will occur once the prestress has been neutralised and the flexural tensile strength at the soffit has been exceeded. The strain at any load is obtained from the combined effect of the strain profile due to prestressing and that due to the applied load. The magnitude of strain required to decompress the prestressing force is equal to and opposite to ε_{p2}. Fig. 5.2.2 shows the conditions in a composite brickwork section with an enclosed cavity just before cracking. The cracking strain is given by:

$$\varepsilon_{cr} = \varepsilon_r + \varepsilon_{p2}$$

... 5.2.13

where

$$\varepsilon_r = f_r/E'_m$$

... 5.2.14a

ε_r = ultimate tensile strain of brickwork
f_r = the modulus of rupture of the section

When the concrete cavity extends to the soffit of the beam there is a contribution from concrete. ε_r is then given by:

$$\varepsilon_r = [f_r/E'_m] \, . \, [b \, /((b - b_c) + b_c . \, m')]$$

... 5.2.14b

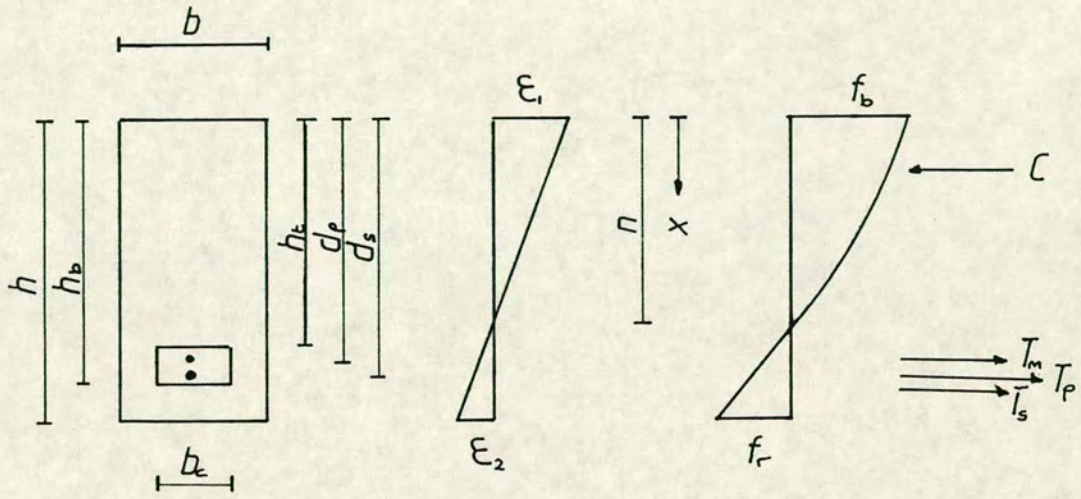

section resultant strain profile stress distribution

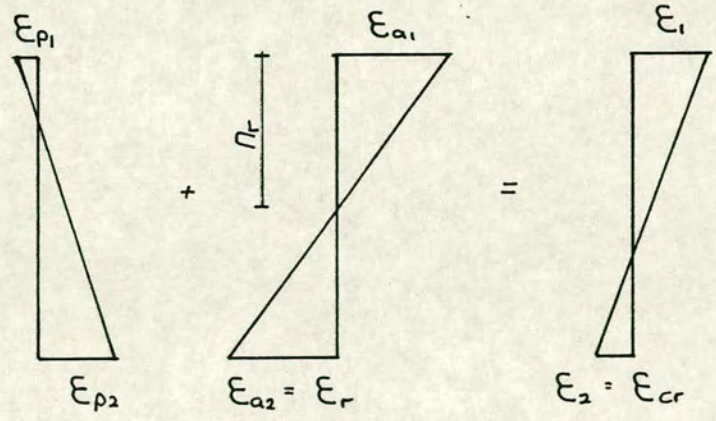

prestrain applied strain resultant

Fig. 5.2.2 Conditions Immediately Before Cracking

The cracking moment is obtained by equating the tensile and compressive forces in the section and taking moments of the resultant forces about the soffit of the section. For the general case where the neutral axis is beneath the concrete cavity ($n > h_b$), the compressive force is obtained from:

$$C = b \int_0^{ht} F_m(\varepsilon)\ \delta x + b_c \int_{ht}^{hb} F_c(\varepsilon)\ \delta x + (b - b_c) \int_{ht}^{hb} F_m(\varepsilon)\ \delta x + b \int_{hb}^{n} F_m(\varepsilon)\ \delta x$$

... 5.2.15a

If the neutral axis falls within the concrete cavity ($h_t < n < h_b$):

$$C = b \int_0^{ht} F_m(\varepsilon)\ \delta x + b_c \int_{ht}^{n} F_c(\varepsilon)\ \delta x + (b - b_c) \int_{ht}^{n} F_m(\varepsilon)\ \delta x$$

... 5.2.15b

With the neutral axis above the cavity ($n < h_t$):

$$C = b \int_0^{n} F_m(\varepsilon)\ \delta x$$

... 5.2.15c

The tensile strain ε is given by:

$$\varepsilon = \varepsilon_1 - \varepsilon_1 . (x/n)$$

... 5.2.16

and

$$n = [\varepsilon_1/(\varepsilon_1 + \varepsilon_2)] . h$$

... 5.2.17

The tensile force in the section is made up of that contributed by the tensioned and non-tensioned reinforcement and that due to the masonry and concrete cavity.

The Tensile Force in the Tensioned Reinforcement:

The strain in the tensioned reinforcement is the sum of that due to the prestress ε_{pp}, that induced by the brickwork at the level of the tendon due to prestress ε_{pe} and that due to the applied load ε_{pa}. Before tensile strains can occur in the brickwork at the level of the tendon, the precompression at that level must be overcome. Assuming that full bond exists between the tendon,

concrete and brickwork shell, an equal strain will be induced in the tensioned reinforcement, ε_{pe}. The strain due to the applied loading is given by :

$$\varepsilon_{pa} = \varepsilon_{a2} [(d_p - n_r)/(h - n_r)]$$

... 5.2.18

where
n_r = centroid of the uncracked transformed section

The total strain in the tensioned steel is thus given by:

$$\varepsilon_p = \varepsilon_{pp} + \varepsilon_{pe} + \varepsilon_{pa}$$

... 5.2.19

and the corresponding tensile force is:

$$T_p = A_p F_p(\varepsilon_p)$$

... 5.2.20

where
A_p = area of tensioned steel
$F_p(\varepsilon_p)$ = stress-strain relationship for the tensioned steel

The Tensile Force In The Non-Tensioned Reinforcement:

This is made up of that due to applied loads ε_{sa} and that due to the precompression in the brickwork at the level of the non-tensioned reinforcement ε_{se}.

Similar to the strain in the tensioned reinforcement due to applied loads, ε_{sa} is given by:

$$\varepsilon_{sa} = \varepsilon_{a2} [(d_s - n_r)/(h - n_r)]$$

... 5.2.21

The total strain in the non-tensioned reinforcement is:

$$\varepsilon_s = \varepsilon_{sa} + \varepsilon_{se}$$

... 5.2.22

and the corresponding tensile force is given by:

$$T_s = A_s F_s(\varepsilon_s)$$

... 5.2.23

where
A_s = area of non-tensioned steel
$F_s(\varepsilon_s)$ = stress-strain relationship for the non-tensioned steel

The Tensile Force in Brickwork/Concrete Composite:

Assuming linear elastic behaviour in tension, the tensile force in the brickwork is given by:

$$T_m = b.\ f_r.\ (h - n)/2$$

... 5.2.24

With an enclosed cavity where $n > h_t$, using the value of f_r for brickwork leads to an underestimate for T_m as the presence of concrete which has the higher value of flexural tensile strength will lead to a higher value of T_m. However, this difference is small and has no significant impact on the results obtained. When the concrete cavity extends to the soffit of the beam and the neutral axis depth is above or within the cavity, the value of f_r is that of the composite brickwork and concrete (see Chapter 3). For equilibrium,

$$C = T$$

... 5.2.25

where $T = T_p + T_s + T_m$.

Equilibrium is assumed to be satisfied when

$$0.98 \leqq C/T \leqq 1.02$$

... 5.2.26

The cracking moment is obtained by taking moments of the resultant forces C and T about the soffit of the beam. The distance from the centroid of the compression zone to the soffit of the beam, l_a for the general case ($n > h_b$) is given by:

$$l_a = \left[b\int_0^{h_t} F_m(\varepsilon)(h-x)\delta x + (b-b_c)\int_{h_t}^{h_b} F_m(\varepsilon)\,(h-x)\delta x + b_c\int_{h_t}^{h_b} F_c(\varepsilon)(h-x)\,\delta x + b\int_{h_b}^{n} F_m(\varepsilon)(h-x)\delta x \right] \div C$$

... 5.2.27a

when $n < h_t$ then,

$$l_a = \left[b\int_0^{n} F_m(\varepsilon)(h - x)\,\delta x \right] \div C$$

... 5.2.27b

For $h_t < n < h_b$,

$$I_a = \left[\begin{matrix} b\int_0^{ht} F_m(\varepsilon)(h-x)\delta x + (b - b_c)\int_{ht}^{n} F_c(\varepsilon)(h - x)\ \delta x \\ b_c \int_{ht}^{n} F_m(\varepsilon)(h - x)\delta x \end{matrix} \right] \div C$$

... 5.2.27c

The cracking moment is given by:

$$M_{cr} = C.\ I_a - [T_p(h-d_p) + T_s(h-d_s) + T_m((h-n)/3)]$$

... 5.2.28

and the curvature is:

$$\phi = [\varepsilon_1 - \varepsilon_2]/h$$

... 5.2.29

The M-ϕ relationship from prestressing up to cracking is obtained by applying increments of ε_{cr} to the extreme tension fibre. Initially a neutral axis depth n_r due to the applied loading is assumed to be h/2 or the depth of the centroidal axis of the transformed section. This gives the strain in the brickwork and the tensile reinforcement due to the applied loading. Using equations 5.2.19, 5.2.20, 5.2.22, 5.2.15, 5.2.23 and 5.2.24, the internal forces are equated. If 5.2.26 is not satisfied a revised value of n_r is used until equilibrium is attained. The moments and curvatures are then given by equations 5.2.28 and 5.2.29.

5.2.3.3 M-ϕ From Cracking to the Ultimate Flexural Moment

Once the flexural tensile strength in the extreme tension fibre has been exceeded, the beam will crack. The crack will travel towards the neutral axis but will terminate short of it because of the tensile strength in brickwork (or concrete) which is less than the ultimate value. This analysis assumes that the crack extends to the neutral axis. However, this assumption does not alter the validity of the analysis as the value of the flexural tensile strength is relatively low.

For the general case (see Fig. 5.2.3) the equation for equilibrium becomes:

$$b\int_0^{ht} F_m(\varepsilon)\delta x + (b-b_c)\int_{ht}^{hb} F_m(\varepsilon)\delta x$$

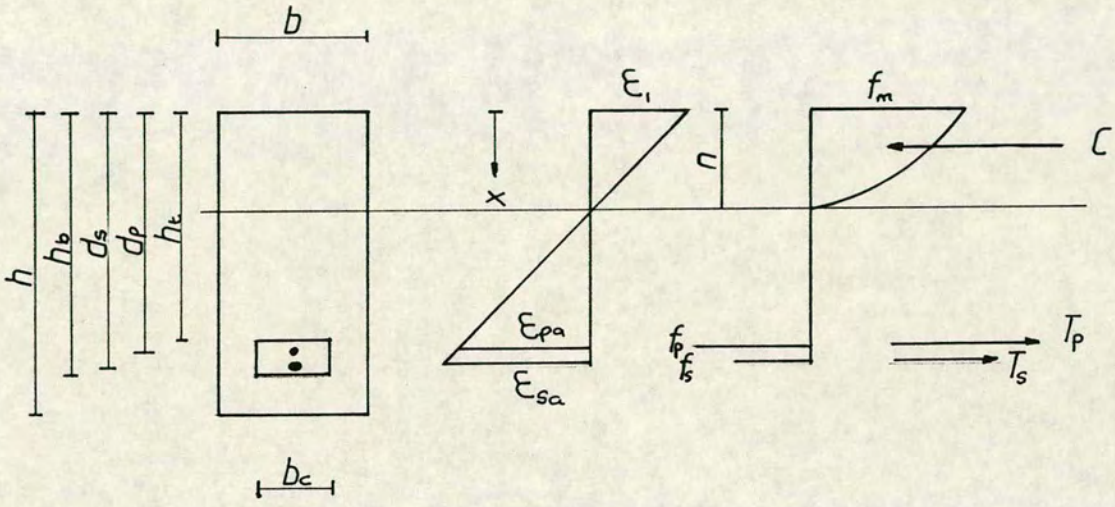

section strain profile stresses

Fig. 5.2.3 Conditions after Cracking

$$+ b_c \int_{ht}^{hb} F_c(\varepsilon)\delta x + b \int_{hb}^{n} F_m(\varepsilon)\delta x$$

$$= A_p F_p(\varepsilon_p) + A_s F_s(\varepsilon_s)$$

... 5.2.30a

where

$$\varepsilon = \varepsilon_1 - \varepsilon_1 . x/n$$

... 5.2.16

when the neutral axis lies within the cavity i.e. $h_t < n < h_b$, in equation 5.2.30a, the fourth term on the left hand side disappears and h_b is replaced by n. With the neutral axis above the cavity, the equation for equilibrium is reduced to:

$$b \int_0^n F_m(\varepsilon)\, dx = A_p F_p(\varepsilon_p) + A_s F_s(\varepsilon_s)$$

... 5.2.30b

When the flexural tensile strength is attained in the extreme tension fibre, the section can be in one of two states: the uncracked state, see Section 5.2.3.2 and the cracked state. In the cracked state,

$$M_{cr} = C . I_a - [T_p(h - d_p) + T_s(h - d_s)]$$

... 5.2.31

As neither the compressive or tensile strains are known, they are evaluated by simultaneous solution of equations 5.2.28 and 5.2.31.

The M–ϕ relationship after cracking is obtained by applying increments of compressive strain to the extreme compression fibre and equating the internal forces using 5.2.30. The moment is obtained from:

$$M = C . I_a - [T_p(h - d_p) + T_s(h - d_s)]$$

... 5.2.32

The corresponding curvature is obtained from:

$$\phi = [\varepsilon_1 + \varepsilon_2]/h$$

... 5.2.33

The ultimate flexural moment is reached when the extreme compression fibre attains the crushing strain of the material.

5.2.4 The Tension Stiffening Effect

In the previous section, a method of obtaining the M-ϕ relationship across a crack was described. Besides giving valuable information on the ductility of a section, the M-ϕ relationship is an important step in the determination of the load-deflection response. The deflection at any particular point is a reflection of average behaviour rather than that at a crack. Thus in the computation of the deflection, it is the average curvature which is important. The average curvature can be considerably less than that at a crack. This is due to the contribution to stiffness given by the concrete/brickwork in the tensile zone between cracks which results from bond action between the concrete and steel. This contribution is known as the tension stiffening effect.

In prestressed brickwork, two expressions[11,12] have successfully used to account for the tension stiffening effect. These are based on the proposal made by Rao et al[68] for reinforced concrete. In this section, this method is described as well as the modifications which were necessary for its application to prestressed concrete and brickwork.

The theory put foward by Rao et al[68] assumes a single layer of tensile reinforcement with all bars having the same mechanical properties. In the case of partially prestressed beams which contain two levels of tensile reinforcement with different mechanical properties, Walker[12] suggested the use of an effective area of steel A_{se}, acting at an effective depth d_e. In sections containing tensioned steel and deformed bars:

$$A_{se} = A_p + A_s . f_{sy}/f_{py} \qquad \text{... 5.2.34}$$

and

$$d_e = [A_p.d_p + A_s.f_{sy}.d_s/f_{py}]/A_{se} \qquad \text{... 5.2.35}$$

Where f_{py} and f_{sy} are the yield strengths of the tensioned and non-tensioned steel respectively.

The variation in steel stress between a cracked and an uncracked section is due to bond stresses between the steel and the surrounding concrete. Fig. 5.2.4 shows the distribution of tensile stresses between cracks in a flexural

member under a constant moment. The actual distribution of bond stresses is extremely difficult to determine. A possible distribution is also indicated in Fig. 5.2.4.

Considering the equilibrium of a section midway between cracks:

$$a_o \, s_m \, \tau_b/2 = A_{se}(f_{se} - f_{se}')$$

... 5.2.36

where
a_o = sum of perimeters of reinforcement
s_m = mean crack spacing
τ_b = bond stress
f_{se} = tensile stress in equivalent area of tensioned reinforcement at a crack
f_{se}' = tensile stress in equivalent area of tensioned reinforcement away from a crack

The difference is steel strain at this point is:

$$\varepsilon_{se} - \varepsilon_{se}' = (f_{se} - f_{se}')/E_s$$

... 5.2.37

where ε_{se} and ε_{se}' are the strains corresponding to f_{se} and f_{se}' respectively.

The mean strain will be given by:

$$\varepsilon_{sem} = \varepsilon_{se} - C_o(f_{se} - f_{se}')/E_s$$

... 5.2.38

For equilibrium, the internal resisting moment at a crack must equal that midway between two cracks. From Fig. 5.2.5;

$$A_{se}.f_{se}.j_1.d_e = A_{se}.f_{se}'.j_3.d_e + A_t.f_{mt}.j_2.d_e$$

... 5.2.39a

where A_t is the area of the transformed section and f_{mt} is the mean tensile stress in the brickwork.

As

$$j_3.d \simeq j_1.d$$

... 5.2.39b

$$A_t = C_1.\ b.\ d_e$$

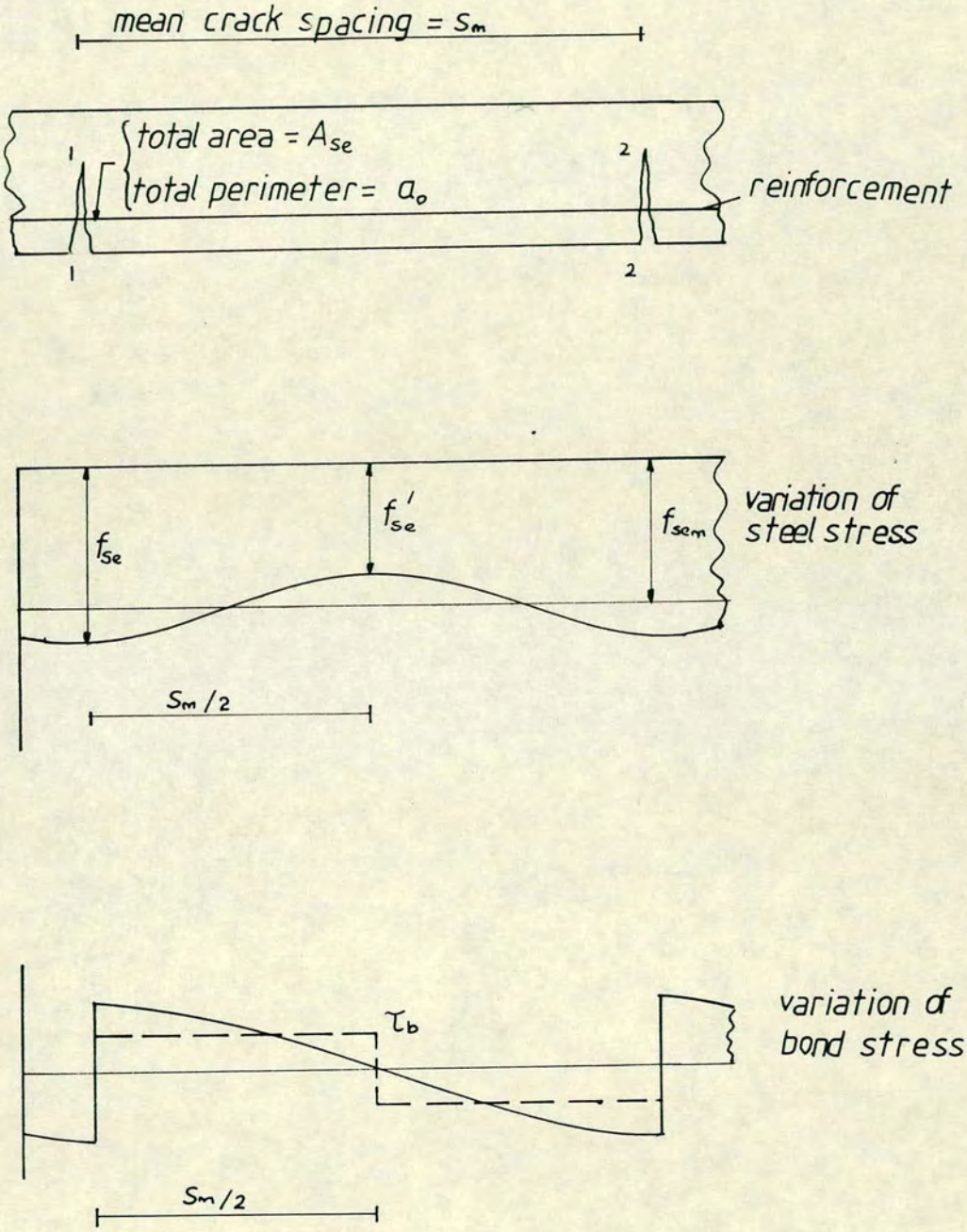

Fig. 5.2.4 Tensile and Bond Stress Distribution Along the Reinforcement

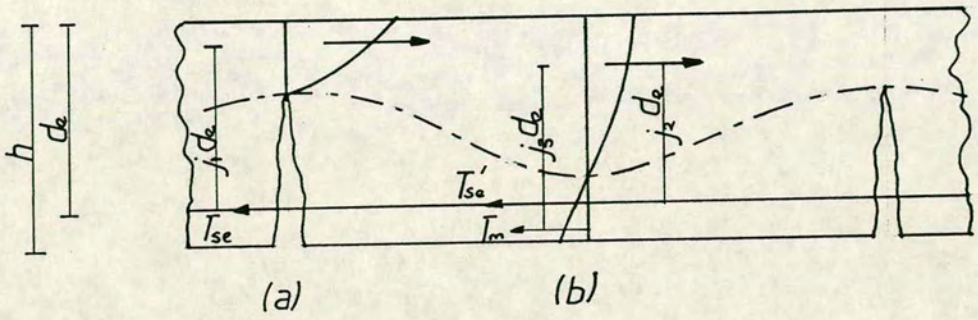

Fig. 5.2.5 Stress Distribution Over the Depth of:

(a) Cracked Section

(b) Mid-Section between Cracks

... 5.2.39c

$$f_{mt} = C_2 \cdot f_r$$

... 5.2.39d

Equation 5.2.39a can be rewritten as:

$$f_{se} - f_{se}' = C_1 \cdot C_2 \cdot j_2/j_1 \cdot f_r \cdot b.d_e/A_{se}$$

... 5.2.40

Substituting 5.2.40 into 5.2.38 gives:

$$\varepsilon_{sem} = \varepsilon_{se} - C_o.C_1.C_2 \cdot j_2/j_1 \; f_r/E_s \; b.d_e/A_{se}$$

... 5.2.41

With $k = C_o \; C_1 \; C_2 \; j_2/j_1$

$$\varepsilon_{sem} = \varepsilon_{se} - k \; f_r/E_s \; b.d_e/A_{se}$$

... 5.2.42

where $b \; d_e/A_{se} = 1/\rho$
ρ = percentage area of reinforcement

Equation 5.2.42 can be rearranged to give:

$$k = (\varepsilon_{se} - \varepsilon_{sem}) \; E_s \; \rho/f_r$$

... 5.2.43

The value of k cannot be determined analytically because no precise information can be obtained concerning C_o, C_1 & C_2. The value of k is obtained empirically.

The steel strain at a crack, ε_{se} can either be obtained theoretically (Rao et al[68]) or from experimental results (Walker[12] and Pedreschi[11]). The average steel strain ε_{sem} is obtained from experimental measurements. As all the other quantities in 5.2.43 are known, k can be calculated. It is then possible to obtain a relationship between k and the degree of cracking $f_{secr}/f_{se)}$ where f_{secr} is the stress in the equivalent area of tensioned reinforcement at a crack at the cracking moment. The expression for k can be substituted back into 5.2.42 to obtain the average steel strain at any load level.

Similarly, the average compressive strain at the extreme fibre will be less

than that across a crack. It has been shown that this difference is very small and can be neglected[11,12].

The average curvature is thus given by:

$$\phi_{av} = [\varepsilon_1 + \varepsilon_{sem}]/d_e$$

... 5.2.44

The average M–ϕ relationship from cracking up to the ultimate is thus obtained by reducing the steel strain across a crack by equation 5.2.42 and using the average steel strain in equation 5.2.44.

The main differences between the method proposed by Rao et al[68] and that used by Pedreschi[11] was in the definition of ε_{se} and ε_{sem} and in the method used to obtain ε_{sem}. Rao et al[68] defined ε_{se} and ε_{sem} as the strain across a crack and the mean strain in the tensile reinforcement respectively. This is the obvious definition for a reinforced concrete beam. For a prestressed section, it seems logical to use the additional strain in the tensile reinforcement due to applied loads so that the prestrain is neglected. This was the definition used by Pedreschi[11] and Walker[12]. Also, the additional strain in the tensile reinforcement across a crack was obtained from experimental measurements[11,12] rather than theoretically from a cracked section as by Rao et al[68]. Walker's[12] proposal was similar to Pedreschi's[11] but for the use of an effective area of steel acting at an effective depth (equations 5.2.34 and 5.2.35).

The following expressions were obtained for the relationship between k, the tension stiffening coefficient and the degree of cracking f_{secr}/f_{se}:

Rao et al[68]: Reinforced concrete

$$k = 0.18\,[f_{secr}/f_{se}]$$

... 5.2.45

Pedreschi[11]:

$$k = 1.0 - 0.97\,f_{secr}/f_{se}$$

... 5.2.46

Walker[12]:

$$k = 0.02 + 0.06[1 - f_{secr}/f_{se}] + 0.77[1 - f_{secr}/f_{se}]^2$$

... 5.2.47

The expression for reinforced concrete (5.2.45) and fully prestressed brickwork (5.2.46) are linear while that for partially prestressed brickwork (equation 5.2.47) is non-linear. Also, the expression for reinforced concrete is contradictory to those obtained for fully and partially prestressed brickwork i.e. in reinforced concrete, the tension stiffening effect decreases with increasing load while the converse was found to be the case in prestressed brickwork.

The non-linear form of Walker's[12] equation (5.2.47) for partially prestressed brickwork was attributed to the non-linear material characteristics of steel and brickwork and also to the post-yield behaviour of steel. In this region large increases in strain correspond to small increases in stress. The value of k thus increases with applied load. However, this increase cannot keep up with the increase in strain and thus results in a non-linear relationship. Pedreschi's[11] expression for k in fully prestressed brickwork beams was obtained from a relatively small number of beams some of which showed a significant variation from equation 5.2.46. Walker's expression is more representative and will be adopted for the brickwork beams reported in this work.

5.2.4.1 Proposed Method for the Calculation of the Tension Stiffening Coefficient k in Prestressed Concrete

It was of interest to find out whether the expression proposed by Rao et al[68] for reinforced concrete was also applicable to this study on prestressed concrete. Using the additional steel stresses and strains obtained experimentally (that is the stresses and strains due to applied load) a relationship between the tension stiffening coefficient k and the degree of cracking f_{secr}/f_{se} was obtained from a least square analysis. The experimental results from the partially prestressed beams were not included in this analysis. This was because every gauge length over which strain measurements were taken contained a crack so that the additional strain across a crack was thus the same as the mean strain. The results are presented in Fig. 5.2.6 along with the best fit equation:

$$k = 0.0063 + 0.192[1 - f_{secr}/f_{se}]^3 \quad \ldots 5.2.48$$

As in brickwork, the tension stiffening coefficient in prestressed concrete is

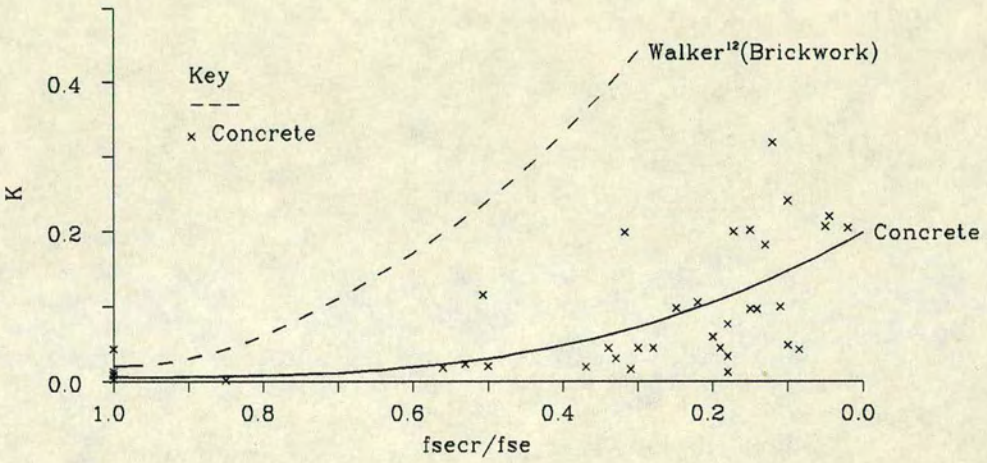

Fig. 5.2.6 Relationship Between Tension Stiffening Coefficient K, and the Degree of Cracking, f_{secr}/f_{se}

non-linear and increases with the load level. This is different from the relationship obtained for reinforced concrete by Rao et al[68] which was linear and decreased with load level (see Equation 5.2.45).

Comparing the expressions for the tension stiffening coefficient in prestressed brickwork and concrete (see Fig. 5.2.6) show a greater tension stiffening effect in brickwork.

5.2.5 Evaluating the Deflection from the M-ϕ Relationship

The relationship between the curvature ϕ and the deflection y along the span of the beam was given in equation 5.2.2 i.e

$$\phi = \delta^2 y/\delta x^2$$

The analytical solution of the above equation is not possible, and so the finite difference method, which is an approximate method for solving differential equations was used to obtain the deflection.

This method of numerical integration is only applicable to problems in which the values of the independent variable, in this case ϕ is known. The object is then to find the values of the dependent variable, y, by first converting the problem to that of solving a set of linear simultaneous equations. A full account of the derivation of the finite difference equations can be found in any reputable text book on structural analysis[73,74]. In this problem, the determination of the curvature ϕ is dependent on the knowledge of the shape and magnitude of the bending moment diagram.

The process of obtaining the load-deflection response of a beam involves the application of the load in increments and calculating the bending moment at the nodes from a knowledge of the bending moment diagram. From the M-ϕ relationship, the curvatures are then obtained. As the only unknowns in the finite difference equations these can be substituted along with the boundary conditions and solved for the deflection y.

The large number of computations required to obtain the load-deflection response have been incorporated into a computer program[12].

5.3 EXPERIMENTAL RESULTS AND DISCUSSION

In this section, experimental results obtained from full scale tests on prestressed brickwork and concrete beams, identical in section and of similar compressive strengths are compared. The cross sections and material properties are given in Chapter 3. A comparison is also made with theoretical results obtained from the direct method using the stress-strain relationship of each material at all stages of loading up to failure.

5.3.1 The M-ϕ Relationship Across a Crack

These relationships were obtained from strain readings taken on the surface of the brickwork/concrete at various depths in the region of constant and maximum moment. The slope of the strain profile represents the curvature. The curvature across a crack was obtained when a crack formed within a gauge length. When more than one gauge length contained a crack, the average curvature across a crack was obtained from equation 5.2.44 i.e.:

$$\phi_{av} = [\varepsilon_1 + \varepsilon_{sem}]/d_e$$

where
ε_1 = the average compressive strain
ε_{sem} = the average additional strain in the reinforcement across a crack.

This method was found to be more representative than simply combining the curvature at each gauge length where a crack appeared.

5.3.1.1 The M-ϕ Relationship Across a Crack for the Fully Prestressed Beams

The M-ϕ relationships across a crack for the fully prestressed beams are presented in Figs. 5.3.1-5.3.2. In Fig. 5.3.1, the relationships for the beams containing 0.274% area of tensioned steel are presented. In both cases, the three distinct phases associated with under-reinforced sections are evident. Phase I represents linear elastic behaviour with the entire section acting. The second phase represents inelastic behaviour with the reinforcement still elastic. The inelastic behaviour results from cracking and the non-linear material properties of the brickwork/concrete. In the third phase, the tensile

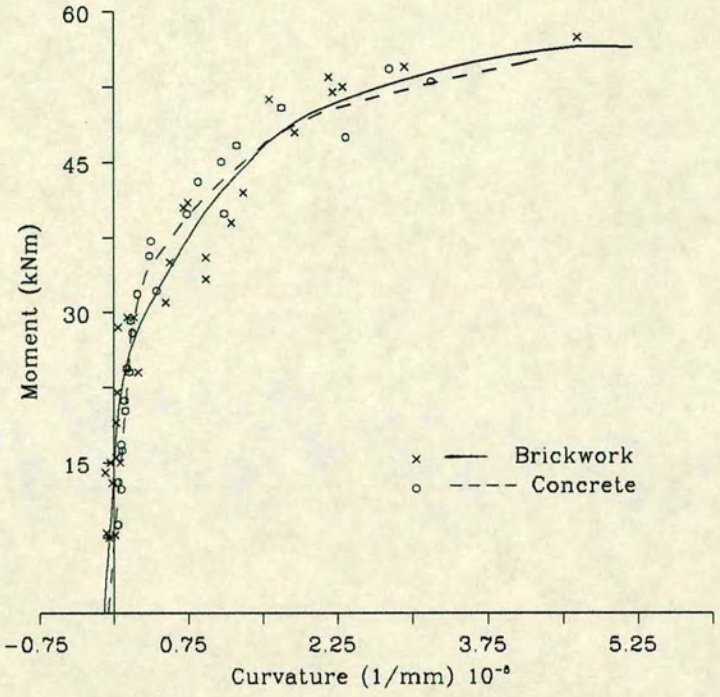

Fig. 5.3.1 Moment–Curvature Relationship Across a Crack, A_p=0.274%

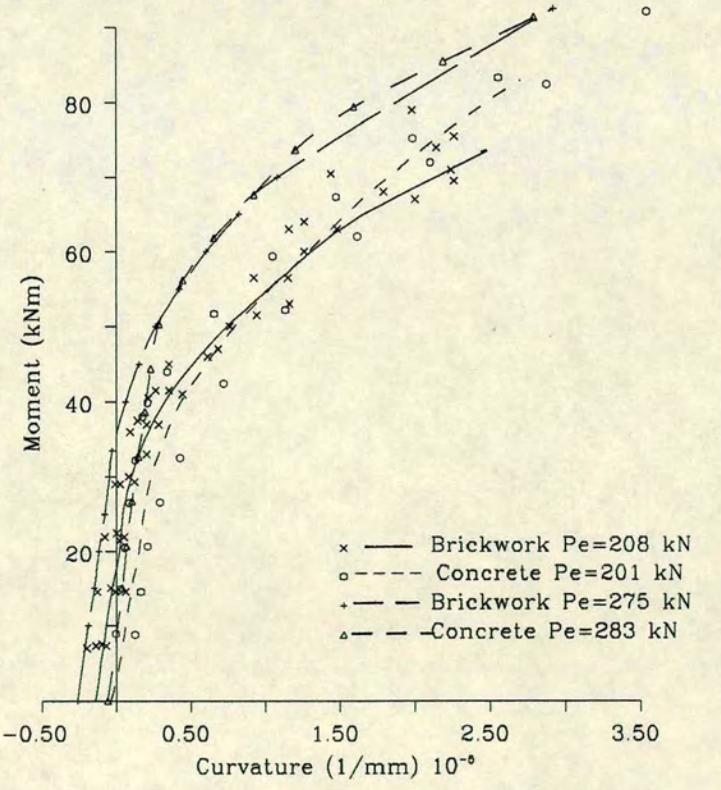

Fig. 5.3.2 Moment–Curvature Relationship Across a Crack, A_p=0.548%

reinforcement has yielded. A small increase in applied load thus corresponds to a large increase in tensile strain and hence curvature. The M-ϕ relationship thus becomes virtually parallel to the x-axis. This is typical of a ductile failure.

The camber due to the eccentric prestressing force is larger in brickwork than in concrete. This is due to the modulus of elasticity of concrete which is higher than the modulus of elasticity of brickwork (see Chapter 3). During the application of external load, cracking begins earlier in brickwork as a result of the lower modulus of rupture when compared with concrete. However, from Fig. 5.3.1, the higher stiffness of concrete is not very obvious during the linear phase as can be seen from the relative slopes of the M-ϕ relationships. This is because these slopes represent the average stiffness up to cracking. In concrete, the higher modulus of rupture causes higher compressive stresses before cracking. The modulus of elasticity thus suffers a larger reduction before cracking.

After cracking, as indicated by the relative steepness of the post-cracking curves, the stiffness in brickwork is higher. This is partly due to the higher stress levels in concrete and its associated reduction in the modulus of elasticity mentioned above. Also, at cracking the tensile force previously carried by the uncracked concrete/brickwork is tranferred to the tensile reinforcement. This being larger in concrete corresponds to a larger tensile strain and hence curvature. Further, as a result of the non-homogeneous nature of brickwork, the path of a crack is through alternate brick/mortar interfaces and brick unit or horizontally along the bed joint. The tensile strength at each of these locations is different. For example that of a brick unit is much higher than that at the brick/mortar interface. The net effect is to slow down the upward propagation of cracks. With increasing load, the relationships for brickwork and concrete become very close until failure. The largest difference occurs when concrete cracks with brickwork into its inelastic phase.

The relationships for the beams containing 0.548% area of tensioned steel are presented in Fig. 5.3.2. The effect of an increased prestressing force in increasing the cracking moment and camber is clearly illustrated by comparing both sets of curves. In brickwork an increased prestressing force also increased the shear strength so that the ultimate moment was increased. In Fig. 5.3.2, the third phase of the M-ϕ relationship which is associated with

post-yield behaviour of the tensile reinforcement is absent in brickwork. This was due to shear failure. The concrete beams however failed in flexure but at this area of steel, the beam containing the higher prestressing force was close to that required for a balanced section. Therefore, the concrete crushed soon after the steel yielded. The concrete beam section with the lower prestressing force was further away from the balanced condition so that crushing of the brickwork occurred long after the steel had yielded. Larger curvatures were thus measured and the flattening out of this relationship was more evident.

As in the beams with 0.274% area of steel the camber was much larger and cracking began earlier in brickwork. However, the differences in camber and the higher post-cracking stiffness of the brickwork beams ensured that up to and beyond cracking, the curvature in brickwork was smaller than in concrete. In the beams with the higher prestressing force, the differences in curvature in the post-cracking phase was insignificant until primary shear failure in brickwork. In the beams with less prestress, the differences in the post-cracking phase was more significant than in the former case but were quite small in comparison to the total curvature when the brickwork beams failed in shear.

5.3.1.2 M-ϕ Relationship Across a Crack for the Partially Prestressed Beams

The M-ϕ relationship across a crack for the partially prestressed beams with shear span to effective depth ratios of 1.5 and 3.0 are given in Figs. 5.3.3 a and b respectively. The post yield behaviour of both relationships appear to be absent. This was because these brickwork and concrete beams failed either in primary or secondary shear before all of the tensile reinforcement had yielded. The flattening out of these relationships was therefore absent.

Previous work[12] has shown that there is a change in slope within the inelastic phase when two levels of tensile reinforcement with different yield strengths are present. This is because the distance between each level is such that it is impossible for both tensile reinforcements to yield simultaneously (see Chapter 4). The yielding of each layer thus corresponds to a change in slope within the inelastic phase. This accounts for the absence of a flattening M-ϕ relationship even though in some beams, some of the tensile reinforcement had yielded.

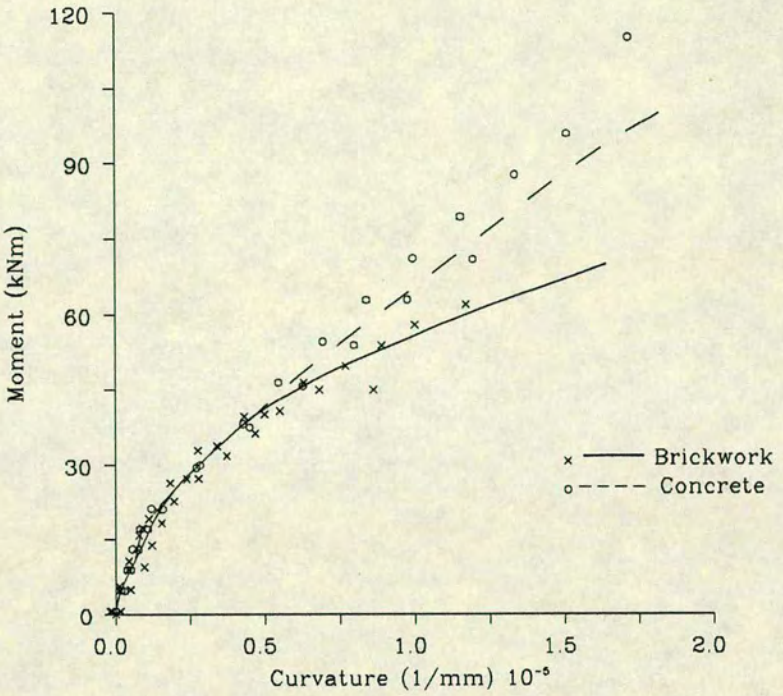

Fig. 5.3.3a Moment–Curvature Relationship Across a Crack, A_{st}=0.856%, a/d=1.5

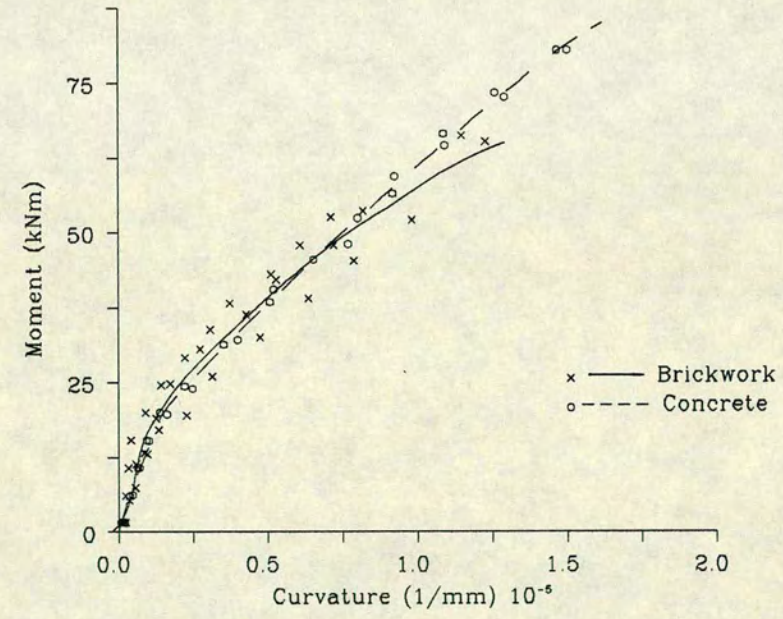

Fig. 5.3.3b Moment–Curvature Relationship Across a Crack, A_{st}=0.856%, a/d=3.0

In these beams, the prestressing force produced virtually no camber in brickwork or concrete when the self weight was acting. These contained one prestressing strand stressed to 70% of the ultimate load (87.5 kN). The relatively short lengths resulted in very high lock-off losses as mentioned in Chapter 3. The higher cracking moment in concrete observed in the previous cases was not very obvious in these beams. This is due to the composite brickwork section (see Chapter 3) in which the concrete cavity extended to the soffit thereby increasing the modulus of rupture of the brickwork beam. However, the higher modulus of elasticity in concrete is reflected in the relative slopes of the elastic phase.

Unlike in the fully prestressed beams, the inelastic phase of the M-ϕ relationships for the partially prestressed beams showed similar post-cracking stiffnesses for brickwork and concrete. This is probably due to the fact that in these beams the average curvature and that across a crack were the same. This was because in the brickwork and concrete beams the crack spacings were such that each gauge length contained a crack (see Chapter 6). With increasing load in the beams with shear span/effective depth ratio (a/d) of 1.5, there was a marked reduction in the stiffness of brickwork when compared with concrete so that the relationships diverged until shear failure in brickwork. This was due to the more significant 'tied arch' action in the concrete beams at this shear span to effective depth ratio. In the beams with a/d ratio of 3.0, 'tied arch' action is less significant than at the previous a/d ratio so that these relationships were very similar until just before the failure of the brickwork beams.

The M-ϕ relationships for the partially prestressed brickwork beams with shear span/effective depth ratios of 4.5 and 6.0 were similar to those with a shear span/effective depth ratio of 3.0.

5.3.2 The Average M-ϕ Relationship

These were obtained using a similar method to those across a crack. However, the average compressive strain and the average additional strain in the tensile reinforcement were obtained from every gauge length.

5.3.2.1 The Average M-ϕ Relationship for the Fully Prestressed Beams

The average M-ϕ relationship is a better representation of the behaviour of a beam than that across a crack which represents behaviour at a cracked section. At a given moment after cracking, the average curvature will be less than that across a crack because of the tension stiffening action of the brickwork/concrete in the tension zone between cracks (see Section 5.2.4). The average M-ϕ relationships are presented in Figs. 5.3.4-5.3.5. The basic shapes of these curves are similar to those obtained for the M-ϕ relationships across a crack.

The relationships for the beams containing 0.274% area of steel are given in Fig. 5.3.4. In the linear elastic phase, the higher stiffness of the concrete beams are better reflected than in the relationship across a crack. As before cracking occurred earlier in brickwork but at a higher moment than in the relationship across a crack. This enhanced cracking moment is due to the fact that in brickwork, cracks are initiated at the brick/mortar interface. The adjacent brick unit and mortar joint have considerably higher tensile strengths. Therefore when cracking begins the reduction in stiffness is localised. On the other hand, concrete is a comparatively homogeneous material. Although cracking also commences at the weakest section, the variation in tensile strength along the member is comparatively small. It consequently suffers a more general loss in stiffness at cracking.

When cracking begins, the averaged M-ϕ relationships, unlike those across a crack, are very similar for brickwork and concrete. This is because of the higher cracking moment in brickwork and the improved post-cracking stiffness in concrete. With increasing load, the average M-ϕ relationships diverge with brickwork having smaller curvatures. This results from the better tension stiffening effect in brickwork when compared to concrete (see Fig. 5.2.6). The differences increase with load level. Like in the relationship across a crack, these relationships also flatten out so that they became virtually parallel to the x-axis indicating ductile behaviour.

The average M-ϕ relationship for the beams containing 0.548% area of tensioned steel are shown in Figs. 5.3.5. These relationships are very similar to those obtained across a crack. In brickwork, the relationships at both prestress levels were virtually unchanged. This is because the crack spacings (see

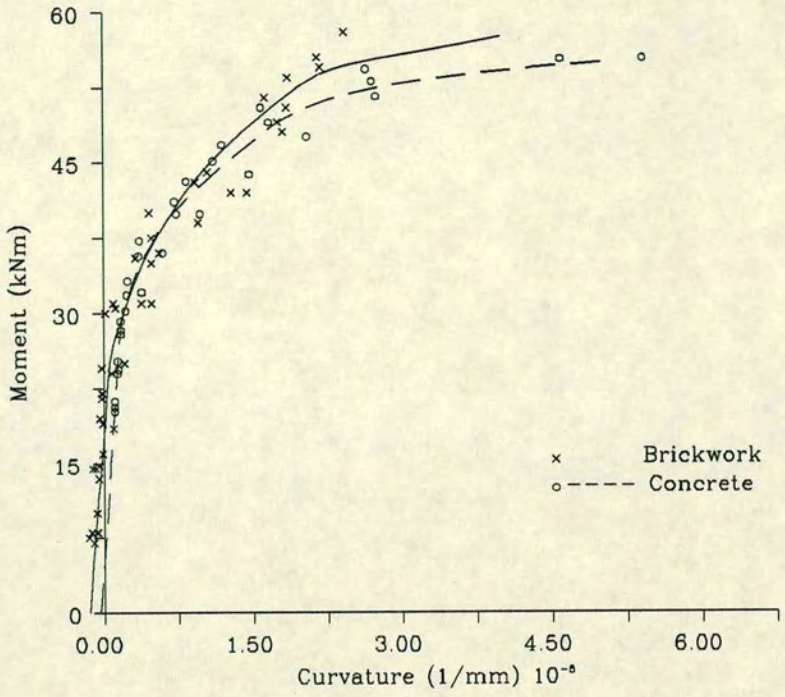

Fig. 5.3.4 Moment–Average Curvature Relationship
A_p=0.274%

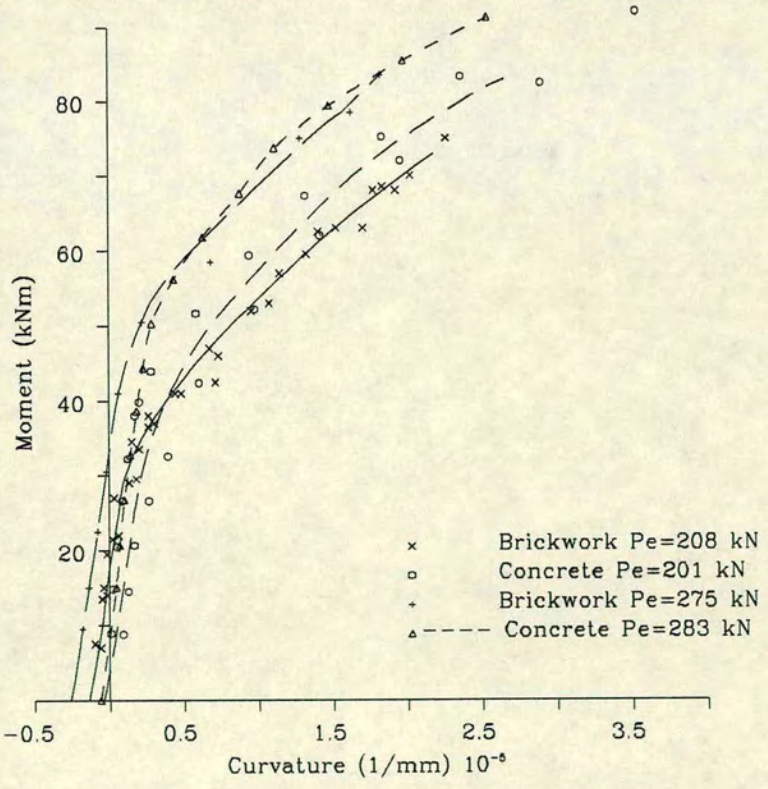

Fig. 5.3.5 Moment–Average Curvature Relationship
A_p=0.548%

Chapter 6) were such that each gauge length contained a crack. The average M-ϕ was thus the same as that across a crack. In concrete the crack spacings were larger so that some gauge lengths did not contain cracks. The average curvature was thus less than in brickwork. The differences in these relationships towards failure can be attributed to primary shear failure in the brickwork beams.

5.3.2.2 The Average M-ϕ Relationships for the Partially Prestressed Beams

The average M-ϕ relationship for the partially prestressed beams in both brickwork and concrete were the same as across a crack (see Figs. 5.3.3). This was because the crack spacings were such that each gauge length contained a crack.

5.3.3 The Load-Deflection Relationships

The load-deflection relationships take the same form as the M-ϕ relationships. Initially, the relationship is linear up to the cracking load. Beyond this point, deflection increases more rapidly with load as it enters the inelastic phase. Finally, after the tensile reinforcement has yielded, the relationship becomes virtually parallel to the x-axis as small increases in load produce large increases in deflection.

Like the M-ϕ relationship, the load-deflection response for a particular beam depends on whether the section is under- or over-reinforced and also on the mode of failure, flexure or shear. In an under-reinforced section which fails in flexural tension, all phases will be present. When the section is over-reinforced the third phase will be absent. If failure is in shear however, the relationship can terminate in any phase.

Unlike the M-ϕ relationships, the applied load-deflection response obtained experimentally began at the origin. This was because it was not possible from the experimental procedure to measure the camber due to prestressing or that if any due to the combined effect of prestress and self weight. The origin of these relationships therefore represent the situation with the beam under the combined effect of prestress and self weight. Brickwork however, has a higher camber due to prestress and also a smaller self weight

(see Chapter 3).

The relationships between the applied load and deflection for similar prestressed brickwork and concrete beams are presented in Figs. 5.3.6–5.3.10.

5.3.3.1 Load–Deflection Relationships for the Fully Prestressed Beams

In Fig. 5.3.6, the relationships for the beams containing 0.274% area of tensioned steel are shown. In each case, all three phases are present. The higher load at which cracking occurs in concrete as well as the more rapid reduction in stiffness after cracking are also illustrated in Fig. 5.3.6. However, up to failure, the differences in both relationships were insignificant. This similarity, like the ultimate moment discussed in Chapter 4, can be attributed to the under–reinforced section. The behaviour of an under–reinforced section is controlled by the tensile reinforcement which was identical in both cases.

In the elastic phase the largest difference occurred at the cracking load of concrete with brickwork already in the inelastic phase. This was 1.5 mm. In the inelastic phase, the difference increased to 2.5 mm. These differences are however quite small. In the post–yield phase, the usefulness of the load–deflection relationship is rather qualitative. It gives an indication of whether or not in overload conditions, the beam possesses sufficient ductility to warn of impending collapse. Fig. 5.3.6 shows that in this case, the brickwork and concrete beams are equally ductile.

The relationships for the beams containing 0.548% area of tensioned reinforcement with the higher prestressing force (Aprox. 280 kN) are shown in Fig. 5.3.7. The features of the M–ϕ relationships discussed in Sections 5.3.1 and 5.3.2 are also evident here. At any given load up to primary shear failure in brickwork, the deflection appears to be smaller in the concrete beams. However, as mentioned above, the effect of the camber which is higher in brickwork has been ignored so that the differences reflected here are exaggerated. The M–ϕ relationships Figs. 5.3.2 and 5.3.5 therefore give a more accurate estimate of the differences to be expected. The largest differences in deflection will occur when concrete cracks with brickwork in the inelastic phase. The absence of the third phase in the brickwork beam results from shear failure.

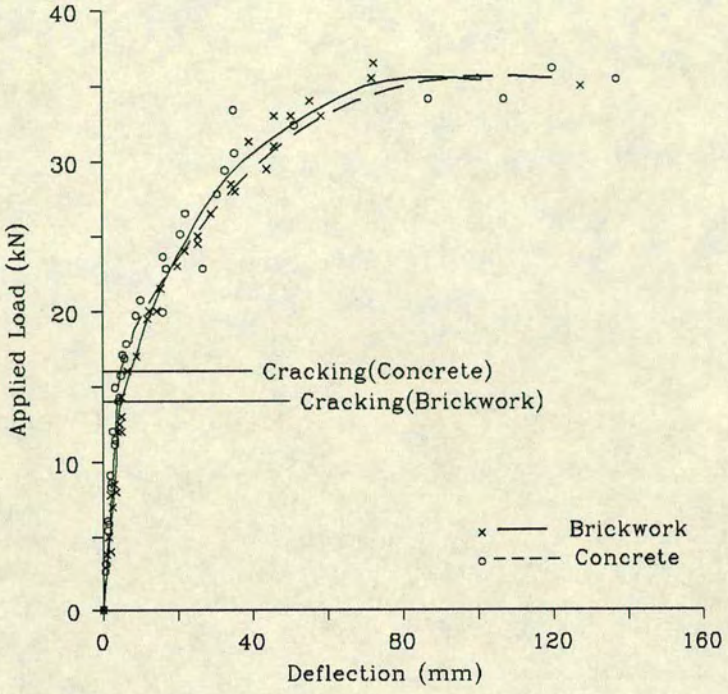

Fig. 5.3.6 Load–Deflection Response
Fully Prestressed Beams A_p = 0.274%

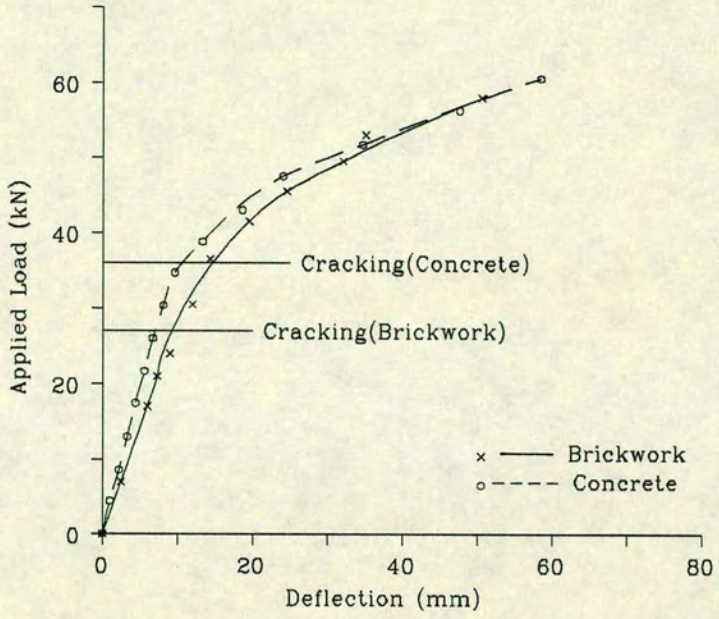

Fig. 5.3.7 Load–Deflection Response
A_p=0.548%, P_e=280 kN

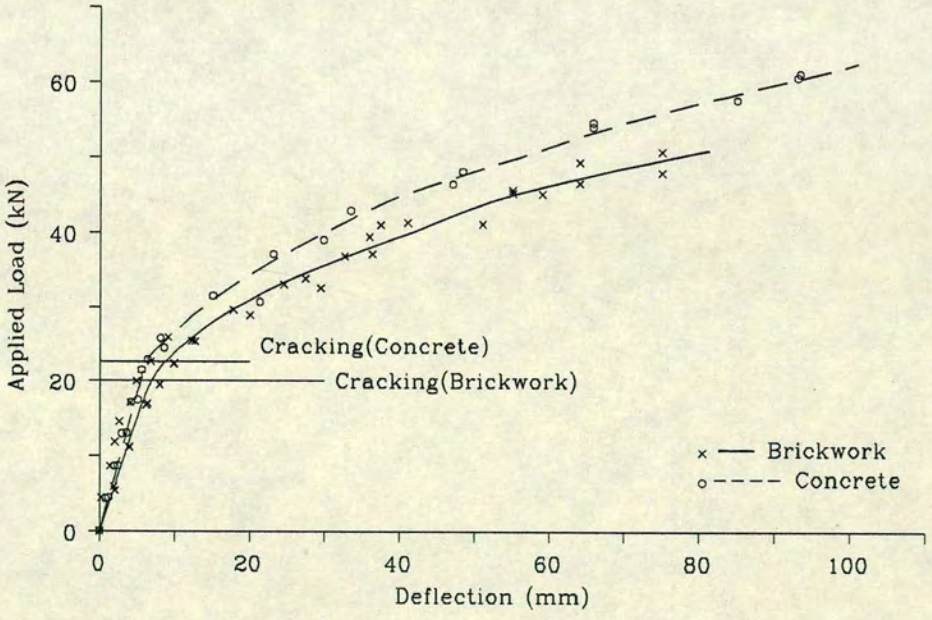

Fig. 5.3.8 Load–Deflection Response
A_p=0.548%, P_e=200 kN

The relationships for the beams containing the same area of steel but with less prestressing force (Aprox. 200 kN) are presented in Figs. 5.3.8. All the features of the average M-ϕ relationships discussed in Section 5.3.2 are also in evidence here. The increased differences in deflection at a given load observed here is also due to the larger camber in brickwork which has not been taken into account.

Comparing Figs. 5.3.7 and 5.3.8 clearly illustrates the effect of increasing the prestressing force on the load-deflection response. The load at which cracking occurs increases and smaller deflections are obtained at a given load after cracking. Also, as mentioned in Sections 5.3.1 and 5.3.2, in beams which fail in shear, the ultimate moment is increased by an increase in the prestressing force.

5.3.3.2 Load-Deflection Relationship for the Partially Prestressed Beams

The load-deflection response for the partially prestressed beams with shear span to effective depth ratios of 1.5 and 3.0 are presented in Figs. 5.3.9 and 5.3.10 respectively. These figures also show all the features of the M-ϕ relationships shown in Figs. 5.3.3. These relationships are very similar until failure of the brickwork beams in primary or secondary shear. Here, unlike in the beams containing tensioned reinforcement only, the camber in both brickwork and concrete due to the eccentric prestressing force was very small. As a result, the larger deflections in brickwork observed in the fully prestressed beams were not present here.

Compared to the beams containing tensioned steel only, the post-cracking stiffness in the partially prestressed beams are much higher. This results from the large area of the deformed bar and its location close to the soffit.

5.3.4 Comparison With Theory

In this section, the experimental M-ϕ and load-deflection relationships are compared with those obtained from the direct method described in Section 5.2.3. The stress-strain relationship of each material (see Chapter 3) was used at all stages of loading.

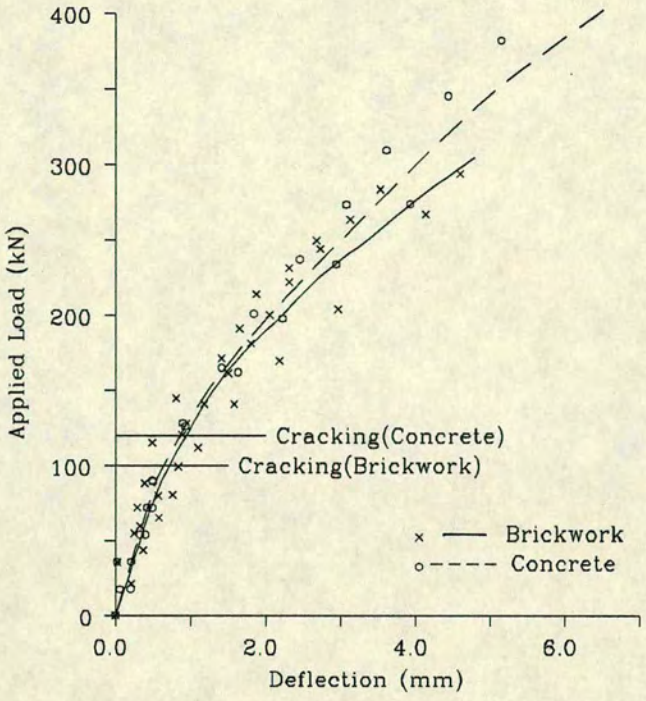

Fig. 5.3.9 Load–Deflection Response
Partially Prestressed Beams (a/d=1.5)

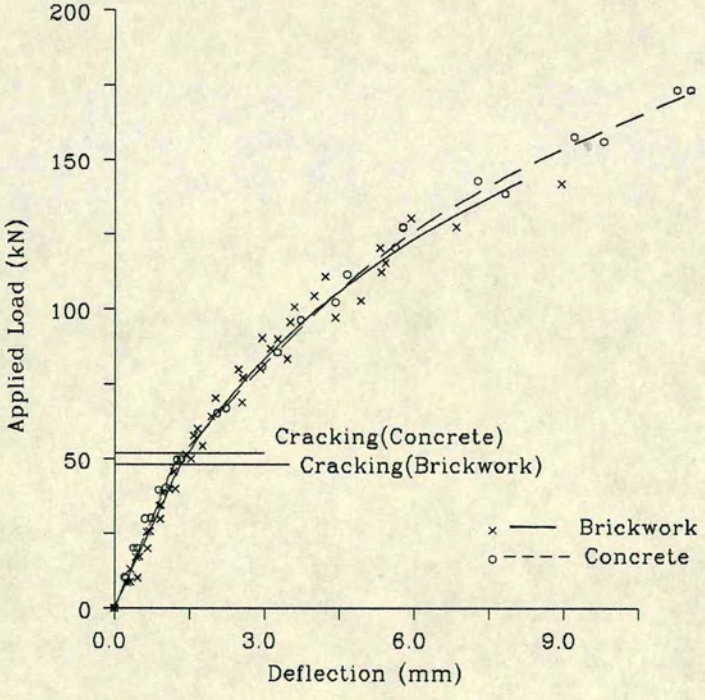

Fig. 5.3.10 Load–Deflection Response
Partially Prestressed Beams (a/d=3.0)

In Figs. 5.3.11–5.3.14, the averages M–ϕ relationships and those across a crack are compared with theoretical results. Combining both relationships on the same graph highlights the differences between the maximum and average curvature.

5.3.4.1 M–ϕ Relationship for Different Steel Areas

In Figs. 5.3.11a and b, the M–ϕ relationships for brickwork and concrete respectively, containing 0.274% area of tensioned steel are presented. In general, in both brickwork and concrete a good agreement with experimental results was obtained. However, towards failure, particularly in brickwork, the theory overestimated both the maximum and average curvatures. This is due to the underestimate in the ultimate moment (see Chapter 4).

The results for the beams containing 0.548% area of tensioned steel with the lower effective prestressing force (approximately 200 kN) are presented in Figs 5.3.12a and b. For the brickwork beams, Fig 5.3.12a, in the inelastic phase, an underestimate of curvature was given by the theory. This increased until failure. This was because primary shear failure occurred in brickwork while the theory assumed a flexural failure. The similarity in the maximum and average curvatures mentioned in Sections 5.3.1 and 5.3.2 is cleary illustrated here. The concrete beams failed in flexure so that the theory was in better agreement with experimental results up to failure.

The relationship for the beams containing the same area of steel but with the higher prestressing force (approx. 280 kN) are given in Figs. 5.3.13 a and b. In this case, the relationships for brickwork are in better agreement with that predicted by the theory. This results from the increased prestressing force which increased the ultimate moment. As above, the experimental maximum and average curvatures were very similar.

The results for the partially prestressed beams with a/d ratio of 3.0 are presented in Figs. 5.3.14 a and b. After cracking, in both cases, the theoretical predictions underestimated experimental results. This was more so in concrete and results from the mode of failure which was in shear rather than in flexure as assumed by the theory.

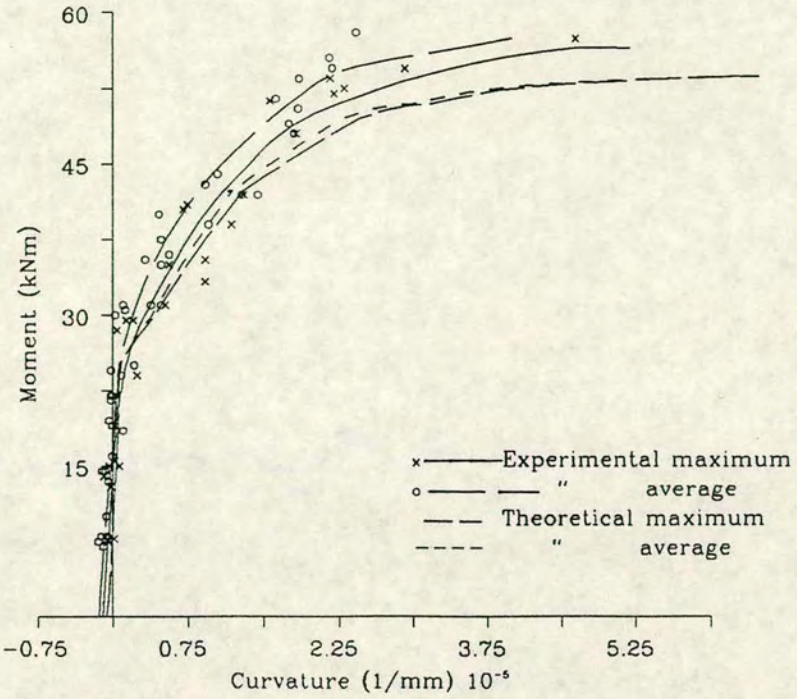

Fig. 5.3.11a Moment–Curvature Relationship, Brickwork Beams, A_p=0.274%

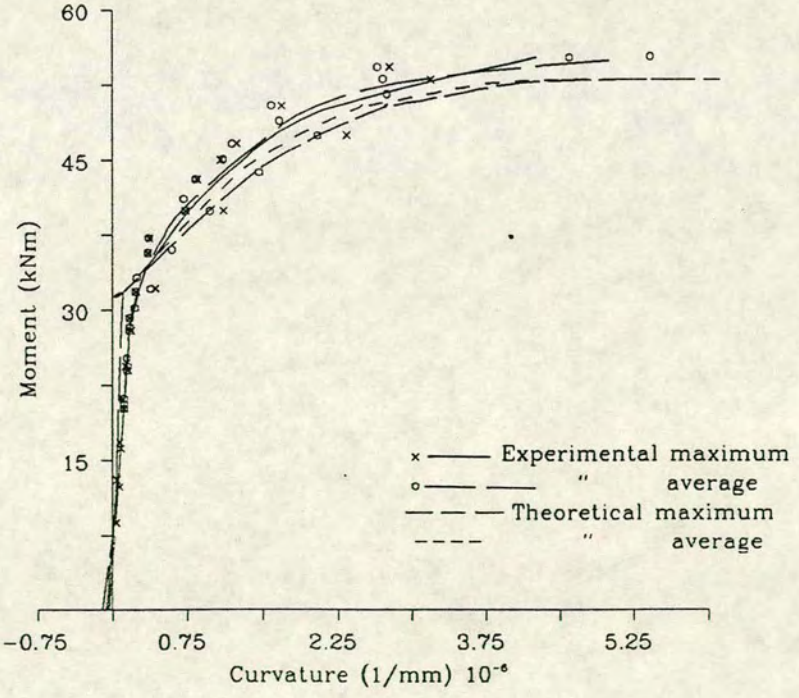

Fig. 5.3.11b Moment–Curvature Relationship, Concrete Beams, A_p=0.274%

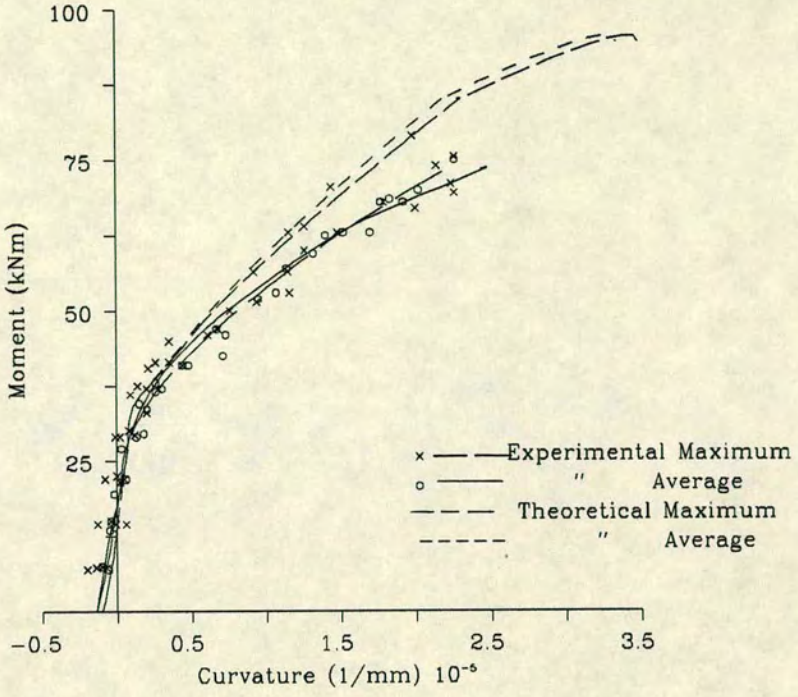

Fig. 5.3.12a Moment–Curvature Relationship
Brickwork Beams, A_p=0.548%, P_e=208 kN

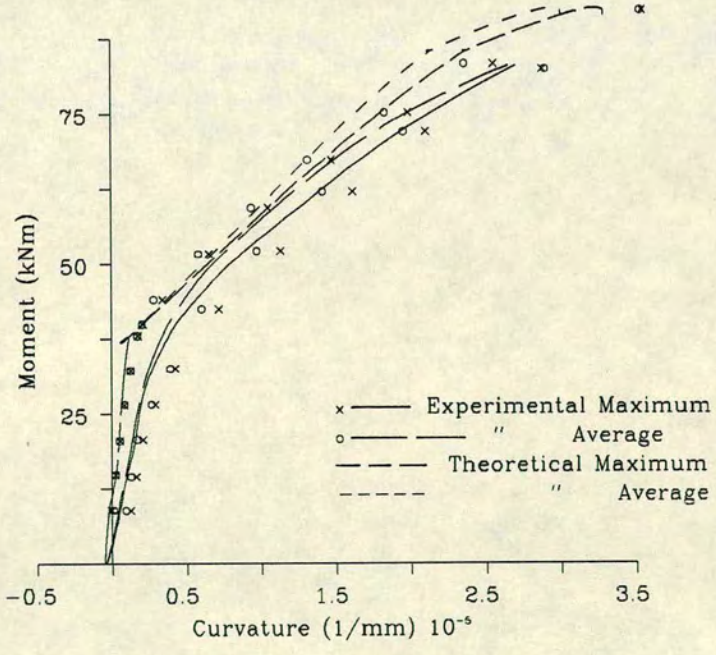

Fig. 5.3.12b Moment–Curvature Relationship
Concrete Beams, A_p=0.548%, P_e=201 kN

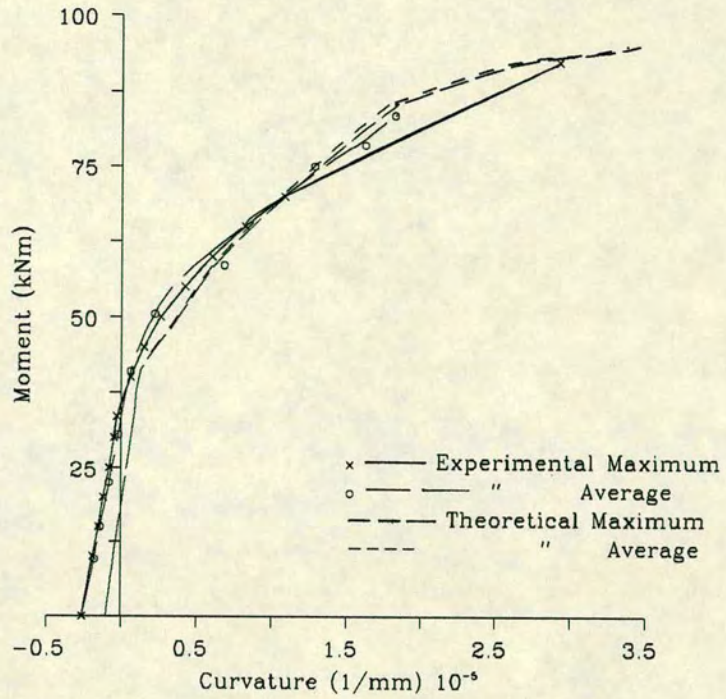

Fig. 5.3.13a Moment–Curvature Relationship
Brickwork Beams, A_p=0.548%, P_e=275 kN

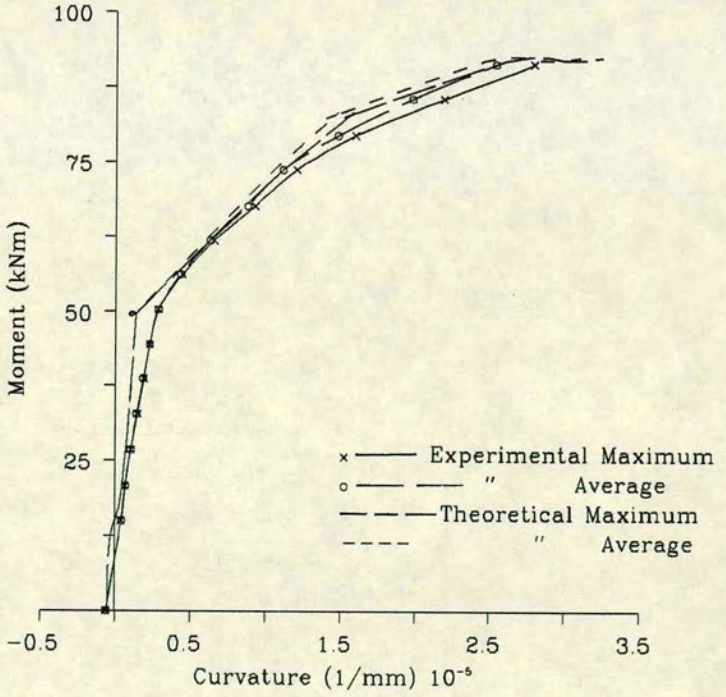

Fig. 5.3.13b Moment–Curvature Relationship
Concrete Beams, A_p=0.548, P_e=283 kN

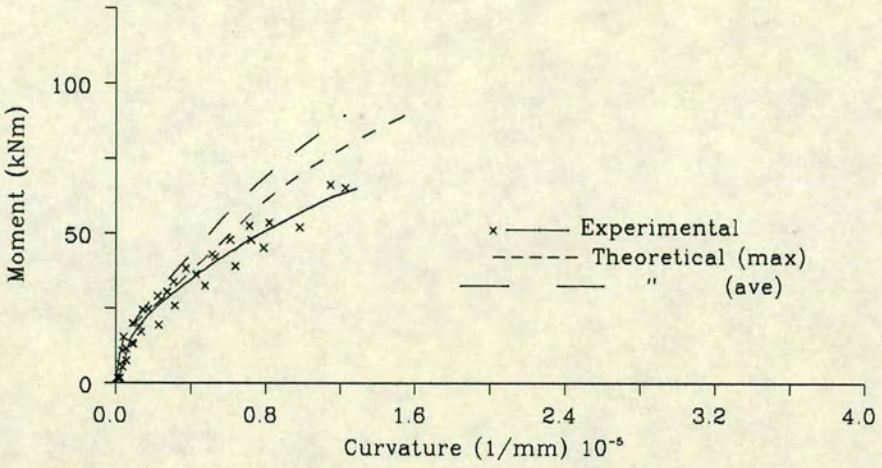

Fig. 5.3.14a Moment–Curvature Relationship

Brickwork Beams, A_{pe}=0.341%, a/d=3.0

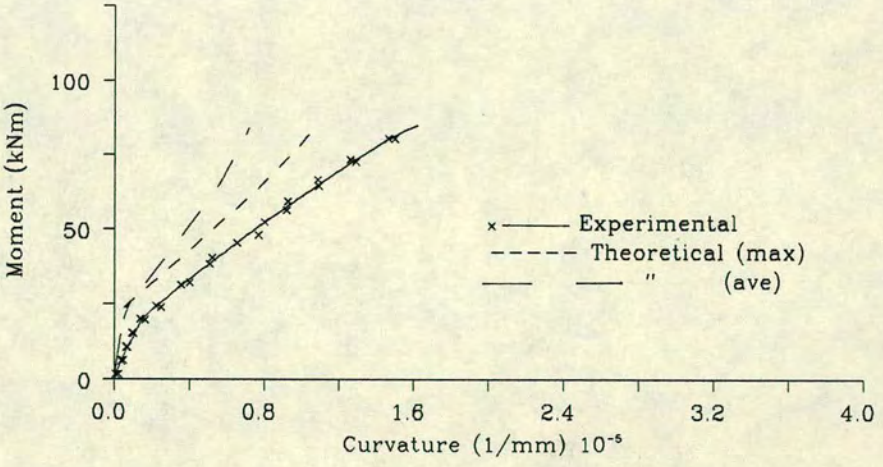

Fig. 5.3.14b Moment–Curvature Relationship
Concrete Beams, A_{pe}=0.341%, a/d=3.0

5.3.4.2 Comparison Between Experimental and Theoretical Load-Deflection Relationships

In Figs. 5.3.15-5.3.18, the load-deflection relationships are compared with theoretical results. Figs. 5.3.15a and b show the relationships for brickwork and concrete containing 0.274% area of steel. In both cases, a good agreement was obtained with experimental results. However, as in the M-ϕ relationships, the theory overestimated the deflections particularly towards failure. This arose from the underestimate in the ultimate moment (see Chapter 4).

The relationships for the beams containing 0.548% area of steel with approximately 200 kN prestressing force are presented in Figs. 5.3.16a and b for brickwork and concrete respectively. In concrete, a better agreement was obtained with experimental results. This was because these beams failed in flexure. However, towards failure, the theoretical results underestimated deflections. In brickwork, the theory underestimated the deflections particularly towards failure. After cracking the differences between experimental and theoretical results increased until primary shear failure.

In the beams with the same area of steel but a higher prestressing force (approx. 280 kN), there was a good agreement with theory in both brickwork, Fig. 5.3.17a and concrete, Fig 5.3.17b. In brickwork, this results from the increase in ultimate moment obtained by increasing the prestressing force in beams which fail in shear. However, as the beam still failed in shear, there was a discrepancy in the ultimate load and deflection. In concrete however, a good agreement was obtained throughout the loading history.

In Figs. 5.3.18a and b, the experimental and theoretical relationships are given for the partially prestressed brickwork and concrete beams respectively. As in the moment-curvature relationships, the theoretical predictions underestimated experimental results. However, in brickwork, a better correlation was obtained in the initial portion of the inelastic phase. Thereafter, the theory predicted smaller deflections than were obtained experimentally. In concrete, a poor correlation was obtained after cracking up until failure.

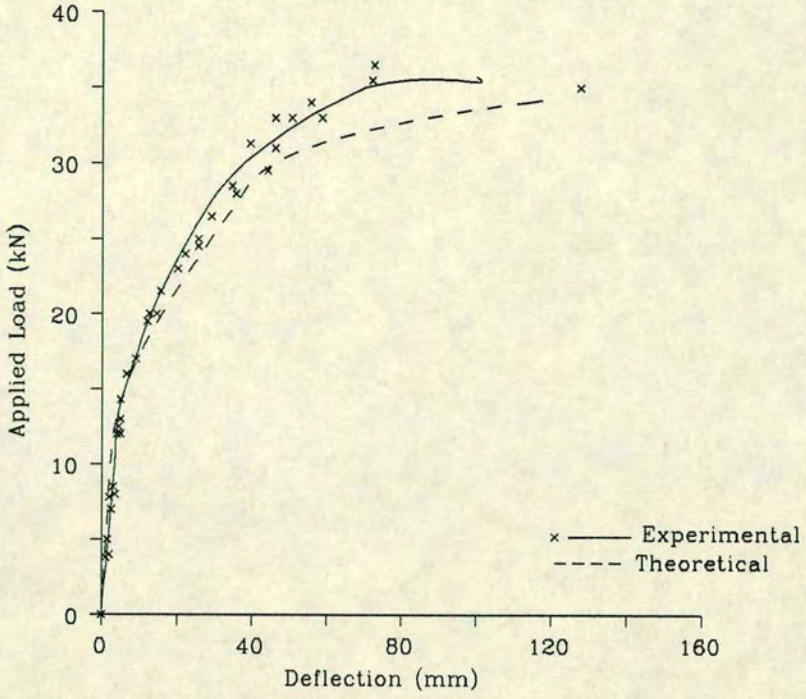

Fig. 5.3.15a Load–Deflection Response
Brickwork Beams, A_p=0.274%

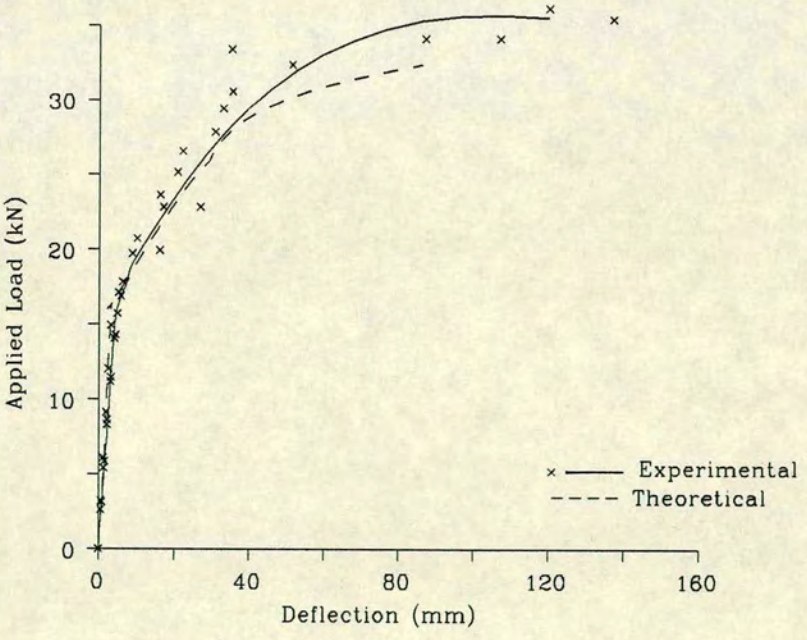

Fig. 5.3.15b Load–Deflection Response
Concrete Beams, A_p=0.274%

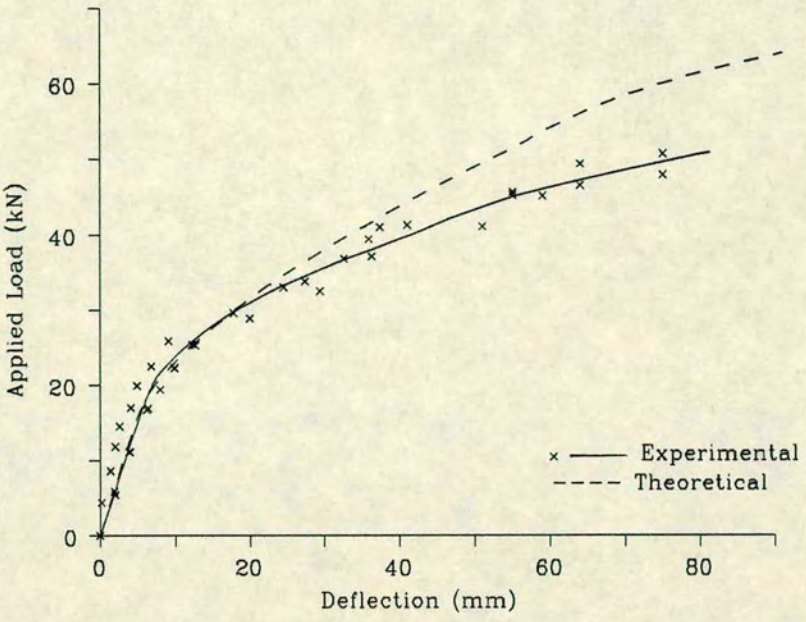

Fig. 5.3.16a Load–Deflection Response, Brickwork Beams, A_p=0.548, P_e=208 kN

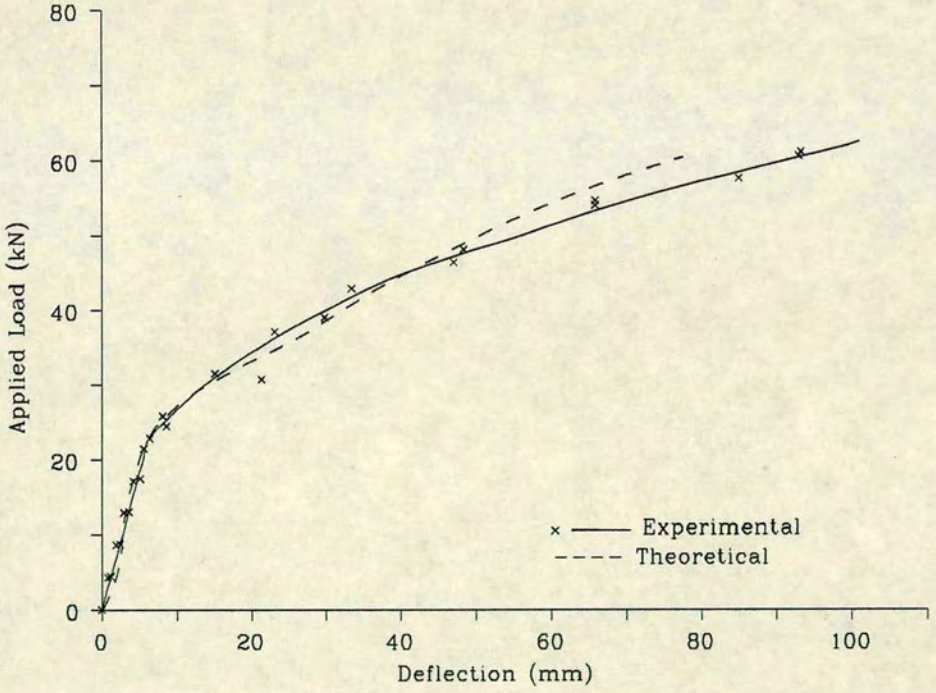

Fig. 5.3.16b Load–Deflection Response, Concrete Beams, A_p=0.548%, P_e=201 kN

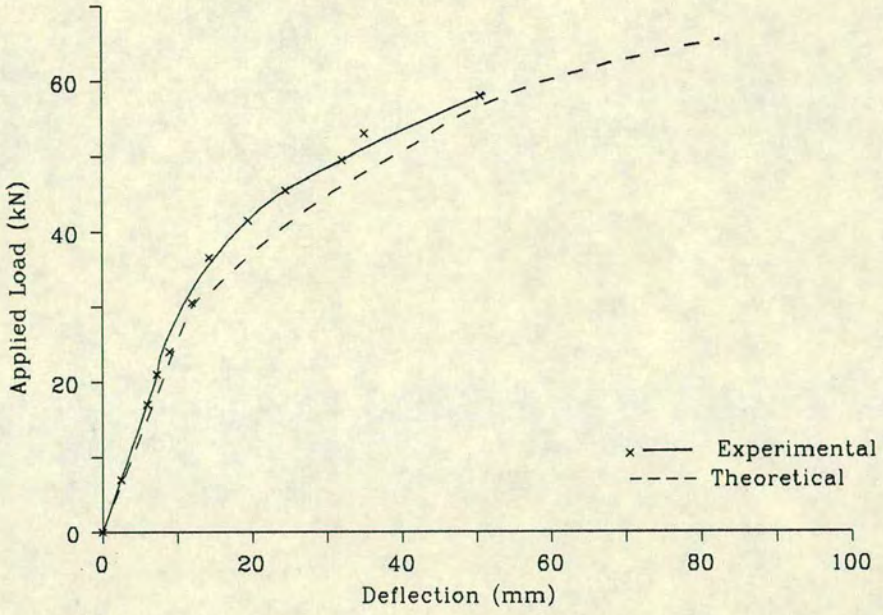

Fig. 5.3.17a Load–Deflection Response, Brickwork Beams, A_p=0.548%, P_e=275 kN

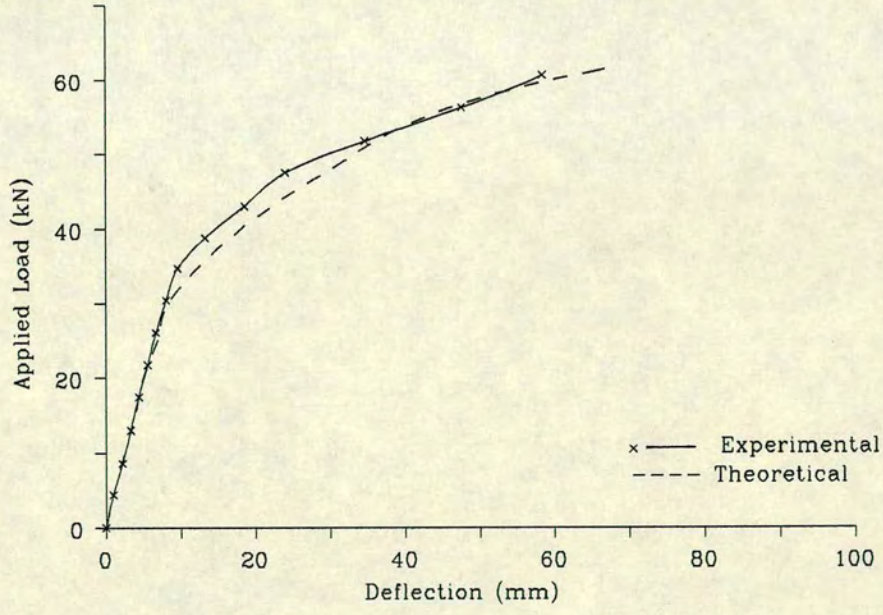

Fig. 5.3.17b Load–Deflection Response, Concrete Beams, A_p=0.548%, P_e=283 kN

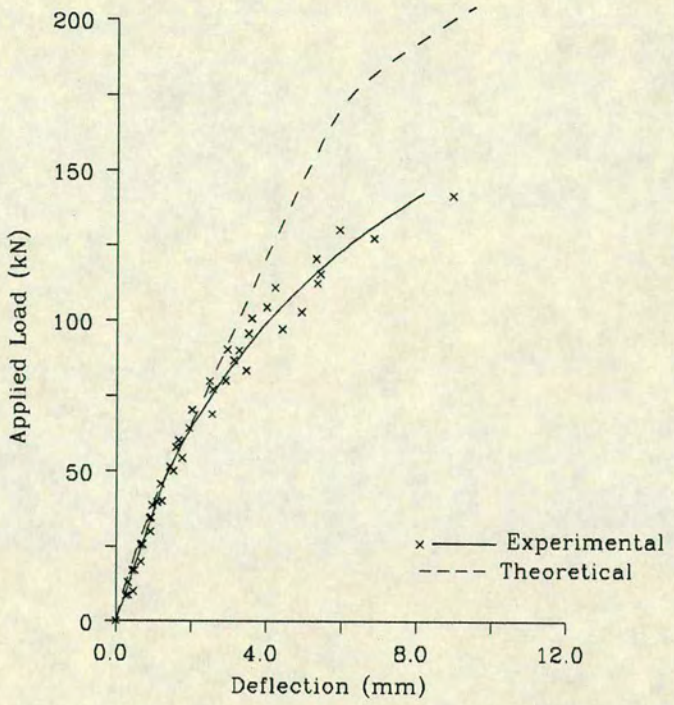

Fig. 5.3.18a Load–Deflection Response, Brickwork Beams, A_{st}=0.856%, a/d=3.0

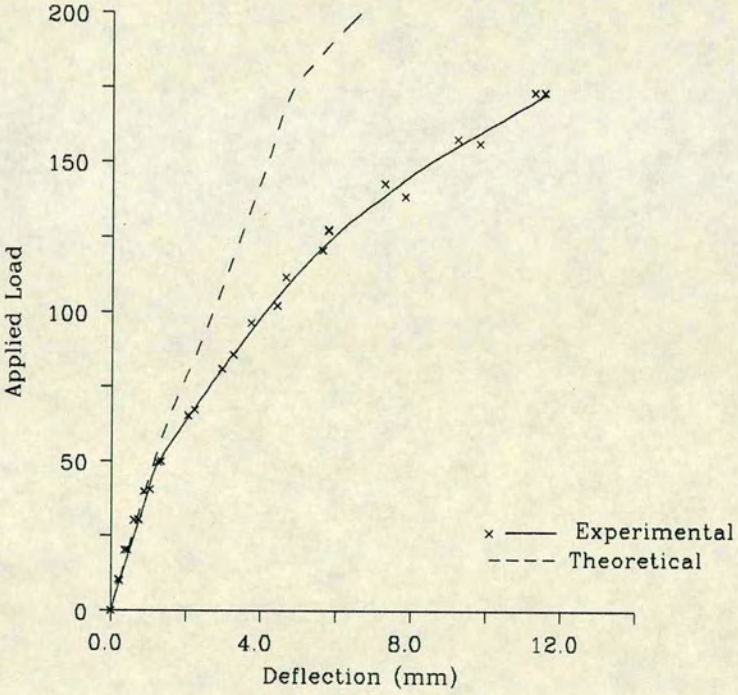

Fig. 5.3.18b Load–Deflection Response, Concrete Beams, A_{st}=0.856%, a/d=3.0

5.4 THE DESIGN OF PRESTRESSED BRICKWORK FOR DEFLECTION

The serviceability requirements for deflection in the code of practice[1] are given as deemed-to-satisfy rules. For example, the deflection of a simply supported beam should not exceed span/250. The deflection may be calculated using the elastic theory. The moment of inertia is obtained on the basis of the gross section rather than the transformed section which accounts for the presence of the tensile reinforcement. The code contains no provisions for cracking under service loads so that an uncracked section is implied. The above method is therefore adequate.

As will be seen in Chapter 6, prestressed brickwork may be allowed to crack under working loads without compromising on safety. The previous sections have shown a similarity in the load-deflection responses of similar prestressed brickwork and concrete sections which fail in flexure over the entire loading history. Also noted was that the post-cracking stiffness in brickwork was higher than in concrete. Further, Walker[12] has shown that prior to the yielding of the tensile reinforcement, partially prestressed brickwork beams showed almost complete recovery on the removal of load. As cracking is allowed in concrete, from the point of view of deflection, cracking may also be allowed in prestressed brickwork.

As in concrete, the calculation of deflection in a cracked prestressed brickwork section requires a cracked section analysis. The elastic method has been used by Walker[12] and Pedreschi[11] to calculate the deflection in a cracked prestressed brickwork section. Using the characteristic compressive strength f_{k2}, given by the code of practice[1] (obtained from Table 3A and Fig. 1(a) of the code) and a material partial safety factor of 1.0, Walker[12] obtained very large overestimates of deflection in the post-cracking phases. This was attributed to the very conservative values given by the code for f_{k2} (see also, Chapter 4). Pedreschi[11] recommended the use of Branson's method[70] to account for the tension stiffening effect of the uncracked brickwork between cracks and the sections of the beam which remain uncracked in flexure. Branson's equation for the effective moment of inertia is given by:

$$I_e = [M_{cr}/M]^3 I_g + [1 - (M_{cr}/M)^3] I_{cr}$$

where
I_e = effective moment of inertia
I_g = gross moment of inertia
I_{cr} = moment of inertia of the cracked section
M = moment at which deflection is required
M_{cr} = cracking moment

Using the value obtained from the experimental results in Appendix D of the code[1] and Branson's equation, the load-deflection relationship was obtained using a material partial safety factor of 1.0. The result is shown in Fig. 5.4.1.

In the elastic phase, the deflections obtained using Branson's formula overestimated the experimental deflections but were satisfactory. However, in the post-cracking phases, gross overestimates were given.

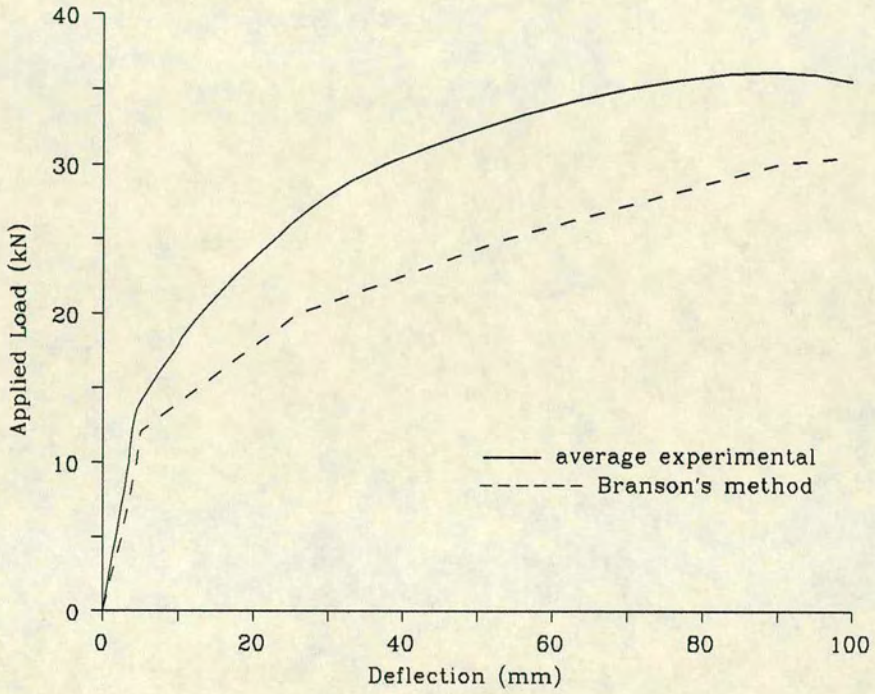

Fig. 5.4.1 Typical Load–Deflection Response
Using Branson's Method

5.5 CONCLUSIONS

The moment-curvature and load-deflection relationships of identical prestressed sections of brickwork and concrete of similar compressive strength have been compared. The following conclusions can be made:

1. When the brickwork and concrete beams fail in flexural tension, similar load-deflection and moment-curvature relationships were obtained.

2. In the case of primary or secondary shear failure in brickwork alone or in both the brickwork and concrete beams, although the failure load in the brickwork beams were lower, the load-deflection and moment-curvature relationships were not significantly different over the entire loading history.

3. The relationship between the tension stiffening coefficient k and the degree of cracking f_{secr}/f_{se} is non-linear in prestressed brickwork and concrete and increases with the load level. The tension stiffening effect is greater in prestressed brickwork.

4. The direct method using the non-linear stress-strain relationship for brickwork and concrete gave good predictions of the moment-curvature and load-deflection relationships for prestressed brickwork and concrete beams which failed in flexure.

5. The cracked section analysis of prestressed brickwork and concrete using Branson's expression for the effective moment of inertia gives very poor estimates of deflection after cracking until failure.

CHAPTER 6
FLEXURAL CRACKING

6.1 INTRODUCTION

Cracking in brickwork and concrete can result from a variety of actions which include bending stress, volumetric change, drying shrinkage and creep under sustained load. This chapter is concerned with cracking caused by tensile stress developed due to bending.

The tensile strength of brickwork and concrete is very low, hence the flexural members of both materials will crack at some point in their loading history. It is important that the width of these cracks should be kept as small as possible for two reasons. Firstly, for aesthetic reasons; large cracks impair the appearance of a member and may cause feelings of alarm. Under these circumstances, the maximum crack width that may be considered nondetrimental depends on the position of the member, the type of finishings to be applied and the intended use of the structure. Aesthetic acceptability is difficult to assess as this varies from individual to individual. The maximum crack width which has been found to be acceptable lies between 0.25 mm and 0.38 mm[75]. Secondly, for the protection of the reinforcement against corrosion; the performance of a member can be considerably hampered if the cracks are large enough to permit the penetration of corrosive elements to the main reinforcement. The resulting corrosion reduces the cross-sectional area of the reinforcement thereby increasing the steel stress with a consequent reduction in the factor of safety. Corrosion can also cause unsightly spalling of the surrounding concrete. Under these circumstances, the maximum crack width depends on the exposure conditions of the member. Crack widths of up to 0.41 mm[75] have been found to be satisfactory but in adverse environmental conditions, these are limited to 0.1 mm[76].

The serviceability limit state of cracking specifies maximum crack widths at the surface of a member which may not be exceeded in a given type of environment. The British Code of Practice for the structural use of concrete[58] specifies a value of 0.1 mm for members in very severe environments and a value of 0.2 mm in all other environments.

In the load factor and elastic methods of design previously used in concrete and brickwork respectively, the permissible stress in the reinforcement was low. The crack widths which were found to be directly related to the stress in the reinforcement, were thus assumed to be satisfactory as long as the rules governing the arrangement of the reinforcement were followed. However, the use of high strength steel and the introduction of the limit state method of design required a better understanding of the factors which affect the crack widths so that these could be adequately predicted. The bulk of the earlier research into cracking in concrete[76,77,78] was confined to reinforced concrete members only. At that time only class I prestressed concrete members were catered for in design in which no tension was allowed under service loads. However, with the inclusion of two additional categories of prestressed members namely class II, in which tensile stresses but not cracking is allowed and class III members in which cracking is allowed under service loads, research work on cracking has expanded to cover prestressed concrete members.

As with most aspects of structural design, the need for a more detailed understanding of cracking behaviour in concrete came earlier than in brickwork. This is reflected in the current British Code of Practice for concrete and structural brickwork BS 8110[58] and BS 5628[1] respectively. Only the former contains recommendations for cracking. It is not surprising therefore, that the bulk of information on cracking pertains to concrete. However, previous investigations have shown that cracking in concrete is more complex than in brickwork[11,12]. This is because, cracking in concrete is random in nature so that a crack can form anywhere within a region of maximum moment. However, in brickwork, the cracks will occur at the brick/mortar interface since the interface bond strength is much lower than that of the mortar or bricks. Thus cracks in brickwork occur at discrete locations defined by multiples of the distance between adjacent mortar joints although cracks may not necessarily form at every joint. This therefore defines the crack spacing which is essential in the prediction of crack widths thereby eliminating a vital parameter which has been the subject of several complex formulae in concrete. Further, the information gathered so far on concrete has been found to be applicable to brickwork by previous researchers[11,12].

In an attempt to develop a rational theory for cracking, a large number of experimental investigations have been carried out on reinforced and

prestressed concrete. A large number of variables have been found to affect the crack widths. These include the steel stress, the type of reinforcement, the concrete cover, the concrete area in tension, the number and diameter of prestressing reinforcement and non-tensioned bars in the tension zone and the strength of concrete. The complexity of this problem led to a large number of approximate, semi-theoretical and empirical formulae for predicting crack widths using different sets of variables.

In the following sections, the main methods of predicting the

1. The average crack width

2. The maximum crack width

3. The crack spacing

in concrete and its applicability to brickwork will be examined. In addition, a method for predicting the maximum crack width in prestressed brickwork based on the steel stress has been proposed. A relationship between the crack spacing and the steel stress in concrete was also derived. The validity of these methods will be checked against experimental results obtained from prestressed brickwork and concrete beams. The cracking behaviour of similar prestressed brickwork and concrete beams will also be compared.

6.2 THEORETICAL PREDICTION OF CRACK WIDTH

As mentioned previously, early investigations into cracking were centred around reinforced concrete. In an attempt to develop a rational theory for cracking, a large number of experimental investigations were carried out. However, the large number of variables on which cracking depends and also, the large scatter to which crack widths are subject to led to the development of a large number of semi-theoretical and experimental equations. Nevertheless, these investigations have identified the major variables which affect the width and spacing of cracks in reinforced concrete as:

1. The tensile stress in the reinforcement and its bond characteristics

2. The concrete cover as measured from the centroid of the reinforcing bar

closest to the soffit of the beam

3. The area of concrete in tension

Based on these variables, methods for predicting the crack widths can be categorized thus:

1. The fictitious tensile stress method

2. Methods in which the crack width is related to the average steel strain or the average strain on the surface of the concrete

3. Methods which relate the crack widths to the steel stress

6.2.1 The Fictitious Tensile Stress Method

The fictitious tensile stress is defined as that stress which would exist in brickwork/concrete if it were of sufficient strength to remain uncracked. Experimental results on concrete[79,80] have shown a linear relationship between the average crack width and the fictitious tensile stress. In its simplest form, the relationship is given by:

$$w_{av} = k.\ c.\ f_{ct}'$$

... 6.2.1

where
w_{av} = average crack width
c = concrete cover
f_{ct}' = fictitious tensile strength
k = a constant obtained experimentally

This relationship has also been shown[80] to be dependent on the area of steel which has lead to its inclusion in equation 6.2.1. According to Krishna Raju et al[80]:

$$w_{av} = R/\rho_s.\ c.\ f_{ct}'$$

... 6.2.2

where
R = a factor defining the bond characteristics of the steel
ρ_s = percentage of non-tensioned reinforcement

However, more recent investigations[81] have shown that the crack widths are affected by the total area of tensile reinforcement rather than that of the non-tensioned steel only.

Experimental results have also shown a linear relationship between the average crack widths and the fictitious tensile stress in brickwork. Further, previous researchers[11,12] have suggested that the joint spacing, b_j is the controlling parameter in brickwork rather than the cover to the reinforcement, c. These developments led to a modified form of equation 6.2.2 for brickwork[12] thus:

$$w_{av} = k_1 (f_{ct}' - f_r) b_j / \rho_s \qquad \text{... 6.2.3}$$

where
f_{ct}' = fictitious tensile stress in brickwork (N/mm^2)
f_r = modulus of rupture (N/mm^2)
b_j = joint spacing (mm)
ρ_s = percentage area of tensile reinforcement
k_1 = 132×10^{-6} mm^2/N for partially prestressed beams(strands and deformed bars)
= 420×10^{-6} mm^2/N for fully prestressed beams (strands only)

Walker[12] introduced f_r into equation 6.2.3 on the basis that cracking will not commence until the modulus of rupture has been exceeded. The different constants for fully and partially prestressed beams were attributed to the different bond characteristics of the tensile reinforcement closest to the soffit and probably, to the cover. While the fully prestressed beams had covers between and 95 mm and 121 mm, those in the partially prestressed beams varied between 25 mm and 50 mm.

Before the inclusion of the area of steel in equations relating the average crack width to the fictitious tensile stress, a major criticism was its total exclusion of the tensile reinforcement. Inspite of the modifications which have been made for concrete beams (Krishna Raju et al[80]) and for brickwork beams (Walker[12]), this method does not give an accurate reflection of beam behaviour especially after the tensile reinforcement has yielded. The main advantage of this method is in its relative simplicity; it is much easier to calculate the fictitious tensile stress in an uncracked section than to carry out a cracked section analysis to determine the stress or strain in the tensile reinforcement as required by the other methods (see Sections 6.2.2 and 6.2.3). Its relative

simplicity makes it suitable for design.

6.2.2 Methods Relating the Crack Widths to the Average Steel Strain or the Average Surface Strain in Concrete/Brickwork

In concrete, the relationship between the crack width and the average steel strain/surface strain is given by Beeby[82], Desayi[83] and Bennet et al[79] as:

$$w_{av} = s_m . \varepsilon \qquad \text{... 6.2.4}$$

where
s_m = mean final crack spacing
ε = average steel strain/surface strain at the depth where crack widths are required

In prestressed brickwork, the crack spacing is related to the joint spacing b_j. The relationship between the average crack width and the average steel strain in fully prestressed brickwork was found by Pedreschi[11] to be given by:

$$w_{av} = (N_j + 0.41)\, b_j . \varepsilon \qquad \text{... 6.2.5a}$$

where N_j is the number of joints between cracks.

The term 0.41 in equation 6.2.5a was included to account for the likelyhood of the actual crack spacing being greater than the predicted spacing. The expression for partially prestressed beams tested by Walker[12], which contained non-tensioned reinforcement close to the soffit was somewhat simplified as the crack spacing was found to be constant at b_j:

$$w_{av} = b_j . \varepsilon \qquad \text{... 6.2.5b}$$

When ε is the average steel strain, equations 6.2.4 and 6.2.5 are approximations as there will be some residual surface strain in the brickwork/concrete between cracks which will reduce the average steel strain. As this reduction is quite small compared to the total steel strain, it is often ignored, or otherwise taken into account by tension stiffening. Also, in methods using the steel strain, the strain has been defined differently by various researchers[11,12,79,83]. In reinforced concrete or brickwork, the strain is obviously the total steel strain due to the absence of a prestrain. In prestressed concrete, ε has been defined

as that corresponding to the stress induced from the stage of decompression[79,83] while in prestressed brickwork, ε has been taken as the additional strain in the reinforcement after cracking[11,12]. In either case, ε is obtained from a cracked section analysis. The average surface strain in the concrete/brickwork is obtained by assuming a linear variation in strain and also with computations based on a cracked section.

The main limitation of this method is the dependence on the mean final crack spacing s_m which will be discussed in Section 6.3. However, as shown in reference 11 and 12, these methods are capable of reflecting beam behaviour even beyond the yielding of the tensile reinforcement.

6.2.3 Methods Which Relate the Crack Widths to the Steel Stress

The steel stress has long been identified as the single most important variable which affects the width of cracks. Thus it is to be expected that methods which incorporate the steel stress give the most accurate predictions of crack widths. Consequently, a large number of equations have been proposed which contain the steel stress. A recent proposal by Suri and Dilger[81] is:

$$w_{max} = k.\ f_s.\ c.\ (A_t/A_s)^{0.5} \qquad \text{... 6.2.6}$$

where
k = constant depending on the type and combination of prestressed and non-prestressed steel ($mm^2/N \times 10^{-6}$)
f_s = steel stress after decompression in the reinforcement located closest to the extreme tensile fibre
c = concrete cover
A_t = area of concrete in tension
A_s = total area of tensile reinforcement
w_{max} = maximum crack width

Equation 6.2.6 was obtained from a statistical analysis carried out on maximum crack width data obtained from a wide variety of sources. The following types and combinations of non-tensioned and tensioned steel were investigated: deformed bars and strands (k = 2.55), strands only (k = 2.65), deformed bars and tensioned wires (k = 3.51) and a combination of tensioned and non-tensioned wires (k = 4.50).

Comparing the results of the analysis for the different types and

combinations of tensioned and non-tensioned steel, the combination which gave the smallest crack widths were the prestressing strands and deformed bars. The combination of tensioned and non-tensioned wires gave the largest crack widths. In between these extremes were the combination of deformed bars and tensioned wires and strands only with the latter giving smaller crack widths. While these observations were in keeping with generally observed experimental results, the differences between the crack widths given by deformed bars and strands and strands only were insignificant in view of the large differences observed experimentally. This was attributed to the differences in cover. This could not be treated as a statistical variable as it was virtually unchanged within each combination of tensile reinforcement but varied between each category. For beams containing strands only, the cover varied between 50 and 60 mm while in those which also contained deformed bars this was between 25 and 30 mm.

6.2.4 Proposed Method for Calculating the Crack Width in Brickwork Beams

To the author's knowledge, methods which have so far been proposed for the calculation of the crack widths in brickwork have not included a relationship with the steel stress. Further, to date, maximum crack widths in prestressed brickwork are obtained by establishing a statistical relationship with the average crack width. It therefore seemed timely for a statistical analysis similar to that carried out on concrete beams by Suri and Dilger[81], to be carried out on maximum crack width data in prestressed brickwork beams. To compensate for the dearth of data on prestressed brickwork, it was necessary to use all the available information on cracking in brickwork and also current knowledge on concrete.

Previous works on prestressed brickwork beams [11,12] have shown that methods which have been used for crack width calculations in concrete are also equally applicable to brickwork as long as the joint spacing b_j rather than the concrete cover c, is taken into consideration (see Sections 6.2.1 and 6.2.2). This is not unexpected in view of the similarities in their stress-strain relationships (see Chapter 3) and general flexural behaviour observed so far. Thus, the major variables which have been found to affect crack widths in prestressed concrete will also affect those in prestressed brickwork with the exception of the cover. The following variables were thus considered in the

statistical analysis:

1. The steel stress, f_s

2. The total area of tensile reinforcement, A_s

3. The area of brickwork in tension, A_t

4. The joint spacing, b_j

The steel stress

In relating the steel stress to the crack width, several states have been chosen as a reference point for the steel stress. A common reference point is that of decompression, either of the entire section[84], the extreme tensile fibre[85], or at the level of the tensile reinforcement closest to the tensile face[81]. Each of these states have advantages. Decompression of the entire concrete section is an attempt to bring the cross-section to a condition identical to a conventionally reinforced section subject to an axial force and bending moment. Thereafter, the section is analysed in the same manner as the working stress analysis for reinforced concrete. This is particularly advantageous for cracked section analysis. However, at the state of decompression of either the entire section or the extreme tension fibre, the stresses in the non-tensioned steel can be significantly compressive if time-dependent effects such as creep and shrinkage are considered. This can be avoided by using the reference point as the decompression of the concrete/brickwork at the level of the tensile reinforcement closest to the extreme tensile fiber[81]. Another reference state, recommended by ACI committee 224[85], is that at cracking, although it is acknowledged that it is difficult to determine the cracking load accurately. In view of the above, the reference state adopted in this analysis was that at the decompression of the brickwork at the level of the tensile reinforcement closest to the soffit.

The Area of Brickwork in Tension

In this study, the area of brickwork in tension is defined as that below the neutral axis. This definition of A_t, was chosen for the following reasons:

- The crack width prediction is based on the tributary area that contributes to the crack width and

- A_t changes with the applied load, so that the effect of load level on crack widths is better represented in the crack width equation

The experimental data on which this statistical analysis was carried out was obtained from reference 11 and also from this work. These results were analysed in two categories: beams containing strands only and those containing a combination of strands and deformed bars. A least squares analysis produced the following equation:

$$w_{max} = k_b . b_j . (A_t/A_s)^{0.5} . f_s \qquad \text{... 6.2.7}$$

where
$k_b = 1.28 \times 10^{-6}$ mm^2/N for beams with strands only
$= 0.63 \times 10^{-6}$ mm^2/N for beams with deformed bars and strands

It is interesting to note that the product $k_b . b_j$ has virtually the same value in both cases. Equation 6.2.7 will be compared with experimental results in Section 6.4.

6.3 METHODS OF PREDICTING THE CRACK SPACING

In methods which relate the crack width to the average steel strain or surface strain (see Section 6.2.2), an essential variable is the crack spacing, s_m. In order to obtain accurate estimates of the crack width from these methods accurate estimates of the crack spacing are necessary.

In Section 6.3.1, the general theory of crack spacing in reinforced concrete is given as well as it application to prestressed concrete and brickwork. This theory is quantitative in that it proposes limits within which the average crack

spacing will fall. In brickwork, this is sufficient to result in specific values for the average crack spacing. In concrete however, the prediction of the crack spacing is rather more complex. As a result, in Section 6.3.2, the methods which have been proposed for the average crack spacing in concrete are examined and a method is proposed.

6.3.1 The Theory of Crack Spacing

When the first crack forms in a flexural member, the surface stresses will be zero at the edge of the crack (see Fig. 6.3.1). With increasing distance away from the crack, the surface stresses increase until a point S_o in Fig. 6.3.1 is reached beyond which stresses are unaffected by the presence of the crack. Within S_o, it is unlikely that another crack will form as the surface stresses have been reduced below the level necessary to cause cracking. Hence, S_o is the minimum crack spacing. If two adjacent cracks form at a distance greater than 2 S_o, then within this length, there will be a region in which surface stresses have not been reduced below that necessary to cause cracking. A crack is therefore likely to form between them. If on the other hand the spacing between adjacent cracks is less than 2 S_o, it is unlikely that a third crack will form between them. These points are illustrated in Fig. 6.3.1. The maximum spacing is thus 2 S_o. The final crack spacing will fall between S_o and 2 S_o. The issue is now that of determining the minimum crack spacing S_o.

Prior to the work of Beeby[82], there were two main theories on crack spacing in reinforced concrete. These were the '**classical**' and '**no-slip**' theories which appeared to be contradictory. However, Beeby[82] suggested that these theories and their resulting equations were, rather, partial descriptions of the same phenomenon. Beeby's theory suggested that the final crack pattern is the result of the interaction between the crack spacing controlled by the proximity to the reinforcement and that controlled by the initial crack height.

The crack spacing controlled by the proximity to the reinforcement is obtained from the assumption that at the formation of the first crack, full bond exists between the reinforcement and the concrete. As such, there is '**no-slip**' and plane sections can not remain plane. This situation is illustrated in Fig. 6.3.2. The crack just penetrates to the surface of the bar where it will have zero width. Applying the elastic theory, it was shown that the minimum crack

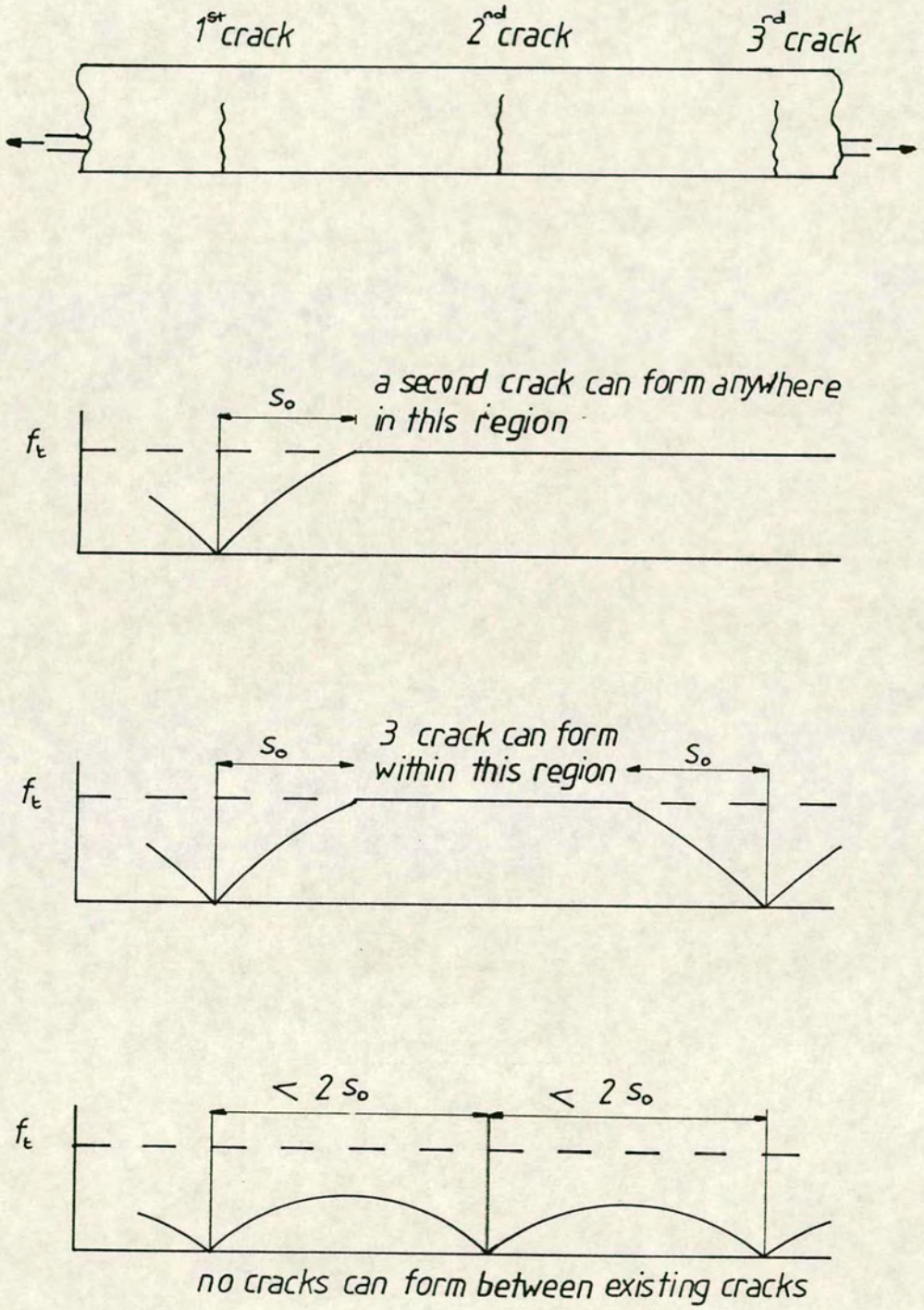

Fig. 6.3.1 Conditions on the Surface of an Axially Reinforced Tension Member

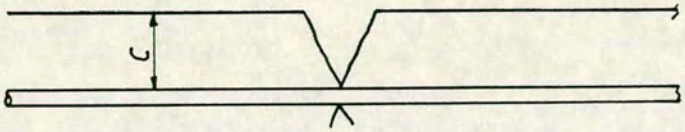

Fig. 6.3.2 Conditions at a crack when the Reinforcement is Fully Bonded to the Concrete (No-Slip Theory)

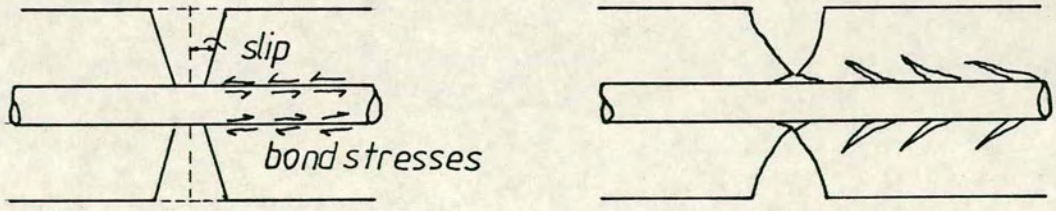

(a) Plain Bar (b) Deformed Bar

Fig. 6.3.3 Slip and Internal Concrete Deformation

spacing S_o is equal to the cover of the reinforcement, Fig. 6.3.2.

The next occurrence of a crack is determined by the surface characteristics of the reinforcement. In a plain bar, further loading will cause the reinforcement to slip relative to the concrete (see Fig. 6.3.3a). Thus bond failure will occur at points where the reinforcement crosses the crack. The transfer of force between the reinforcement and concrete takes place through bond stresses acting at the interface. On a further assumption that since bond failure does occur, the distribution of bond stress is a function of the ultimate bond stress, the following relationship results:

$$S_o = k_2 . D/\rho' \qquad \ldots 6.3.1$$

where
D = bar diameter
ρ' = reinforcement ratio
k_2 = a constant

The above treatment for plain bars constituted the **'bond-slip'** or **'classical'** approach to crack spacing.

In a deformed bar, slip as shown in Fig. 6.3.3a does not occur along the bar-concrete interface. Rather, the distortion of the concrete is accomodated by a series of internal cracks (see Fig. 6.3.3b). Studies on the nature of cracking around a deformed bar under increasing load have suggested that initially the situation is as described by the 'no-slip' theory. Thereafter, internal cracking takes place at successively greater distances from the main crack. This effectively reduces the rate of transfer of stress from the steel to the concrete thereby increasing the minimum crack spacing from the cover c towards S_o in equation 6.3.1. The spacing between cracks will thus depend on the amount of internal cracking which occurred before the formation of an adjacent crack. The mean crack spacing s_m, thus consists of two components, the minimum cover multiplied by a constant and the average effect of internal failure which results in:

$$s_m = k_1 . c + k_2 . D/\rho' \qquad \ldots 6.3.2$$

where
k_1, k_2 are constants
c = minimum cover

D and ρ' are as defined in equation 6.3.1.

The above derivations have been obtained from considerations of an axially loaded tension member. As the conditions at the soffit of a flexural member are not necessarily the same, further experiments were carried out by Beeby[82] on unreinforced concrete columns subjected to eccentric loads. If the load is at sufficient eccentricity to induce tension in one face (see Fig. 6.3.4), under increasing load, a controlled and stable crack pattern results. This pattern constitutes the spacing controlled by the initial crack height. If the initial crack height is h_o, applying the elastic theory and using the same argument as before, the final crack spacing will be expected to fall within the range h_o and 2 h_o. The addition of tensile reinforcement to a flexural member increases the depth of the neutral axis thereby reducing the initial crack height.

The minimum crack spacing is thus defined between the limits set by the cover and the initial crack height with both effects interacting to produce the crack pattern at any particular section. In very deep beams under flexure, the conditions at the soffit approach that under pure tension. In such cases the crack spacing will be dominated by the cover. Conversely, in shallow sections with a low percentage of steel, the initial crack height will be the controlling factor.

6.3.1.1 The Crack Spacing in Prestressed Concrete

Although, the theory given in Section 6.3.1 was for reinforced concrete, it can also be applied to prestressed concrete as long as the initial crack height h_o is defined. In reinforced concrete, this is the height of the crack immediately after the cracking moment has been exceeded. The relationship between the crack height and moment for reinforced concrete is shown in Fig. 6.3.5a. Once the cracking moment has been exceeded, there is a decrease in the moment capacity as the crack height increases. Since the applied load is not being removed, the crack will travel until it reaches a point A shown in Fig 6.3.5a where the moment of resistance is again at the cracking moment. Beyond this point, any increases in crack height is insufficient to change the crack pattern.

In prestressed concrete, as illustrated in Fig. 6.3.5b, the situation is

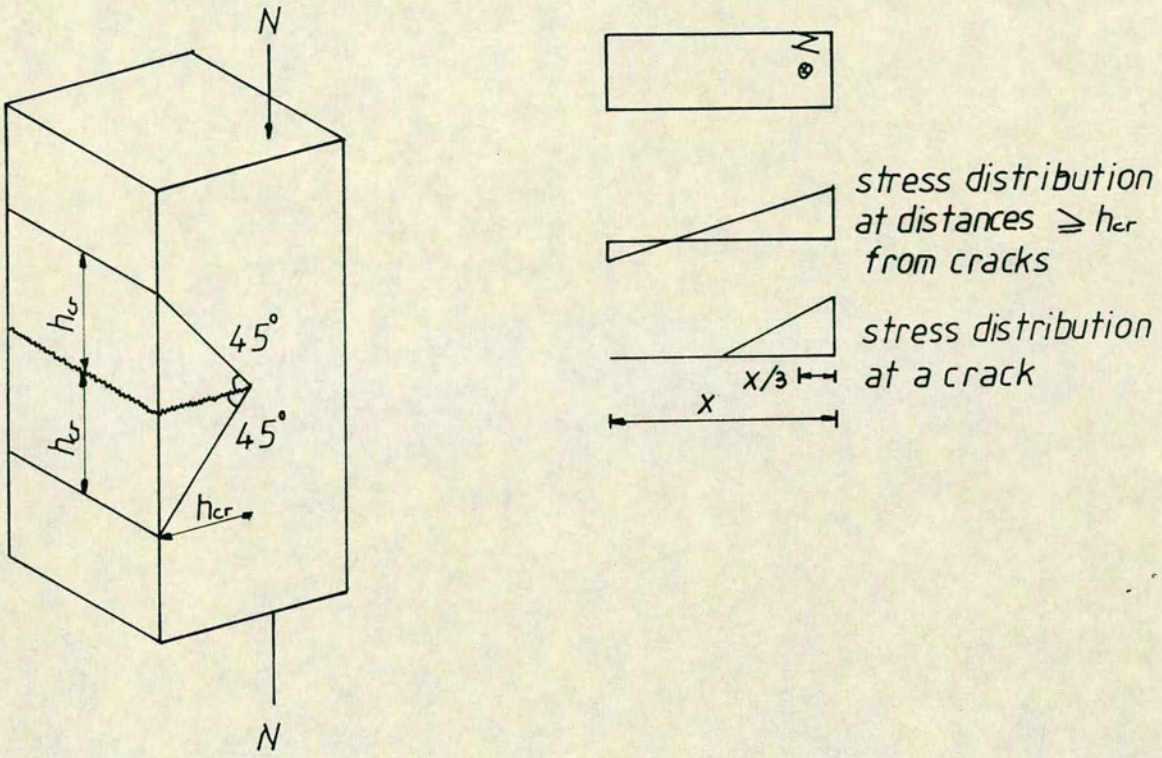

Fig. 6.3.4 Cracking in an Unreinforced Concrete Column

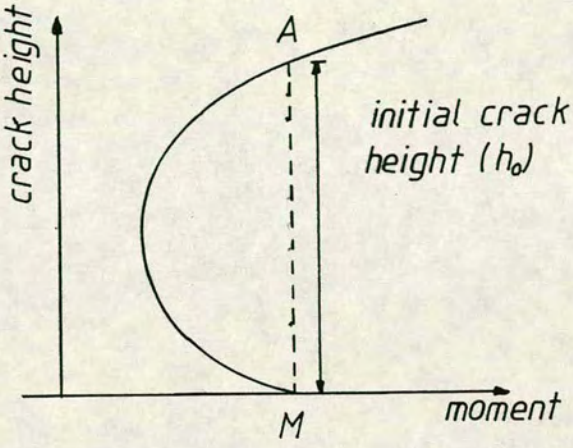

(a) Reinforced Concrete

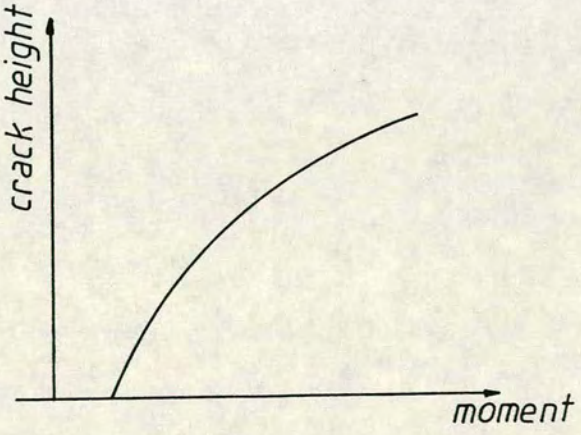

(b) Prestressed Concrete

Fig. 6.3.5 Relationship Between the Crack Height and Moment

somewhat different. There is no initial crack height as at the onset of cracking, the cracks are theoretically infinitely short and small. To overcome this obstacle and still maintain the integrity of this method, Beeby et al[86] have suggested that in the absence of an initial crack height, a 'controlling' crack height should be used defined by:

$$\delta(h_o/h)/\delta(M/bd^2f_r) = 1 \qquad \text{... 6.3.3}$$

i.e the controlling crack height is obtained when the rate of increase in crack height equals that of the moment. For practical purposes, it has been suggested that the controlling crack height in prestressed concrete can be taken as equal to the depth of the tension zone[86].

6.3.1.2 Application of the Theory of Cracking to Prestressed Brickwork

In principle, the theory given in Sections 6.3.1 and 6.3.1.1 should also be applicable to bonded prestressed brickwork. However, a few matters require consideration.

Firstly, the tensile strength along a brickwork member is variable. The tensile strength of the brick unit is much higher than that of the mortar which is in turn higher than that at the brick/mortar interface. Therefore, cracking will be initiated at the brick/mortar interface and the crack spacing will be a multiple of b_j within the limits set by the cover and the initial or controlling crack height. If the cover is greater than the minimum joint spacing, then the average crack spacing will be greater than b_j. If however, the converse is the case, the average crack spacing will be equal to b_j. If the initial or controlling crack height h_o is greater than 2 b_j but less than 3 b_j, then, the average crack spacing will be 2 b_j and so on.

Secondly, consideration has to be given to the definition of the initial or controlling crack height in brickwork. Experimentally[11,12], it has been found that the height to which a crack rises on formation is dependent on the area of steel, the cover and the presence of non-tensioned steel close to the soffit. These are all related to the neutral axis. Previous researchers[11,12] have thus taken h_o to be the depth of the tension zone with satisfactory results.

6.3.2 Determination of the Average Crack Spacing

The theory of crack spacing (Section 6.3.1) is rather qualitative. It proposes that the crack spacing is made up of two terms (equation 6.3.2) and sets limits within which the average crack spacing will fall. In brickwork, this was sufficient to lead to specific values for the average crack spacing. In concrete however, the prediction of the average crack spacing is more complex and in this section, previous methods will be examined and a method proposed.

6.3.2.1 Existing Methods for Prediction the Average Crack Spacing in Concrete

The mean crack spacing is usually derived by assuming that at cracking, bond failure occurs between the reinforcement and the concrete i.e. the '**classical**' or '**bond-slip**' approach (see Section 6.3.1). The average crack spacing is then obtained by equating the total tensile force transferred from the steel to the concrete, to the resistance of the concrete area in tension. This leads to an equation in the following form:

$$s_m = k.\ A_t.\ f_t / \Sigma\ O.(f'_c{}^{0.5}) \qquad ...6.3.4$$

where
s_m = average crack spacing
k = a constant obtained experimentally
A_t = an appropriate area of concrete in tension
f_t = the tensile strength of concrete
Σ O = sum of reinforcing perimeters
f'_c = compressive strength of concrete

The term $A_t\ f_t$ represents the resistance of the concrete area in tension. The area of concrete in tension, $[A_t]$ over which the transfer of force takes place has been defined differently by various researchers[83,87]. Desayi[83], used a value equal to twice the cover less the bar diameter. The area of concrete in tension used by Nawy[87] is shown in Fig. 6.3.6. $S_m.\ \Sigma\ O.\ f'_c{}^{0.5}$ represent the total tensile force transferred from the steel to the concrete by bond stresses over the average crack spacing. The maximum bond stress is a function of $f'_c{}^{0.5}$ and hence its presence in equation 6.3.4.

There are two limitations to the use of equation 6.3.4 in the calculation of the average crack spacing. Firstly, theory has suggested that the crack spacing

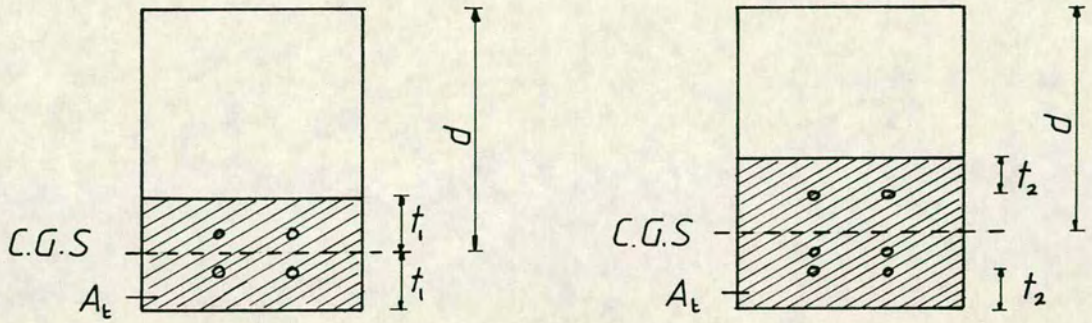

Fig. 6.3.6 Nawy's[67] Definition of the Concrete Area in Tension in a Rectangular Beam

is described by two terms obtained from the '**no-slip**' and '**bond-slip**' theories. Equation 6.3.4 is therefore a partial description of the average crack spacing. Secondly, recent evidence suggests that the area of tensile reinforcement, which is not represented in equation 6.3.4, greatly affects the spacing of cracks[87,81].

Beeby[76,86] found that the average crack spacing controlled by the initial crack height was given by:

$$s_m = 1.33\ h_o \qquad \text{...6.3.5}$$

However, this only applies when the percentage area of steel is small or the beam is shallow. Otherwise, the cover plays a more significant role in the crack spacing so that equation 6.3.5 becomes inadequate.

6.3.2.2 Proposed Method for Calculating the Crack Spacing in Concrete

It is suggested by the author that a suitable form for the average crack spacing in concrete is given by :

$$s_m = k_1 + k_2 . (A_t/A_s)^{0.5} . c \qquad \text{... 6.3.6}$$

where
s_m = average crack spacing
c = minimum concrete cover
A_t = area of concrete in tension
A_s = total area of tensile reinforcement
k_1, k_2 = constants

This proposal is based on the following:

The crack width is dependent on the crack spacing so that the factors which affect the former will also affect the latter. In methods which relate the crack widths to the steel strain or the average surface strain, the crack spacing is explicitly represented (see equation 6.2.4). As the steel strain and stress are also directly related, it is implied that in methods which employ the steel stress, the crack spacing is implicitly represented. This is confirmed by Nawy's equation[87] which relates the maximum crack width to the steel stress or steel strain thus:

$$w_{max} = k.\ s_m.\ (\Delta f_s)^{\alpha}$$

or

$$w_{max} = k'.\ s_m.\ (\varepsilon_s)^{\alpha}$$

... 6.3.7

where
Δf_s = net stress in the prestressed reinforcement
k, k', α are constants to be determined experimentally

Therefore, in such equations, besides the steel stress, it can be argued that the remaining terms describe the crack spacing. This is confirmed by Beeby's formula[76]:

$$w = k.\ D/P'.\ f_s$$

... 6.3.8

where
k = constant
D = nominal bar diameter
P' = effective reinforcement ratio (A_s/b.d)

The term D/P' has been used to describe the crack spacing[82].

From equation 6.2.6 which was considered to be the best relationship relating the maximum crack widths to the steel stress, $(A_t/A_s)^{0.5}$ c can be said to represent terms in the crack spacing equation with a dimensional constant to mentain dimensional integrity.

The use of $(A_t/A_s)^{0.5}$. c in the crack spacing equation has the following advantages:

- It reflects the reduction in crack spacing with an increase in the area of steel as was found experimentally by Nawy[87].

- The crack spacing is based on the concrete area in tension which affects it

- The definition of the concrete area in tension as that below the neutral axis is an adequat representation of the increase in crack height with increasing moment. This is particularly useful in prestressed beams where at the onset of cracking, this is very small, and increases under increasing applied moment.

The presence of k_1 in equation 6.3.6 is to account for the fact that there will be a minimum crack spacing even in the absence of tensile reinforcement.

A regression analysis on all the crack spacing data obtained from the concrete beams tested in this work resulted in k_1 = 184 mm and k_2 = 0.109. These constants are subject to the limitations of the data. Wider use of equation 6.3.6 will require verification from a wider and more varied data set.

6.4 EXPERIMENTAL RESULTS AND DISCUSSION

In this section, the experimental flexural cracking behaviour of similar prestressed beams of brickwork and concrete are compared. These include the crack spacing and pattern and the average and maximum crack widths. A comparison is also made with theoretical results.

6.4.1 The Crack Spacing

In brickwork, cracking was always initiated at the brick/mortar interface at the soffit of the beam. As mentioned earlier, this results from the tensile strength at these locations being the lowest in a brickwork member. The crack spacing was always in multiples of the joint spacing, b_j illustrated in Fig. 6.4.1 and was dependent on the area and distribution of tensile reinforcement.

The crack spacing reduced with an increase in the area of tensile reinforcement. In beams containing 0.274% area of tensioned steel, 84% of the spacing between crack fell between 2 x b_j (2 x 110 mm) and 3 x b_j (3 x 110 mm). The most common was 2 x b_j at 49% (see Fig. 6.4.2a). In beams with 0.548% area of tensioned steel, 92% of the cracks were spaced between b_j and 2 x b_j with 55% at b_j (see Fig. 6.4.2b). In comparing these beams, the effect of the cover has been ignored. However, previous results[11] have shown that increasing the area of steel with the cover constant reduces the crack spacing. In the partially prestressed beams, the crack spacing was constant at b_j (225 mm). This confirms a previous finding[12].

In concrete, the first crack(s) appeared in the region of maximum moment. As in brickwork, the crack spacing decreased with an increase in the area of

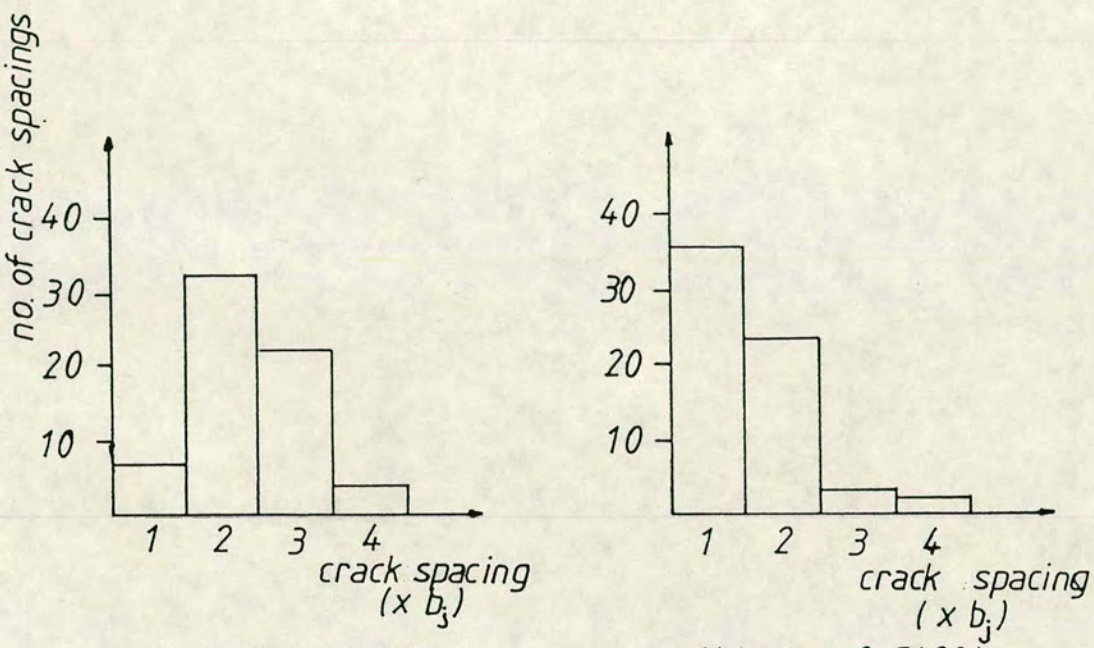

(a) $A_p = 0.274\%$ (b) $A_p = 0.548\%$

Fig. 6.4.2 Distribution of Crack Spacing in Brickwork

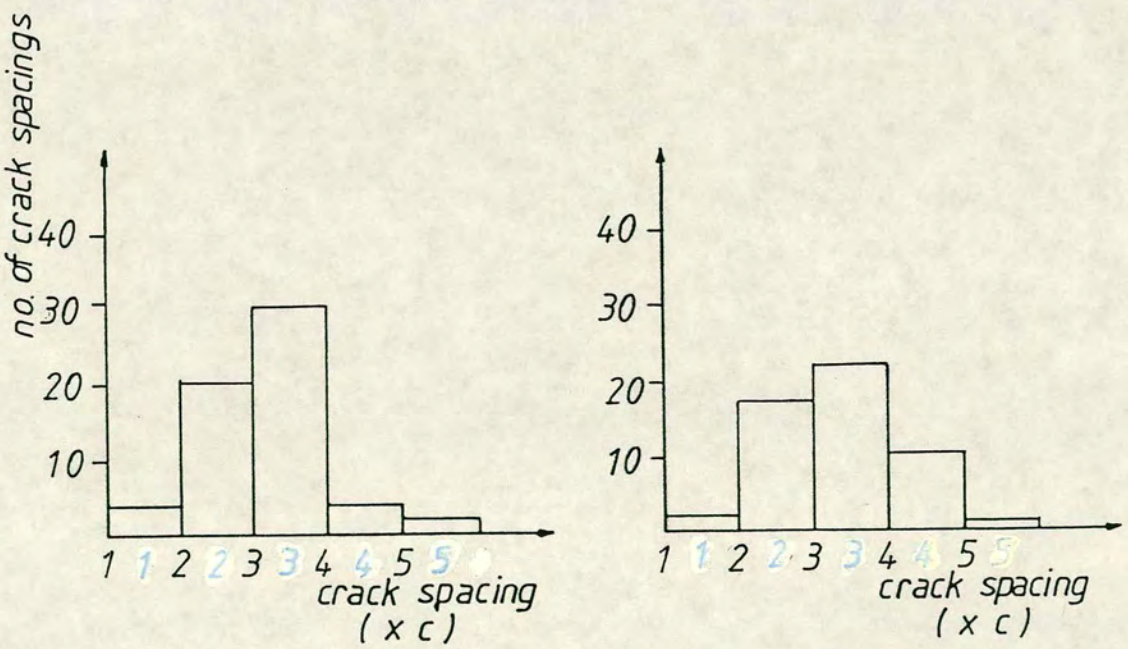

(a) $A_p = 0.274\%$ (b) $A_p = 0.548\%$

Fig. 6.4.3 Distribution of Crack Spacing in Concrete

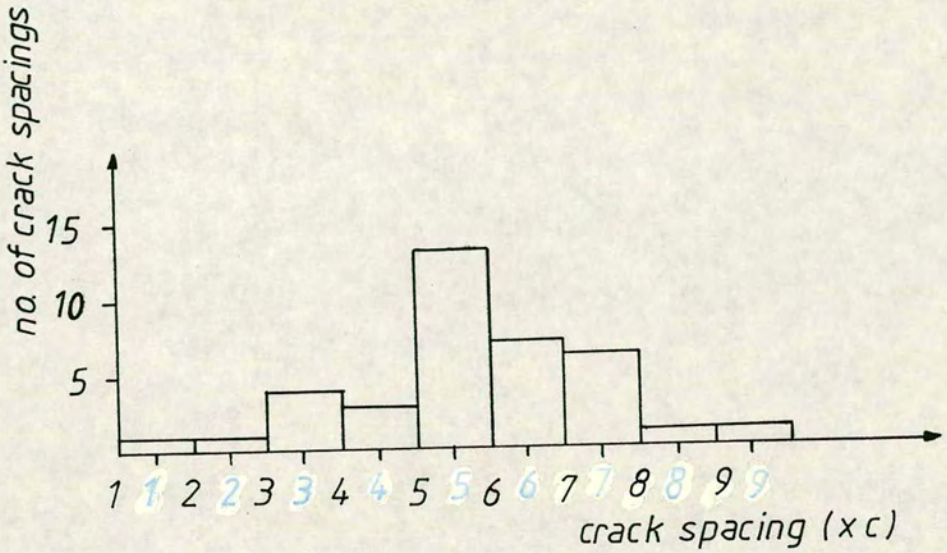

(c) Partially Prestressed Concrete Beams

Fig. 6.4.3 (contd.)

steel. In beams containing 0.274% area of steel, the most common range of crack spacing was between 363 and 484 mm (3c–4c where c is the minimum cover) with an average of 391 mm (see Fig. 6.4.3a). In beams containing 0.548% area of steel, the most common range of crack spacings had reduced to 285–380 mm (3c–4c) with an average value of 317 mm (see Fig. 6.4.3b). The cover to the tensile steel also varied so that its effect could not be isolated. However, previous research[87] has noted a decrease in the crack spacing with an increase in the area of tensile reinforcement. The crack spacing in the partially prestressed concrete beams had also reduced when compared with the fully prestressed beams. The most common range was 187.5–225 mm (5c–6c) with an average value of 221 mm (Fig. 6.4.3c).

From Figs. 6.4.2 and 6.4.3 which show the distribution of crack spacing in brickwork and concrete respectively, the most common range of crack spacings and the average were smaller in brickwork. In both cases, increasing the area of tensile steel reduces the crack spacing. This results from the increased stiffness of the section and the reduction in the depth of the tension zone. This reduces the initial crack height, h_o, which as mentioned in Section 6.3.1 affects the upper limit of crack spacing. In brickwork, the minimum crack spacing was the joint spacing b_j and in concrete, this approaches the cover.

The presence of non-tensioned steel close to the soffit as in the partially prestressed beams resulted in a reduced crack spacing. This can be attributed to the increased area of steel close to the soffit of the beam and the reduced cover. The large area of steel close to the soffit increases the influence of the cover on the crack spacing. In this case, the resulting crack spacings in brickwork and concrete were comparable.

In Tables 6.4.1a and b, the crack spacings are compared with theoretical results. The cover c refers to the distance from the soffit to the centroid of the nearest tensile reinforcement, h_o is taken as the depth of the tension zone and is obtained from a cracked section analysis. Using the guide lines set out in Section 6.3.1.2 for brickwork, the predicted values for all beams are in excellent agreement with the experimental results. In Table 6.4.1b, the average crack spacings obtained in concrete using the methods described in Section 6.3.2 are presented. The average crack spacings obtained experimentally are also presented. The results obtained from Beeby's method[76,86], equation 6.3.5 are given in column

Table 6.4.1a Comparison Between Predicted and Experimental Average Crack Spacings in Brickwork

% area of steel A_p #	P_e	cover+	h_o*	b_j	Exp.	Theo.
	kN	mm	mm	mm	mm	mm
0.274	135	121	188	110	220	220
0.548	275	95	111	110	110	110
0.548	208	95	69	110	110	110
0.341	62	37.5	183	225	225	225

Table 6.4.1b Comparison Between Predicted and Experimental Average Crack Spacings in Concrete

% area of steel A_p #	P_e	cover+	h_o*	Ave Exp	Theoretical		
					Beeby[76]	Nawy[87]	Eq. 6.3.6 (proposed)
	kN	mm	mm	mm	mm	mm	mm
0.274	128	121	271	391	374	910	449
0.548	283	95	226	341	279	456	329
0.548	201	95	188	317	324	456	330
0.341	62	37.5	236	221	327	261	226

Notes
+ distance from the centroid of the lowest tension bar to the soffit
* obtained from a cracked section analysis ($h_{cr} = h - n$)
# equivalent area of tensioned steel

6. Inspite of the random nature of cracking in concrete, the results obtained for the fully prestressed beams are very good. This is due to the relatively small area of steel and the large covers so that the crack spacing controlled by the initial crack height h_o, dominates. However, for the partially prestressed beams, this was not the case. The larger area of steel and the smaller concrete cover causes the pattern controlled by the cover to play a more significant role which is not represented in equation 6.3.5. Nawy's formula[87] was derived from the 'bond-slip' theory, equation 6.3.4 with k = 0.151 in SI units. These results are presented in column 7. In all cases, a poor estimate is given of experimental results. Column 8 contains the average crack spacing obtained from the proposed equation 6.3.6. Unlike previous methods, a good correlation of average crack spacings were obtained in all the concrete beams. However, equation 6.3.6 was obtained from limited data. On a wider perspective, all that can be said is that the basic form of equation 6.3.6 shows promise in the determination of the average crack spacing in concrete.

The Crack Pattern

The flexural crack pattern in the constant moment region at failure for each group of brickwork and concrete beams are given in Figs. 6.4.4a-c. In concrete, at the initial stages of cracking, the cracks travelled vertically, in the region of constant and maximum moment. In the fully prestressed beams, towards failure, these cracks began to fan out so that they travelled horizontally. The distance from the top of the beam where the cracks fanned out increased with the percentage area of steel. In the partially prestressed concrete beams, the crack pattern depended on the ultimate moment at failure. For those beams in which the failure moment was equal to or greater than the flexural moment of resistance, there was considerable horizontal propagation of cracks. In beams which failed before the flexural moment had been reached, this was absent.

In brickwork, the initial height and direction of propagation of cracks was dependent on the area and distribution of steel. In the bottom course, the cracks always travelled vertically along the brick/mortar interface. With a low percentage area of steel (0.274%), on first appearance, these travelled vertically upwards in the beam section through a combination of brick units and brick/mortar interfaces. With increasing area of steel (0.548%) and non-tensioned reinforcement close to the soffit (the partially prestressed

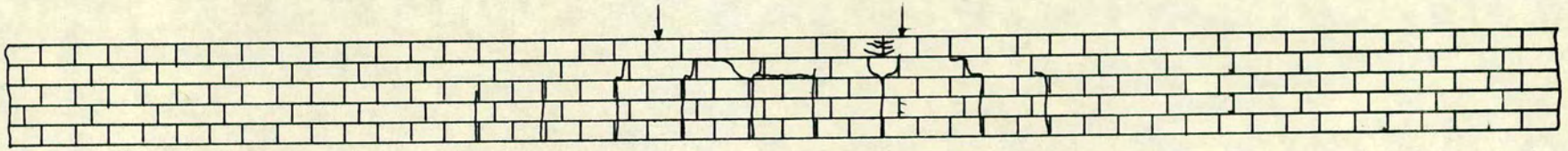

Brickwork

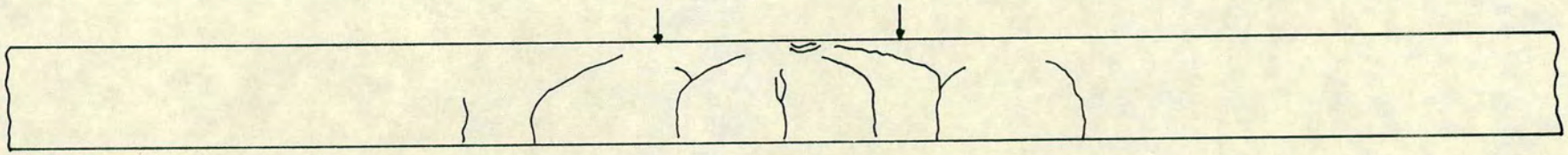

Concrete

Fig. 6.4.4 a Crack Pattern for Fully Prestressed Beams A = 0.274 %

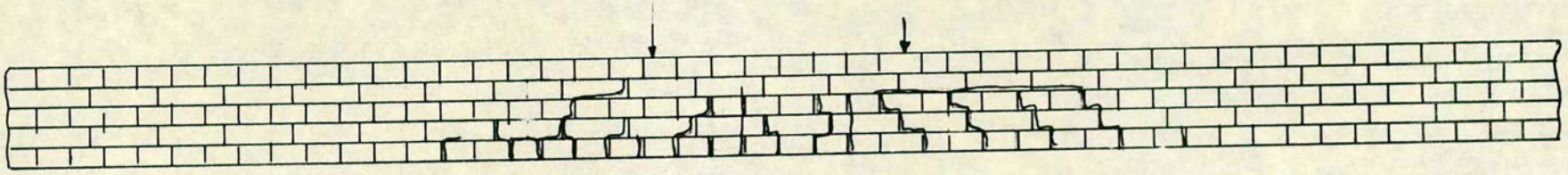

Brickwork

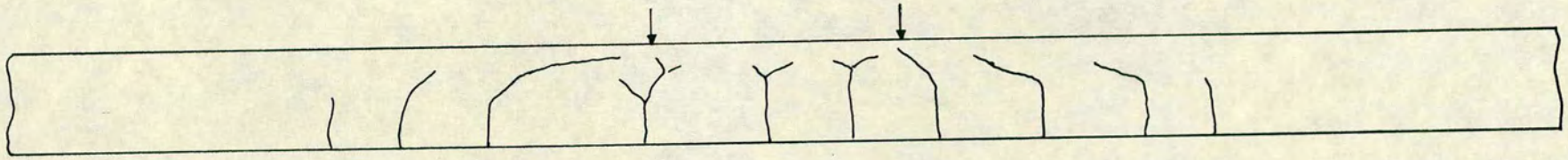

Concrete

Fig. 6.4.4 b Crack Pattern for Fully Prestressed Beams $A_p = 0.548\%$

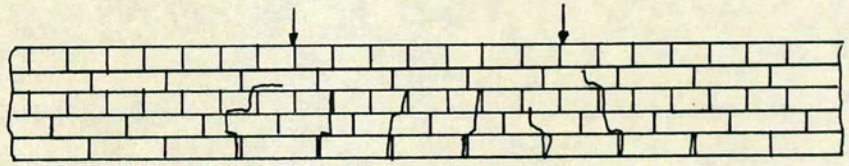

Brickwork

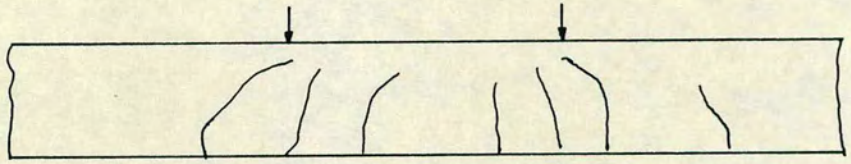

Concrete

Fig. 6.4.4 c Typical Flexural Crack Pattern for Partially Prestressed Beams

beams), these cracks began to travel upwards through a combination of header and bed joints. In all the brickwork beams described here, only those with the least area of steel failed in flexure so that the complete flexural crack pattern in the other beams were not developed.

6.4.2 The Average Crack Width

The average crack width is the arithmetic mean of all the crack widths measured in the constant moment region at each load increment for a particular beam. Given the scatter of experimental results, the relationships between the moment and the crack widths were obtained by fitting a curve. The relationships between the 'total moment' and the 'additional moment after cracking' ($M-M_{cr}$) were each plotted against the average crack width. The former enabled a comparison to be made over the entire loading history so that the effects of the differences in the cracking moments could be investigated. Bennett et al[79] found that the increase in crack width was proportional to the additional moment after cracking rather than the total moment. In order to compare the rates of increase in crack width between brickwork and concrete, the $M-M_{cr}$ vs average crack width relationships were also plotted. In the latter relationship, the differences in the cracking moments were not reflected and also, slight variations in the prestressing forces could be allowed for.

6.4.2.1 Fully Prestressed Beams

In Figs. 6.4.5 and 6.4.6, the moment-average crack width relationship for similar fully prestressed beams of brickwork and concrete are compared. The fully prestressed beams were taken from reference 11.

At the commencement of cracking, the reinforcement was still in the elastic range. This resulted in a quasi-linear relationship particularly obvious in the beams with the higher percentage area of steel. With increasing moment these relationships tended to flatten out. Eventually, in beams which failed in flexure by yeilding of the tensile reinforcement, the moment-average crack width relationship becomes virtually parallel to the x-axis so that small increases in moment produce large increases in crack widths. Generally, from Figs. 6.4.5 and 6.4.6, at a given moment, smaller crack widths were obtained in

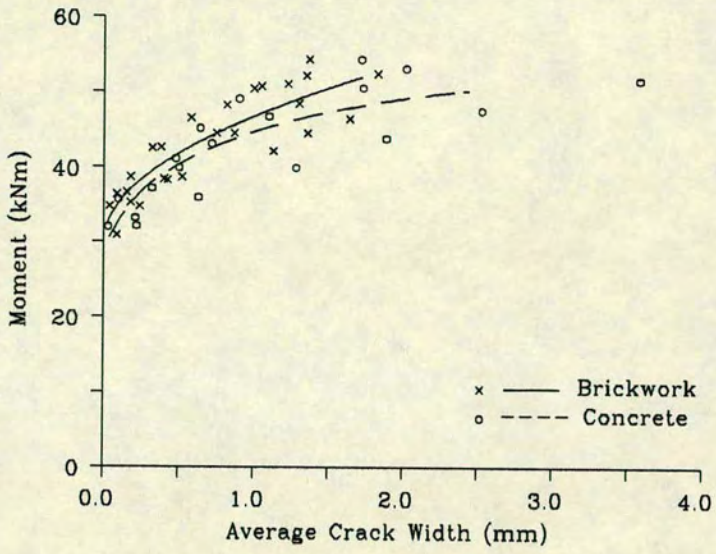

Fig. 6.4.5a Moment–Average Crack Width
A_p=0.274%

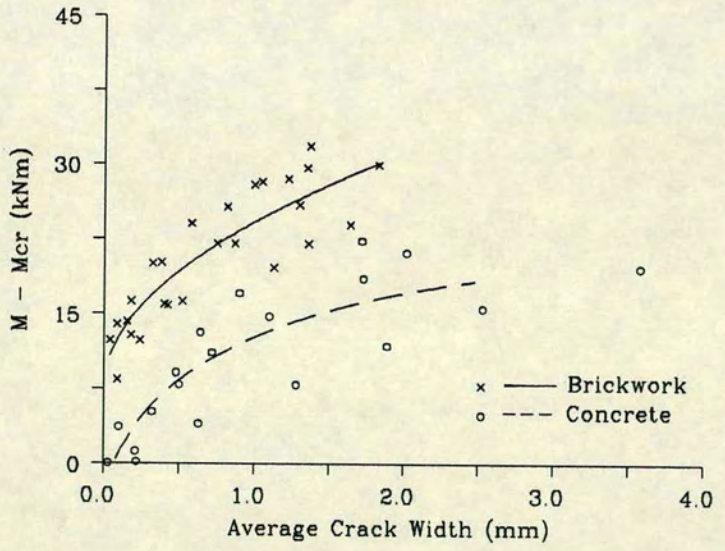

Fig. 6.4.5b M – M_{cr} vs Average Crack Width
A_p=0.274%

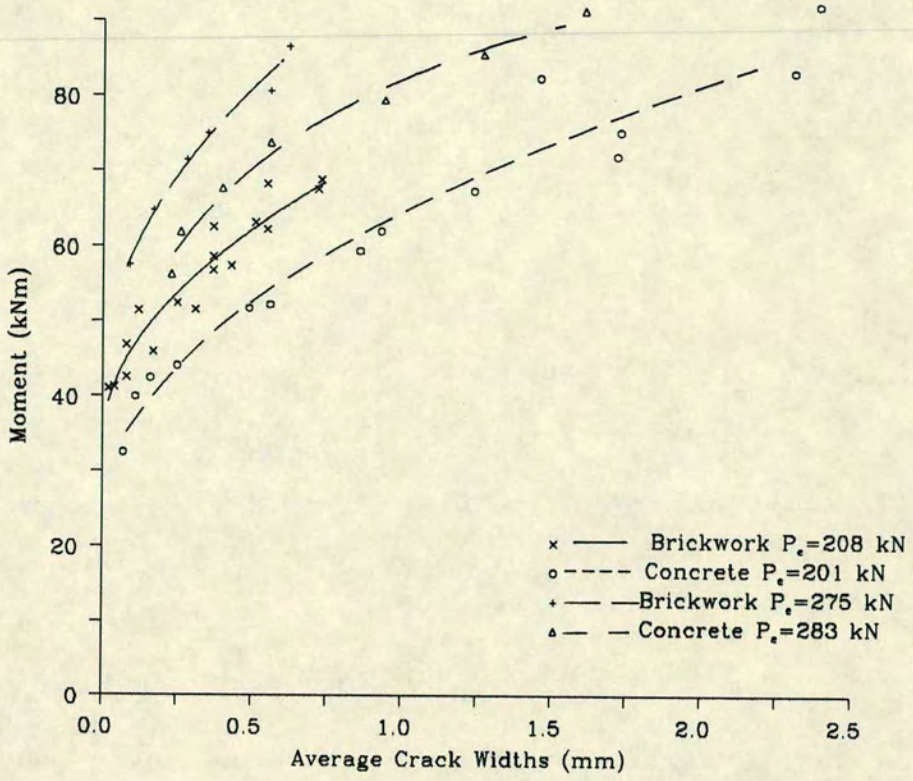

Fig. 6.4.6a Moment–Average Crack Width
A_p=0.548%

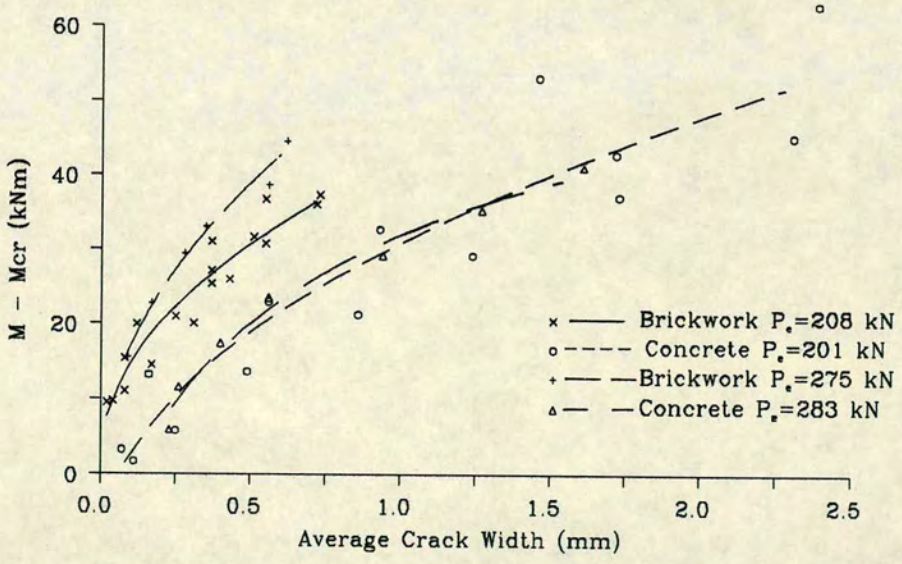

Fig. 6.4.6b M – M_{cr} vs Average Crack Width
A_p=0.548%

brickwork than in concrete at all percentage areas of steel inspite of the fact that cracking began earlier in the brickwork. This can be attributed to the differences in the nature of brickwork and concrete. As observed in the Section 6.4.1, the spacing between cracks is generally larger in concrete than in brickwork owing to the presence of brick/mortar interfaces in the latter. Therefore, there are generally more cracks in brickwork than in concrete. It is implied in Section 6.2.2 from equation 6.2.4 that the total width of cracks is related to the elongation of the steel. In brickwork this is divided among a larger number of cracks than in concrete which results in smaller crack widths in the brickwork beams. For the same reason, the rate of increase in the width of cracks as given by the $M-M_{cr}$ vs average crack width relationship, Figs. 6.4.5b and 6.4.6b is higher in concrete than in brickwork.

The brickwork and concrete beams containing 0.274% area of steel (see Fig. 6.4.5a) failed in flexure by the yielding of the tensile reinforcement and therefore there was a considerable flattening of the moment-average crack width relationship before failure. The differences in crack width between the brickwork and concrete beams tended to increase towards failure. However, within the serviceability limits for crack widths in concrete[58] (up to 0.2 mm) the crack widths in brickwork and concrete were comparable.

The relationships between the moment and average crack width for the brickwork and concrete beams containing 0.548% area of tensile steel are presented in Figs. 6.4.6. In Fig. 6.4.6a, the higher moment at which cracking occurs in the beams containing the higher prestressing force is reflected by the smaller crack widths at all moments when compared with those with less prestressing force. This results from the increased stiffness imparted by the higher prestressing force. The moment-average crack width relationships for these beams follow the same trend as for the beams with 0.274% area of steel with the exception that here, the quasi-linear portion (Fig. 6.4.6a) is more in evidence. Also, in brickwork and to a lesser extent in concrete, the moment-average crack width relationships do not become parallel to the x-axis towards failure. This is due to the larger area of steel which results in a stiffer section. The beams with the lower prestressing force show a flatter relationship towards failure. This results from the reduced stiffness of the cracked section. The brickwork beams failed primarily in shear so that at ultimate, the tensile reinforcement had not yielded.

The additional moment after cracking is plotted against the average crack width in Fig. 6.4.6b. Once again, it is evident that after cracking, the cracks widen more rapidly in concrete. However, while the rate of crack widening was found to be virtually constant in concrete irrespective of the prestressing force, an increase in the rate of crack widening with decreasing prestress was observed in brickwork.

6.4.2.2 Partially Prestressed Beams

Figs. 6.4.7 a and b show the moment-average crack width relationship for similar partially prestressed beams of brickwork and concrete. The relationships were quasi-linear throughout the loading history. This was partly due to the increased stiffness arising from the relatively large area of steel close to the soffit of the beam and also to the mode of failure. These beams failed in either primary or secondary shear before all of the tensile reinforcement had yielded. The flattening portion of these relationships which result from the yielding of the tensile reinforcement was therefore absent.

The average experimental curves were very similar with brickwork again having narrower cracks at a given moment. These differences reduced towards failure of the brickwork beams. The similarity in both relationships result from the area of tensile reinforcement and also its distribution. In Section 6.4.1, it was mentioned that increasing the area of tensile steel results in smaller crack spacings. Also, the presence of non-tensioned steel close to the soffit (i.e reduced cover) also reduces the crack spacing. In brickwork, this was reduced to the minimum possible spacing for this bonding arrangement i.e b_j (225 mm). In concrete, this was reduced to a value comparable to b_j (221 mm). Similar crack spacings with identical tensile reinforcement lead to similar crack width and hence the similarity between the average measured crack widths in the partially prestressed brickwork and concrete beams.

6.4.2.3 A Comparison Between the Experimental and Theoretical Average Crack Widths

The computer program described in Chapter 5 is capable of predicting the average crack width using the average steel strain method (Section 6.2.2). Therefore with an accurate allowance for the tension stiffening effect (see

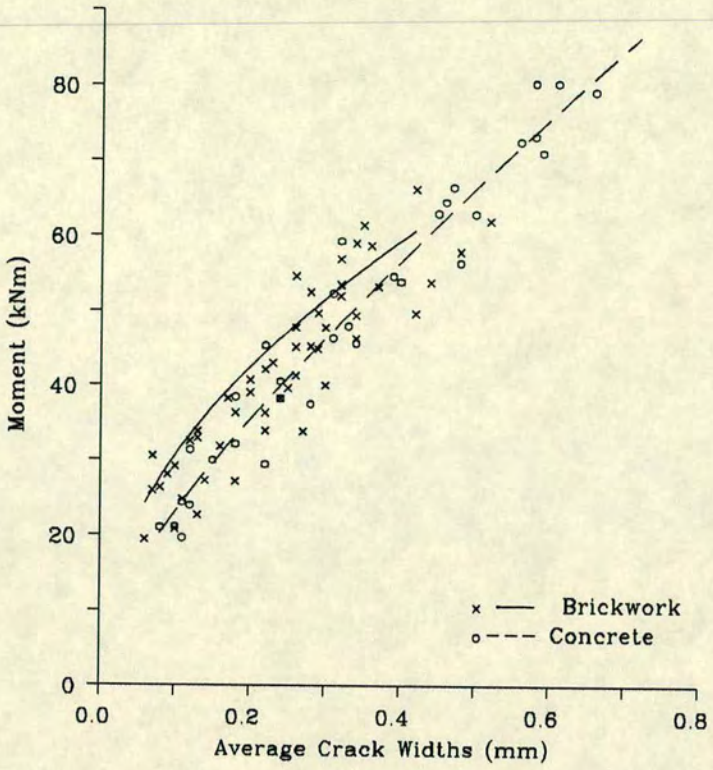

Fig. 6.4.7a Moment–Average Crack Width
A_{ps}=0.341%

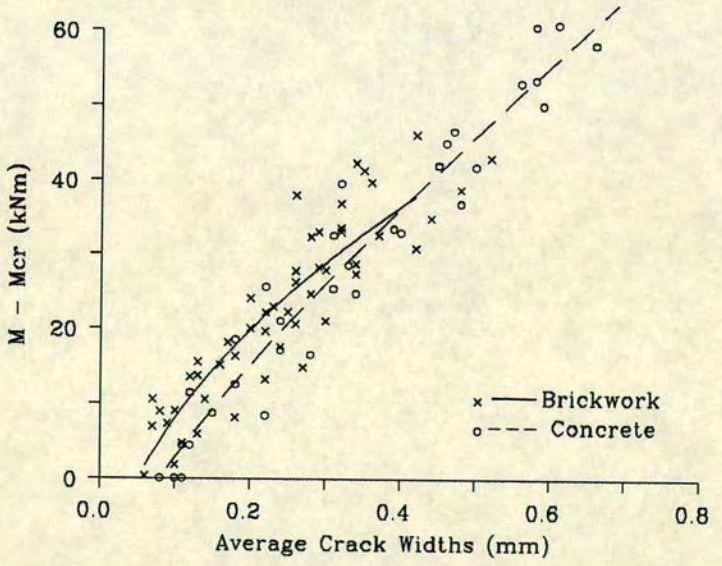

Fig. 6.4.7b M – M_{cr} vs Average Crack With
A_{ps}=0.341%

Chapter 5), the average crack widths can be predicted as long as the crack spacing can also be determined. The moment–average crack width relationship for the beams tested here are compared with those obtained theoretically from this method. The results are presented in Figs. 6.4.8–6.4.13.

In Fig. 6.4.8–6.4.10, these relationships for the concrete beams are presented. In all cases with the exception of the partially prestressed beams, the theoretical predictions were very good. In the partially prestressed concrete beams, Fig. 6.4.10, when the tension stiffening effect is taken into account as described in Chapter 5, the average crack widths were underestimated. Without the effects of tension stiffening, a better estimate of the average crack widths were obtained. Initially, both relationships are coincident. With increasing load, the theoretically obtained crack widths become increasingly smaller than those measured. These discrepancies between theory and experimental results can be attributed to the mode of failure of the beam which was in shear.

The moment–average crack width relationship for the brickwork beams are compared with theoretical predictions in Figs. 6.4.11–6.4.13. For the beams containing 0.274% area of steel, Fig. 6.4.11, good predictions were obtained. For all other brickwork beams Figs. 6.4.12 and 6.4.13, the theoretical average crack widths were smaller than those measured. This can be attributed to the occurrence of shear failure rather than a flexural failure as assumed by the theory.

6.4.3 The Maximum Crack Width

The maximum crack width is the largest recorded at each load increment after cracking in the region of constant and maximum moment. The relationship between the moment and the maximum crack widths for the brickwork and concrete beams are presented in Figs. 6.4.14–6.4.16. For the beams containing tensioned steel only (Figs. 6.4.14 and 6.4.15), the maximum crack widths in brickwork were smaller than those in the corresponding concrete beams. In the partially prestressed beams however, the maximum crack widths in the brickwork and concrete beams were coincident until shear failure of the brickwork beams.

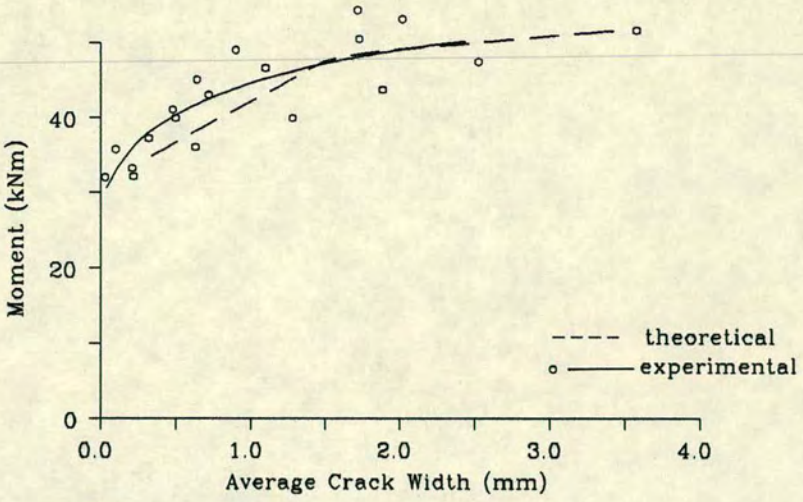

Fig. 6.4.8 Moment–Average Crack Width
Concrete Beams, A_p=0.274%

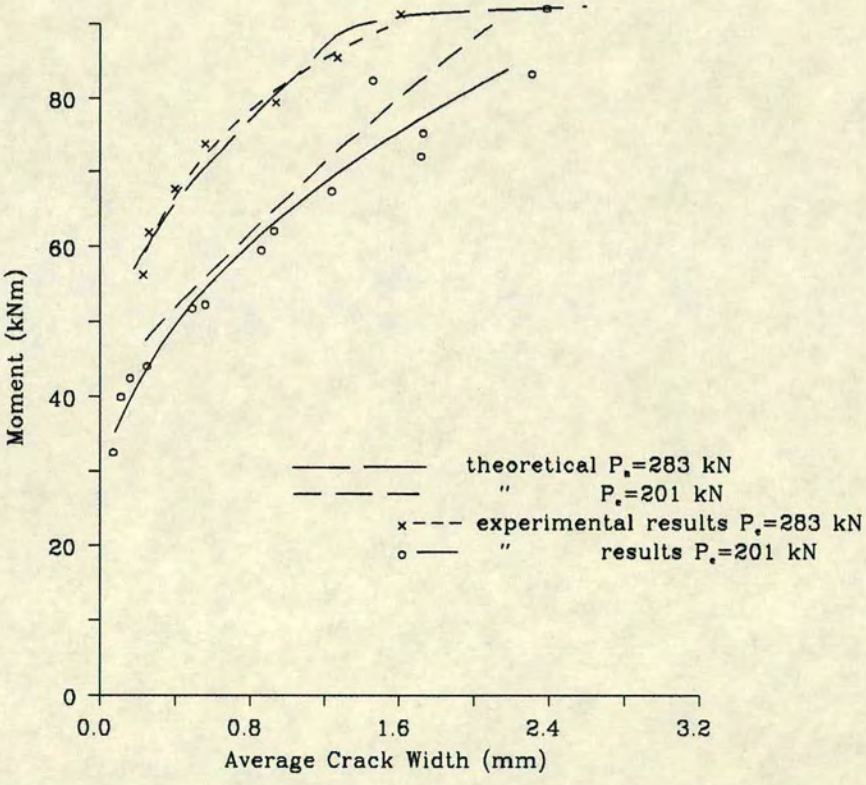

Fig. 6.4.9 Moment–Average Crack Witdh
Concrete Beams, A_p=0.548%

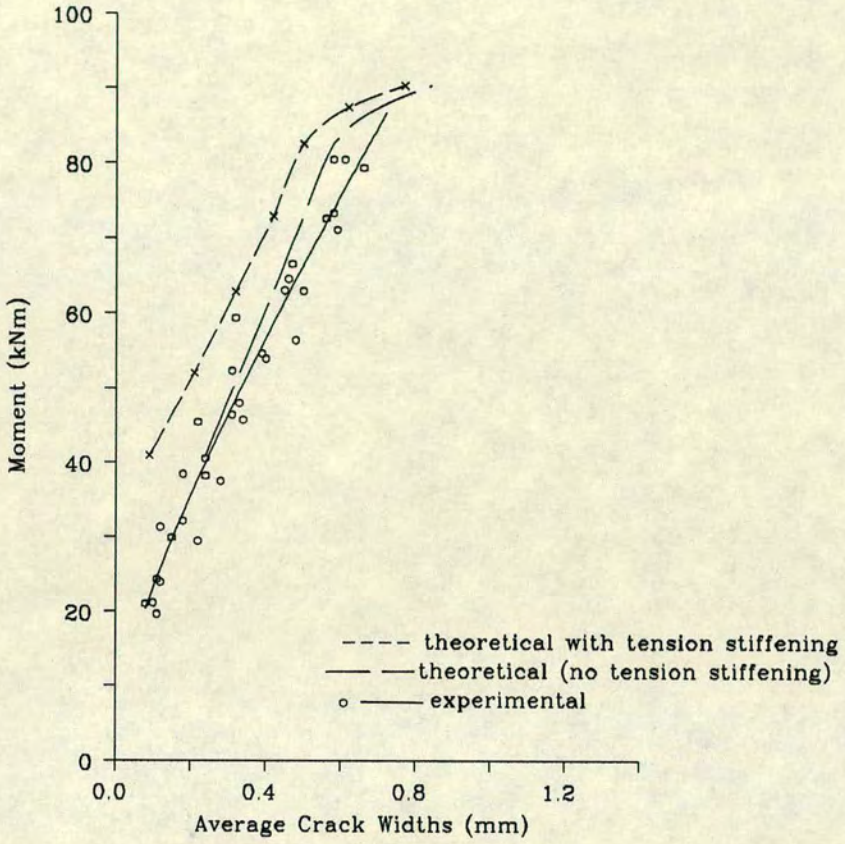

Fig. 6.4.10 Moment–Average Crack Width
Concrete Beams, A_{ps}=0.341%

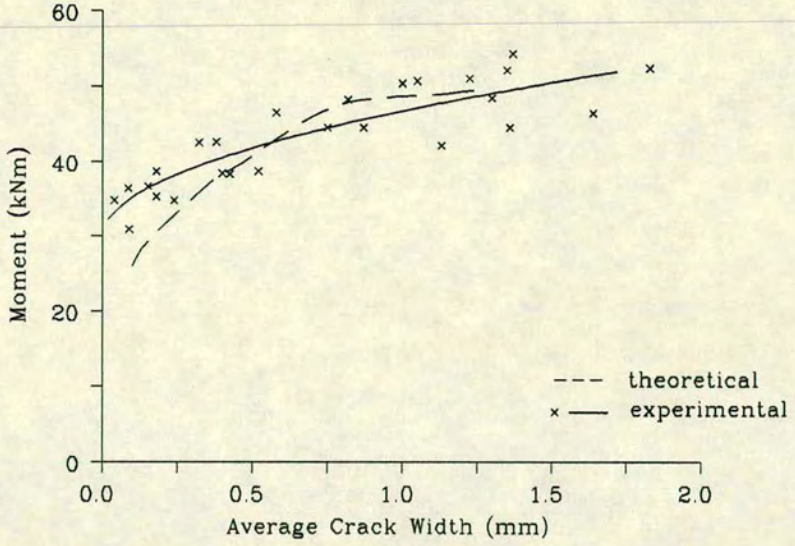

Fig. 6.4.11 Moment–Average Crack Width
Brickwork Beams, A_p=0.274%

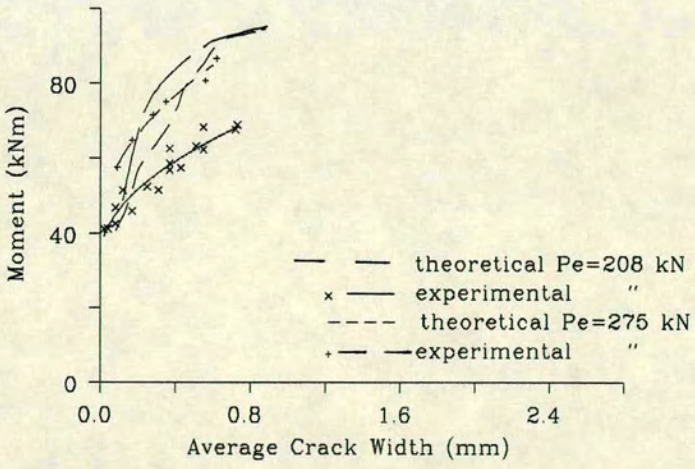

Fig. 6.4.12 Moment–Average Crack Width
Brickwork, A_p=0.548%

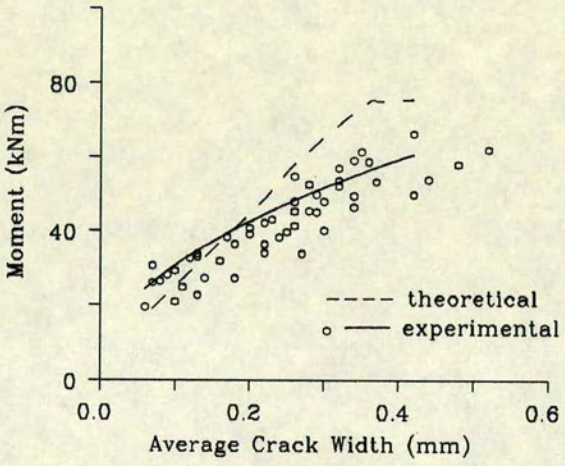

Fig. 6.4.13 Moment–Average Crack Width
Brickwork Beams, A_{ps}=0.341%

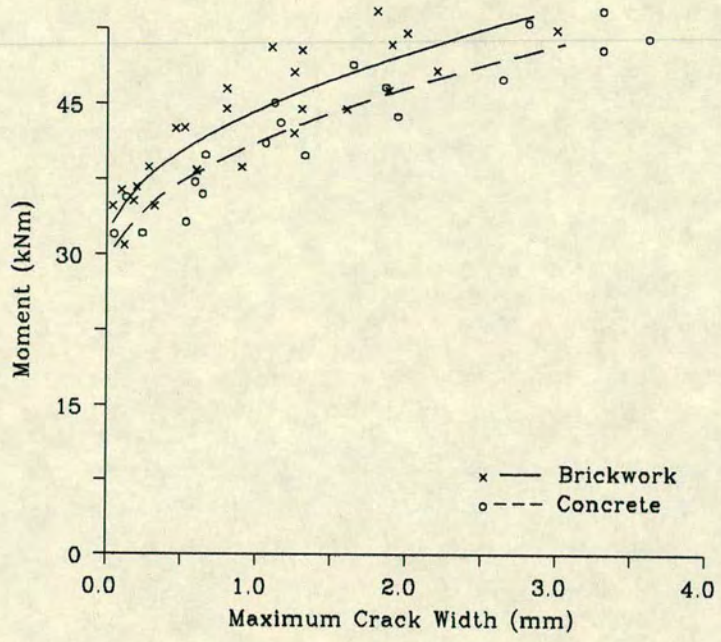

Fig. 6.4.14 Moment–Maximum Crack Width
A_p=0.274%

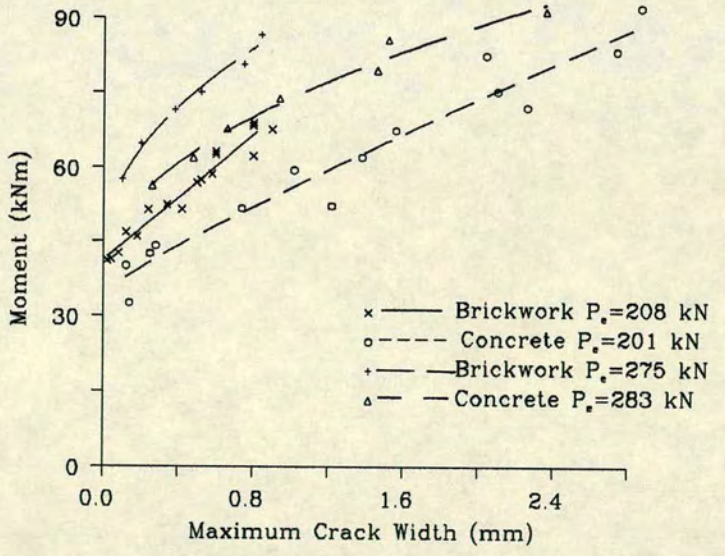

Fig. 6.4.15 Moment–Maximum Crack Width
A_p=0.548%

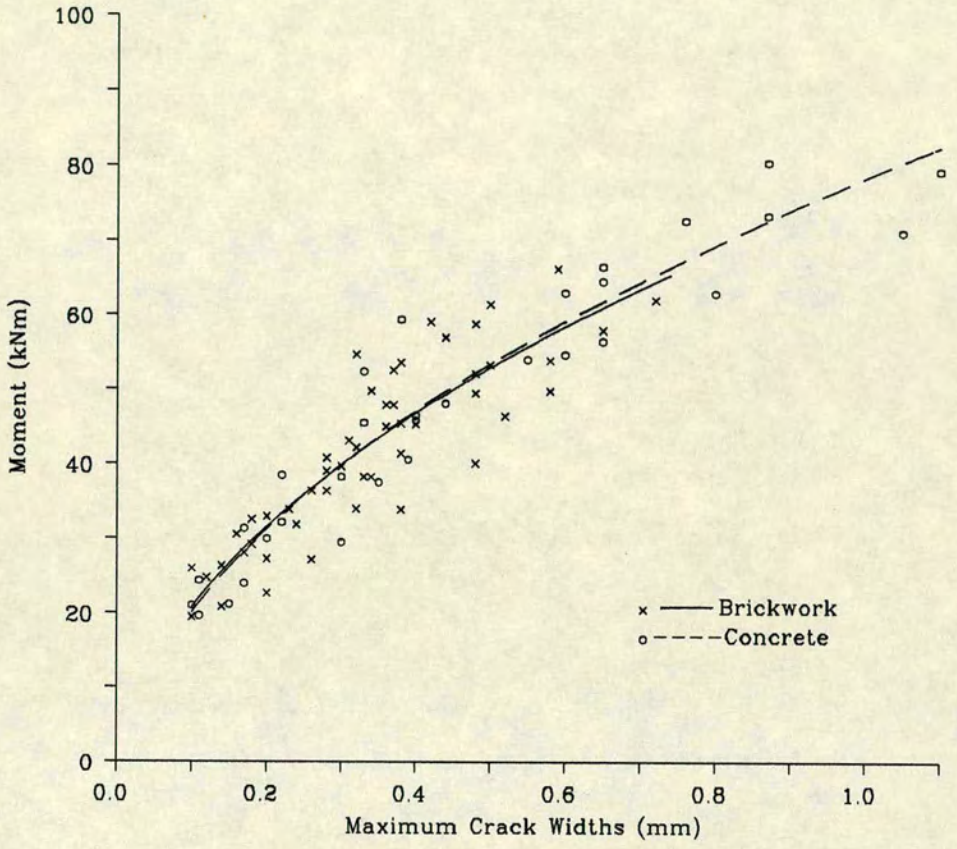

Fig. 6.4.16 Moment–Maximum Crack Width
A_{ps}=0.341%

6.4.3.1 Relationship Between the Maximum and Average Crack Widths

The serviceability limit state of cracking specifies maximum crack widths which may not be exceeded under certain conditions of exposure. Therefore, although the average crack width is important, it is the maximum which is the controlling parameter in design. This is because a crack considerably wider than the mean may permit the penetration of corrosive elements to the tensile steel and thereby hamper its efficiency. Previous researchers[11,12] have calculated the maximum crack width by establishing a relationship between the maximum and average crack width. This has been done with the aid of histograms which show the frequency by which the maximum crack width exceeds the mean by a given amount. This method has also been employed here.

In Figs. 6.4.17 a, b and c, frequency histograms are presented for brickwork and concrete at each percentage area of steel. Also shown on these figures, are the 95% confidence limits i.e the ratio of the maximum to average crack width which was exceeded by 5% of the results. Figs. 6.4.17 show that the distribution of maximum crack widths varies with the percentage area of steel.

In the beams containing 0.274% area of steel, Fig. 6.4.17a, the most commonly occurring ratio of maximum to mean crack width in brickwork was 1.3 while in concrete, this was between 1.0 and 1.1. More importantly, the 95% confidence limit was 1.7 and 2.1 in brickwork and concrete respectively reflecting the wider scatter of experimental results in the concrete beams. At 0.548% area of steel Fig. 6.4.17 b, the most frequent ratio had increased to 1.4 and 1.2 in brickwork and concrete respectively. Again, the 95% confidence limit in brickwork at 1.6 was lower than in concrete at 2.0. The distribution of maximum crack widths in the partially prestressed brickwork and concrete beams were very similar, Fig. 6.4.17c. The most frequently occurring ratio of the maximum to mean crack width was 1.4 in both cases. This value was also obtained by Walker[12] from results on a large number of partially prestressed brickwork beams containing varying amounts of tensioned and non-tensioned steel. The 95% confidence limits were 1.9 and 1.7 in brickwork and concrete respectively. This value for brickwork was also in good agreement with that obtained in a previous work[12] of 2.0.

Combining the results of all the concrete beams and all the brickwork

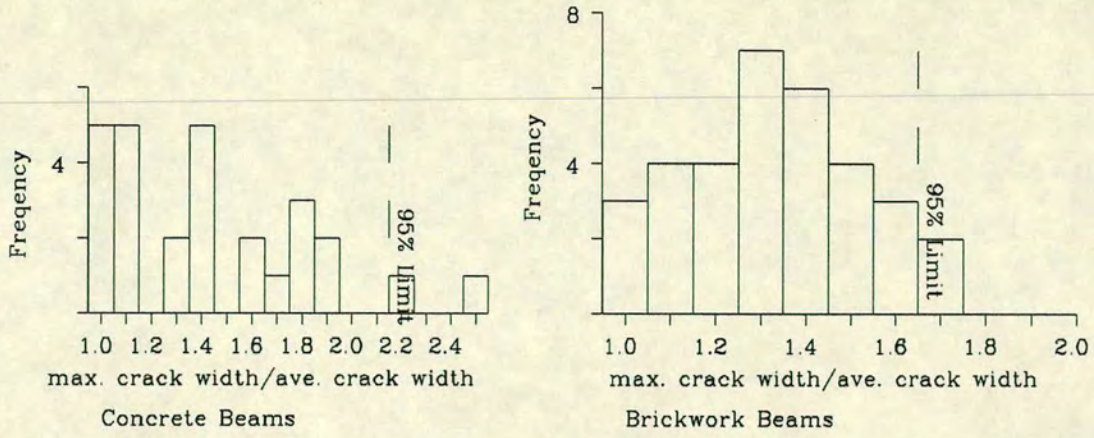

Fig. 6.4.17a Distribution of Crack Widths, A_p=0.274%

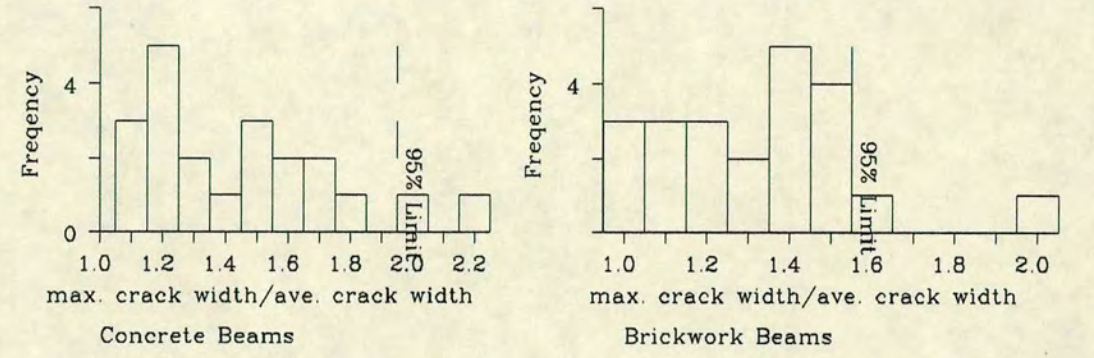

Fig. 6.4.17b Distribution of Crack Widths, A_p=0.548%

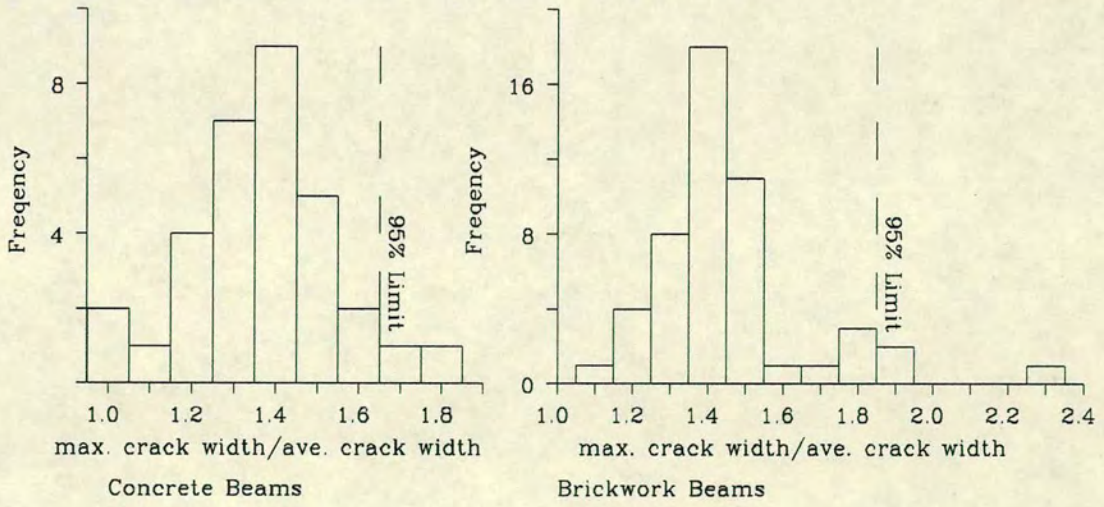

Fig. 6.4.17c Distribution of Crack Widths, A_{pc}=0.341%

beams produce Figs. 6.4.18 a and b respectively. The most frequent ratio of maximum to mean crack width was 1.4 in both cases. The 95% confidence limits were 1.9 and 1.8 in concrete and brickwork respectively. Therefore in concrete:

$$w_{max} = 1.9\ w_{av} \qquad \ldots 6.4.1$$

and from equation 6.2.4,

$$w_{max} = 1.9.\ s_m.\ \varepsilon \qquad \ldots 6.4.2$$

Similarly, for brickwork;

$$w_{max} = 1.8.\ s_m.\ \varepsilon \qquad \ldots 6.4.3$$

where
s_m = average crack spacing
ε = average strain at the depth where crack widths are required

6.4.3.2 Comparison Between Experimental and Theoretical Maximum Crack Widths

The maximum crack widths are compared with the predictions given by the Suri-Dilger equation[81] and the proposed method (see Section 6.2.3) for concrete and brickwork respectively. A comparison is also made with those obtained from a statistical relationship between the maximum and average crack widths (equations 6.4.2 and 6.4.3). The theoretical average crack widths were obtained from Section 6.4.2.3.

Figs. 6.4.19 to 6.4.22 show the experimental and theoretical relationships for concrete. In the beams containing 0.274% area of steel, Fig. 6.4.19, the Suri-Dilger Equation overestimated the crack widths up to failure. However, the general shape of the curve is in good agreement with the experimental relationship. The relationship obtained from equation 6.4.2 is also plotted in Fig. 6.4.19. This also overestimated the maximum crack width but to a lesser degree than the previous method. It also formed a lower bound to the experimental data, a direct result of using a 95% confidence limit.

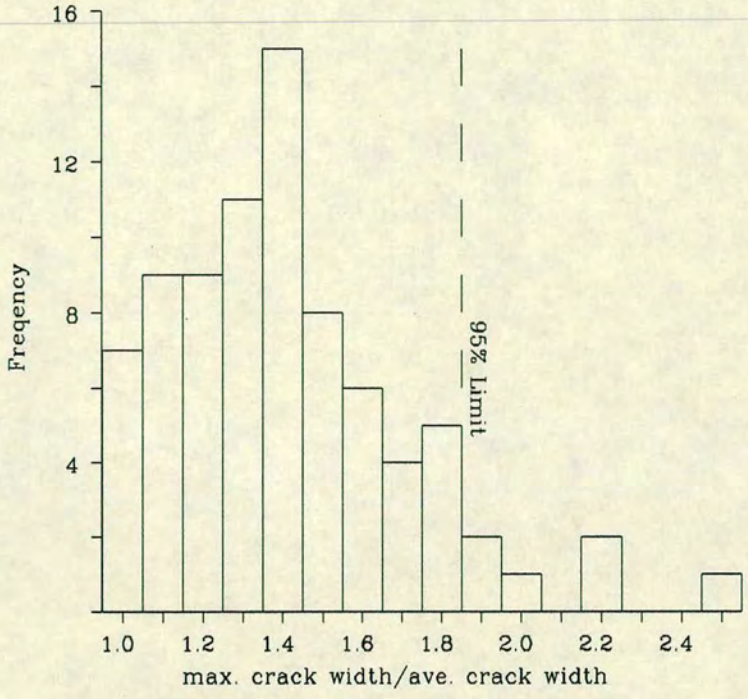

(a) Concrete Beams

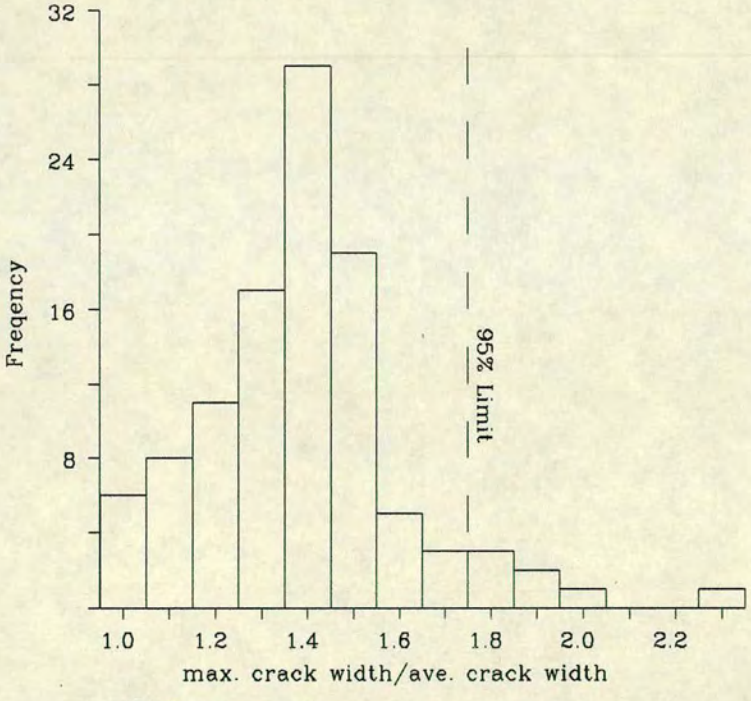

(b) Brickwork Beams

Fig. 6.4.18 Distribution of Maximum Crack Widths in Brickwork and Concrete Beams

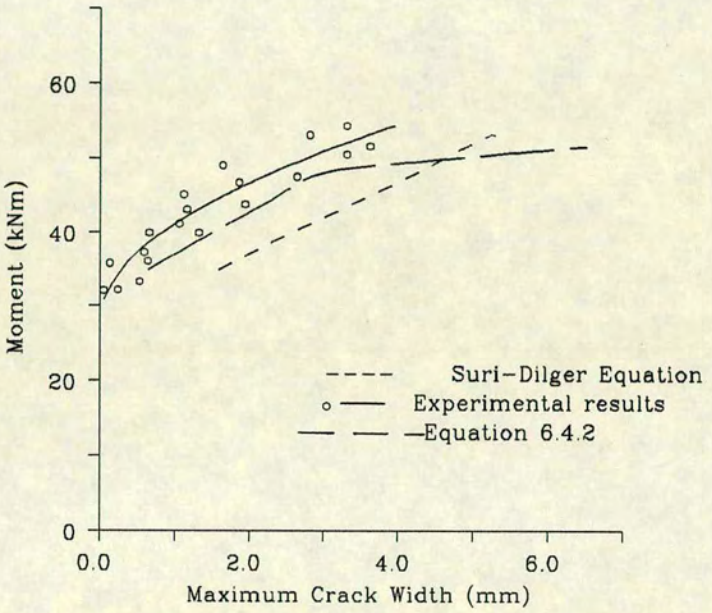

Fig. 6.4.19 Moment–Maximum Crack Width
Concrete Beams, A_p=0.274%

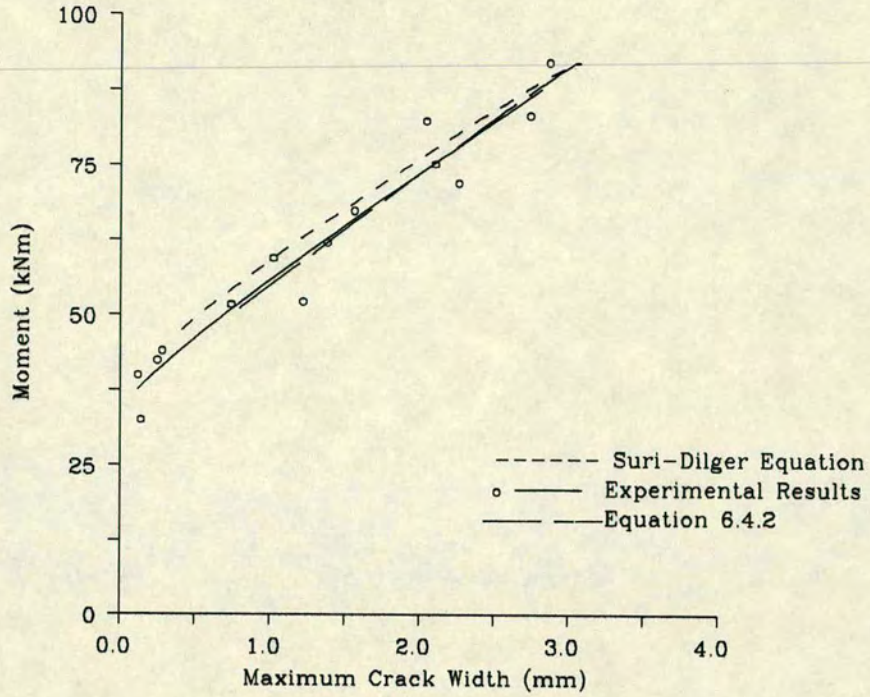

Fig. 6.4.20 Moment–Maximum Crack Width
Concrete Beams, A_p=0.548%, P_e=200 kN

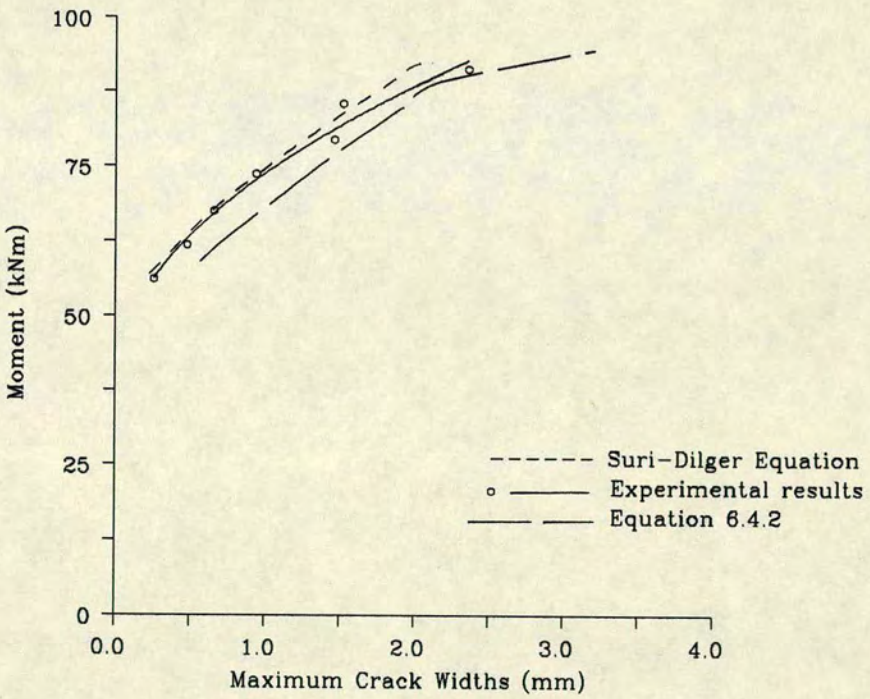

Fig. 6.4.21 Moment–Maximum Crack Width
Concrete Beams, A_p=0.548%, P_e=283 kN

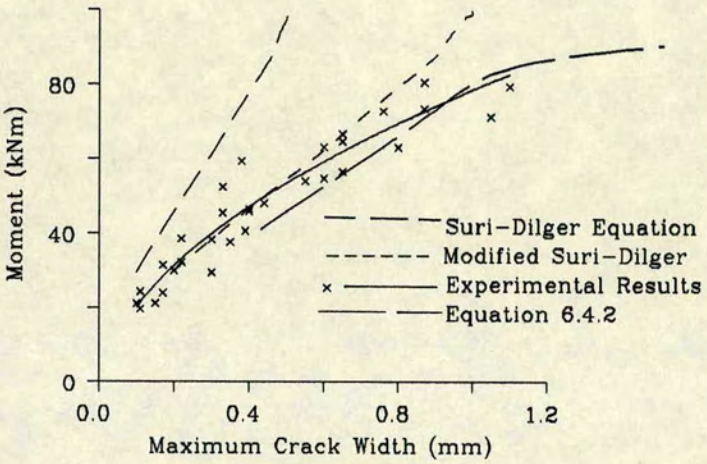

Fig. 6.4.22 Moment-Maximum Crack Width
Concrete Beams, A_{pe}=0.341%

The relationships for the beams containing 0.548% area of steel are presented in Fig. 6.4.20 and 6.4.21 for the beams with the lower and higher prestressing forces respectively. In both cases, both theoretical methods show very good agreement with experimental results. For the beams with an effective prestressing force of 201 kN, equation 6.4.2 gives an excellent correlation. The Suri-Dilger equation also gives a good agreement with experimental results although a slight underestimate was obtained. For the beam with an effective prestressing force of 283 kN, Fig. 6.4.21, the Suri-Dilger equation gave an excellent correlation with the maximum crack widths obtained experimentally. Equation 6.4.2 slightly overestimates experimental results.

The experimental and theoretical moment-maximum crack width relationship for the partially prestressed concrete beams are presented in Figs 6.4.22. The Suri-Dilger equation underestimated the experimental results especially towards failure. This was because of the constant given for this combination of tensile reinforcement (deformed bar and strand) in Equation 6.2.6. This constant along with that for beams containing strands only are given in Table 6.4.2. As mentioned in Section 6.2.3, the relative values of the constants for these combinations of tensile reinforcement are inconsistent with experimental observations which show large differences in crack widths for strands only and the combination of strands and deformed bars. Suri et al[81] attributed this anomaly to the differences in cover. For this reason a regression analysis was carried out on the maximum crack width data for the partially prestressed concrete beams tested in this work. The results are also contained in Table 6.4.2. The value of the constant obtained was 5.0×10^{-6} mm^2/N. Using this value in the Suri-Dilger equation resulted in a much better correlation with experimental results (see Fig. 6.4.22). However, a constant with a value of 5.0×10^{-6} N/mm^2 appears to be inconsistent with the values obtained by Suri and Dilger[81]. This discrepancy also results from the cover. Firstly, the range of covers for the beams with strands and deformed bars analysed by Suri and Dilger[81] were between 20 and 30 mm, less than the cover in the beams tested here which was 37.5 mm. Further, the fact that the cover can not be treated as a variable in the statistical analysis being fairly constant within each combination of tensile reinforcement by varying across the different combinations. The resulting theoretical relationship in the partially prestressed concrete beams was initially, coincident with experimental results but with increasing load underestimated the crack width. Equation 6.4.2 gave

Table 6.4.2 The constants in the equations for predicting the maximum crack width in brickwork and concrete

Equation	Type of steel	k x 10^{-6}	correlation	standard deviation
Concrete				
$w_{max}=k.f_s.(A_t/A_s)^{0.5}.c$	strands only	2.65	0.98	0.083
(equation 6.2.6)	strands and deformed bars	5.00 (2.55)*	0.87	0.136
Brickwork				
$w_{max}=k_b.f_s.(A_t/A_s)^{0.5}.b_j$	strands only	1.28	0.82	0.214
(equation 6.2.7)	strands and deformed bars	0.63	0.89	0.084

Note
* value obtained by Suri and Dilger[80]

an overestimate of experimental results until just before failure.

The relationship for the brickwork beams are presented in Figs. 6.4.23–6.4.26. For beams containing 0.274% area of steel, equation 6.4.3 overestimated the maximum crack width for the better part of the loading history. The proposed method also gives an overestimate up to the yielding of the steel. However, predictions by the proposed method were more conservative prior to the yielding of the steel and formed a lower bound to the experimental results.

Figs. 6.4.24 and 6.4.25 show the relationships for the beams with 0.548% area of steel with effective prestressing forces of 208 kN and 275 kN respectively. For beams with the lower prestressing force, initially, both methods overestimated the maximum crack widths with the proposed method giving the better estimate. Thereafter, both methods give underestimates, which is neglible in the method proposed in Section 6.2.4. The abrupt termination of the experimental result well short of the predictions was due to primary shear failure. For beams containing the higher prestressing force, Fig. 6.4.25, similar trends were exhibited by both methods but as in the previous group of beams, equation 6.4.3 gave a better estimate than in the previous case. The proposed method also slightly overestimated experimental results up to the primary shear failure of the beam.

The results for the partially prestressed brickwork beams are shown in Fig. 6.4.26. Initially, both methods give a good estimate of experimental results. With increasing load, the predicted results by Eq 6.3.4 become increasingly smaller than obtained experimentally. The proposed method however gave a good estimate until failure.

The graphs, Figs. 6.4.19–6.4.26 show that each method has its advantages. Relating the maximum crack widths to the steel strain, equations 6.4.2 and 6.4.3 via the average steel strain is better able to reflect observed cracking behaviour for those beams which fail in flexure by the yielding of the tensile reinforcement. This is because in the stress–strain relationship for steel, it is the strain which undergoes large changes in value upon yielding. Therefore methods which use the steel strain as a variable are are better able to reflect post–yield behaviour. Conversely, no sudden changes occur in the steel stress at yielding. Consequently, methods which contain the steel stress as a variable are unable to reflect post–yield behaviour. However, it is most unlikely that

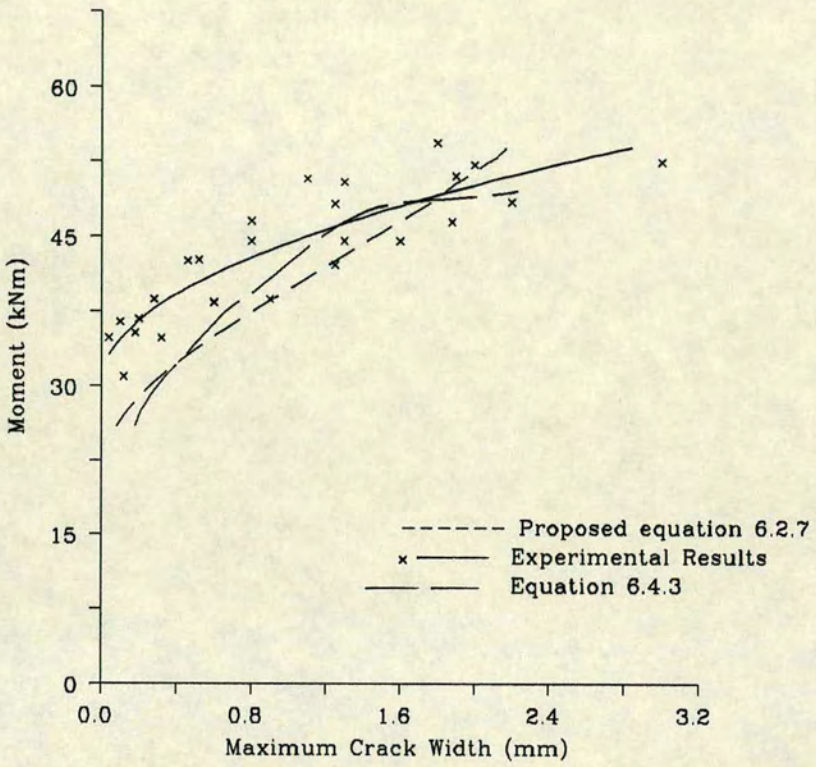

Fig. 6.4.23 Moment–Maximum Crack Width
Brickwork Beams, A_p=0.274%

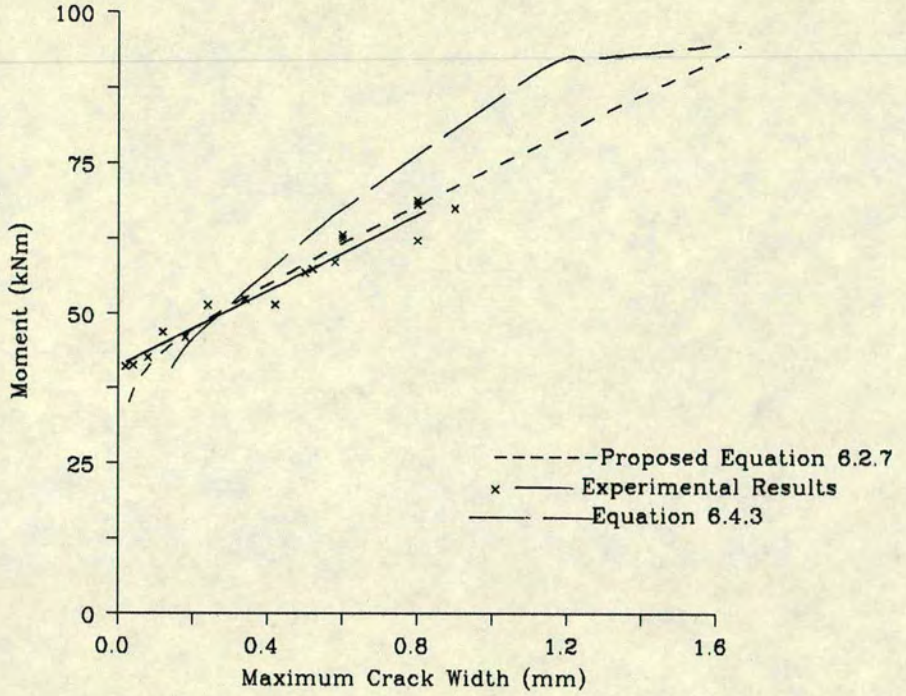

Fig. 6.4.24 Moment–Maximum Crack Width
Brickwork Beams, A_p=0.548%, P_e=208 kN

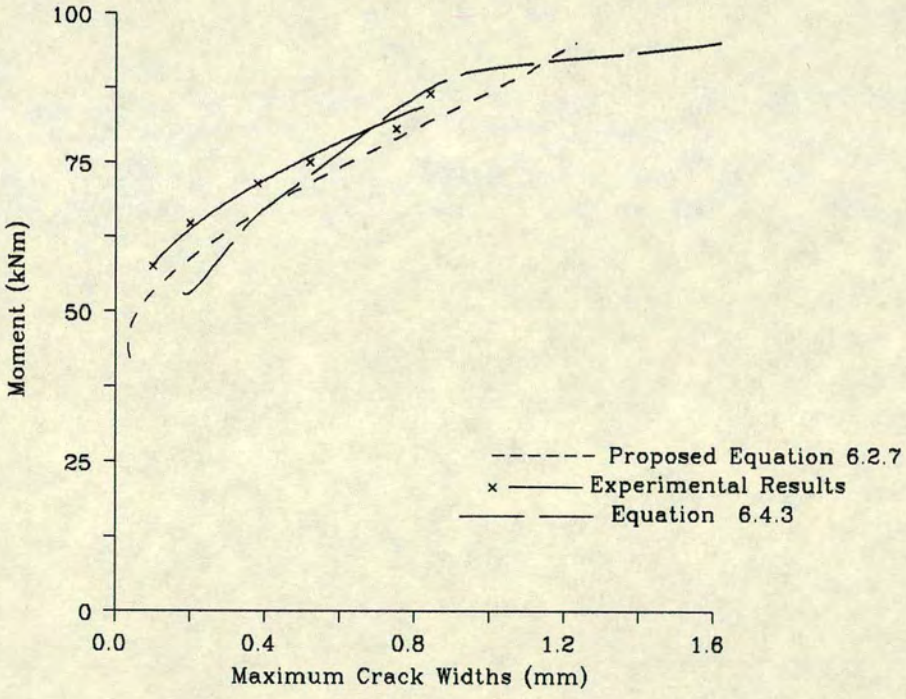

Fig. 6.4.25 Moment–Maximum Crack Width
Brickwork Beams, A_p=0.548%, P_e=275 kN

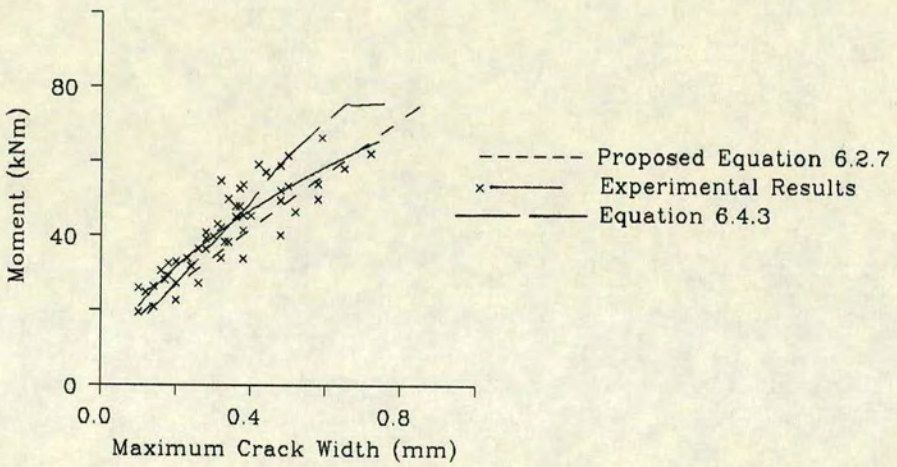

Fig. 6.4.26 Moment–Maximum Crack Width
Brickwork Beams, A_{ps}=0.341%

crack widths will be accurately required after the yielding of the steel.

Equations 6.4.2 and 6.4.3 depend on the accuracy of the prediction of the average crack widths (see Section 6.4.2) and are therefore subject to the same limitations. Also, the relationship between the maximum and average crack widths was derived from a statistical relationship obtained from experimental results. The statistical nature of these equations result in overestimates of the maximum crack width in most cases. Conversely, the Suri-Dilger equation for concrete and that proposed here are independent of statistical data. Within the service load limits in concrete considered to be of the order of 0.41 mm[75], these methods give an accurate reflection of cracking behaviour. The Suri-Dilger equation and that proposed herein for brickwork and equations 6.4.2 and 6.4.3 are all dependent on a cracked section analysis.

6.5 CLASSIFICATION OF PRESTRESSED BRICKWORK BEAMS

Prestressed concrete members are classified as class I, II or III[58]. On the other hand no classifications exist in prestressed brickwork. Using the same criteria for prestressed brickwork, the service load moments obtained for brickwork and concrete beams have been compared in the following sections:

1 Class I Members

In a class I member, no tension is allowed to develop under service load. Therefore, in brickwork and concrete beams containing the same effective prestress, the service loads should be the same.

In Table 6.5.1, the service load moments for similar prestressed brickwork and concrete class I beams are presented. The partially prestressed beams have been omitted as their definition excludes them from this class. In all cases, service load moments for the brickwork beams are practically identical to those for the concrete beams, the slight differences resulting from the differences in the effective prestressing force. In all cases, factors of safety based on the ultimate flexural moments of resistance, were well in excess of an assumed satisfactory value of 1.5. The highest factors of safety were obtained for the beams containing 0.548% area of tensioned reinforcement in

Table 6.5.1 Service Load Moments

% area of steel	P_e kN	M_{ult} kNm	Class I $M_{cl(1)}$	Class I $\frac{M_{ult}}{M_{cl(1)}}$	Class II $M_{cl(2)}$	Class II $\frac{M_{ult}}{M_{cl(2)}}$	Class III $M_{cl(3)}$	Class III $\frac{M_{ult}}{M_{cl(3)}}$	Defl. mm
Brickwork Beams									
0.274	135	54	16	3.38	24	2.25	29	1.86	3.5
0.548	275	95	34	2.88	41	2.32	58	1.64	15.0
0.548	208	95	25	3.80	33	2.88	46	2.07	15.5
0.341	62	103	–	–	–	–	30	3.43	1.95
Concrete Beams									
0.274	128	53	16	3.31	32	1.66	32	1.66	3.5
0.548	283	92	34	2.71	51	1.80	56	1.64	9.0
0.548	201	91	25	3.64	41	2.22	41	2.22	7.0
0.341	62	101	–	–	–	–	31	3.26	1.95

which some of the strands were not stressed to the allowable limit. These beams are also referred to as partially prestressed beams and will not normally be designed as Class I members. The lowest factors of safety were obtained in the beams containing the same area of steel but with the higher prestressing force.

The only differences which may arise between prestressed brickwork and concrete class I beams will be that the brickwork will have slightly more camber under the same effective prestress compared with concrete but this can be insignificant as was seen from the M–O relationships in Chapter 5 (Figs. 5.3.1–5.3.6) and can be an advantage at higher load levels.

2 Class II Members

In a class II member, tension is allowed to develop but no visible cracking is permitted under service loads. The service load moment of a class II member is thus limited by the magnitude of the tensile stress which can be sustained before cracking begins i.e the modulus of rupture. Its value in concrete is higher than in brickwork of comparable compressive strength. Consequently, the difference between the service load moments of a class I and a class II member in brickwork is smaller than in concrete.

The service load moments for class II brickwork and concrete beams are presented in Table 6.5.1. The higher moments obtained over class I members result in reduced factors of safety. The lower service load moments in the brickwork beams when compared to the concrete beams result in higher factors of safety. The beams with the highest factors of safety were those containing 0.548% area of tensioned steel in which not all the tendons were stressed to the maximum limit. The partially prestressed beams are also excluded from this class.

3 Class III Members

In a class III member, cracking is allowed up to a maximum crack width of 0.2 mm. The service load moment thus depends on the rate of increase in crack widths after cracking. The service load moments obtained for class III members are also given in Table 6.5.1. The maximum crack widths were

obtained from the Suri-Dilger equation (equation 6.2.6) for the concrete beams and from the proposed method in brickwork, equation 6.2.7.

In concrete, the differences between the service load moment for classes II and III members were either very small or non-existent. This is due to the rapid widening of cracks as seen in Fig. 6.4.5b-6.4.7b. In the concrete beams containing 0.274% area of steel, immediately after cracking, the crack widths were larger than 0.2 mm. The service load moments of the classes II and III beams were thus identical. The same also occurred in the beams with 0.548% area of steel with the lower prestressing force. In brickwork however, there is a marked increase in service load for all beams. An increase of 42.5% was obtained for the beam with the highest prestressing force compared with an increase of 10% in the similar concrete beam. The increased service load in the brickwork beams however result in reduced factors of safety. The partially prestressed beams containing a combination of strand and deformed bar had very high factors of safety, much higher than is usually required in design. The factors of safety in both materials were however similar.

Also presented in Table 6.5.1 are the deflections at a crack width of 0.2 mm. In all cases, these were less than span/360.

6.6 CONCLUSION

The flexural cracking behaviour of prestressed beams of brickwork and concrete of similar cross-sectional properties and of similar compressive strengths have been compared. The following conclusions can be drawn:

1. Once the cracking moment has been exceeded in the beams containing tensioned reinforcement only, the crack widths and the rate of increase in the width of cracks with load increment is larger in concrete when compared to brickwork.

2. In the prestressed beams containing tensioned reinforcement only, the spacing between cracks were larger in the concrete beam than in a similar brickwork beam. In brickwork, cracks form at the brick/mortar interface which is largely dictated by the bond pattern.

3. In the prestressed beams containing tensioned and non-tensioned reinforcement, the crack spacing, crack widths and the rate of increase in the crack widths with load increment were similar in the brickwork and concrete beams.

4. The maximum crack widths in prestressed brickwork beams can be accurately estimated using the method proposed in this work.

5. The average crack spacing in prestressed concrete beams can be obtained from the equation proposed in this work. In the case of prestressed brickwork, the method proposed by Walker[12] gave accurate results.

6. The classification of prestressed brickwork beams can be based on limiting the tensile stresses under service loads as is currently done for concrete[58].

CHAPTER 7
THE SHEAR STRENGTH OF PRESTRESSED BEAMS

7.1 INTRODUCTION

In the previous chapters, (4, 5 and 6), it has been shown that the behaviour of prestressed brickwork and concrete beams with identical cross-sectional properties and of similar compressive strength which fail in flexure are very similar up to failure. However, when the brickwork beams, which have the lower shear strength, fail primarily in shear, the ultimate moment is less than in the concrete beams because of the lower shear strength of brickwork. As mentioned in the literature review, (Chapter 2), unlike in concrete beams, the introduction of shear reinforcement into a brickwork beam to increase the shear strength is not always straightforward and can lead to impracticable design details. This imposes a limitation on the structural performance of prestressed brickwork beams when compared with prestressed concrete beams as shear failures, which can occur at a lower moment than the ultimate flexural moment of resistance, can be sudden, brittle and devastating. Hence there is a need for rational methods of predicting the shear strength in general and of brickwork beams in particular.

The shear strength of concrete beams has received a lot of attention particularly in the last three decades. Various theories have been developed for predicting the shear strength of reinforced and prestressed concrete beams. Because of the many variables which have been found to affect the shear strength, a large number of these theories are empirical and were obtained from a correlation with specific test results. More recently however, the plastic theory[88,89] and the 'concept of the compressive force path'[90,91,92,93,94] have been developed to predict the shear strength of reinforced and prestressed concrete beams. Compared to concrete, little attention has been given to the shear strength of brickwork beams. This is probably due to the added complication of the presence of mortar joints which act as planes of weakness. Shear strength theories on brickwork beams have so far been empirical but for the application of the plastic theory[11]. The main disadvantage of the plastic theory when applied to prestressed brickwork is its dependence on an

effectiveness factor which was introduced to compensate for the fact that brickwork is not a plastic material as assumed in the plastic theory. The effectiveness factor is obtained from experimental results on beams which failed in shear. For this reason, the possibility of applying the concept of the compressive force path to prestressed brickwork beams is investigated in this chapter. The theoretical study also included a finite element analysis of prestressed brickwork beams in order to determine the magnitude of the principal tensile stress at failure.

In the literature review (Chapter 2), it was mentioned that experimental studies on the shear strength of prestressed brickwork has so far concentrated on fully prestressed beams. No experimental work has been carried out with the specific aim of studying the shear strength of partially prestressed brickwork beams. To this aim, an experimental program was carried out in which sixteen partially prestressed brickwork beams containing tensioned and non-tensioned tensile reinforcement were studied. The variable considered was the shear span to effective depth ratio between 1.5 and 6.0. The ultimate moment and failure modes of these beams were given in Chapter 4. In this chapter, experimental results pertaining to the shear strength are presented. A comparison is made with theoretical results and with other experimental results on fully prestressed brickwork beams. Four partially prestressed concrete beams with shear span to effective depth ratios of 1.5 and 3.0 were also tested for comparison with similar brickwork beams.

7.2 FACTORS WHICH AFFECT THE SHEAR STRENGTH

A large number of variables have been found to affect the shear strength. A detailed description of these variables is given elsewhere[95]. The most important variables are the shear span to effective depth ratio (a/d) (or the moment to shear depth ratio (M/V.d)), the area of tensile reinforcement and the compressive strength in the case of concrete beams.

7.2.1 The Effect of the Shear Span to Effective Depth Ratio on the Shear Strength

The most important variable which has been found to affect the shear

strength of brickwork and concrete beams is the shear span to effective depth ratio (a/d) or in the case of non-rectangular sections, the moment to shear depth ratio (M/V.d). For a constant cross-section and area of tensile reinforcement, the shear strength increases with decreasing shear span to effective depth ratio.

By relating the flexural capacity of a beam and the mode of failure to the shear span to effective ratio, four types of behaviour have been identified in concrete beams of which three have also been reported in prestressed brickwork beams:

1. Flexural failure - This type of failure was fully discussed in Chapter 4. The shear span to effective depth ratio above which this type of failure occurs in brickwork and concrete beams is dependent on the area of steel. In concrete, this type of failure is generally associated with a value in excess of 5.0[95,96,97]. In prestressed brickwork beams, no value has been suggested. In reinforced brickwork however, this value is around 5.0[7].

2. Diagonal tension failure - This type of failure is characterised by an inclined crack in the shear span which forms as an extension to the flexural crack nearest the support. This crack gradually bends over and travels towards the load point. There may also be a horizontal propagation along the level of the tensile reinforcement towards the support. Beams which fail in diagonal tension exhibit a reduction in flexural capacity with decreasing shear span to effective depth ratio. Prestressed brickwork beams also exhibit diagonal tension failure[11].

3. Shear compression failure - The inclined cracks which develop in the shear span of these beams are independent of flexural cracks. The flexural moment capacity increases from the critical value of diagonal tension failure with decreasing shear span to effective depth ratio up to the full flexural moment capacity. The limiting shear span to effective depth ratio below which the full flexural capacity is attained or exceeded is also dependent on the area of steel. However, the critical shear span to effective depth ratio which demarks the transition from diagonal tension failure to shear compression failure is independent of the area of steel and has been given a value in concrete beams of around

2.5[95,96,97,98,99,100]. In beams which fail in shear compression, the appearance of the inclined crack transforms the beams into a 'tied arch' and may be capable of sustaining more load before failure. In brickwork, at low shear span to effective depth ratios, the formation of an inclined crack also transforms a beam into a 'tied arch' and such a beam may have residual strength before failure. Although researchers in reinforced brickwork[7,8,101] have also observed an increase in the flexural moment capacity when the shear span to effective depth ratio is decreased below a value of between 2.0 and 3.0 evidence of this is not conclusive in prestressed brickwork beams.

4. Deep beam failure – Failure of a deep beam is characterised by an inclined crack joining the support to the load point. Flexural cracking may or may not be present in the shear span. After inclined cracking, in the absence of web reinforcement, this type of beam is transformed into a 'tied arch' which may fail in a number of ways:

    a. Anchorage failure of the tension reinforcement which is usually combined with dowel splitting effect.

    b. Crushing failure at the reactions

    c. Flexural failure either of the tension reinforcement due to yielding or fracture, or of the 'crown of the arch' where the concrete crushes

    d. Tension failure of the 'arch rib' by cracking over the support; followed by

    e. Crushing along the crack.

    In a directly loaded deep beam, the full flexural capacity is surpassed. The critical shear span to effective depth ratio at which this type of behaviour occurs is dependent on the area of steel. Although no single shear span to effective depth ratio has been specified to represent the transition from shear compression to deep beam failure, a value of 1.0[95,100] is commonly assigned. Kani[96] from experimental evidence suggested a value of 1.5. Although some reinforced[8] and prestressed[11] brickwork beams have failed in shear along a line joining the support and

the load points, there is no evidence of deep beam failure in these beams as the ultimate moments were less than the flexural moment capacity.

7.2.2 The Percentage Area of Tensile Reinforcement

The second most important variable which has been found to affect the shear strength of concrete beams is the percentage area of steel. An increase in the percentage area of steel increases the shear strength of a concrete beam. This has not been found to be the case in prestressed or reinforced brickwork beams except in grouted cavity reinforced brickwork beams[102].

Increasing the percentage area of steel in reinforced and prestressed concrete beams increases the shear span to effective depth ratio which demarks the transition from diagonal tension to flexural failure. The shear span to effective depth ratio which seperates shear compression failures from deep beam failure in concrete beams is reduced when the percentage area of steel is increased. Insufficient experimental evidence exists on the effect of the percentage area of steel in prestressed brickwork beams on the mode of shear failure. However, in reinforced brickwork like reinforced and prestressed concrete, an increase in the area of steel increases the shear span to effective depth ratio which demarks the transition from diagonal tension to flexural tension failures. Also, at shear span to effective depth ratios less than 2.0, the ratio of the ultimate moment due to shear failure to the ultimate flexural moment in a reinforced brickwork beam increases with decreasing area of steel.

7.2.3 The Compressive Strength

The shear strength of reinforced and prestressed concrete beams increases with the compressive strength. This has not been found to be the case in brickwork beams[102].

7.3 THEORY

7.3.1 Existing Methods for Predicting the Shear Strength

The following methods are among those which have so far been used to predict the shear strength of prestressed concrete beams:

- The Principal Tensile Stress Theory

- The Plastic Theory

- The Concept of the Compressive Force Path

The method which shall be proposed for the prediction of the shear strength of prestressed brickwork beams in this work is based on the 'concept of the compressive force path' and will be presented in Section 7.3.2. In this section, the principal tensile stress theory and the plastic theory will be outlined and their limitations highlighted.

7.3.1.1 The Principal Tensile Stress Theory

Shear failure is always preceeded by an inclined crack in the shear span. In the principal tensile stress method, it is assumed that inclined cracking will occur when the principal tensile stress exceeds a specified value - the tensile strength of concrete/brickwork. The principal tensile (and compressive) stresses are produced by shear stresses.

As mentioned in Section 7.2 an inclined crack can form before flexural cracking occurs - a web-shear crack or after flexural cracking - a flexure-shear crack. Although some beams may have residual strength after inclined cracking, in beams without shear reinforcement, this is not reliable and the inclined cracking load is usually considered to be the practical ultimate load for such beams.

Web-Shear Cracks

As the beam is uncracked before the formation of a web-shear crack, the principal tensile stress computation can be based on elastic theory. The

inclined cracking load can be obtained using the Mohr's Failure Theory[95] for concrete/brickwork subjected to combined shear and normal stresses.

From a Mohr's circle, it can be shown that the shear stress, v_{cw}, which corresponds to reaching the tensile strength of concrete, f_t, at the neutral axis of a beam with an axial stress f_{pc} is given by:

$$v_{cw} = f_t (1 + f_{pc}/f_t)^{0.5} + V_p/b_w \; t \text{ (psi)}$$

... 7.3.1

where
V_p = the vertical component of the prestressing force in beams with curved tendons
b_w = the width of the web

Equation 7.3.1 has been approximated to a straight line by the ACI code given as:

$$v_{cw} = 3.5 (f'_c)^{0.5} + 0.3 f_{pc} + V_p/b_w \; d \text{ (in psi)}$$

... 7.3.2

f'_c = the compressive strength of concrete obtained from cylinders

The above approach is also adopted in the British Code of Practice for Concrete BS 8110[58] Section 4.3.8.4 and for a beam with straight tendons, the design ultimate shear resistance of a section uncracked in flexure given by:

$$V_{co} = 0.67 \; b_v \; h \; (f_t^2 + 0.8 \; f_{cp} \; f_t)^{0.5} \text{ (in N/mm}^2\text{)}$$

... 7.3.3

where
b_v = breadth of member, or for T-, I- and L-beams, the breadth of the rib
h = height of the beam
f_t = maximum design principal tensile stress
f_{cp} = design compressive stress at the centriodal axis due to prestress, taken as positive
V_{co} = design ultimate shear resistance of a section uncracked in flexure

This approach has been suggested by Roumani and Phipps[23,24] for unbonded prestressed brickwork beams.

Flexure-Shear Cracks

As the beam is already cracked in flexure before the formation of the inclined crack, the method of analysis employed for web-shear cracking is not

applicable. The mechanism by which a flexure-shear crack forms is not fully understood and although the concept of the concrete cantilever[96,100] has been used to idealise the mechansim of flexure-shear cracks, the load corresponding to the formation of a flexure-shear is estimated by semi-rational expressions.

In a prestressed concrete beam, for flexure-shear cracking, the inclined cracking load has been expressed in terms of the shear necessary to cause a flexural crack at a point located d/2 to d towards the reaction (d being the effective depth) from the section under consideration, plus an increment of shear necessary for this flexural crack to develop into an inclined crack. The ACI code expression for the flexure-shear cracking load in a prestressed concrete beam is given[95] as:

$$V_{ci} = M_{cr}/(M/V - d/2) + 0.6(f'_c)^{0.5}\, b_w\, d \text{ (psi)}$$

... 7.3.4

The first term represents the shear necessary to cause the initiating flexural crack and the second term expresses the additional increment in shear necessary to convert the flexural crack to an inclined crack. The external moment necessary to cause cracking at the point under consideration is M_{cr}.

The above approach has also been adopted in BS 8110[58] for prestressed concrete containing flexure-shear cracks. The equation is given by:

$$V_{cr} = (1 - 0.55\, f_{pe}/f_{pu})\, v_c\, b_v\, d + M_o\, V/M$$

... 7.3.5

M_o = moment necessary to produce zero shear stress in the concrete at the extreme tension fibre (in this calculation only 0.8 of the stress due to prestress is taken into account)
V,M = are the design shear force and bending moment values at the section due to the particular ultimate load condition
f_{pe} = design effective prestress in the tendons after all losses have occurred, which should not be taken as greater than 0.6 f_{pu}.

Roumani and Phipps[24] have suggested an expression for the inclined cracking load of unbonded prestressed brickwork beams already cracked in flexure. This expression is however based on a Mohr's circle which as previously mentioned is only applicable to an uncracked beam.

To the author's knowledge, the principal tensile stress theory has not been applied to bonded prestressed brickwork beams. There are two main

reasons for this:

1. The limiting principal tensile stress - the principle tensile stress in brickwork is dependent not only on the magnitude of the principal compressive stress but also on the orientation of the bed joints and it is thus difficult to specify a limiting value. This value has been found to increase with shear span to effective depth ratio[23,24] and the overall depth of the beam[24].

2. The difficulty in calculating the principal tensile stress in a cracked member, (as a brickwork member is usually cracked in flexure before diagonal cracking) with the added complication of the presence of mortar joints.

In order to investigate the magnitude of the principal tensile stress at failure in the partially prestressed brickwork beams tested in this work, a non-linear finite element analysis was carried out using a finite element package **Lusas** as described below. The results are presented in Section 7.4.

7.3.1.2 Finite Element Analysis

A finite element analysis was carried out in order to estimate the magnitude of the principal tensile stresses of flexurally cracked partially prestressed brickwork beams at shear failure. Although several finite element programs have been written for masonry, these have been developed for specific purposes and are therefore narrow in their applications. For example, the program developed by Dhanasekar[103] does not account for geometric nonlinearity. In the partially prestressed brickwork beams tested in this work, the deformations were quite significant so that geometric nonlinearity needed to be accounted for. Other authors have included Page[104] and Samarasinghe[105] for unreinforced masonry walls/panels subjected to in-plane loading. In this work, the finite element analysis has been carried out using a general purpose package, Lusas. Among the facilities available in Lusas include nonlinear material models, geometric non-linearity and graphic output. A comprehensive description of Lusas and the non-linear iterative procedure incorporated therein can be found elsewhere[106,107]. In this section, a brief description of the constitutive material models used for brickwork and steel are

presented.

Brickwork

Brickwork has been modelled as a homogeneous material. The non-linear material model (material model 24 in Lusas) developed for concrete was used to model the behaviour of brickwork. A comprehensive description of this material model can be found elsewhere[107].

The constitutive model is able to represent the non-linear loss of stiffness associated with tensile and compressive failures. Failure is referred to a stress envelope formulated in terms of the principal stress components as shown in Fig. 7.3.1. The formation of tensile cracks in this model is represented by the smeared crack approach in which a single discrete crack is represented by a number of finely spaced or 'smeared cracks'. Cracking is assumed to occur when one or both of the principal stresses are in violation of the cracking criterion as defined by the tensile failure envelope. Two smeared crack planes are permitted. The crack plane(s) form in the direction(s) perpendicular to the principal stresses which cause it. The material represented by the cracked gauss point subsequently becomes orthotropic with local material axes being defined parallel and perpendicular to the crack direction. Once formed, the crack directions are assumed to remain fixed but may unload and reload following subsequent stress redistribution.

The gradual release of stress from the cracked material is modelled numerically using a strain softening or tension stiffening curve. This is implemented as a descending branch of the stress-strain relationship in tension as shown in Fig. 7.3.2. The transfer of the normal component of stress across a crack is reduced gradually via the strain softening curve.

The continued ability of a cracked beam to transfer shear stress across the surfaces of a crack is described in the model by multiplying the shear modulus of the uncracked section by a factor α (where α is between 0.0 and 1.0). This factor is known as the shear retention factor and is usually assumed to be constant.

Steel

The deformational responses of the tensile reinforcement was represented

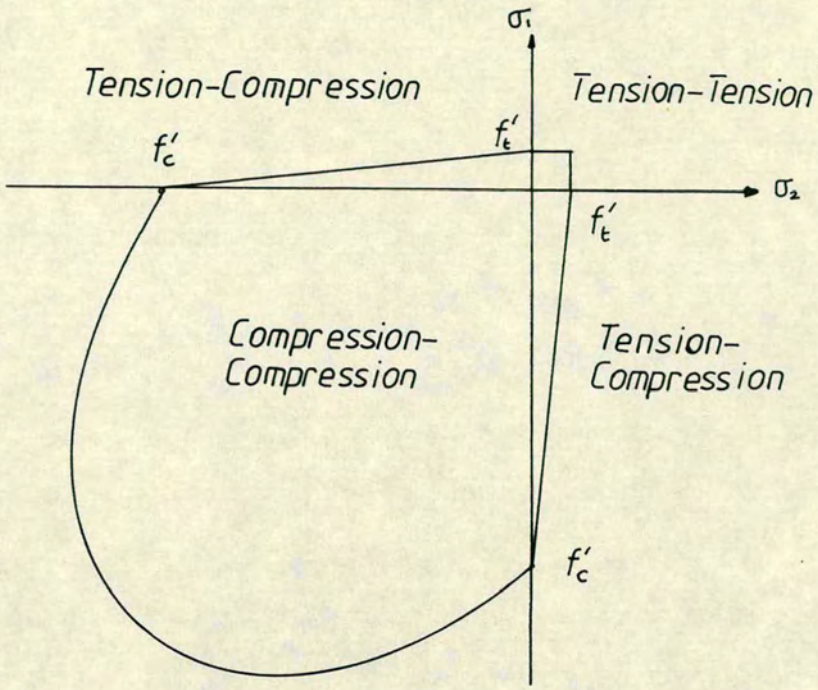

Fig. 7.3.1 Failure Envelope for Concrete

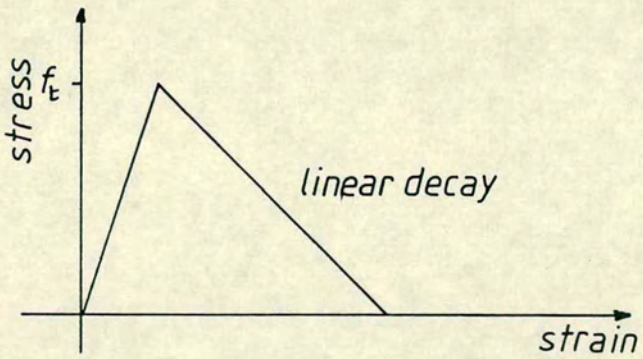

Fig. 7.3.2 Strain Softening Curve

by the tri-linear stress-strain relationships shown in Chapter 3.

7.3.1.3 The Plastic Theory

The plastic theory has been used to predict the shear strength of reinforced and prestressed concrete beams with and without shear reinforcement[88,89] and also, fully prestressed and reinforced brickwork beams without shear reinforcement[11]. A full treatment of the plastic theory and its applications to reinforced and prestressed concrete can be found elsewhere[88]. In this section, the application of the plastic theory to brickwork and concrete beams without shear reinforcement is outlined.

Assumptions

A beam is assumed to be made up of compression and tension stringers which behave in a rigid-perfectly plastic manner. The brickwork/concrete in the web is also assumed to be rigid-perfectly plastic with yielding controlled by a modified Coloumb yield criterion in which the tensile strength is assumed to be zero (see Fig. 7.3.3). In brickwork, this assumption was made possible by the results of biaxial tests on masonry panels carried out by Page[104] which showed that a rectangular surface could be approximated under biaxial compression-compression which is not significantly affected by the orientation of the principal stresses to the bed joint (see Fig. 7.3.3b).

To account for the lack of ductility in brickwork and concrete as assumed in the theory, the compressive strength is multiplied by an effectiveness factor ν which has a value between 0.0 and 1.0.

The Upper Bound Solution

An upper bound solution is obtained by assuming a failure mechanism and equating the rates of external and internal work. The failure mechanism assumed[88,11] for beams without shear reinforcement and subjected to concentrated loading is shown in Fig. 7.3.4.

The lowest upper bound equations (in the case of brickwork beams) are as follows:

$$\tau/f_m = \nu/2[((a/h)^2 + 4\Phi(\nu - \Phi)/\nu^2)^{0.5} - a/h]$$

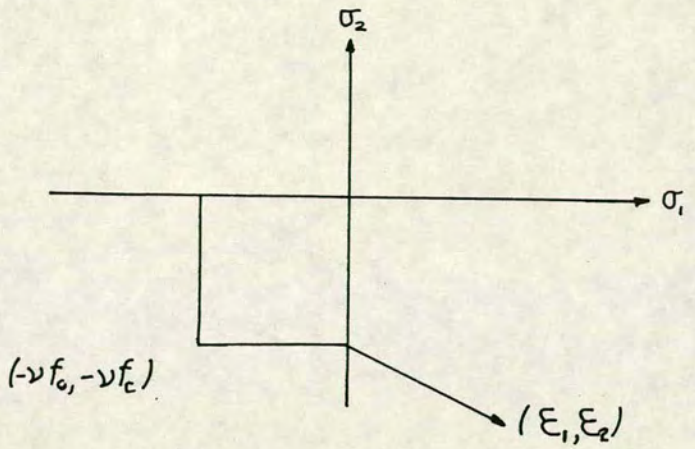

Fig. 7.3.3a Yield Locus for Concrete

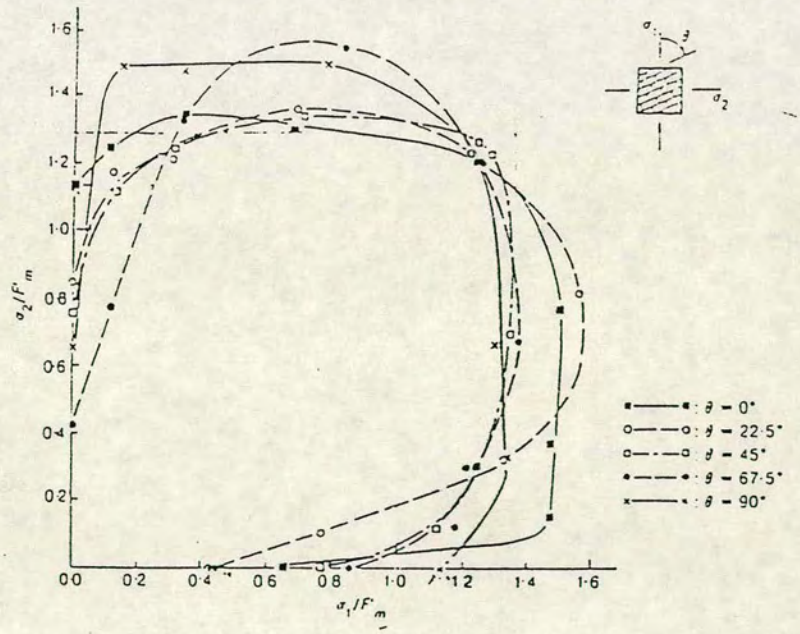

Fig. 7.3.3b Failure Surface for Masonry Under Biaxial Compression - Compression (After Page[104])

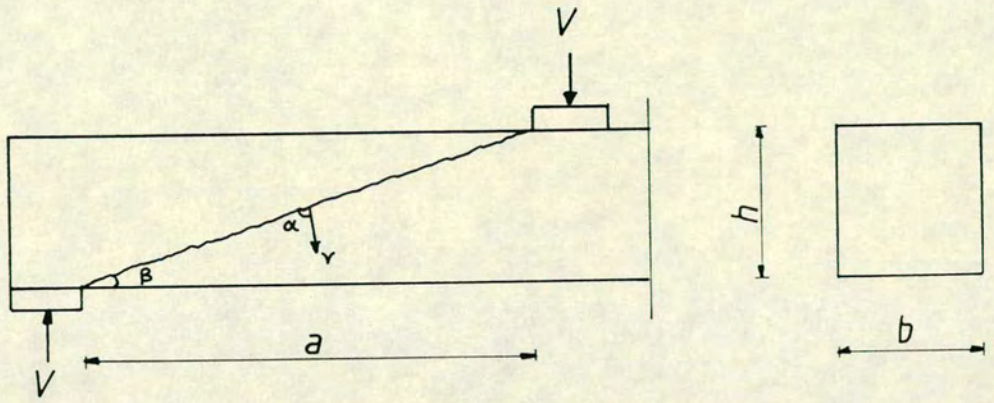

Fig 7.3.4 Assumed Failure Mechanism for an Upper-Bound Solution

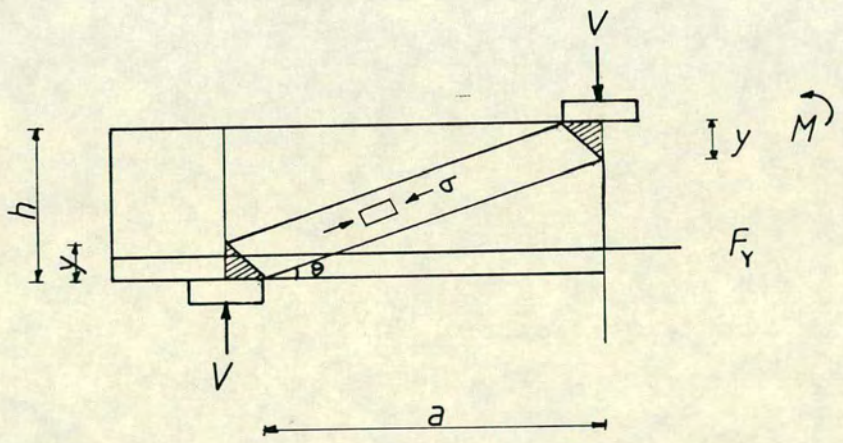

Fig. 7.3.5 Stress Distribution in the Shear Span Subject to Concentrated Loading (Lower-Bound Solution)

... 7.3.6a

valid for $\Phi < \nu/2$

and

$$\tau/f_m = \nu/2[((a/h)^2 + 1)^{0.5} - a/h]$$

... 7.3.6b

valid for $\Phi > \nu/2$

τ and Φ are the shear strength and the reinforcement index respectively and are defined as follows:

$$\tau = V/b.h$$

... 7.3.7

$$\Phi = F_y/b.h.f_m$$

... 7.3.8

where
f_m = compressive strength of brickwork obtained from single course prisms
ν = effectiveness factor
a = shear span (measured from the centre of the support to the centre of the load point)
h = height of the beam

Lower Bound Solution

The lower bound solution is obtained by assuming a statically admissible stress distribution and calculating the corresponding load. The assumed stress distribution is shown in Fig. 7.3.5.

The highest lower bound solution is the same as the lowest upper bound solution (equation 7.3.6), therefore, the exact plastic solution is obtained.

The Effectiveness Factor ν

For brickwork beams, the web effectiveness factor is obtained by making ν the subject of the formula in Equation 7.3.6a i.e

$$\nu = [(\tau/f_m)^2 + \Phi^2]/[(\Phi - a/h \,.\, \tau/f_m)]$$

... 7.3.9

ν is obtained from beam test results at ultimate when failure is in shear and this constitutes a major disadvantage of the application of the plastic theory to brickwork beams.

The effectiveness factor in concrete beams is also obtained from a correlation with test data but in this case, the volume of data available enabled a statistical analysis to be carried out which identified the variables which influence the effectiveness factor and produced relationships between these variables and the effectiveness factor.

The effectiveness factor in a partially prestressed concrete beam is given by the following empirical formula:

$$\nu = f_1(\sigma_c)\ f_2(h)\ f_3(\rho)\ f_4(a/h)\ f_5(\sigma_{eff}/\sigma_{0.2})$$

... 7.3.10

where f_1, f_2, ... are functions of the variables indicated and are given by:

$$f_1(\sigma_c) = 3.5/(\sigma^{0.5}) \quad (5 < \sigma_c < 60)\ (N/mm^2)$$

$$f_2(h) = 0.27(1 + 1/h^{0.5}) \quad (0.08 < h < 0.7) \quad (h \text{ in } m)$$

$$f_3(\rho) = 0.15\ \rho + 0.58 \quad (\rho < 4.5\%) \quad (\rho \text{ in } \%)$$

$$f_4(a/h) = 1.0 + 0.17(a/h - 2.6)^2 \quad (a/h < 5.5)$$

$$f_5(\sigma_{eff}/\sigma_{0.2}) = 1.1[1.0 + 0.81(\sigma_{eff}/\sigma_{0.2})]$$

... 7.3.11

σ_{eff} is the effective prestress and $\sigma_{0.2}$ is the 0.2% stress of the prestressing reinforcement. σ_c is the compressive strength of concrete and ρ is the percentage area of tensile reinforcement.

$f_4(a/h)$ is a variable which is only active in a reinforced concrete beam and obviously, $f_5(\sigma_{eff}/\sigma_{0.2})$ is absent in such a beam.

7.3.2 Proposed Method for Prestressed Brickwork Beams: Compressive Force Path Method

The proposed method for predicting the shear strength of a prestressed brickwork beam is based on the concept of the compressive force path previously developed for concrete[90,91,92,93,94]. This concept has resulted in a comprehensive description of the causes and mechanisms of the various

modes of shear failure in concrete beams. It has been verified experimentally[93] and by finite element analysis[91,92]. This concept is also compatible with other published experimental results[90,91,92,93,94]. These factors encouraged its application to the prestressed brickwork beams reported in this work.

The fundamental principle which underlies the 'compressive force path concept' is that the various modes of shear failure observed in reinforced and prestressed concrete are associated with the multiaxial stress conditions which exists in the region of the path along which the compressive force is transferred from support to support. In Section 7.2, it was seen that shear failure is always characterised by an inclined crack in the shear span. The path along which the compressive force is transferred is obtained from the shape of the inclined crack. It was also stated in Section 7.2 that only the diagonal tension failure and 'tied arch' failure have been observed in prestressed brickwork beams. In this section therefore, the concept of the compressive force path is applied to prestressed brickwork beams which fail in diagonal tension and as a tied arch (shear compression). The resulting equations for concrete beams failing in diagonal tension, shear compression and deep beam failure will be presented in Section 7.3.3. A full description of the compressive force path concept for concrete beams can be found elsewhere[90,91,92,93,94].

7.3.2.1 Diagonal Tension Failure in Prestressed Brickwork Beams

The shape of the inclined crack which characterises diagonal tension failure is curved and made up of two near-linear portions at an angle joined together by a smooth curve (see Fig. 7.3.6). For equilibrium, this change in direction of the compressive force indicated by the near-linear portions generates a tensile force T_1 in Fig. 7.3.7, in the region of the curved connection, bisecting the obtuse angle formed by the near-linear portions. This tensile force imposes a limit on the magnitude of the compressive force which can be transmitted along the path. The resulting compression-tension region may also be affected by the predominantly tensile force field which exists at the tip of the flexural crack closest to the support (T_2 in Fig. 7.3.7). When the capacity of the region to sustain the combined stress field is exceeded, an inclined crack appears leading to complete collapse.

It has been shown that the stress conditions in the shear span and the

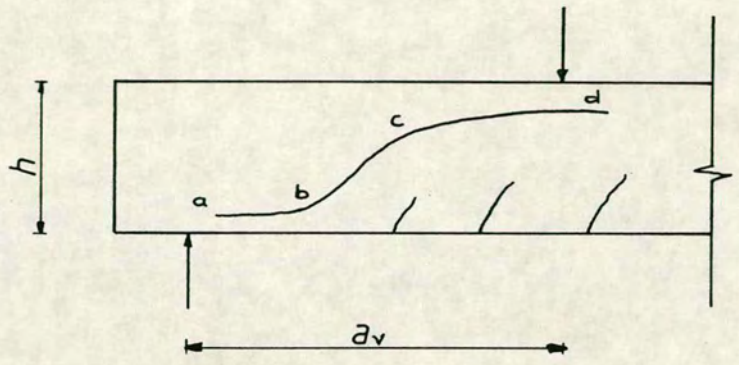

Fig. 7.3.6 Shape of the Inclined Crack Characterising Diagonal Tension Failure

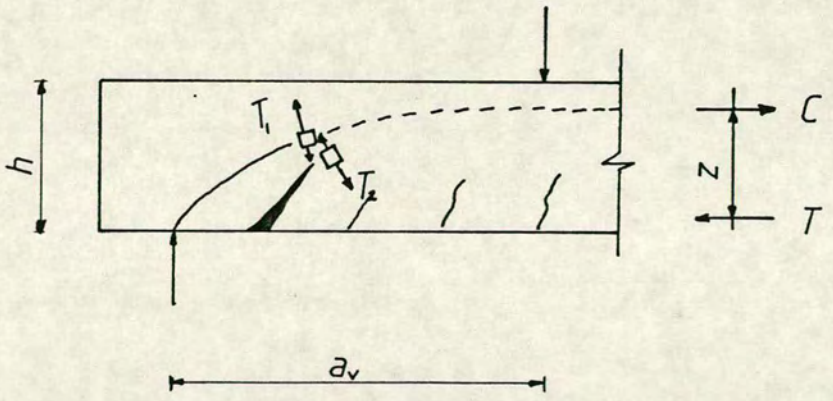

Fig. 7.3.7 Compressive Force Path in a Beam which Fails in Diagonal Tension

internal actions C and T (in Fig. 7.3.7) which cause them are independent of the shear span to effective depth ratio[90]. Therefore, it can be considered that the internal condition for diagonal tension failure is reached when the shear force attains a critical value V_{cr} independent of the shear span to effective depth ratio, a_v/d. The flexural capacity of a beam is therefore given by:

$$M_{cr} = V_{cr}.a_v \qquad \ldots 7.3.12$$

When a_v increases to a value a_{vf} dependent on the percentage area of steel ρ_s (= $A_{se}/b.d_e$), M_{cr} becomes equal to the full flexural capacity M_f. Equation 7.3.12 becomes:

$$M_f = V_{cr}\ a_{vf} \qquad \ldots 7.3.13$$

Eliminating V_{cr} from equations 7.3.12 and 7.3.13 and normalising a_v and a_{vf} by d_e gives:

$$M_{cr}/M_f = (a_v/d_e)/(a_{vf}/d_e) \qquad \ldots 7.3.14$$

Also from equation 7.3.13,

$$a_{vf} = M_f/V_{cr} = A_{se}\ f_{se}\ z/V_{cr} \qquad \ldots 7.3.15$$

Where
f_{se} = stress in the effective area of tensile steel
A_{se} = effective area of tensile steel
z = lever arm of internal forces acting on a cross-section within the 'flexure' span (see Fig. 7.3.7)

From equation 7.3.15, a reduction in the area of steel corresponds to a reduction in not only the ultimate flexural moment, M_f but also a_{vf}, the shear span to effective depth ratio which demarks flexural from diagonal tension failure. As will be seen in Section 7.4, this is compatible with experimental results on prestressed brickwork beams.

The above is a qualitative analysis. In order to obtain the shear strength from this concept for brickwork beams, the use of some additional information is required:

A common feature of reinforced and prestressed brickwork beams which fail in shear[7,11,12,20,29] is horizontal splitting along the top bed joint. This splitting is akin to that of a three course prism tested in axial compression (see Chapter 3). Further, under four point loading, this horizontal splitting progresses into the constant moment region after which the beam fails in shear. We know that the constant moment region is essentially under uniaxial compression[90] (the same as in the three course prism). Therefore, the condition for splitting in the constant moment region is given by the splitting strain in a three course prism. As will be seen in Section 7.4, this is verified from experimental results. Knowledge of the splitting strain and the location of the top bed joint can be used to obtain the shear strength of a brickwork beam as described below.

The conditions which cause horizontal splitting in the top bed joint is independent of the shear span to effective depth ratio and is therefore compatible with the compressive force path concept for diagonal tension failure (from above).

Procedure for Calculating the Shear Strength of Prestressed Brickwork Beams

- Let the splitting strain = ε_j and the distance from the top of the beam to the top bed joint = d_j

- Bed joint splitting will occur when

$$\varepsilon_{ms} = \varepsilon_j[n/(n - d_j)] \qquad \text{... 7.3.16}$$

where
ε_{ms} = top fibre strain at shear failure

and assuming a value for the neutral axis depth, n.

- From ε_{ms}, the compressive stress at the top fibre f_f can be obtained from the stress-strain relationship of brickwork, and hence the total compressive force

- Hereafter, the procedure is the same as for the ultimate flexural strength calculation i.e the object is to balance the compressive and tensile forces

- When this has been achieved, the ultimate moment in shear is given by

$$M_v = F_p(d_p - \lambda_2.n) + F_s(d_s - \lambda_2.n)$$

... 7.3.17

- The corresponding shear strength is given by:

$$\tau = M_v/a_v.b.d_e$$

... 7.3.18

For a beam which will not fail in shear, it is impossible to balance the total tensile and compressive forces when the top bed joint strain is given a value of ε_j as this value is incompatible with the crushing strain being attained at the top fibre. The value of ε_j is discussed in Section 7.4.

7.3.2.2 Shear Compression or Tied Arch Failure in Brickwork

Before inclined cracking, the shear span in a member which fails in shear compression is subject to combined bending and shear and the path along which the compressive force is transmitted to the support is similar to that in members which exhibit diagonal tension failure (see Fig. 7.3.8a), i.e it is curved and for equilibrium gives rise to tensile stresses developing across. When the strength of this region under the compression-tension stress field becomes critical, an inclined crack forms. The formation of the inclined crack may be coincident with failure. Otherwise, the presence of the inclined crack may cause a stress redistribution which results in a new near-linear force path running from the support to the load point (see Fig. 7.3.8b).

It has been suggested[90] that the distribution of compressive stresses across the path is such that with increasing load, the stresses in the region of the load point are the first to increase to a level close to the compressive strength. Under this stress level, the expansion of this region across the compressive force path is significantly larger than that of the adjacent regions and as a result, it is restrained by the surrounding brickwork. Such a restraint causes a triaxial compressive state of stress which may increase the load carrying capacity of the region. Therefore, under increasing load, it is unlikely that the diagonal crack will propagate through this region of triaxial

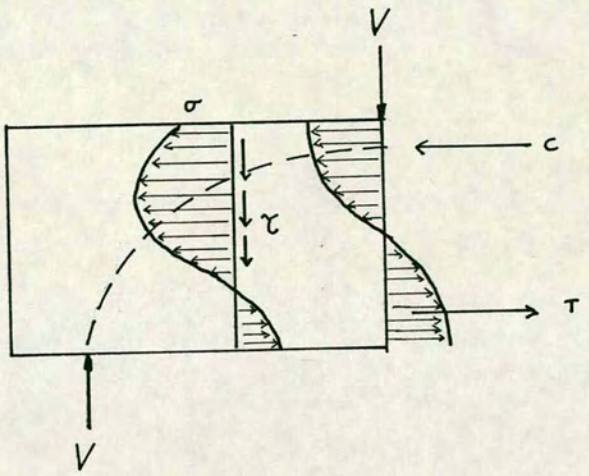

(a) Before Inclined Cracking

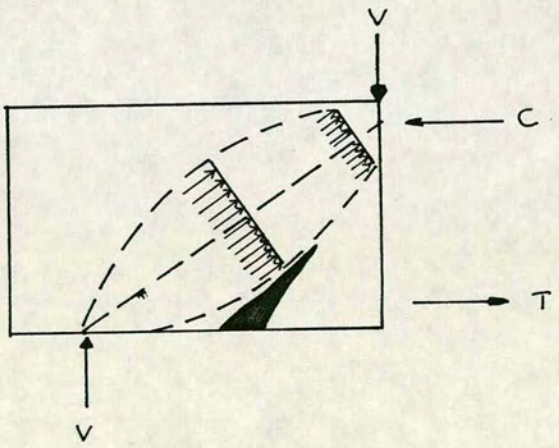

(b) After Inclined Cracking

Fig. 7.3.8 Stress Conditions in the Shear Span of Members which Fail in Shear Compression

compression. Rather, in order to avoid this region, the cracks should branch out horizontally towards the compression zone of the middle span which is essentially under uniaxial compression. Therefore, a brickwork beam which fails in shear compression will also exhibit bed joint splitting in the constant moment region.

In such a member, the slope of the diagonal crack to the horizontal axis of the beam will increase with decreasing shear span to effective depth ratio. Also, it can be proved theoretically that for a given load, an increase in the slope of the diagonal crack causes a decrease in the tensile force near the tip of the crack[90]. A higher compressive force will therefore be required for crack branching. This is reflected in the increase in the flexural capacity with decreasing a/d ratio as observed in reinforced brickwork beams. However, these increases can be quite small and unreliable.

For a given beam geometry and area of longitudinal reinforcement, a simplified expression for the variation of the compressive force C with a_v/d may be given by:

$$C = C_o \, (a_{vo}/d_e)/a_v/d_e)$$

... 7.3.19

Where
C_o = value of C when brickwork developes its full uniaxial compressive strength
a_{vo} = value of a_v at which $C = C_o$

The flexural capacity of the beam is given by

$$M_c = C \, z = C_o \, z \, (a_{vo}/d_e)/a_v/d_e)$$

... 7.3.20

When a_v decreases to a_{vo}, then M_c increases to $M_o=C_oz_o$ where z_o is the lever arm corresponding to M_o. For an under-reinforced section, this is equal to the full flexural capacity $M_f = A_{se} \, f_{se} \, z_f$, z_f being the lever arm corresponding to M_f i.e

$$M_o = M_f = C_o \, z_f$$

... 7.3.21

Assuming that z, z_o, z_f are approximately equal, then equations 7.3.20 and 7.3.21 give:

$$M_c/M_f = (a_{vo}/d_e)/(a_v/d_e)$$

... 7.3.22

Although M_f increases with A_{se}, M_c is independent of A_{se} since as discussed earlier in this section, collapse of the beam is caused by failure of the brickwork in the compressive zone. As a result, M_c/M_f decreases with increasing A_{se}. As will be seen in Section 7.4, this trend is compatible with experimental results.

7.3.3 The Shear Strength of a Concrete Beam Obtained from the Concept of the Compressive Force Path

A comprehensive description of the compressive force path concept as applied to concrete beams failing in diagonal tension[90,91,93], shear compression[90,92] and deep beam failure[90,94] are given in the references indicated. In the following sections, the resulting equations will be presented.

7.3.3.1 Diagonal Tension Failure (Shear Span to Effective Depth Ratio > 2.5)

For concrete beams which fail in diagonal tension, it has been demonstrated[93] that the empirical formula proposed by Bobrowski et al[108] for sections under the influence of bending moment and shear is compatible with the concept of the compressive force path. This formula gives the ultimate shear strength and also the location of the critical section. It is as follows:

$$M_{cx} = 0.875\ a_{vx}\ d\ (0.342\ b_1 + 0.3\ M_{fx}/d^2(z/a_{vx})^{0.5}).$$
$$(16.66/\rho_w.f_y)^{0.25}$$

... 7.3.23

where
the subcripts x denotes a given cross-section at a distance x from the support
M_{cx} = moment capacity of the beam at a given section (combined flexure and shear) (Nmm)
M_{fx} = flexural capacity (Nmm)
a_{vx} = shear span defined as the ratio Max/Vax (mm)
Max,Vax = applied bending moment (Nmm) and shear force (N) respectively at a given section x
z = lever arm (mm)
d = effective depth (mm)
ρ_w = (area of tension steel (Ae))/(web area of concrete to effective depth (b_1d))

f_y = characteristic strength of tension steel (N/mm^2)
b_1 = effective width (mm) as defined in reference 109 (for a rectangular section)

The procedure for obtaining the ultimate moment in shear, M_{cx} and its location x is as follows:

1. Determine M_{fx} as shown in Chapter 4.

2. At various distances from the support along the shear span x, calculate M_{cx} from equation 7.3.23 and the corresponding V_{cx} ($=M_{cx}/x$). A curve of M_{cx} vs V_{cx} is then plotted giving the failure envelope (see Fig. 7.3.9)

3. Bending moment (M) and shear force (V) diagrams can be used to construct M-V diagrams describing the combinations of M and V which a beam under a given load is subject to along its span. The point of contact between the M-V and M_{cx}-V_{cx} envelopes when superimposed on each other defines the combinations of M and V causing failure. The ratio $a_{ax}=M_{ax}/V_{ax}=M_{cx}/V_{cx}$ indicates the location of failure (see Fig. 7.3.9).

7.3.3.2 Shear Compression and Deep Beam failures (Shear Span to Effective Depth Ratio < 2.5)

The force path which characterises shear compression and deep beam failures are similar - a line joining the support and loading points. Also, the shear span to effective depth ratio demarking shear compression and deep beam failure in concrete is not well defined and as such there is some overlap between these types of failure. For this reason deep beam failure will be considered as an extension to shear compression failure and will both be treated in this section.

A comprehensive description of the compressive force path concept for concrete beams which fail in shear compression and those which exhibit deep beam failures can be found elsewhere[90,92,94]. In summary, the inclined crack forms when the compression-tension stress field along this path becomes critical. The beam may have residual strength after inclined cracking.

The method proposed by Zielinski, described in reference 110 is compatible with the concept of the compressive force path for these types of

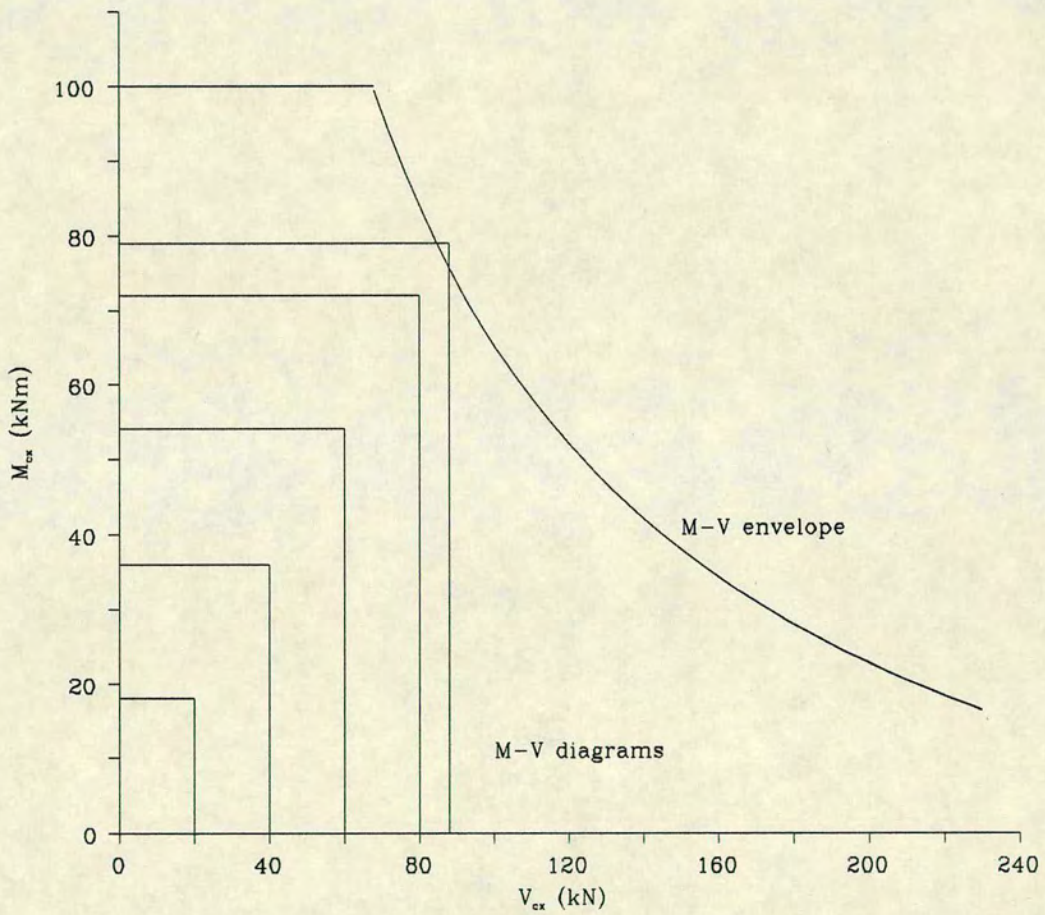

Fig. 7.3.9 Typical M-V Envelope

failure. In this method, the strength along the line joining the support to the loading point under biaxial compression-tension is used to obtain the ultimate shear force. It is assumed that the appearance of an inclined crack will not cause collapse of the member as long as sufficient web reinforcement (including longitudinal reinforcement) is provided to take over the splitting force.

For simplification, the actual curvilinear variation of the biaxial stresses between the support and load point is replaced by a rectangular stress. This assumption is comparable to the simplifiction of the flexural compression zone in reinforced concrete beams according to the ultimate flexural strength method[110]. The following variables are defined in Fig. 7.3.10 for a beam without web reinforcement:

f_{ct} = compressive stress in concrete subject to biaxial tension-compression
f_{tc} = tensile stress in concrete subject to biaxial tension-compression
f'_c = compressive cylinder strength of concrete
f_t = tensile strength of concrete
a = shear span (measured from the centre of the support to the centre of the load area)

$$\alpha = \tan^{-1} h/a$$

$$V = S \sin \alpha$$

$$H = S \cos \alpha$$

... 7.3.24a

The biaxial stress condition depends on the geometry of the support segment and can be defined as:

$$f_{ct} = S \cos \alpha/b\ h = H/b\ h$$

... 7.3.24b

$$f_{tc} = S \sin \alpha/a\ b = V/a\ b$$

... 7.3.24c

$$f_{ct}/f_{tc} = H\ a/V\ h = a^2/h^2$$

... 7.3.24c

Using Suwalski-Zalewski criterion[110] for the biaxial compression-tension stress state, the limiting value of f_{tc} at which diagonal splitting occurs is given as:

$$f_{tc} = f'_c/[f'_c/f_t + (a/h)^2]$$

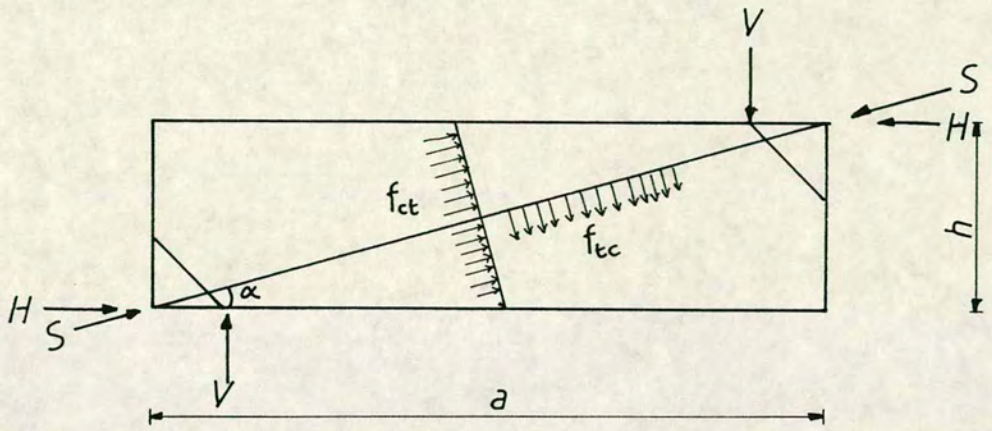

Fig. 7.3.10 Assumed Stress Distribution Under Shear Compression (After Zielinski[110])

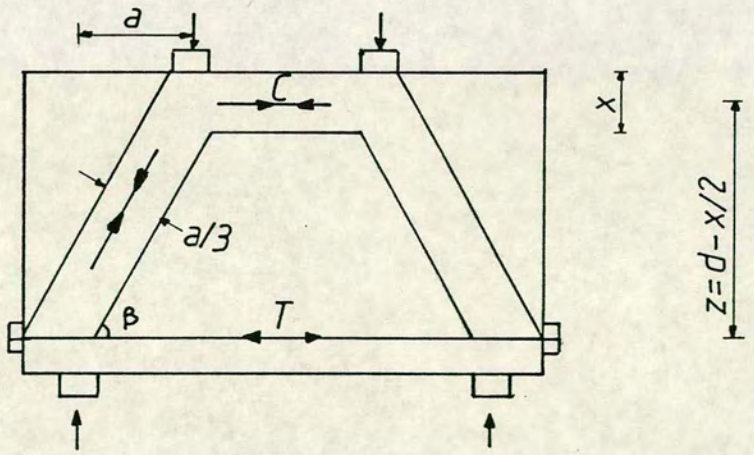

Fig. 7.3.11 Simplified Force Path for a Deep Beam

... 7.3.25

when a/h < 1, a and h are interchanged. The corresponding load is given by:

$$V_s = f_{tc}\ a\ b = f'_c\ a\ b/[f'_c/f_t + (a/h)^2]$$

... 7.3.26a

The effect of the longitudinal tensile reinforcement is to increase the splitting force as follows;

$$V_s = f_{tc}\ a\ b + f_s\ A_s \cos\psi + f_p\ A_p \cos\psi$$

... 7.3.26b

f_s = steel stress at cracking = $E_s\ \varepsilon_t$ (ε_t=0.0001 to 0.0002),
f_p = stress in the tensioned steel at cracking = $E_p\ \varepsilon_t$ (ε_t = prestrain + 0.0001 to 0.0002)
A_s = area of non-tensioned steel
A_p = area of tensioned steel
ψ = angle between the tensile steel and the principal tension direction

In terms of f_{ct}, the transverse load can be expressed as:

$$V_s = f_{ct}\ b\ h^2/a = [f_t\ b\ h^2]/[f_t/f'_c + h^2/a^2]$$

... 7.3.27a

Including the effect of the tensile steel:

$$V_s = f_{ct}\ b\ h^2/a + E_s/E_c\ [A_s \sin\psi + A_p \sin\psi]$$

... 7.3.27b

Equations 7.3.26 and 27 were derived on the basis of a theoretically applied concentrated load. However such loads are usually applied over loading areas and supported over bearing areas. These have the effect of reducing the splitting force. To allow for this effect a reduction coefficient $\kappa = a_i/a$ has been proposed which accounts for the ratio of the clear span a_i measured between the bearing and loading plates to the total length of the shear span, a (measured from the centre of the support to the centre of the loading plate).

Diagonal splitting is accompanied by a sudden increase in the steel stress. This occurs because after diagonal splitting, the total tension force must be carried by the longitudinal reinforcement. Therefore, when insufficient tensile reinforcement is provided, the beam collapses. If the splitting force can be

adequately sustained by the tensile reinforcement, the member will be able to carry more load until the reinforcement yields or the concrete fails in diagonal compression. The ultimate load defined by the yielding of the steel is given by:

$$V_u = A_s f_{sy} \cos \psi + A_p f_{py} \cos \psi$$

... 7.3.28

A deep beam is capable of sustaining considerably higher loads. Therefore, failure will occur by crushing of the concrete along the inclined crack. In order to check the adequacy of the concrete along the inclined crack when the steel yields, Kotsovos[94] modelled a deep beam as a 'tied frame with inclined legs' as shown in Fig. 7.3.11. Using the symbols as defined in Fig.7.3.11, when the steel yields, the following relationship exists between the total tensile and compressive forces:

$$C = b.x.f_c = A_s f_{sy} + A_p f_{py}$$

... 7.3.29

and the adequacy of the concrete along the inclined crack is checked by:

$$C. \cos \beta. \quad < b. (a/3). f_c$$

... 7.3.30

If the shear span to effective depth ratio (a/d) is less than the width of the bearing plate, then the width of the inclined leg is equal to that of the plate.

If failure occurs by crushing of the concrete along the inclined crack, in reference 110, the ultimate load is defined as follows:

$$\sigma = (V/\sin \alpha)/(B/\sin \alpha)$$
$$= V/B$$

This gives:

$$V_u = \sigma_{comp} B = Q. f'_c. B$$

... 7.3.31

where
V = shear force
B = bearing area
Q = stress reduction coefficient (assumed in reference 110 to be 0.7)
σ_{comp} = compressive strength

7.4 EXPERIMENTAL RESULTS AND COMPARISON WITH THEORY

In Chapter 4, the ultimate moment and failure mode for all the prestressed brickwork and concrete beams reported in this work were presented. In this section, experimental results pertaining to the shear strength of all the beams which failed in primary and secondary shear will be presented. Also, a comparison is made between the experimental results and those predicted by the application of the compressive force path concept and the plastic theory. Finally, the results of the finite element analysis are presented and discussed and a comparison is made with experimental results. Where possible, results obtained from shear strength investigations into fully prestressed brickwork beams are also presented with the aim of establishing trends of shear strength behaviour in prestressed brickwork.

7.4.1 The Shear Strength of Partially Prestressed Beams

In Chapter 4, the shear strength at failure, irrespective of the mode of failure, for all the prestressed brickwork and concrete beams reported in this work were presented. In Table 7.4.1, the shear strength of all the beams which failed in shear are summarised. The shear strength of the partially prestressed brickwork beams is plotted against the shear span to effective depth ratio (a/d) in Fig. 7.4.1. This figure shows an increase in the shear strength with a decrease in the a/d ratio. In the beams with a/d ratio of 1.5, the average shear strength at failure was 2.5 N/mm^2 while at an a/d ratio of 6.0, the average shear strength at failure was reduced to 0.62 N/mm^2. This is in keeping with other experimental results on reinforced[7,8,23,101] and prestressed[11] brickwork and concrete beams.

Also plotted in Fig. 7.4.1, is the relationship between the shear strength and the shear span to effective depth ratio for the fully prestressed brickwork beams containing 0.548% area of steel[11]. In order to compare both sets of results, the total area of steel in the partially prestressed beams is presented as an equivalent area of tensioned steel, being 0.341%. In a previous work[11] on fully prestressed brickwork beams, it has been shown that increasing the area of tensioned steel with the prestressing force kept constant has no effect

Table 7.4.1 Experimental Results

Beam	a/d	$\frac{V}{b.d^2}$ N/mm^2	$\frac{M_{exp}}{M_f}$
B1	1.5	2.25	0.68
B2	1.5	2.91	0.88
B12	1.5	2.36	0.68
CB11	1.5	3.92	1.16
CB12	1.5	3.31	0.96
B3	3.0	1.44	0.87
B7	3.0	1.25	0.75
B11	3.0	1.04	0.61
B15	3.0	1.16	0.68
CB9	3.0	1.50	0.88
CB10	3.0	1.63	0.95
B4	4.3	0.91	0.77
B5	4.5	0.78	0.69
B6	4.5	1.07	0.95
B13	4.5	0.80	0.71
B8	6.0	0.62	0.71
B9	6.0	0.75	0.90
B10	6.0	0.78	0.95
B14	6.0	0.60	0.70
BB1	11.21	0.66	0.93
BB2	11.21	0.55	0.78
BB3	11.21	0.55	0.77
BB4	11.21	0.57	0.81

Notes:
M_f = flexural moment of resistance
M_{exp} = ultimate moment at failure

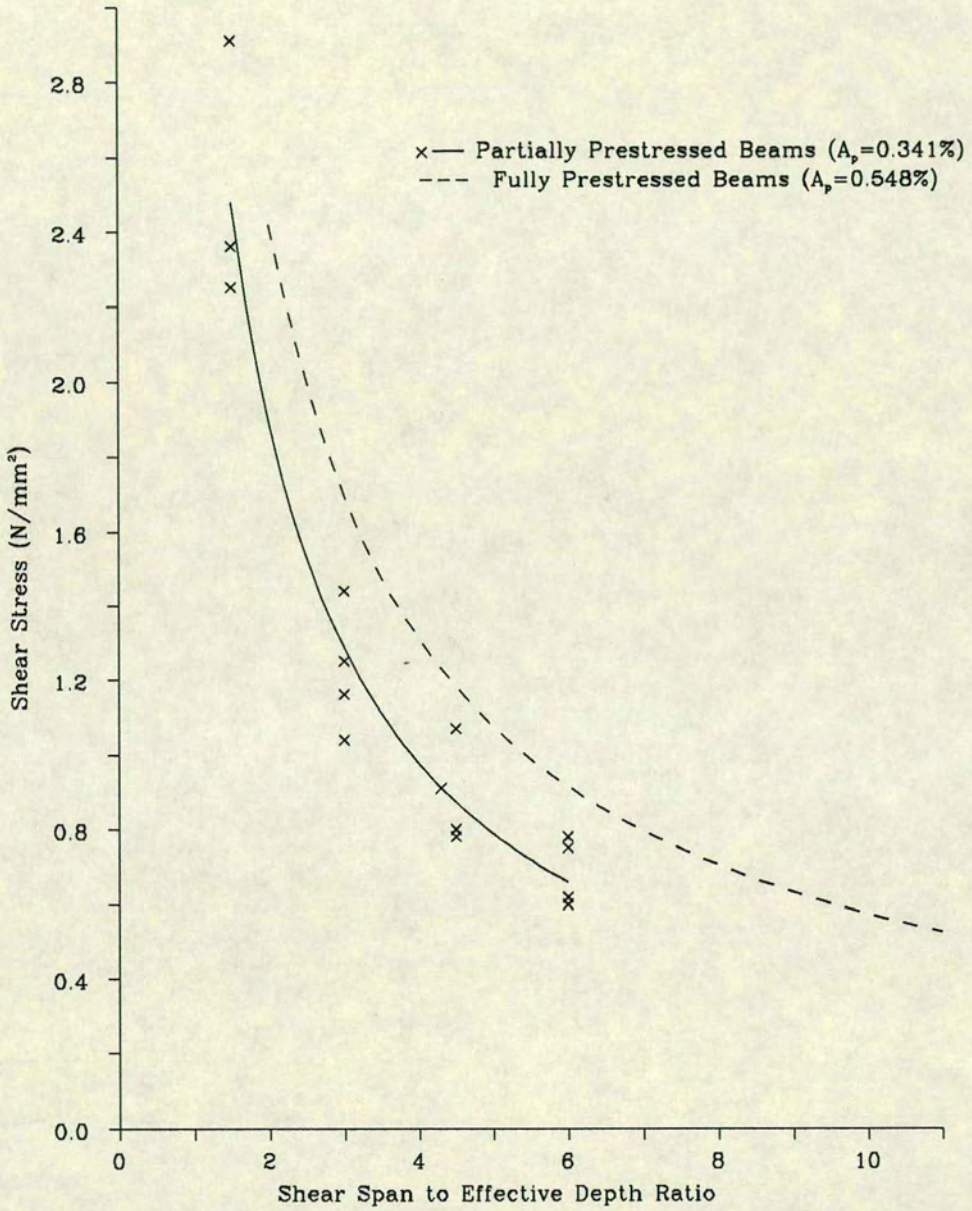

Fig. 7.4.1 Relationship Between the Shear Strength and the Shear Span to Effective Depth Ratio for Prestressed Brickwork Beams

on the shear strength. Thus if we ignore the effect of the area of steel, then partially prestressed beams will have a lower shear strength when compared to fully prestressed beams.

The shear strength of the partially prestressed concrete beams are also presented in Table 7.4.1. As in the brickwork beams, there is an increase in the shear strength with decreasing a/d ratio. At an a/d ratio of 1.5, the average shear strength at failure was 3.61 N/mm^2. When the shear span to effective depth ratio was increased to 3.0, the average shear strength was reduced to 1.57 N/mm^2. Expectedly, the shear strength in the concrete beams were also higher than those in the corresponding brickwork beams. At an a/d ratio of 1.5, the shear strength in the concrete beam was 44% higher than that in the brickwork beams. At an a/d ratio of 3.0, the shear strength of the concrete beams was 28% higher than in the brickwork beams.

The higher shear strength in concrete could be due to the larger amount of shear which can be transferred by aggregate interlock which is much less in brickwork and the absence of mortar joints which act as planes of weakness.

7.4.2 Shear Cracks in Partially Prestressed Beams

7.4.2.1 Partially Prestressed Brickwork Beams

In all beams, flexural cracking had extended into the shear span before failure and was confined to that half of the shear span closest to the loading point. Two types of inclined cracks were observed in the partially prestressed brickwork beams; flexure-shear and web-shear cracks. Flexure-shear cracks were observed in the brickwork beams with a/d ratio between 3.0 and 6.0. The initiating flexural crack was that closest to the support and was generally located at the middle of the shear span. With increasing load, the initially vertical flexural crack became inclined and travelled in the direction of the load point in a step-wise manner. On reaching the top bed joint, there was a horizontal propagation of this crack along the bed joint and into the constant moment region (see Fig. 7.4.2). There was also a horizontal propagation of this crack along the bottom bed joint towards the support.

The flexure-shear crack is consisitent with diagonal tension failure. It is

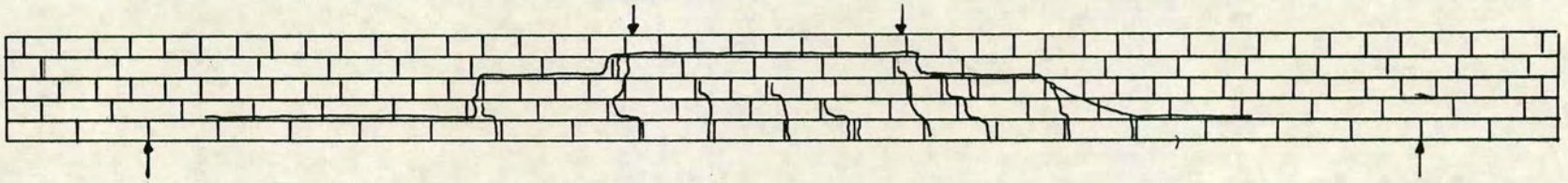

Fig. 7.4.2 Flexure-Shear Crack in a Partially Prestressed Brickwork Beam (a/d = 6.0)

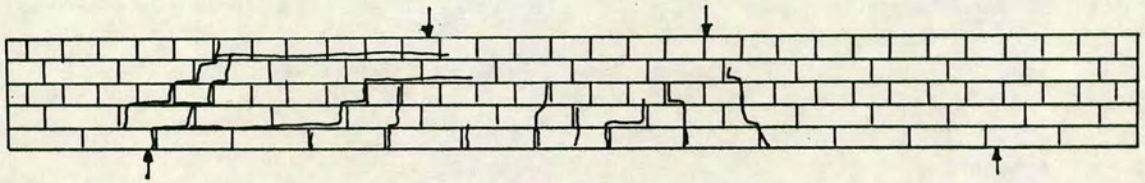

Fig. 7.4.3 Web-Shear and Flexure-Shear Cracks in a Partially Prestressed Brickwork Beam (a/d = 3.0)

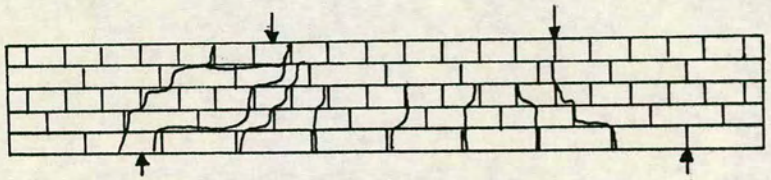

Fig. 7.4.4 Web-Shear Crack in a Partially Prestressed Brickwork Beam (a/d = 1.5)

also compatible with the force path for diagonal tension failure postulated by the compressive force path concept, which as seen in Section 7.3 is characterised by a change in direction of the compressive force path between the loading and supporting points.

In the beams with shear span to effective depth ratios of 4.5 and 3.0, as well as the flexure-shear crack in the shear span, web-shear cracks were also present at failure (see Fig. 7.4.3) and were the cause of failure. Irrespective of whether shear failure was caused by flexure-shear cracking or web shear cracking, there was always a horizontal propagation of the crack along the top bed joint into the constant moment region at failure.

In the beams with an a/d ratio of 1.5, the inclined crack which caused failure was independent of flexural cracking. It travelled from the support in the step-wise fashion at a steep angle to the horizontal axis of the beam (about 60°) into the top of the beam. There was also a horizontal propagation of this crack into the constant moment region terminating just beyond the load point (see Fig. 7.4.4). This crack pattern is thus similar to those for the beams with a/d ratios of 3.0 to 6.0 described above. The behaviour of B16, a partially prestressed brickwork beam with a shear span to effective depth ratio of 1.5 was very different from the other beams in this group. The failure of this beam was due to a weak bond and has therefore been excluded from the discussion in this chapter.

7.4.2.2 Partially Prestressed Concrete Beams

In the partially prestressed concrete beams, flexural cracking had also extended into the shear span. In the beams with shear span to effective depth ratio of 1.5, this occurred very close to the loading point while for those with the higher a/d ratio (3.0), flexural cracking as in the partially prestressed brickwork beams, was confined to that half of the shear span nearest the loading point.

In the concrete beams with a/d ratio of 3.0, shear failure was caused by a flexure-shear crack and the initiating flexural crack was located at the middle of the shear span. There was also a horizontal propagation of this crack towards the support (see Fig. 7.4.5). In the direction of the load point, this initially vertical crack became inclined and travelled into the constant moment

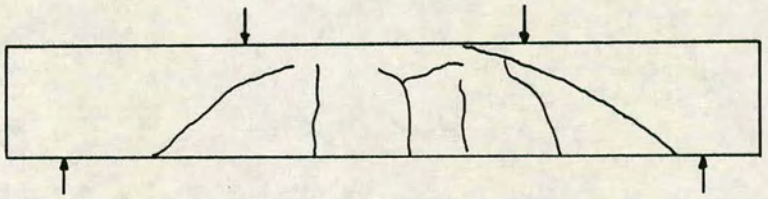

Fig. 7.4.6 Web-Shear Crack in a Partially Prestressed Concrete Beam (a/d = 1.5)

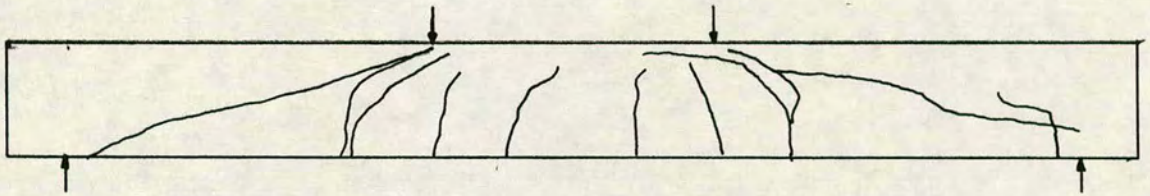

Fig. 7.4.5 Flexure-Shear Crack in a Partially Prestressed Concrete Beam (a/d = 3.0)

region where failure occurred when this crack had penetrated into the top of the beam.

In the beam with a/d ratio of 1.5, the inclined crack was independent of flexural cracking and travelled in a straight line from the inner edge of the bearing plate to a point beneath the line of action of the point load. Thereafter, it penetrated into the constant moment region and caused crushing of the concrete just beyond the loading point (see Fig. 7.4.6). This is compatible with the compressive force path concept for members which fail in shear compression or exhibit deep beam failure.

7.4.3 Degradation in the Ultimate Moment Due to Shear Failure

The degradation in the ultimate moment due to shear failure when compared with the flexural moment of resistance of the section based on the single course prism for the brickwork beams is plotted against the shear span to effective depth ratio in Fig. 7.4.7. This relationship shows an increase in the ratio of the ultimate moment due to shear failure to the ultimate flexural moment for beams with a shear span to effective depth ratio of 1.5, when compared with beams with a shear span to effective depth ratio of 3.0. Assuming, as in reinforced brickwork, that the transitional shear span to effective depth ratio between diagonal tension and tied arch failure is around 2.5, Fig. 7.4.7 shows an increase in the ratio of the ultimate flexural moment attained at shear span to effective depth ratios below 2.5. This appears to be different from the trend in fully prestressed brickwork beams, also plotted in Fig. 7.4.7. The apparent absence of an increase in the ratio of the ultimate moment due to shear failure to the ultimate flexural moment in fully prestressed brickwork beams at a/d ratios less than 2.5 can be attributed to the following;

- The range of shear span to effective depth ratio tested; as seen from Section 7.2, the transition shear span to effective depth ratio between tied arch action and diagonal tension is between 2.0 and 3.0 and results at a shear span to effective depth ratio of 2.0 can obscure the trend.

- The tied arch action is less significant in prestressed brickwork.

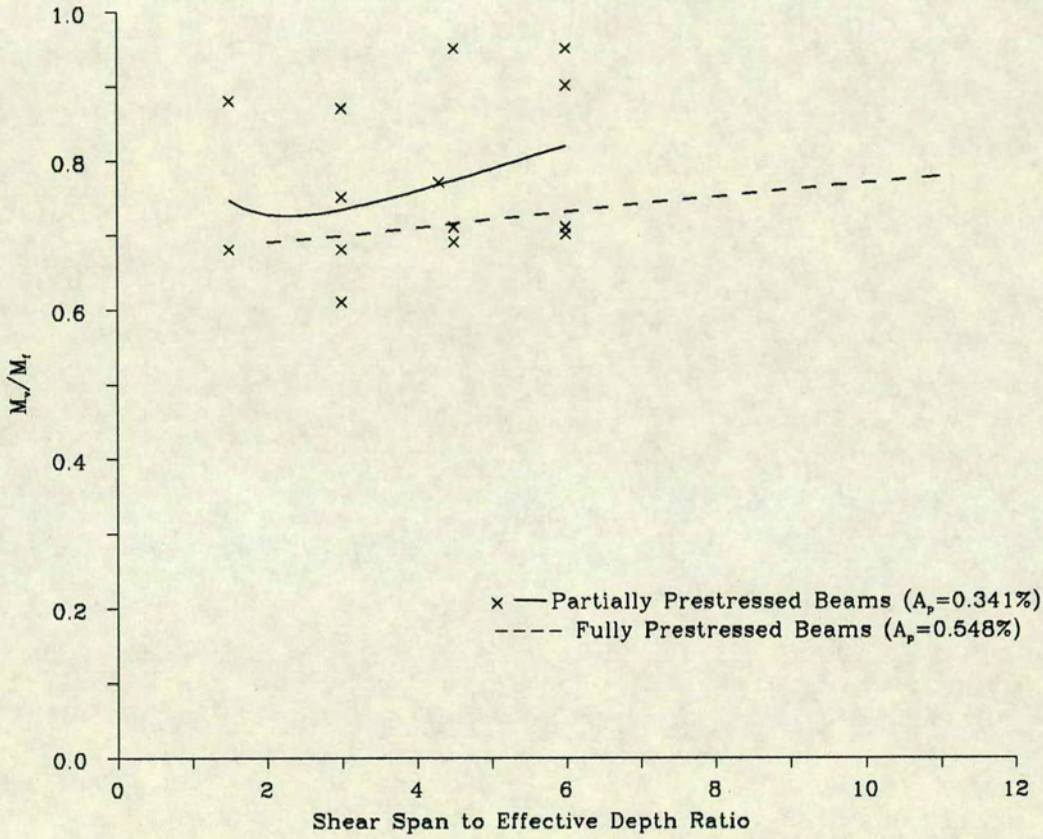

Fig. 7.4.7 Degradation in Failure Moment due to Shear

After inclined cracking, the total shear force across a crack in a beam without web reinforcement must be carried by dowel action of the longitudinal reinforcement, aggregate interlock across the crack surfaces and by the compression zone above the crack. Reinforced brickwork usually has higher steel areas than prestressed brickwork. The increased area may increase the contribution of the dowel action in the steel to the shear strength. Also, the tendon used for the prestressed beam is much more flexible than ordinary reinforcement and may not be very effective in transmitting shear due to dowel action. Negligible dowelling forces have been indicated in straight longitudinal prestressing reinforcement[111].

Some of the partially prestressed brickwork beams failed in secondary shear after the non-tensioned steel had yielded. In these beams, the degradation in the ultimate moment due to shear failure was small. For example, in B10 which had a shear span to effective depth ratio of 6.0, a ratio of the failure moment to ultimate flexural moment of 0.95 was obtained. In the beams which failed in primary shear, a ratio as low as 0.61 was obtained (B11 a/d = 3.0).

Comparing the results of the fully and partially prestressed brickwork beams in Fig. 7.4.7 shows that the a/d ratio which demarks the transition from diagonal tension to flexural failure increases with the increasing area of steel. This is in keeping the with the concept of the compressive force path (see Equation 7.3.15).

For the partially prestressed concrete beams, there is an increase in the ratio of the ultimate moment to the flexural moment of resistance with decreasing a/d ratio. For beams with a/d ratio of 1.5, an average value of 1.06 was obtained while in the beams with the higher a/d ratio, 3.0, this ratio was 0.91 (see Table 7.4.1).

7.4.4 The Splitting Strain in Brickwork

The proposed method for calculating the shear strength of prestressed brickwork beams (see Section 7.3) was dependent on the strain at which bed joint splitting occurs in a brickwork beam. Uniaxial tests on three course prisms of the format shown in Chapter 3, exhibit bed joint splitting. Up until now, there has been no real interest in the strain at which this type of bed

joint splitting occurs and references to it have been rather vague. Using 'raw' data on three course prisms obtained from reference 11 and defining the splitting strain in a three course prism as that beyond which the prism ceased to behave monolithically, the range of splitting strains obtained from the strain distribution was between 0.00044 and 0.00065 with an average value of 0.00058.

To confirm that the ultimate failure in shear occurred due to splitting in the bed joint in the constant moment region, the splitting strain obtained from the three course prism was used to calculate the compression and tensile forces in the beam at failure by trial and error. The tensile forces so calculated were compared with the values measured in the beam tests from electrical resistance strain gauges which were attached to the steel. These results are presented in Table 7.4.2. In all cases, the ratio between the measured and calculated values of the tensile force at shear failure was between 0.91 and 1.21 with an average value of 1.08.

Also, in Table 7.4.2, the maximum strain at the top bed joint for the partially prestressed brickwork beams tested in this work are presented. The range of the average splitting strain for all the beams was between 0.00045 and 0.00066 with an average value of 0.00055 which compares very well with the values of splitting strain obtained from the three course prisms.

For the purpose of calculating the shear strength of the prestressed brickwork beams contained in this work, the splitting strain shall be taken as 0.00058 - the average value obtained from the three course prisms.

7.4.5 Comparison Between Experimental and Predicted Results

In Table 7.4.3, the shear strength predicted from the concept of the compressive force path for the partially prestressed brickwork and concrete beams reported in this work which failed in shear are presented. In all cases, there was very good agreement between the experimental and theoretical results. The ratio of the experimental to the predicted shear strength varied from 0.84 to 1.28 with an average value of 1.06. The concept of the compressive force path was also used to predict the shear strength of some fully prestressed brickwork beams which failed in shear which were obtained from reference 11. These results are shown in Table 7.4.4. In this case the

Table 7.4.2 Tensile Forces at Shear Failure Obtained from the Splitting Strain in Brickwork

Beam	T_{exp} kN	T_{cal} kN	$\frac{T_{exp}}{T_{cal}}$	ε_{j_5} 10^{-5}
B1	287.6	276.9	1.04	60
B2	235.7^{+}	201.3^{+}	1.17	-
B12	314.5	276.9	1.14	50
B3	85.0^{+}	75.6^{+}	1.12	45
B7	264.9	276.9	0.96	51
B11	311.1	275.6	1.13	51
B15	253.9	277.8	0.91	-
B4	320.9	277.9	1.15	62
B5	269.5	277.8	0.97	58
B6	225.9*	201.3*	1.12	52
B13	285.9	277.9	1.03	-
B8	266.2	277.8	0.96	66
B9	339.3	278.1	1.21	-
B10	322.1	280.5	1.15	54
B14	310.8	277.9	1.12	51
Average			1.08	55

Notes:
+ Tendon force only
* Force in the reinforcing bar only
T_{exp} is the measured tensile force at failure (total)
T_{cal} is the calculated tensile force at failure using a splitting strain of 58×10^{-5}
ε_j is the strain at which bed joint splitting occurred in the beam tests

Table 7.4.3 Comparison Between Experimental and Theoretical Shear Strengths

Beam	a/d	τ_{exp} N/mm^2	τ_{comp} N/mm^2	$\frac{\tau_{exp}}{\tau_{comp}}$	a/h	ν	Φ	τ_{plas} N/mm^2	$\frac{\tau_{exp}}{\tau_{plas}}$
B1	1.5	2.25	2.47	0.91	1.04	0.34	0.137	2.66	0.85
B2	1.5	2.91	2.48	1.18	1.04	0.34	0.137	2.66	1.09
B12	1.5	2.36	2.47	0.95	1.04	0.34	0.137	2.66	0.89
CB11	1.5	3.92	3.06	1.28	1.04	0.58	0.129	3.60	1.09
CB12	1.5	3.31	3.06	1.08	1.04	0.58	0.129	3.60	0.92
B3	3.0	1.44	1.25	1.15	2.27	0.34	0.137	1.39	1.04
B7	3.0	1.25	1.24	1.01	2.27	0.34	0.137	1.39	0.90
B11	3.0	1.04	1.24	0.84	2.27	0.34	0.137	1.39	0.75
B15	3.0	1.16	1.25	0.93	2.27	0.34	0.137	1.39	0.84
CB9	3.0	1.50	1.35	1.11	2.27	0.43	0.129	1.63	0.92
CB10	3.0	1.63	1.35	1.20	2.27	0.43	0.129	1.63	1.00
B4	4.3	0.91	0.88	1.04	3.37	0.34	0.137	0.95	0.95
B5	4.5	0.78	0.84	0.93	3.46	0.34	0.137	0.93	0.84
B6	4.5	1.07	0.85	1.27	3.46	0.34	0.137	0.93	1.15
B13	4.5	0.80	0.84	0.95	3.46	0.34	0.137	0.93	0.86
B8	6.0	0.62	0.64	0.97	4.68	0.34	0.137	0.66	0.89
B9	6.0	0.75	0.64	1.17	4.68	0.34	0.137	0.69	1.08
B10	6.0	0.78	0.64	1.22	4.68	0.34	0.137	0.69	1.13
B14	6.0	0.60	0.64	0.95	4.68	0.34	0.137	0.69	0.87

Table 7.4.4 Comparison Between Experimental and Theoretical Shear Strengths for Fully Prestressed Brickwork Beams[11]

Beam	a/d	τ_{exp} N/mm^2	τ_{comp} N/mm^2	$\frac{\tau_{exp}}{\tau_{comp}}$	a/h	ν	Φ	τ_{plas} N/mm^2	$\frac{\tau_{exp}}{\tau_{plas}}$
BB1	11.21	0.66	0.45	1.47	7.33	0.341	0.186	0.56	1.19
BB2	11.21	0.55	0.44	1.26	7.33	0.341	0.186	0.56	0.98
BB3	11.21	0.55	0.44	1.26	7.33	0.341	0.186	0.56	0.98
BB4	11.21	0.57	0.44	1.31	7.33	0.341	0.186	0.56	1.02
BB5	4.0	1.33	1.10	1.21	2.66	0.341	0.186	1.48	0.90
BB6	4.0	1.27	1.09	1.17	2.66	0.341	0.186	1.48	0.86
BB7	2.0	2.15	2.17	0.99	1.33	0.341	0.186	2.73	0.79
BB8	2.0	2.71	2.16	1.25	1.33	0.341	0.186	2.73	0.99
BB9	7.0	0.75	0.54	1.40	4.77	0.341	0.186	0.85	0.89
BB10	7.0	0.70	0.54	1.30	4.77	0.341	0.186	0.85	0.83

ratio of experimental to theoretical shear strength was generally between 0.99 and 1.31. The predicted shear strength of the beam containing the highest prestressing force, BB1 was underestimated by 47%. This is probably due to the fact that this beam was very close to flexural failure. In the beams with the shorter shear spans, the predicted shear strengths were much closer to the expermental values.

In the concrete beams with an a/d ratio of 1.5, one of the beams failed at an ultimate moment which was higher than the predicted flexural moment of resistance (CB11) while the other failed at a lower moment than the flexural moment. In this case, there might have been overlap between shear compression and deep beam failure. Using Equation 7.3.30 indicated a residual strength along the inclined crack after the yielding of the tensile reinforcement. Assuming that failure will occur when the tensile reinforcment has yielded gave a predicted shear strength of 3.43 N/mm^2 with a ratio to the experimental shear strength of 1.14 and 0.97 for CB11 and CB12 respectively. In design the minimum value will be adopted.

The shear strength predicted by the plastic theory is also shown in Tables 7.4.3 and 7.4.4. As mentioned in Section 7.3, an essential parameter required for the application of the plastic theory is the effectiveness factor ν. In a previous work in which the plastic theory was applied to brickwork[11], the effectiveness factor was obtained from three different sets of results. These were obtained from Sinha[7], Suter and Hendry[8] and the experimental work carried in the reference[11]. The average effectiveness factors obtained in each case were 0.33, 0.35 and 0.34 respectively. From these figures one might conclude that the web effectiveness factor in brickwork is constant. Using an effectiveness factor of 0.34 for the partially prestressed brickwork beams tested in this work, the predicted shear strengths are also given in Table 7.4.3.

The plastic theory gave a slight overestimate the shear strength. The ratio of experimental to predicted shear strength was between 0.75 and 1.15 with an average value of 0.97. Using Equation 7.3.9 for the partially prestressed brickwork beams tested in this work, an average effectiveness factor of 0.29 was obtained with a range between 0.211 and 0.388 indicating that the similar effectiveness factors obtained from the previous work[11] were indeed coincidental.

The effectiveness factor in brickwork, as has been demonstrated for concrete[88], is not constant but is likely to be dependent of several variables. From the results of reinforced and fully prestressed brickwork, one can conclude that the factors in equation 7.3.10 which will influence the effectiveness factor is the overall height of the beam, h and the ratio of the effective prestress to the 0.2% proof stress of the tensioned reinforcement, $\sigma_{eff}/\sigma_{0.2}$. This is because as mentioned is Section 7.2, the strength of the brickwork and the percentage area of steel have been found to have little if any effect on the shear strength[102]. Referring to Fig. 7.4.1 in which the shear strength of fully and partially prestressed brickwork beams were compared, the differences in the shear strength can be attributed to $\sigma_{eff}/\sigma_{0.2}$ as in these cases, the height was constant.

In Fig. 7.4.8 and 7.4.9, the results predicted by the concept of the compressive force path and the plastic theory for the partially and fully prestressed brickwork beams respectively are compared with experimental results.

7.4.6 The Results of the Finite Element Analysis

The finite element analysis required as part of the data input, a value for the shear retention factor mentioned in Section 7.3. A value of 0.33 was found to be suitable for the partially prestressed brickwork beams with a shear span to effective depth ratios between 3.0 and 6.0. However for the partially prestressed brickwork beams with the shear span to effective depth ratio of 1.5, a the higher value of 0.5 was found to be more appropriate. A secant modulus of elasticity at an average stress of 30 N/mm^2 was used in this analyis.

7.4.6.1 Verification of the Finite Element Analysis for Brickwork Beams

To verify the finite element analysis for the behaviour of flexurally cracked brickwork beams, the predicted deflections were checked against the experimental deflections obtained from the beam tests. These results are presented in Figs. 7.4.10–7.4.13. In all cases, very good predictions were obtained.

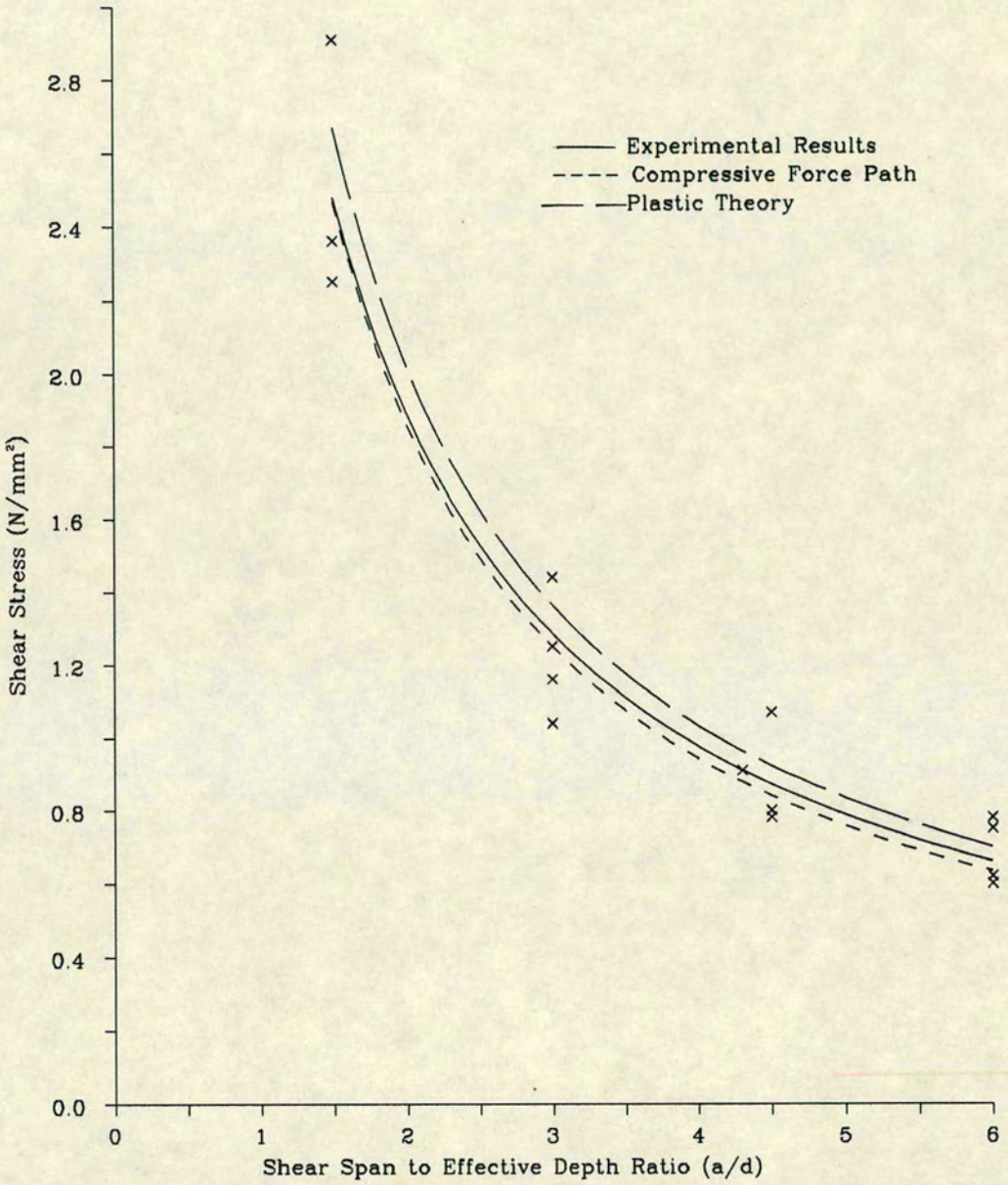

Fig. 7.4.8 Comparison Between Experimental and Predicted Shear Strengths for Partially Prestressed Brickwork

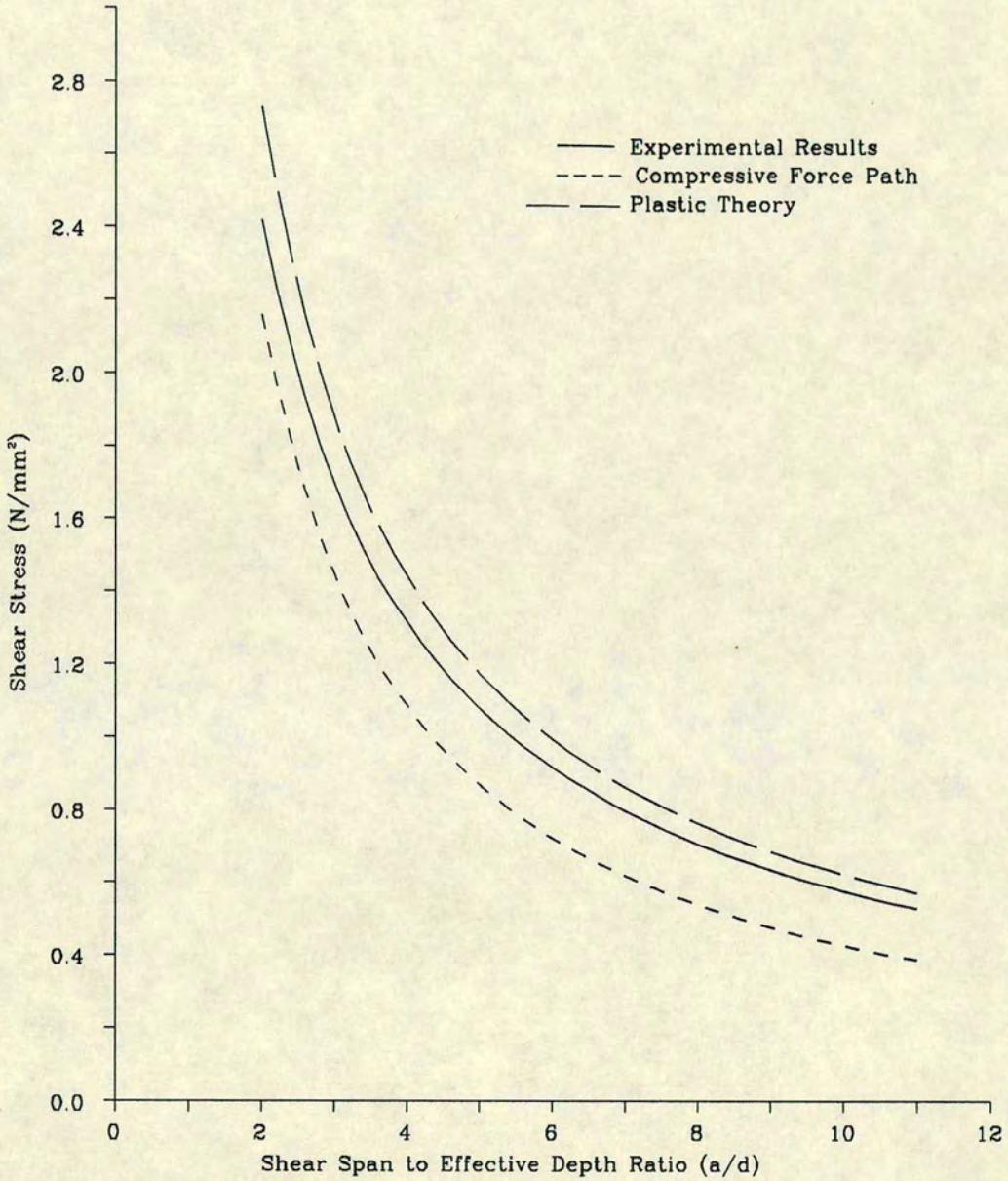

Fig. 7.4.9 Comparison Between Experimental and Predicted Shear Strengths for Fully Prestressed Brickwork

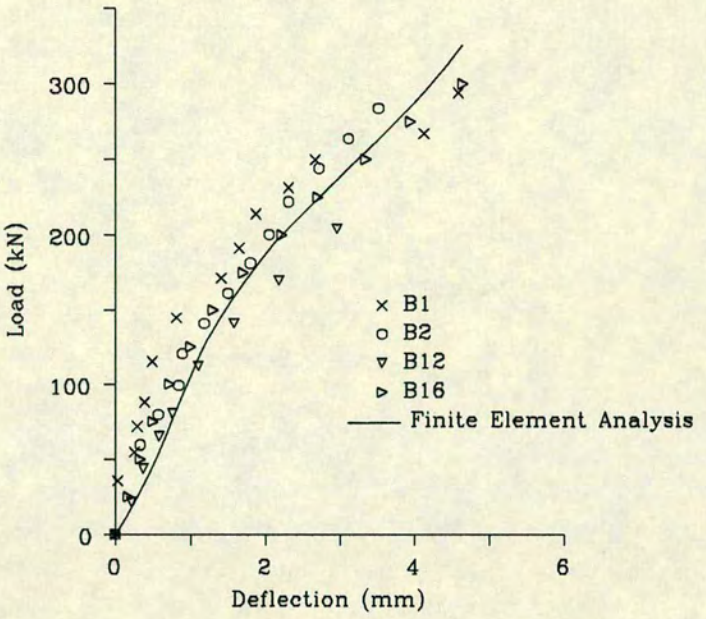

Fig. 7.4.10 Load – Deflection Relationship
Shear Span to Effective Depth Ratio = 1.5

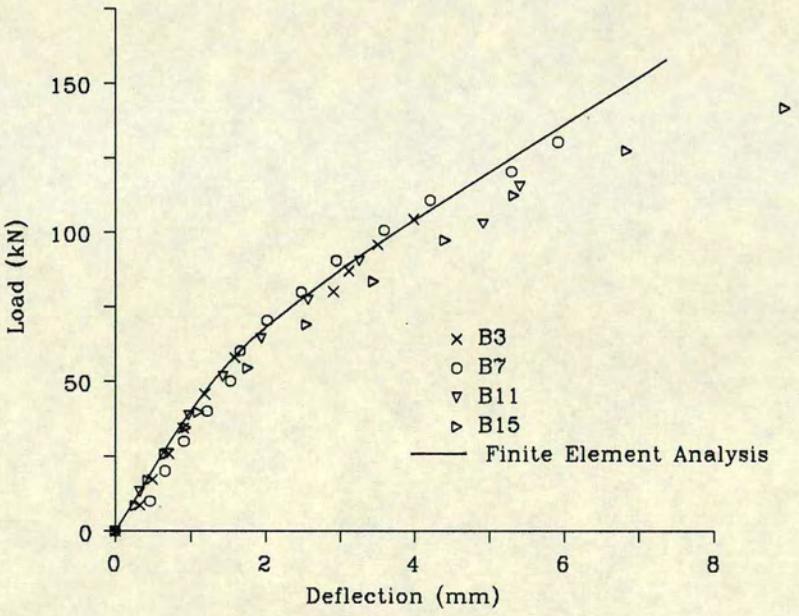

Fig. 7.4.11 Load – Deflection Relationship
Shear Span to Effective Depth Ratio = 3.0

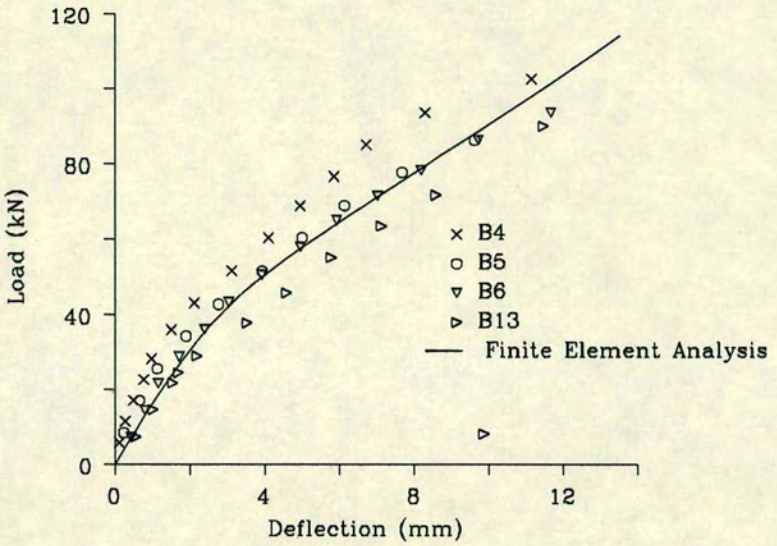

Fig. 7.4.12 Load – Deflection Relationship
Shear Span to Effective Depth Ratio = 4.5

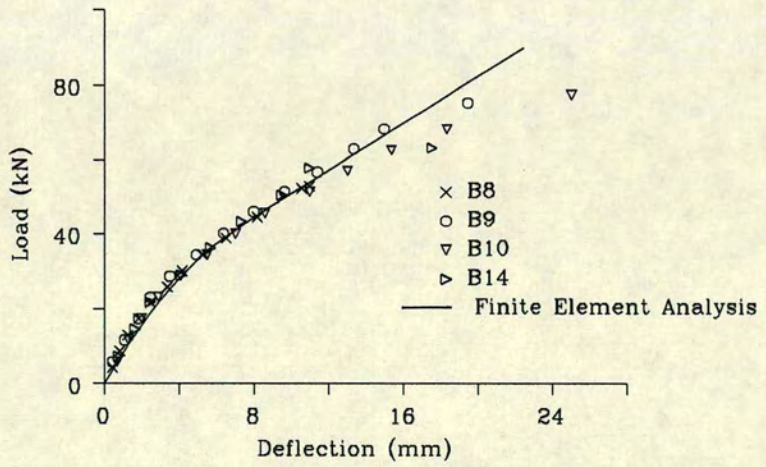

Fig. 7.4.13 Load – Deflection Relationship
Shear Span to Effective Depth Ratio = 6.0

The top fibre strain and the force in the tensioned and non-tensioned steel predicted by the finite element analysis also compared favourably with the experimental results. In all cases, the predicted results were always within 15% of the experimental values. These results are presented in Table 7.4.5.

Using the tangent modulus of elasticity obtained in Chapter 3, the strain at the level of the top bed joint at shear failure obtained from the finite element analysis was 0.00059 which is in very good agreement with the average value obtained experimentally from the beam tests (0.00055) and at bed joint splitting of the three course prisms (0.00058).

7.4.6.2 The Principal Stresses

In Figs. 7.4.14-7.4.17, the contour plots for the principal tensile and compressive stresses in the partially prestressed brickwork beams at failure obtained from the finite element analysis are presented.

Beams with Shear Span to Effective Depth Ratios between 3.0 and 6.0

In these beams, the principal compressive stresses at failure was always less than the compressive strength of brickwork indicating that in these beams, crushing of the brickwork did not occur. The maximum values were obtained in the top fibre of the compression zone in the maximum moment region and these values increased with increasing shear span to effective depth ratio. These predictions are in keeping with experimental results. Also, the principal compressive stresses in all cases were confined to the areas expected for beam bending i.e to the compression zone of the beams.

As can be seen from Fig. 7.4.14-7.4.16, the principal tensile stresses were distributed over the entire beam except in the lightly loaded areas at the top of the beam close to the support and the tensile zone of the constant moment region which was cracked in flexure. The maximum principal tensile stresses in all cases occurred at a section under the loading point close to the neutral axis depth (see Fig. 7.4.14-7.4.16). These values for the beams with shear span to effective depth ratios of 3.0, 4.5 and 6.0 were 1.71 N/mm^2 at an angle of 22° (to the horizontal axis of the beam), 1.89 N/mm^2 at an angle of 5.5° and 2.11 N/mm^2 at an angle of 4.5° respectively. This indicates that there was an increase in the value of the maximum principal tensile stress at failure with

Table 7.4.5 Comparison Between Experimental and Finite Element Analysis (F.E.A) Strains at Failure

a/d	Top Fibre Strain		Additional Tendon Strain		Strain in Re Bar	
	Exp	FEA	Exp	FEA	Exp	FEA
1.5	0.00133	0.00153	0.00108	0.00111	0.00261	0.00247
3.0	0.00150	0.00149	0.00114	0.00106	0.00222	0.00196
4.5	0.00148	0.00169	0.00118	0.00118	0.00194	0.00215
6.0	0.00180	0.00176	0.00162	0.00141	0.00219	0.00229

+ Tension
- Compression

CONTOUR VALUE

A	-1.135
B	-0.7569
C	-0.3785
D	-0.1388E-16
E	0.3785
F	0.7569
G	1.135
H	1.514

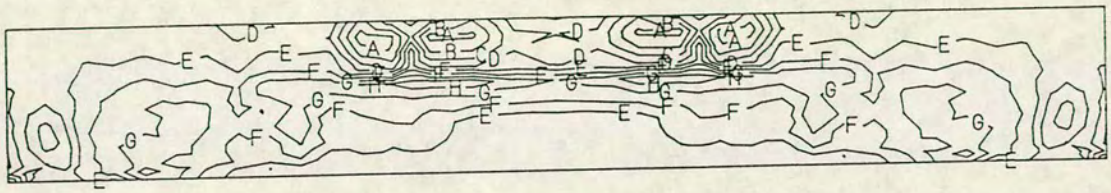

Principal Stress Contours at the Last Load Increment
Partially Prestressed Brickwork Beams
Shear Span to Effective Depth Ratio = 3.0

CONTOUR VALUE

A	-19.07
B	-16.34
C	-13.62
D	-10.90
E	-8.172
F	-5.448
G	-2.724
H	-0.3331E-15

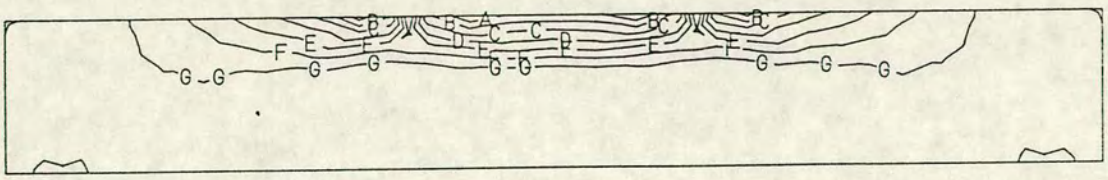

Principal Stress Contours at the Last Load Increment
Partially Prestressed Brickwork Beams
Shear Span to Effective Depth Ratio = 3.0

Fig. 7.4.14

+ Tension
- Compression

CONTOUR VALUE	
A	-0.6975
B	-0.3488
C	0.0
D	0.3488
E	0.6975
F	1.046
G	1.395
H	1.744

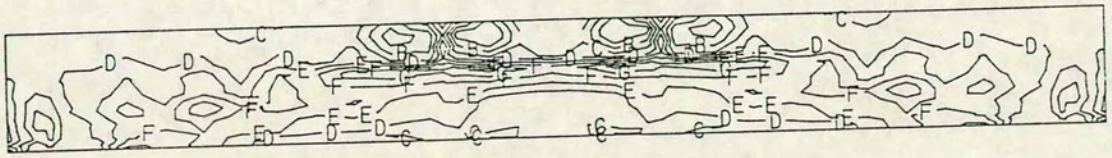

Principal Stress Contours at the Final Load Increment
Partially Prestressed Brickwork Beams
Shear Span to Effective Depth Ratio = 4.5

CONTOUR VALUE	
A	-20.81
B	-17.84
C	-14.87
D	-11.89
E	-8.920
F	-5.946
G	-2.973
H	-0.5551E-15

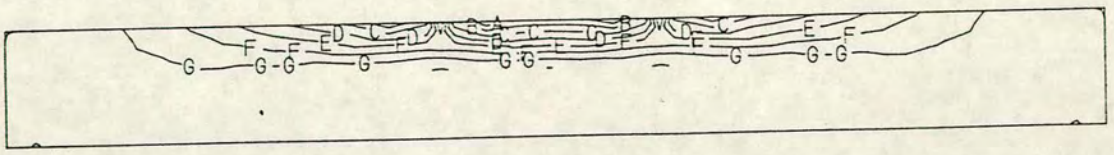

Principal Stress Contours at the Final Load Increment
Partially Prestressed Brickwork Beams
Shear Span to Effective Depth Ratio = 4.5

Fig. 7.4.15

+ Tension

- Compression

CONTOUR VALUE

A	-22.42
B	-19.21
C	-16.01
D	-12.81
E	-9.607
F	-6.404
G	-3.202
H	-0.6661E-15

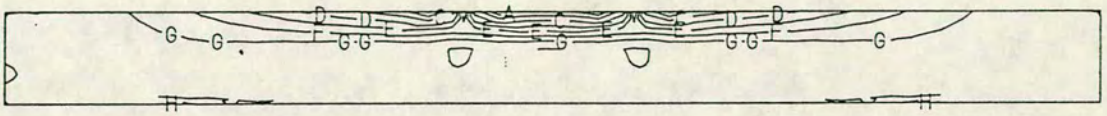

Principal Stress Contours at the Final Load Increment
Partially Prestressed Brickwork Beams
Shear Span to Effective Depth Ratio = 6.0

CONTOUR VALUE

A	-1.292
B	-0.8610
C	-0.4305
D	0.0
E	0.4305
F	0.8610
G	1.292
H	1.722

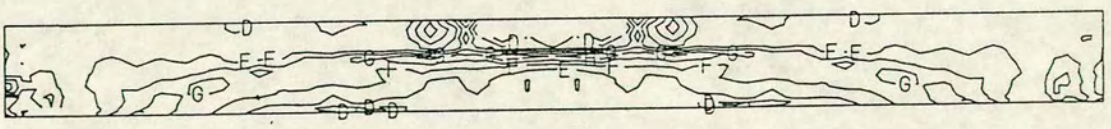

Principal Stress Contours at the Final Load Increment
Partially Prestressed Brickwork Beams
Shear Span to Effective Depth Ratio = 6.0

Fig. 7.4.16

+ Tension
- Compression

CONTOUR VALUE
A -2.471
B -1.854
C -1.236
D -0.6179
E -0.2776E-16
F 0.6179
G 1.236
H 1.854

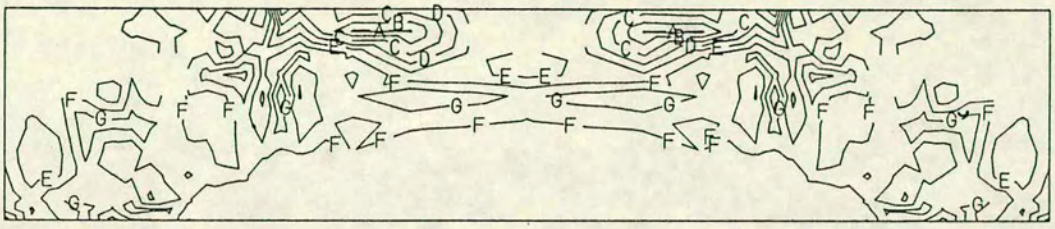

Principal Stress Contours at the Final Load Increment
Partially Prestressed Brickwork Beams
Shear Span to Effective Depth Ratio = 1.5

CONTOUR VALUE
A -26.56
B -22.77
C -18.97
D -15.18
E -11.38
F -7.589
G -3.795
H 0.0

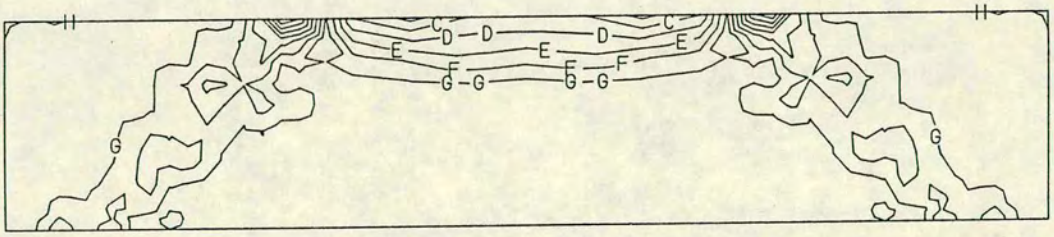

Principal Stress Contours at the Final Load Increment
Partially Prestressed Brickwork Beams
Shear Span to Effective Depth Ratio = 1.5

Fig. 7.4.17

increasing shear span to effective depth ratio. As will be discussed below, this trend is compatible with other experimental results[103,104,105].

Comparing the principal tensile and compressive stress contours clearly shows a region of biaxial compression-tension in the upper region of the shear span within that half of the shear span close to the loading point (see Fig. 7.4.14-7.4.16). This is in keeping with the compressive force path concept which, as presented in Section 7.3, postulates the existence of a biaxial compression-tension stress field in the region of the path along which the shear force is transferred to the support. Also, comparing the principal compressive and tensile stress contours show that the compression zone of the constant moment region of these beams are essentially under uniaxial compression. Hence, the use of three course prisms under uniaxial compression is justified for the determination of the shear strength of brickwork beams as suggested in Section 7.3. The maximum principal tensile stress also occurs in the region of maximum shear force and bending moment.

Biaxial tests on masonry panels have been reported by Page[104], Dhanasekar[103] and Samarasinghe[105]. These tests were carried out on model scale brickwork panels with a range of angles of the bed joints to the principal stresses. Although the trends predicted by these tests in biaxial tension-compression are similar to those which have been obtained by the finite element analysis carried out in this work, the absolute values of principal stresses can not be obtained from the surfaces proposed. This is because the materials used in their tests (one sixth and half scale brickwork) were different from the full scale brickwork tested in this work. The failure surface obtained from the work of Page[104] in biaxial compression-tension is shown in Fig. 7.4.18. As mentioned above, there was an increase in the principal tensile stress with shear span to effective depth ratio between 3.0 and 6.0. There was however, a corresponding decrease in the orientation of the maximum principal tensile stress with increasing value to the horizontal axis of the beam which is indeed the angle to the bed joint. This trend is reflected in Fig. 7.4.18, which shows an increase in the size of the failure envelope with decreasing angle of the principal tensile stress to the bed joint.

Incidentally, it will not be out of point to mention that the value of the tensile stresses at failure obtained from the finite element analysis in a cracked partially prestressed brickwork beam is somewhat similar to the modulus of

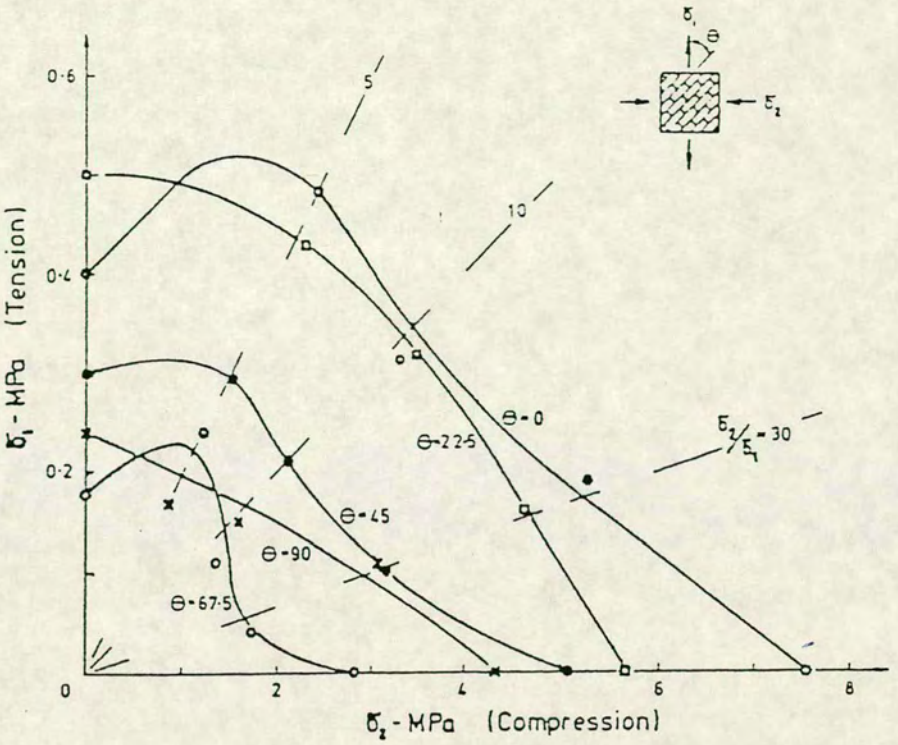

Fig. 7.4.18 Failure Surface for Masonry Under Biaxial Tension - Compression (After Page[103])

rupture which had a value of 1.83 N/mm^2 in the partially prestressed brickwork beams tested in this work (see Chapter 3).

Beams with Shear Span to Effective Depth Ratio of 1.5

The principal stress contours for the partially prestressed brickwork beams with a shear span to effective depth ratio of 1.5 are shown in Fig. 7.2.17.

Unlike in the beams with the higher shear span to effective depth ratios, the compressive stress contours were not confined to the compression zone which characterises a beam in bending, but were also present in the shear span extending from the loading point to the support rather like a 'tied frame' with inclined legs (akin to Kostovos[94] model of a deep beam, see Section 7.3). This indicates that a significant amount of compressive force is transmitted directly from the load point to the support. However, in the constant moment region, there was a reduction in compressive stress with increasing distance from the top fibre – an indication of beam bending.

Principal tensile stresses were present in a large area of the beam with exceptions being in the compression zone of the constant moment region, the areas of the beam which were cracked in flexure and the lightly loaded areas above the support. Like in the beams with shear span to effective depth ratios between 3.0 and 6.0, the maximum principal tensile stresses in these beams were obtained at a section where the shear force and the bending moment were maximum. This value was 1.91 N/mm^2 at an angle of 44° to the horizontal axis of the beam. Above, it was mentioned that there is an increase in the value of the principal tensile strength with decreasing angle of the bed joint to the principal tensile stress. This result for the beams with shear span to effective depth ratio of 1.5 appears to be in contradiction to the above results. However, as can be seen from Fig. 7.4.18, at an orientation of the principal tensile stress to the bed joint of 45°, when the ratio of the principal compressive stress to the principal tensile stress has a value of around 5, higher principal tensile stresses are obtained. In these beams, the ratio of the principal compressive stress to the principal tensile stress at shear failure was 7.

The presence of a high tensile stress in the shear span close to the load point is also compatible with the concept of the compressive force path for members which fail in shear compression (see Section 7.3). Comparing the

principal tensile and compressive stress contours for these beams clearly indicates that the path along which the compressive force is transmitted from the loading point to the support is under a state of biaxial compression-tension - as postulated by the compressive force path concept.

7.5 CONCLUSION

In this chapter, a theoretical and experimental investigation has been carried out into the shear strength of partially prestressed brickwork beams. The following conclusions can be drawn:

1. The shear strength of partially prestressed brickwork beams increases with decreasing shear span to effective depth ratio.

2. There is a degradation in the ultimate moment due to shear failure at all shear span to effective depth ratios. It appears that the maximum degradation in ultimate moment occurs between a shear span to effective depth ratio of 3.0 and 1.5.

3. Diagonal tension failure occurred in the partially prestressed brickwork beams with shear span to effective depth ratio of 3.0 and above. At a shear span to effective depth ratio of 1.5, the partially prestressed brickwork beams exhibited shear compression failure. However, in both types of failure, the shear span of the beams were already cracked in flexure.

4. The compressive force path concept is compatible with the failure modes observed in partially prestressed brickwork beams. The shear strength of prestressed brickwork beams without shear reinforcement can be reliably predicted from the application of this concept.

5. A finite element analysis carried out using a non-linear material model developed for concrete, was modified for brickwork and gave predictions of deflection, top fibre strain and the tensile forces in the non-tensioned and tensioned steel which were in good agreement with the experimental results.

CHAPTER 8
CONCLUSIONS
AND SUGGESTIONS FOR FURTHER STUDIES

8.1 GENERAL

This thesis presents the results of a study which has been carried out to compare the behaviour of fully and partially prestressed beams of brickwork and concrete with identical cross-sectional properties and of similar compressive strength under the ultimate limit states of shear and flexure and the serviceability limit states of deflection and cracking. As the shear strength of brickwork imposes a limitation on the structural performance of prestressed brickwork beams, the work presented in this thesis also included an experimental and theoretical investigation in which the effect of the shear span to effective depth ratio on the shear strength of partially prestressed brickwork beams was investigated. A total of twenty seven full-scale tests on fully and partially prestressed brickwork and concrete beams were carried out as well as a series of small specimen tests from which the material properties used in the theoretical analysis were obtained.

A method for determining the balanced area of steel in a beam containing tensioned and non-tensioned steel at different depths was developed. An expression relating the maximum crack width in a prestressed brickwork beam to the steel stress after decompression was proposed. A method has also been suggested for the determination of the shear strength of prestressed brickwork beams based on the concept of the compressive force path.

8.2 CONCLUSIONS

On the basis of this study, the following general conclusions can be drawn:

1. When failure is in flexural tension, the ultimate moment, moment-curvature and load-deflection relationships of fully and partially prestressed brickwork and concrete beams are very similar up to failure.

However, in the fully prestressed beams containing tensioned steel only, narrower crack widths and smaller crack spacings were obtained in the brickwork. Comparable crack widths and crack spacings were obtained in the partially prestressed brickwork and concrete beams which contained non-tensioned close to the soffit.

2. The shear strength of a prestressed brickwork beam is lower than that of a similar concrete beam.

3. The shear strength of a partially prestressed brickwork beam is dependent on the shear span to effective depth ratio which also influences the mode of shear failure i.e. diagonal tension or shear compression.

4. The flexural crack widths in a fully or partially prestressed brickwork beam is directly proportional to the steel stress after decompression.

5. The balanced area of steel in a partially prestressed brickwork or concrete beam containing tensioned and non-tensioned steel at different depths can be estimated from the method developed in this work.

6. The proposed method of estimating the maximum crack widths in a fully or partially prestressed brickwork beams correlates closely with experimental results.

7. The concept of the compressive force path which has been used to estimate the shear strength of concrete beams can also be successfully applied to fully and partially prestressed brickwork beams.

8. The flexural behaviour and ultimate strength in flexure and shear of fully and partially prestressed brickwork beams can be predicted from the stress-strain relationship and compressive strength of brickwork obtained from uniaxially loaded single course prisms.

9. A non-linear finite element analysis carried out on partially prestressed brickwork beams using a material model developed for concrete and modified to account for the behaviour of brickwork, gave predictions of deflection, the strain in the top brickwork fibre and the tensile forces in

the tensioned and non-tensioned steel which were in good agreement with experimental results.

8.3 SUGGESTIONS FOR FURTHER STUDIES

The work described in this thesis complements previous works[11,12] which have been carried out to establish the behaviour of bonded prestressed brickwork beams. The flexural behaviour of fully and partially prestressed beams and the factors which affect it have been explained and theoretical methods of analysis based on the non-linear material properties proposed which predict the ultimate flexural moment, deflection and cracking.

This study has shown that the structural behaviour of prestressed brickwork beams are comparable to prestressed concrete beams except when the brickwork beams fail in shear. The shear strength of partially prestressed brickwork beams has been studied and a method proposed for calculating the shear strength of prestressed brickwork beams which is based on the non-linear stress-strain relationship for brickwork. An expression has also been proposed which can be used to accurately predict the maximum crack widths.

However, for a better understanding of the behaviour of prestressed brickwork beams and to enable the adoption of prestressed brickwork beams as an alternative to concrete beams in some areas of the civil/structural engineering industry, the following areas are suggested for further research:

1. The long term behaviour of bonded prestressed brickwork beams need to be considered, particularly the magnitude of the prestress losses and the factors which affect them.

2. Research is required into the behaviour of prestressed brickwork beams under repeated loading.

3. The method proposed for the calculation of the shear strength of partially prestressed brickwork beams is based on the strain at which bed joint splitting occurs in the constant moment region of the beam. The value for the splitting strain proposed in this work is only applicable to

brickwork of high strength brick laid in grade I mortar. Values of the splitting strain need to be determined for other combinations of brick and mortar.

4. From a structural engineering point of view the acceptance of prestressed brickwork beams as a viable alternative to concrete beams in housing is dependent on two criteria, the first of which has been the subject of this thesis. The second is one of economic comparability. Research is required in this area.

REFERENCES

1. British Standards Institution, 'Code of Practice for Use of Reinforced and Prestressed Masonry', BS 5628: Part: 2: 1985.

2. Baker, L.R., 'The Flexural Action of Masonry Structures Under Lateral Load', Ph.D. Thesis, Deakin University, Australia, July 1981.

3. Thomas, K., 'Current Post-Tensioned and Prestressed Brickwork and Ceramics in Great Britain', Designing, Engineering and Constructing with Masonry Products, Edited by F. B. Johnson, Gulf, Houston, Texas, 1969, pp 285–301.

4. Schneider, R.R. and Dickey, W. L., 'Reinforced Masonry Design', Prentice-Hall, New Jersey, 1980.

5. Plummer, H.C. and Blume, J.A., 'Reinforced Brick Masonry and Lateral Force Design', Structural Clay Products Ltd., Washington D.C., 1953.

6. Haseltine, B.A. and Tutt, J.N., 'Brickwork Retaining Walls', Brick Development Association publication, Westerham Press, 1979.

7. Sinha, B.P., 'Reinforced Grouted Cavity Brickwork', Building Research and Practice, July/August 1982, pp 226–243.

8. Suter, G.T. and Hendry, A.W., 'Shear Strength of Reinforced Brickwork Beams', The Structural Engineer, June 1975, No. 6, Vol. 53, pp 249–253.

9. Hendry, A.W., 'The Shear Strength of Reinforced Brickwork', International Symposium on Reinforced and Prestressed Masonry, Edinburgh, 1984, pp 104–122.

10. Sutherland, R.J.M, 'The Future of Prestressed Masonry', Proceedings of the 6th International Brick Masonry Conference, Edited by Laterconsult, Rome, 1982, pp 582–593.

11. Pedreschi, R.F., 'A Study of the Behaviour of Post-tensioned Brickwork Beams', Ph.D. Thesis, Department of Civil Engineering and Building Science, The University of Edinburgh, 1983.

12. Walker, P.J., 'A Study of the Behaviour of Partially Prestressed Brickwork Beams', Ph.D. Thesis, Department of Civil Engineering and Building Science, The University of Edinburgh, 1987.

13. Garwood, T.G., 'The Construction and Test Performance of Four Prestressed Brickwork Beams', The 8th International Symposium on Loadbearing Brickwork, London, 1983.

14. Garwood, T.G., 'The Flexural Behaviour of Fully Prestressed and Partially Prestressed "Pier-Bond" Brickwork Beams', International Symposium on Reinforced and Prestressed Masonry, Edinburgh, 1984, pp 411-426.

15. Foster, D., 'Design and Construction of a Prestressed Brickwork Water Tank', Proceedings of the 2nd International Brick Masonry Conference, Edited by H.W.H West and K. Speed, British Ceramic Research Association, Stoke-on-Trent, 1971.

16. Neill, J.A., 'Post-Tensioned Brickwork', Clay Products Technical Bureau, Technical Note, Vol. 1, No. 9, 1966.

17. Curtin, W.G., Shaw, G., Beck, J.K and Pope, L.S., 'Post-Tensioned Free Cantilever Diaphragm Wall Project', Proceedings of the 6th International Brick Masonry Conference, Edited by Laterconsult, Rome, 1982, pp 1645-1656.

18. 'Handbook of Structural Concrete', Edited by F.K Kong, R.H Evans, E. Cohen and F. Roll, Pitman Publishing Inc., London, 1983.

19. Lin, T.Y. and Burns, N.H., 'Design of Prestressed Concrete Structures', Third edition, John Wiley and Sons, New York, 1981.

20. Mehta, K.C. and Fincher, D., 'Structural Behaviour of Pretensioned Prestressed Masonry Beams', Proceedings of the 2nd International Brick

Masonry Conference, Edited by H.W.H. West and K. Speed, Stoke-on-Trent, British Ceramic Research Association, 1971, pp 215-219.

21. Curtin, W.G. and Phipps, M., 'Prestressed Masonry Diaphragm Walls', Proceedings of the 6th International Brick Masonry Conference, Edited by Laterconsult, Rome, 1982, pp 971-980.

22. Williams, E.O.L. and Phipps, M., 'Bending Behaviour of Prestressed Masonry Box Beams', Proceedings of the 6th International Brick Masonry Conference, Edited by Laterconsult, Rome, 1982, pp 981-994.

23. Roumani, N. and Phipps, M.E., 'The Shear Strength of Prestressed Brickwork I and T Sections', Proceedings of the 7th International Brick Masonry Conference, Edited by T. McNeilly and J.C. Scrivener, Melbourne, Australia, 1985, Vol. 2, pp 1001-1014.

24. Roumani, N. and Phipps, M.E., 'The Ultimate Shear Strength of Unbonded Prestressed Brickwork I and T Section Simply Supported Beams', Proceedings of the British Masonry Society, No. 2, April 1988, pp 82-84.

25. Montague, T.I. and Phipps, M.E., 'The Behaviour of Post-tensioned Masonry in Flexure and Shear', International Symposium on Reinforced and Prestressed Masonry, Edinburgh, 1984.

26. Robson, I.J., Ambrose, R.J., Hulse, R. and Morton, J., 'Post-Tensioned Prestressed Brickwork Beams', Proceedings of the British Masonry Society, No. 1, November 1986., pp 100-105.

27. Pedreschi, R.F. and Sinha, B.P., 'Development and Investigation of the Ultimate Load Behaviour of Post-Tensioned Brickwork Beams', The Structural Engineer, Vol. 60B, No. 3, September 1982, pp 63-67.

28. Walker, P.J. and Sinha, B.P., 'Behaviour of Partially Prestressed Brickwork Beams', Proceedings of the 7th International Brick Masonry Conference, Edited by T. McNeilly and J.C. Scrivener, Melbourne, Australia, 1985, pp 1015-1029.

29. Garwood, T.G., 'A Comparison of the Behaviour of Reinforced, Prestressed and Partially Prestressed Brickwork Beams', Proceedings of the British Masonry Society, No.2, April 1988, pp 76-81.

30. Pedreschi, R.F. and Sinha, B.P., 'The Stress/Strain Relationship of Brickwork', 6th International Brick Masonry Conference, Rome, May 1982, pp 321-334.

31. Lenczner, D. and Davies, P., 'Loss of Prestress in Post-Tensioned Brickwork Walls and Columns', International Symposium on Reinforced and Prestressed Masonry, Edinburgh, 1984, pp 76-89.

32. Lenczner, D., 'Brickwork: Guide to Creep', A Structural Clay Product Publication, SCP 17, 1980.

33. Lenczner, D., 'The Loss of Prestress in Post-Tensioned Brick Masonry Members', Masonry International, No. 5, July 1985, pp 9-12.

34. Lenczner, D. and Davies, P., 'Creep Loss of Prestress in Post-Tensioned Brickwork Walls with Previous Stress History', Proceedings of the British Masonry Society, Edited by H.W.H West, No. 2 April 1988, pp 5-7.

35. Bradshaw, R.E., Drinkwater, J. and Bell, S.E., 'A Multi-Purpose Farm Building Incorporating Prestressed Brickwork Diaphragm Walling', Proceedings of the British Ceramic Society, Load Bearing Brickwork (7), Edited by H.W.H West, Stoke-on-Trent, September 1982, pp 308-315.

36. Bradshaw, R.E, Drinkwater, J.P. and Bell, S.E., 'The George Armitage Head Office', Masonry International, No. 1, April 1984, pp 18-21.

37. The Brick Bulletin, The Brick Development Association, 3/82 August 1982 pp 21-25.

38. Allen, L.N., 'Post-Tensioned Brickwork at Rushden Fire Station', Engineers File Note No.1, Published by the Brick Development Association, March 1986.

39. The Brick Bulletin, The Brick Development Association, 2/89 Spring 1989.

40. Leonhardt, F., 'Prestressed Concrete Design and Construction', Published by Wilhelm Ernst & Sohn, Berlin, Munich, 1964.

41. Walker, P.J and Sinha, B.P., 'Compressive Strength of Brickwork on Edge under Axial and Eccentric Loading', Masonry International, No. 6, December 1985, pp 1-8.

42. British Standards Intitution, 'Structural Use of Concrete, Code of Practice for Special Circumstances', BS 8110: Part 2: 1985.

43. British Standards Institution, 'Specification for Clay Bricks, BS 3921, 1985.

44. Page, A.W and Marshall, R., 'The Influence of Brick and Brickwork Prism Aspect Ratio on the Evaluation of Compressive Strength', Proceedings of the 7th International Brick Masonry Conference, Edited by T. McNeilly and J.C. Scrivener, Melbourne, Australia, Vol. 1, 1985, pp 653-664.

45. Sinha, B.P. and Pedreschi, R.F., 'Compressive Strength and some Elastic Properties of Brickwork', International Journal of Masonry Construction, Vol. 3, No. 1, 1983, pp 19-25.

46. British Standards Institution, 'Specification for Ordinary and Rapid-Hardening Portland Cement', BS 12, 1978.

47. British Standards Institution, 'Specification for Building Limes', BS 890, 1976.

48. British Standards Institution, 'Specification for Building Sands from Natural Sources', BS 1200, 1976.

49. British Standards Institution, 'Specification for Aggregates from Natural Sources for Concrete', BS 892, 1983.

50. Maurenbrecher, A.H.P., 'Compressive Strength of Eccentrically Loaded Masonry Prisms', 3rd Canadian Masonry Symposium, Edmonton, 1983.

51. Drysdale, R.C. and Hamid, A.A., 'Effect of Eccentricity on the Compressive Strength of Brickwork', Proceedings of the British Ceramic Society, No. 30, September 1982, pp 140–148.

52. Hodgkinson, H.R. and Davies, S., 'The Stress–Strain Relationship of Brickwork when Stressed in Directions other than Normal to the Bed Face', Proceedings of the 6th International Brick Masonry Conference, Edited by Laterconsult, Rome, 1982, pp 290–299.

53. Sinha, B.P., 'An Ultimate Load Analysis of Brickwork Flexural Members', International Journal of Masonry Construction, Vol. 67, 1970, pp 243–247.

54. Desayi, P. and Krishna, S., 'Equation for the Stress–Strain Curve for Concrete', Journal of the American Concrete Institute, March 1964, pp 345–350.

55. Hognestad, E., 'Confirmation of the Inelastic Stress Distribution in Concrete', Journal of the Structural Division , Proceedings of the American Society of Civil Engineers, Paper 1189, March 1957, pp 1189–1 – 1189–15.

56. ACI–ASCE Report on the 'Ultimate Strength Design', Journal of the American Concrete Institute, January 1956.

57. Hognestad, E., Hanson, N.W., and McHenry, D., 'Concrete Stress Distribution in Ultimate Strength Design', Journal of the American Concrete Institute, Vol. 27, December 1955, pp 455–479.

58. British Standards Institution, 'Structural Use of Concrete, Code of Practice for Design and Construction', BS 8110: Part 1: 1985.

59. Teychenne, D.C., Franklin, R.E. and Erntroy, H.C., 'Design of Normal Concrete Mixes', Department of the Environment, Building Research Establishment, Transport and Road Research Laboratory, London, 1982.

60. Buliding Research Establishment Digest, 'Concrete Mixes: Specification, Design and Quality Control', Digest 244, London, December 1980.

61. Shirley, D.E., 'Introduction to Concrete', Cement and Concrete Association Publication, London, 1980.

62. British Standards Institutions, 'Testing of Concrete', BS 1881, 1983.

63. British Standards Institution, 'Specification for High Tensile Steel Wire and Strand for the Prestressing of Concrete', BS 5896, 1980.

64. British Standards Institution, 'Specification for Hot Rolled Steel Bars for the Reinforcement of Concrete', BS 4449, 1978.

65. Thurlimann, B. A., 'A Case for Partial Prestressing', Structural Concrete Symposium, Department of Civil Engineering, University of Toronto, Toronto, May 1971, pp 253-301.

66. Hutton, S.G. and Loov, R.E., 'Flexural Behaviour of Prestressed, Partially Prestressed and Reinforced Concrete Beams', Journal of the American Concrete Society, Vol. 63 (2), December, 1966, pp 1401-1409.

67. Bennett, E.W., 'Partial Prestressing - A Historical Overview', Journal of the Prestressed Concrete Institute, September-October 1984, pp 104-117.

68. Rao, P.S and Subrahmanyam, B.V., 'Trisegmental Moment-Curvature Relations for Reinforced Concrete Members', Journal of the American Concrete Institute, No. 70-39, May 1973, pp 346-357.

69. Beeby, A.W. and Taylor, H.P.J, 'Short-Term Deformations of Concrete Structures', Cement and Concrete Association Technical Report TRA 408, March 1968.

70. Branson, D.E., 'Deformation of Concrete Structures', MacGraw-Hill, New York.

71. Burns, N.H., 'Moment Curvature Relationships for Partially Prestressed Concrete Beams', Journal of the Prestressed Concrete Institute, Vol 9, 1964, pp 52-63.

72. Priestley, M.J.N., Park, R. and Lu, F.P.S., 'Moment-Curvature Relationships for Prestressed Beams in Constant Moment Zone', Magazine of Concrete Research, Vol 23, No 75-76, June 1971, pp 69-78.

73. Majid, K.I., 'Introduction to Matrix and Numerical Methods for Civil Engineers', Woodstock Publishing, England, 1981.

74. Coates, R.C., Coutie, M.G. and Kong, F.K., 'Structural Analysis', Nelson, 1982.

75. Park, R. and Paulay, T., 'Reinforced Concrete Structures', John Wiley and Sons, New York, 1975.

76. Beeby, A. W., 'An Investigation of Cracking in Slabs Spanning One Way', Cement and Concrete Association Technical Report 433, April 1970.

77. Broms, B.B., 'Crack Width And Crack Spacing in Reinforced Concrete Members', Journal of the American Concrete Institute, October 1965, pp 1237-1255.

78. Base, G.D., Read, J.B., Beeby, A.W. and Taylor, H.P.J., 'Crack Control in Concrete Beams', CERA, Research Report No 6, Cement and Concrete Association, 1966.

79. Bennett, E.W. and Chandrasekhar, C.S., 'Calculation of the Width of Cracks in Class 3 Prestressed Concrete Beams', Proceedings of the Institution of Civil Engineers, Vol 49, 1971, pp 333-346.

80. Krishna Raju, N., Basvarajaiah, B.S. and Ahamed Kutty, U.C., 'Flexural Behaviour of Pretensioned Concrete Beams with Limited Prestress', Building Science, Vol 8, 1973, pp 179-185.

81. Suri, K.M., and Dilger, W.H., 'Crack Width of Partially Prestressed Concrete Members', Journal of the American Concrete Institute, Technical paper, Title No 83-73, September-October 1986 pp 784-796.

82. Beeby, A.W., 'The Prediction of Crack Widths in Hardened Concrete', The Structural Engineer, Vol 10, No 4, July 1982, pp 226-243.

83. Desayi, P., 'A Method for Determinig the Spacing and Width of Cracks in Partially Prestressed Concrete Beams', Proceedings of the Institution of Civil Engineers, Part 2, Vol 59, September 1975, pp 411–428.

84. Tadros, M.K., 'Expedient Service Load Analysis of Cracked Prestressed Concrete Sections', Journal of the American Concrete Institute, Vol 27, No 6, November–December 1982, pp 86–111.

85. ACI Committee 224, 'Control of Cracking in Concrete Structures', Journal of American Concrete Institute, Vol 69, No 12, December 1972, pp 719–752.

86. Beeby, A.W., Keyder, E. and Taylor, H.P.J., 'Cracking and Deformation of Partially Prestressed Concrete Beams', Cement and Concrete Association Technical Report 465 Publication 42.465, 1972.

87. Nawy, E.G., 'Flexural Cracking Behaviour of Pretensioned and Post–Tensioned Beams: The State of Art', Journal of the American Concrete Institute, Title No 82–84, November/December 1985, pp 890–900.

88. Nielsen, M.P., Braestrup, M.W., Jensen, B.C. and Bach, F., 'Concrete Plasticity. Beam Shear – Punching Shear – Shear in Joints', Danish Society for Structural Science and Engineering, Structural Research Laboratory, Special Publication, Technical University of Denmark, Copenhagen, 1978.

89. Nielsen, M.P. and Braestrup, M.W., 'Shear Strength of Prestressed Concrete Beams Without Web Reinforcement', Magazine of Concrete Research, Vol 30, No 104, September, 1978.

90. Kotsovos, M.D., 'Mechanics of "Shear" Failure', Magazine of Concrete Research, Vol 35, No 123, June 1983, pp 99–106.

91. Kotsovos, M.D., 'Behaviour of Beams With Shear Span–to–Depth Ratios Greater Than 2.5', Journal of the American Concrete Institute, Vol 83, No 93, November–December 1986, pp 1026–1034.

92. Kotsovos, M.D., 'Behaviour of Reinforced Concrete Beams with Shear Span to Depth Ratio between 1.0 and 2.5', Journal of the American Concrete Institute, Vol 81, No 27, May–June 1984, pp 279–286.

93. Kotsovos, M.D., Bobrowski, J. and Eibl, J., 'Behaviour of Reinforced Concrete T–Beams in Shear', The Structural Engineer, Vol 65B, No 1, March 1987, pp 1–10.

94. Kotsovos, M.D., 'Design of Reinforced Concrete Deep Beams', The Structural Engineer, Vol 66, No 2, January 1988.

95. Joint ASCE–ACI Task Committee 426 on Shear and Diagonal Tension, 'The Shear Strength of Reinforced Concrete Members', Journal of the Structural Division, June 1973, pp 1091–1187.

96. Kani, G.J.N., 'The Riddle of Shear Failure and its Solution', Journal of the American Concrete Institute, April 1964, pp 441–467.

97. Kong, F.K. and Evans, R.H., 'Reinforced and Prestressed Concrete', Published by Van Norstrand Reinhold, 1980.

98. Freig, S.M. and Smith, K.N., 'Indirect Loading on Beams with Short Shear Spans', Journal of the American Concrete Institute, Vol 74, May 1977, pp 220–222.

99. Bresler, B. and MacGregor, J.G., 'Review of Concrete Beams Failing in Shear', Journal of the Structural Division, Proceedings of the American Society of Civil Engineers, February 1967, pp 5106–5110.

100. Kani, G.N.J., 'Basic Facts Concerning Shear Failure', Journal of the American Concrete Institute, June 1966, pp 675–691.

101. Suter, G.T. and Keller, H., 'Shear Strength of Grouted Reinforced Brick Beams', 4th International Brick Masonry Conference, Bruges, April 1976.

102. Hendry, A.W., 'Structural Brickwork', Published by Macmillan Press, London, 1983.

103. Dhanasekar, M., 'The Performance of Brick Masonry Subjected to In-Plane Loading', Ph.D Thesis, Department of Civil Engineering, University of Newcastle, Australia, 1985.

104. Page, A.W., 'Finite Element Model for Masonry', Journal of the Structural Division, Proceedings of the American Society of Civil Engineers, Vol 104, No ST8, August 1978, pp 1267-1285.

105. Samarasinghe, W., Page, A.W. and Hendry, A.W., 'A Finite Element Model for the In-Plane Behaviour of Brickwork', Proceedings of the Institution of Civil Engineers, Part 2, Vol 71, 1982, pp 171-178.

106. Finite Element Analysis Ltd, 'Lusas finite Element Analysis System User Manual', October 1987.

107. Finite Element Analysis Ltd, 'Non-Linear Concrete Model 24 Internal Report No. FEAI703', June 1987.

108. Bobrowski, J. and Bardhan-Roy, B.K., 'A Method of Calculating the Ultimate Strength of Reinforced and Prestressed Concrete Beams in Combined Flexure and Shear', The Structural Engineer, Vol. 47, No. 5, May 1969, pp 197-209.

109. Design and Detailing of Concrete Structures for Fire Resistance: Interim Guidance by a Joint Committee of the Institution of Structural Engineers and The Concrete Society, London, April 1978.

110. Taner, N., Fazio, P.P and Zielinski, Z.A., 'Strength and Behaviour of Beams-Panels - Tests and Analysis', Journal of the American Concrete Institute, October 1977, Vol 74, No 10, pp 511-519.

111. Bruce, R.N., 'The Action of Vertical, Inclined and Prestressed Stirrups in Prestressed Concrete Beams', Journal of the Prestressed Concrete Institute, Vol 9, Part 1, 1969, pp 14-25.

APPENDIX

Published Papers

During the course of this investigation, the following paper has been published in collaboration with Dr. B. P. Sinha.

"A Comparative Study of Prestressed Beams of Brickwork and Concrete", Proceedings of the first International Masonry Conference, London, United Kingdom, Edited by H.W.H. West, 2nd - 4th December 1986 pp 92-94.